The investigation of the effects of Metformin in Thyroid Cancer

By:

Safar Kheder

A thesis submitted in partial fulfillment of the requirements for the degree of Doctor of Philosophy

Supervisors:

Saba Balasubramanian, Karen Sisley and Sirwan Hadad

The University of Sheffield

Department of Oncology and Metabolism

Medical School

Sheffield, UK.

February 2018

Acknowledgement

This is my pleasure to take this valuable opportunity to show my immense gratitude to my supervisors Dr. Saba Balasubramanian, Dr. Karen Sisley and Dr. Sirwan Hadad for their patience, support, enthusiasm, motivation, and important help during my PhD. I could not expected to have better supervision during my PhD.

Dr. Saba Balasubramanian is very welcoming and has spent time with me during and beyond office hours. He is keen to give me advice and guides me in the right direction with my endless enquiry and questions throughout my PhD.

Dr. Karen Sisley is always keen to help me alongside my laboratory work in the lab or her office and she has trained me very well during my PhD.

Dr. Sirwan Hadad enriched me with his great knowledge on Metformin as an anti-cancer agent and guided me with his excellence supervision.

I would like to thank several people (David Hammond, Claire Greaves, Azeez Salawu, Nawal Al Shammari, Afnan Al Kathiri, Meshal AlHaji Mohammed, Shamsa Ihmed, Dler Kadir) that they have important role in the success of my PhD.

Human Capacity Development Program (HCDP) in Kurdistan Regional Government-Iraq (KRG) sponsored this work and I want to say this work was impossible to complete it without their funds and support.

Finally, I would like to take this opportunity to thank my family for their understanding and unconditional support throughout my PhD.

Abstract

Background: Thyroid cancer is generally associated with an excellent prognosis, but there is significant long-term morbidity with standard treatment, and some sub-types have poor prognosis. Metformin, an oral anti-diabetic drug is shown to have anti-cancer effects in several types of cancer (breast, lung and ovarian cancer). Proposed mechanisms include activation of Adenosine Mono-phosphate-activated Protein Kinase (AMPK) pathway; inhibition of mTOR pathway; reduction in blood glucose and insulin levels by inhibiting hepatic gluconeogenesis and increasing peripheral glucose uptake. OCT1 (organic cation transporter 1) helps in the uptake of Metformin into liver cells.

Aims: Explore the anti-cancer effect of Metformin on the growth and proliferation of thyroid cancer cell lines.

Methods: The effects of Metformin on thyroid cancer cell lines (FTC-133, K1E7, RO82-W-1, 8305C and TT) and normal thyroid follicular cells (Nthy-ori 3-1) were investigated using the MTT (3-[4,5-dimethylthiazol-2-yl]-2,5 diphenyl tetrazolium bromide) assay for cell proliferation; clonogenic assay; Fluorescence-activated Cell Sorting (FACS) analysis for apoptosis (using double staining with Annexin V-FITC stained early apoptotic cells and propidium iodide stained late apoptotic cells) and cell cycle (using propidium iodide staining); and H2A.X phosphorylation (γH2AX) assay for DNA repair. Immunocytochemistry was used to investigate OCT1 expression to evaluate the mechanism of action of Metformin. The effects of Thyroid Stimulating Hormone (TSH), insulin and Insulin-like Growth Factor- 1 (IGF-1) on the response to Metformin treatment were also investigated. Affymetrix assay was used for gene expression profiling of cell lines before and after Metformin treatment.

Results: Metformin inhibited cell proliferation and colony formation at a minimum concentration of 0.03 mM and increased the percentage of apoptotic

cells at concentrations of 0.1 mM and above. Metformin also induced cell cycle arrest in G0/G1 phase at minimum concentration of 0.3 mM. Unlike previous reports, Metformin did not appear to affect response to DNA repair. OCT1 expression was observed in all thyroid cancer cell lines, but no significant difference was observed in the proportion and intensity of OCT1 expression in Metformin treated and non-treated cells. Anti-cancer effects of Metformin (cell proliferation and apoptosis) was amplified in the glucose-free medium compared to glucose-rich medium. Metformin inhibited cell proliferation regardless of the presence of TSH, IGF-1 and insulin in the medium. Metformin modulated the expression of numerous genes and provided clues to the mechanism of action.

Conclusion: Metformin suppresses thyroid cancer proliferation *in vitro* at concentrations within the therapeutic range for diabetic patients. This effect appears to be independent of TSH, insulin, glucose and IGF-1. Further work is needed to determine the molecular mechanisms underlying the observed effects.

Publications

- Research article: Kheder S, Sisley K, Hadad S, Balasubramanian SP., et al., e**ffects of prolonged exposure to low dose Metformin in thyroid cancer.** J Cancer, 2017. **8**(6): p. 1053-1061.
- Poster and oral presentation: Kheder S, Sisley K, Hadad S, Balasubramanian SP **the *in vitro* effects of Metformin on thyroid cancer cell lines** at the 15th International Thyroid Congress, Florida 2015
- Poster presentation: Kheder S, Sisley K, Hadad S, Greaves C, Balasubramanian SP **importance of the OCT1 transporter to the anti-cancer effect of Metformin in thyroid cancer**, presented at the 11th Annual School Research Meeting 2015, The Medical School, University of Sheffield, UK; and 35th BAETS Annual Scientific Meeting Reading/ Henley on Thames 2015
- Oral presentation: Kheder S, Sisley K, Hadad S, Balasubramanian SP **investigation of the role of Metformin in thyroid cancer** presented at the BJS Prize session of the 34th BAETS Annual Scientific Meeting in Liverpool 2014. European Journal of Surgical Oncology (EJSO), Volume 40, Issue 12, December 2014, Pages 1799-1800 http://dx.doi.org/10.1016/j.ejso.2014.07.010http://dx.doi.org/10.1016/j.ejso.2014.07.010
- Poster presentation: Kheder S, Sisley K, Hadad S, Balasubramanian SP **investigation of the role of Metformin in thyroid cancer,** presented at the 10th Annual Research Meeting 2014, The Medical School, University of Sheffield, UK.

Table of contents

List of Figures

List of Tables

List of abbreviations

(I^{131})	Radio-iodine ablation
ACF	Aberrant Crypt Foci
ADP	Adenosine Diphosphate
Akt	Protien kinase
AMPK	Adenosine 5'-monophosphate –activated protein kinase
ATC	Anaplastic Thyroid Cancer
ATJCC	American Joint Committee on Cancer
ATP	Adenosine Triphosphate
BMI	Body Mass Index
BRAF	B-type Raf kinase
Cdk	Cyclin-dependent kinase
CT	Computerized Tomography
DMEM	Dulbecco's Modified Eagle Medium
DMEM-F12	Dulbecco's Modified Eagle's Medium Ham's F-12
DMSO	Dimethyl Sulphoxide
DNA	Deoxyribonucleic acid
DPBS	Dulbecco's Phosphate Buffered Saline
DTC	Differentiated Thyroid Cancer
EDTA	Ethylene-diamine-tetra-acetic-acid
EMEM	Minimum Essential Medium Eagle
FBS	Foetal Bovine Serum

FNAC	Fine Needle Aspiration Cytology
FT3	Free Tri-iodothyronine
FT4	Free Thyroxine
FTC	Follicular Thyroid Cancer
Gy	Gray (units for radiation)
HCC	Hurthle Cell Cancer
IGF-1	Insulin-like Growth Factor 1
IGF-1R	Insulin-like growth factor-1 receptor
IMS	Industrial Methylated Spirits
MAPK	Mitogen Activated Protein Kinase
MCDB	Molecular, Cellular, and Developmental Biology culture
MEN II	Multiple Endocrine Neoplasia type 2
miRNAs	MicroRNAs
mM	Millimoles
MRI	Magnetic Resonance Imaging
MTC	Medullary Thyroid Cancer
mTOR	Mammalian Target of Rapamycin
NEAA	Non-Essential Amino Acids
NSCLC	Non small Cell Lung Cancer
PAX8	Paired boxed gene 8
PPARγ1	Peroxisome Proliferator-Activated Receptor gamma
PTC	Papillary Thyroid Cancer
RAI	Radioactive Iodine
RAS	RAt Sarcoma oncogenes
Rb	Retinoblastoma protein

RET	Rearranged During Transfection gene
RIA	Radioiodine ablation
RNA	Ribonucleic acid
RPMI	Rosewell Park Memorial Institute culture medium
T3	Tri-iodothyronine
T4	Thyroxine
Tg	Thyroglobulin
THIN	The Health Information Network
TNBC	Triple receptor-negative breast cancer
TNM	Tumour Node Metastasis
TPO	Thyroid Peroxidise
TSH	Thyroid Stimulating Hormone
TSHRAb	TSH receptor antibody
OCT 1-3	Organic Cation Transporter 1-3
PMAT	Plasma membrane Monoamine Transporter
MATE 1-2	Multidrug and Toxin Extrusion protein 1-2
VEGF	Vascular Endothelial Growth Factor
USA	United States of America
µg	Microgram
µl	Microlitre
LKB1	Liver kinase B1
GLUT4	Glucose Transporter Type 4
ACC	Acetyle-CoA Carboxylase
HMG-CoA	3-hydroxy-3-methyle-glutargl-coenzyme A reductase
GPAM	Glycerol-3-Phosphate Acyltranferase 1 Mitocondrial

HERT2	Human Epidermal Growth Factor Receptor 2
COX-2	Cyclooxygenase-2
STAT3	Signal Transducer and Activator of Transcription 3
Bcl-2	B-cell lymphoma 2
VEGF	Vascular Endothelial Growth Factor
Bax	Bcl2-associated X
TSC2	Tuberous Sclerosis Complex 2
S6K1	Ribosomal Protein S6 Kinase beta-1
ERK	Extracellular signal-regulated kinase
EGFR	Epidermal Growth Factor Receptor
ATM	Ataxia-telangiectasia mutated
DNA-PK	DNA-dependent protein kinase
FOXO1	Forkhead box O1
PPP1R10	Protein phosphatase 1 regulatory subunit 10
SNORD	Small nucleolar RNA, C/D box
SLC18A3	Solute carrier family 18 member A3
C4B	Complement component 4
BCL10	B-cell lymphoma/leukemia 10
IER3	Immediate early gene X-1
TAF1D	TATA-box binding protein associated factor
TP53BP2	Tumour suppressor p53-binding protein 2
TPT1	Translationally-controlled 1
CASP2	Caspase 2
DAPK1	Death associated protein kinase 1

CHAPTER ONE

Introduction

1.1 Introduction

Thyroid cancer is a relatively uncommon malignancy (less than 1% of all cancers registered in the UK). However, it is the most common endocrine cancer, accounting for more than 90% of these tumours [1, 2]. The majority of thyroid cancer types have an excellent prognosis; but there are concerns over long-term morbidity associated with standard treatment regimes. Some types and subtypes of thyroid cancer are associated with poor prognosis and novel treatment options are being tried.

Metformin (N', N'-dimethybiguanide) is an oral anti-diabetic drug of the Biguanide class and one of the most commonly prescribed drugs worldwide; accounting for nearly 120 million prescriptions a year [3]. It is the first drug of choice in most patients with type 2 diabetes and has been licensed for use in in UK since 1958 [4-6]. Metformin has recently been investigated for possible anti-cancer effects by activating the Adenosine Mono-phosphate-activated Protein Kinase (AMPK) pathway in several types of cancer.

1.2 Thyroid Gland

1.2.1 Thyroid Gland Anatomy

The thyroid gland is situated at the front of the neck (overlying the 2nd, 3rd, and 4th tracheal rings) and consists of two lateral pear-shaped lobes joined by an isthmus in the middle [7, 8]. Thyroid gland is very vascular; being supplied mainly by superior and inferior thyroid arteries. Extensive anastomoses occur between the main thyroid arteries and branches of the tracheal and oesophageal arteries [7]. The veins draining thyroid gland are the superior, inferior and middle thyroid veins [7-9]. There is an extensive lymphatic network within the gland. Although some lymph channels pass directly to the deep cervical nodes, the subcapsular plexus drains principally to the juxta-thyroidal (i.e. pretracheal and paratracheal) nodes and nodes around the superior and inferior thyroid veins before passing to the deep cervical and mediastinal groups of nodes [7].

1.2.2 Thyroid Gland Physiology

The thyroid gland secretes a number of thyroid hormones; of which thyroxine (T4) and Tri-iodothyronine (T3) are the most important (**Figure 1.1**). Other hormones of little physiological significance include reverse T3, T1 and T2 [10]. The production and release of T3 and T4 in the thyroid gland is stimulated by Thyroid Stimulating Hormone (TSH) [7, 11] as part of the hypothalamo-pituitary-thyroid axis. T4 is secreted in much larger amounts by the gland, but is converted by mono-deiodination in the circulation and tissues to the more potent T3. The conversion of T4 to T3 is decreased by many factors such as illness (cancer, heart diseases, liver diseases, kidney diseases and infections), drugs, injury, malnutrition and starvation.

T3 and T4 are lipid soluble hormones and carried in the blood by proteins (thyroid binding globulin, transthyretin and albumin). They cross the cell membrane and bind to thyroid hormone receptors in the nucleus. Thyroid-hormone receptors are nuclear acidic proteins associated with chromatin and bind to specific DNA sequences when activated [7].

Thyroid hormones encourage various metabolic activities in most tissues in the body; thereby increasing the basal metabolic rate. This increases oxygen consumption and body temperature. Thyroid hormones enhance lipid metabolism, increase fatty acid oxidation in tissues and fatty acid concentration in plasma [12]. As a result blood cholesterol and triglyceride levels are decreased. Thyroid hormones stimulate gluconeogenesis and glycogenolysis. Thyroid hormones are necessary for normal growth in children; therefore their deficiency causes growth retardation. They also have effects on growth and development of nervous system (especially in foetal and neonatal brain) [13] and enhance the activity of the sympathetic nervous system - increase heart rate, cardiac contractility and blood flow.

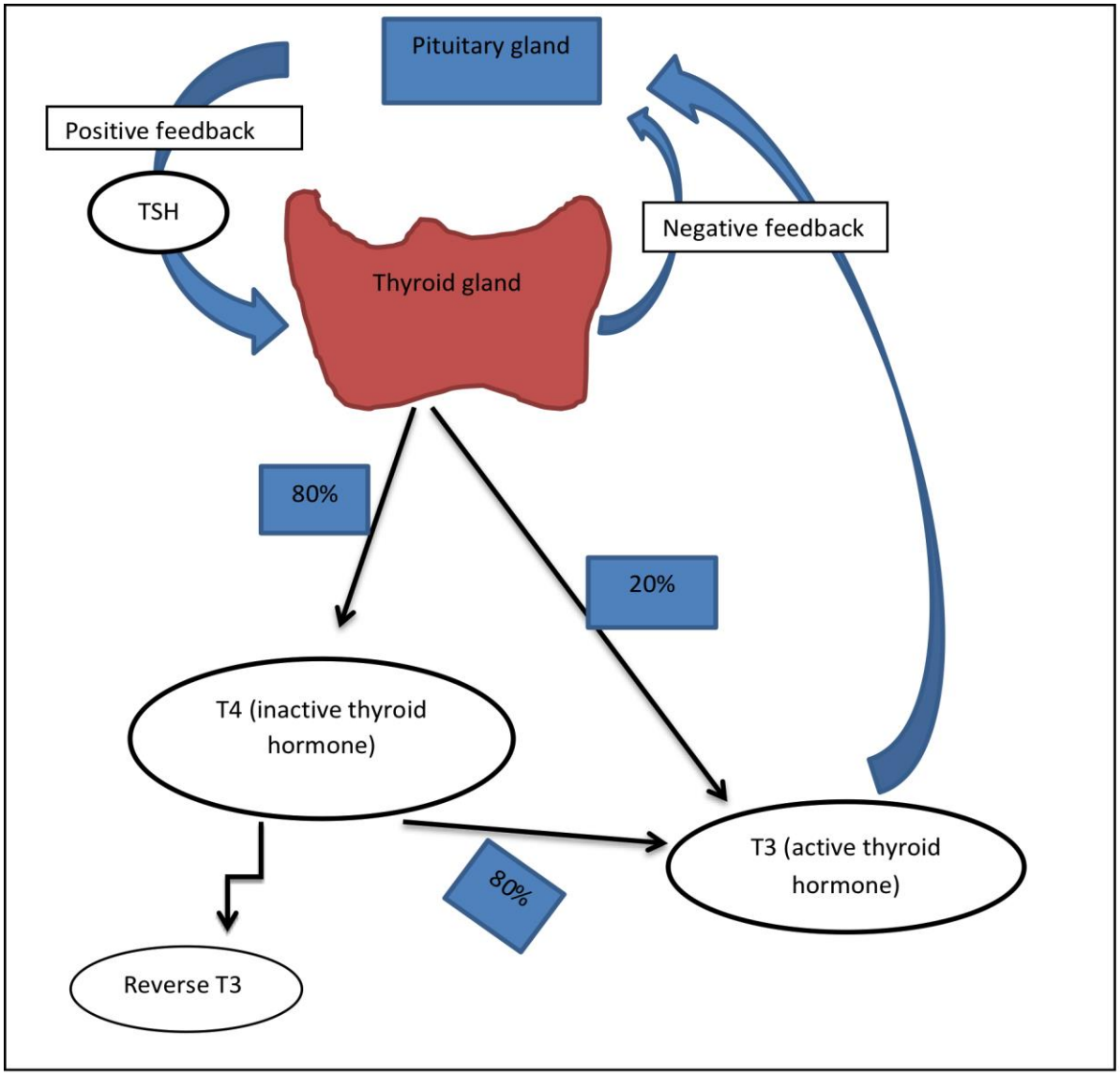

Figure 1.1: Regulation of thyroid hormone synthesis and release.

1.2.3 Thyroid Diseases

Thyroid diseases are often classified on the basis of thyroid function – i.e. hyperthyroidism and hypothyroidism. However, a significant number of thyroid pathologies are due to structural abnormalities where the patient is euthyroid, i.e. has normal thyroid function. These can be categorised as a separate group (thyroid nodules and goitre).

1.2.3.1 Hyperthyroidism

In hyperthyroidism the T4 and T3 levels are raised but TSH is low or undetectable. Occasionally, T3 levels alone (and not T4) can be raised. Hyperthyroidism is much more common in women (~10 times). The prevalence in women is 0.5-2%. It is more common in iodine-deficient areas of the world [1]. In subclinical hyperthyroidism, serum thyrotropin (TSH) is low, but free thyroxine (T4) and serum T3 concentrations are normal [14].

Aetiology

The common causes of hyperthyroidism are Graves' disease (a form of autoimmune thyroiditis), multinodular goitre and autonomously functioning solitary thyroid nodule [14]. Rare causes include drugs (such as amiodarone and lithium), TSH secreting pituitary lesions, differentiated thyroid cancer and ectopic sources of thyroid hormones such as struma ovarii.

Clinical features

The clinical features are numerous and involve a number of different organ systems. They include

1. General - weight loss with a normal or increased appetite, heat intolerance, fatigue, sweating, palmar erythema (redness), spider naevi (a dilated arteriole forming a red papule from which radiated prominent capillaries), onycholysis (separation of nail from its bed), alopecia (loss of hair), pigmentation (colouration of the skin), vitiligo (patches of loss of skin pigmentation), clubbing (nail become convex), pretibial myxoedema (dry firm waxy swelling of skin), gynaecomastia (enlargement of breast tissue in males), lymphadenopathy and osteoporosis (loss of bone tissue and liable to fracture).

2. Gastrointestinal - diarrhoea and steatorrhoea (due to fat malabsorption), anorexia, vomiting.

3. Cardiovascular - palpitations, sinus tachycardia, atrial fibrillation, increased pulse pressure, ankle oedema, angina and dyspnoea on exertion.

4. Respiratory - exacerbation of asthma.

5. Muscular and nervous system - tremor and irritability, hyperreflexia, muscle weakness, proximal myopathy.

6. Reproductive system - amenorrhoea/oligomenorrhoea, infertility, loss of libido, and impotence.

7. Eyes - lid retraction, lid lag, excessive lacrimation, chemosis (conjuctival swelling), exophthalmos (protrusion of eyeballs), corneal ulceration, diplopia, papilloedema (swelling of retina) and loss of visual acuity.

Investigations

Thyroid function tests are used to diagnosis hyperthyroidism (**Table 1.1 and Figure 1.2**). TSH receptor antibody (TSHRAb) levels may be estimated to determine aetiology as in Graves' disease [15]. In some patients (such as those with multinodular goitre) with hyperthyroidism, a radio-isotope scan will be required to determine if a specific nodule is the cause of the problem, as this may influence subsequent management [16].

Treatment

Treatment is aimed at addressing the excess production and release of thyroid hormones. Antithyroid drugs such as Carbimazole or Propylthiouracil are often used to render patients euthyroid in the first instance. The relapse rate following cessation of anti-thyroid drugs is more than 50% and subsequent treatment options such as Radioactive Iodine (RAI) or surgery depend on response to anti-thyroid drugs, age, patient choice and local facilities [17].

Radioactive iodine can be useful in patients who have recurrence of hyperthyroidism following surgery and patients with hyperthyroidism who are older than 40 years [18]. Surgery is often preferred as definitive treatment in patients with large goitres, associated significant Graves' ophthalmopathy and situations where RAI is contraindicated (such as pregnancy or lactation) or less preferred (women with young children) [19]. The surgical approach is usually a total thyroidectomy. Subtotal resections used to be performed in the past, but that was associated with

the risk of recurrence. Disadvantages of surgery include complications such as hypoparathyroidism, recurrent laryngeal nerve injury, and the need for life-long thyroxine [20].

1.2.3.2 Hypothyroidism

Primary hypothyroidism is the most common form of hypothyroidism and is due to a primary pathology in the thyroid gland. In primary hypothyroidism, free T3 (FT3) and free T4 (FT4) levels are low and the TSH is raised. The prevalence of primary hypothyroidism is more common in women [14]. Secondary hypothyroidism is due to pituitary disease. In secondary hypothyroidism FT4 is low and TSH is undetectable.

Subclinical hypothyroidism: is defined by raised (TSH) and normal FT4. The frequency of subclinical hypothyroidism and its impact on physiology and the risk of long-term complications are unclear [14]. Repeat measurements and monitoring is usually done before institution of treatment in symptomatic cases as the condition may be transient [14].

Aetiology

The most common cause of primary hypothyroidism is Hashimoto's thyroiditis. Other causes include spontaneous atrophic hypothyroidism, radio-iodine ablation (I^{131}) and thyroid surgery.

Clinical features

In the early stages, patients are often asymptomatic and the diagnosis is made on routine biochemical testing. Symptoms are often non-specific and diverse. Clinical features include tiredness, weight gain, cold intolerance, hoarseness, goiter, poor hearing, non-pitting edema, myxedema, periorbital puffiness, anemia, bradycardia, hypertension, pericardial and pleural effusion, carpel tunnel syndrome and depression.

Investigations

Thyroid function tests are used to diagnose hypothyroidism (**Table 1.1 and Figure**

1.2). FT3 levels are not routinely measured for the diagnosis of hypothyroidism as they correlate well with FT4 levels and do not independently influence management.

Treatment

Thyroid hormone replacement therapy; Thyroxine should be given as a single dose and is usually started at low doses (such as 50 µg per day). Further dose escalations are titrated to TSH levels and symptoms and are done in increments of 25 µg every few weeks to months. The optimal dose of thyroxine in most patients is the dose that restores serum TSH to the lower part of the normal reference range [21].

Table 1.1: Thyroid function test results in thyroid diseases.

Thyroid diseases	**FT3**	**FT4**	**TSH**
Hyperthyroidism	Raised	Raised	Low
T3 thyrotoxicosis	Raised	Normal	Low
Subclinical hyperthyroidism	Normal	Normal	Low
Primary hypothyroidism	Low	Low	Raised
Secondary hypothyroidism	Low	Low	Low
Subclinical hypothyroidism	Normal	Normal	Raised

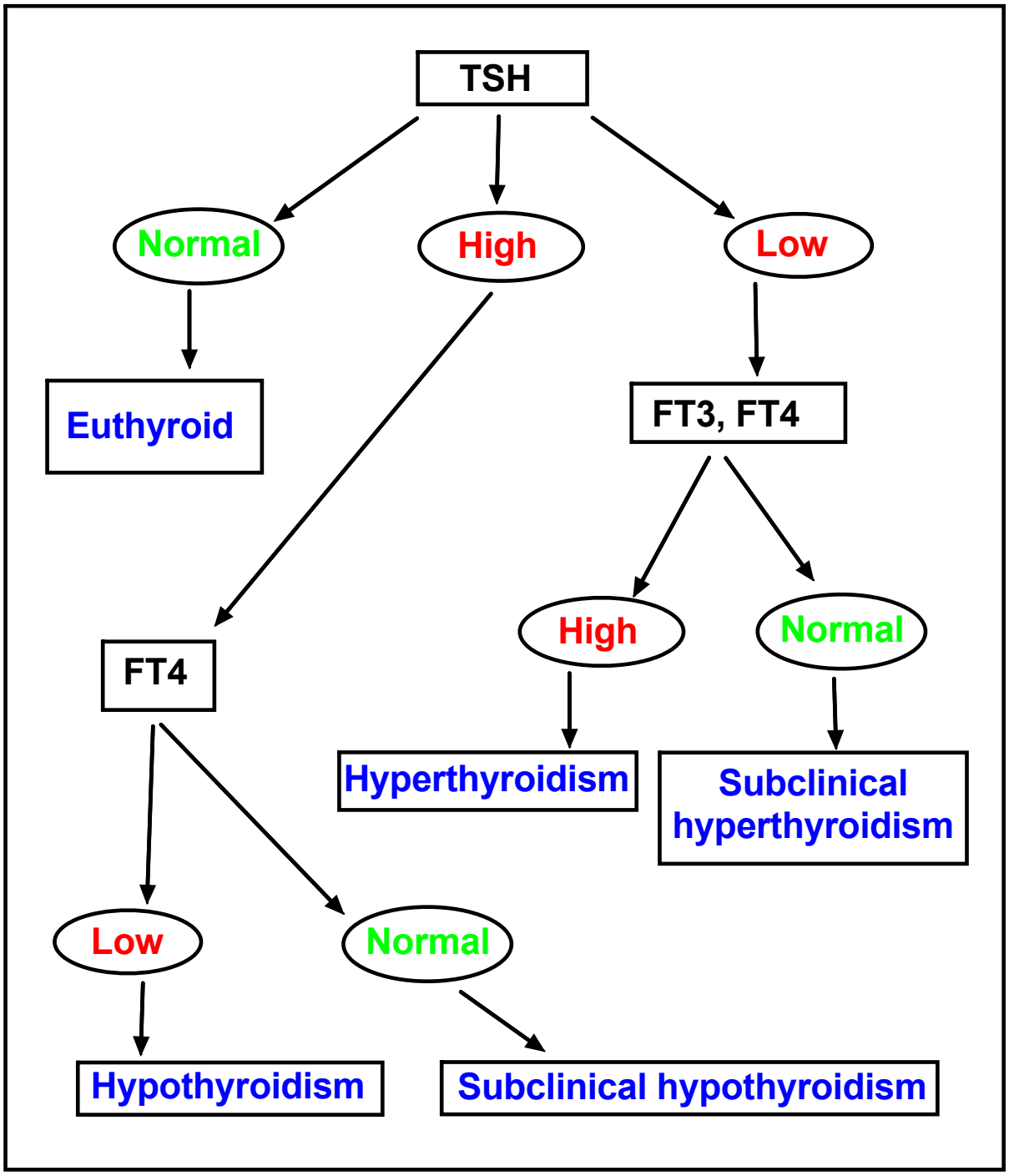

Figure 1.2: An algorithm to explain the diagnosis of thyroid dysfunction.

This is based on biochemical measurements of TSH, FT4 and FT3 levels. The biochemical tests are shown in yellow boxes and the clinical conditions are shown in blue boxes.

1.2.3.3 Thyroid Nodules and Goitre

Thyroid nodules are very common in the population. The prevalence may be as high as 50%; but only up to 5% of patients presenting with thyroid nodules have cancer

[22]. In patients presenting with thyroid nodules, the most important question is whether the nodule is benign or malignant.

Goitre is the term used to describe any single, diffuse or multinodular enlargement of thyroid. Its enlargement during puberty, pregnancy and lactation is called physiological goitre [14].

Thyroid nodule(s) or pathological goitre may be due to a variety of benign and malignant conditions. Benign thyroid neoplasms include follicular adenoma (colloid, simple, fetal, embryonal, and hurthle cell), hyperplastic nodules and rarely papillary adenoma. Rare causes include teratoma, lipoma, c-cell adenoma and dermoid cysts. Non-neoplastic thyroid abnormalities that may present as a thyroid nodule/goitre include colloid goitre, thyroiditis, thyroid cyst, hemi-agenetic thyroid, infections and granulomatous diseases (sarcoidosis). Non-thyroidal lesions that may be considered in the differential diagnoses of a thyroid nodule include lymphadenopathy, thyroglossal cyst, laryngocele, lymphatic cysts, parathyroid cysts and rarely aneurysms.

The vast majority of the above mentioned pathological conditions are independent of thyroid function (hypo- or hyperthyroidism). Occasionally, some conditions such as thyroiditis present with both thyroid dysfunction and a thyroid mass/nodule.

1.2.3.4 Thyroid cancer

Thyroid cancer can be classified according to the cell of origin:

a) Follicular cells

- Differentiated Thyroid Cancer (DTC): Papillary Thyroid Cancer (PTC), Follicular Thyroid Cancer (FTC) and Hurthle Cell Cancer (HCC)
- Undifferentiated Thyroid Cancer: Anaplastic Thyroid Cancer (ATC)

b) Parafollicular C cells: Medullary Thyroid Cancer (MTC)

c) Lymphocytes: Lymphoma

d) Secondaries.

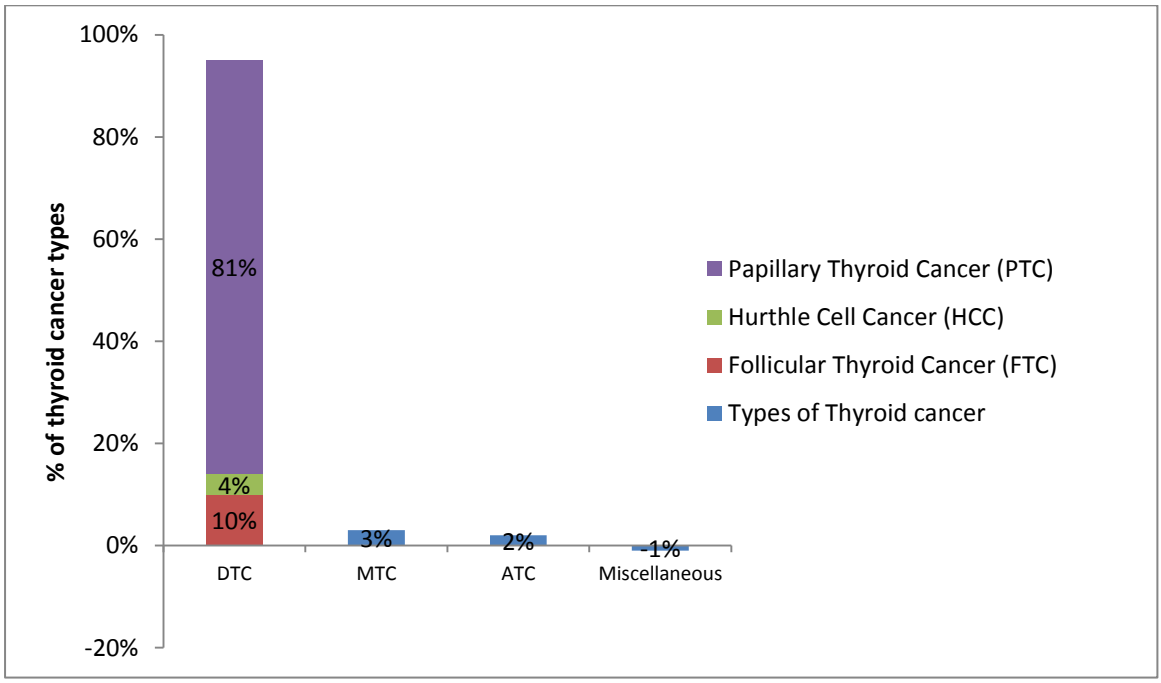

Figure 1.3: Percentage of thyroid cancer types.

(DTC = Differentiated Thyroid Cancer; MTC = Medullary Thyroid Cancer; ATC = Anaplastic Thyroid Cancer).

1.2.3.5 Epidemiology of Thyroid Cancer

As shown in figure 1.3, papillary thyroid cancer is the most common type of thyroid cancer [23, 24] and accounts for around 80% of all differentiated thyroid cancer [25]. The relative proportions of other cancer subtypes are as shown in figure 1.3.

Overall, the incidence of thyroid cancer has increased by 58% in many populations worldwide (Europe, Asia, Oceania and Americas), except in Sweden where the incidence of thyroid cancer decreased by 18% from 1973-2002 [26]. The incidence of thyroid cancer varies according to geographical distribution, age and sex. The highest incidence of thyroid cancer was reported in USA [26, 27] and Israel and the lowest incidence was reported in Uganda from 1973-2002 [26] (**Figure 1.4**).

The incidence of thyroid cancer in UK from 1976-2005 was 13.83/million, 8.88/million, 8.71/million and 8.71/million person/year in Scotland, Northern and Yorkshire, north west and Wales respectively [28].

With regards to the subtypes, the incidence of papillary thyroid cancer has increased significantly over the last thirty years [23]; follicular thyroid cancer and medullary thyroid cancer have remained stable [23]; and the incidence of anaplastic thyroid cancer has remained stable [29] or decreased [23, 27]. The reason for the increase of papillary thyroid cancer is as yet not clear but suggested reasons include over diagnosis and increased exposure to radiation.

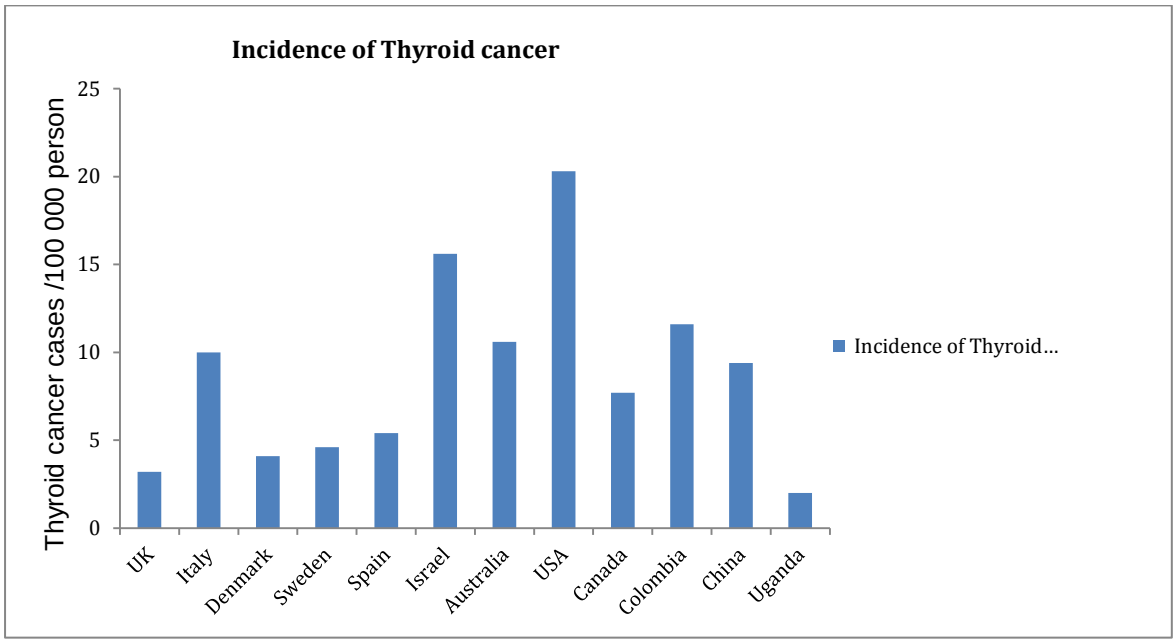

Figure 1.4: Incidence of thyroid cancer.

The figure shows the incidence of thyroid cancer per 100000 people and varied according to worldwide distribution from 1998 to 2002 in both sexes.

The prognosis of papillary and follicular thyroid cancer is very good (>80% 10 year survival) when treated appropriately; that of medullary is intermediate (75% 10 year survival) and anaplastic thyroid cancer is poor (14% 10 year survival) [30]. Anaplastic thyroid cancer accounts for 2% of all thyroid cancer but is the cause of up to 15% thyroid cancer mortality [31].

Thyroid cancer is more common in women than men [23, 32] but the mortality rates are higher in men than women [23]. The risk factors for thyroid cancer include radiation exposure and family history [33]. Radiation exposure can be in the form of external radiotherapy for treatment or exposure to a nuclear accident.

1.2.3.6 Thyroid cancer management

General principles

A patient with suspected thyroid nodule or cervical lymphadenopathy undergoes a detailed clinical assessment to enable a clinical diagnosis to be made. A clinical diagnosis of a thyroid nodule has three components:

1. Structural/anatomical – is it a solitary nodule, dominant nodule in a multinodular goitre, multinodular goitre or a diffuse goitre?
2. Physiological – is the patient clinically euthyroid, hypothyroid or hyperthyroid?
3. Pathological – is the nodule suspicious for cancer?

Investigations are done along the following lines:

1. Blood tests (T4 and TSH) – this is to confirm or exclude thyroid dysfunction. Thyroid Peroxidase (TPO) is an enzyme found in thyroid follicular cells. TPO catalyses important several steps in thyroid hormone synthesis. TPO antibody is formed in blood against TPO in patients with autoimmune thyroid disease. Thyroid peroxidase antibodies are often routinely performed in the investigation of patients with thyroid disease. A high result in a euthyroid patient could be an indication of subsequent hypothyroidism.

2. Fine Needle Aspiration Cytology (FNAC): Fine-needle aspiration is currently the most accurate test in the preoperative diagnosis of thyroid cancer [34-37]. FNAC can diagnose papillary thyroid cancer, medullary thyroid cancer and anaplastic thyroid cancer [24, 34-36]; however it cannot distinguish between follicular adenoma and follicular carcinoma. Core needle biopsies are sometimes recommended when fine-needle aspiration test is suspicious of lymphoma or metastases [34]. The accuracy of fine needle aspiration test is related to the experience of the physician or the person who is performing and evaluating the fine-needle aspiration [34]; however, molecular marker analysis, particularly in indeterminate specimens, is beginning to play a more prominent role [24].

3. Radiological imaging: Ultrasound of the neck is a good non-invasive and radiation-free imaging modality to investigate thyroid lumps; often used as

part of routine assessment in all patients presenting with thyroid nodules. It can differentiate solid from cystic lesions, identify associated lymphadenopathy in the neck and detect non-palpable nodules. Certain features on ultrasound such as vascularity, regularity of margins, presence and nature of calcifications can help differentiate benign from malignant nodules.

Computerised Tomography (CT) of neck and mediastinum can be useful to evaluate thyroid cancer metastasis and to detect laryngeal invasion [34]. It is used in patients suspected of having locally invasive cancers, lymph node metastases and in patients with retrosternal goitre to assess the extent of retrosternal extension. Magnetic Resonance Imaging (MRI) of neck is also occasionally used to assess soft tissue invasion [34].

4. Preoperative screening for phaeochromocytoma and primary hyperparathyroidism should be performed if medullary thyroid cancer is suspected [34]. This enables detection and early treatment of these associated conditions in patients with MEN II (Multiple Endocrine Neoplasia type II) syndrome; of which medullary thyroid cancer is a component.

1.2.3.6.1 Thyroid cancer staging

American Joint Committee on Cancer (AJCC) has designed a staging system using the TNM classification (**Table 1.2**).

Table 1.2: AJCC TNM staging

	DTC < 45 years	**DTC >45 years**	**ATC**	**MTC**
Stage I	Any T, any N, M0	T1, N0, M0		T1, N0, M0
Stage II	Any T, any N, M1	T2 - T3, N0, M0		T2-T4, N0, M0
Stage III		T4, N0, M0 Any T, N1,M0		Any T, N1, M0
Stage IV		Any T, any N, M1	All considered as stage IV	Any T, any N, M1

T= size and extent of the primary tumour (T1≤1cm; 1 cm<T2 ≤4 cm; T3 >4 cm; T4 direct invasion through the thyroid capsule); N = the absence (N0) or presence (N1) of regional node involvement; M= the absence (M0) or presence (M1) of metastases.

Management of specific cancer types:

1. Differentiated Thyroid Cancer (DTC)

- Surgery: The surgical options are unilateral total lobectomy, total thyroidectomy and more extensive resection. Patients with papillary thyroid cancer and follicular thyroid cancer >1 cm undergo a total thyroidectomy [34, 38]. Lymph node dissection is usually performed only when the tumour has metastasised to lymph nodes [34]. Specific surgical complications include recurrent laryngeal nerve injury and hypoparathyroidism [34].

- Radioiodine ablation (RIA): RIA is recommended in most patients following surgery for tumours >1 cm as an adjuvant to reduce risk of local and distant recurrence. Further doses of radio-iodine may be used in patients with residual or recurrent disease [24, 34]. However, an ongoing multi-centre trial in the UK aims to establish the need for RIA in low risk differentiated thyroid cancer.

- TSH suppression therapy: The main goal of thyroxine therapy is to reduce the levels of TSH (that may act as a growth factor) in thyroid cancer patients [39], but potential long term morbidity can occur and these include atrial fibrillation, anxiety, osteopenia and other manifestations of hyperthyroidism.

- External beam radiotherapy has a role in the treatment of differentiated thyroid cancer in advanced cases to provide symptomatic relief where surgery is not possible [2, 24].

- Chemotherapy: Chemotherapy is of no value as an initial therapy in differentiated thyroid cancer and is not recommended [34].

- Follow up and monitoring: Following definitive treatment with surgery, radio-iodine ablation and TSH suppression, patients are usually monitored by regular physical examinations and biochemically by measuring TSH, Tg (thyroglobulin) levels and Tg-antibody levels. An ultrasound scan of the neck is done routinely in some centres but more selectively in others, but only if

persistent or recurrent disease is suspected. Recurrent disease may be treatment by one or more of the following – re-do surgery, RIA and external beam radiotherapy – depending on the presence of symptoms, extent of disease and likelihood of achieving cure.

2. Medullary Thyroid Cancer (MTC)

- As MTC arises from the parafollicular C-cells of the thyroid and not from thyroid follicular cells, RIA and TSH suppression do not play a role. Surgery is the mainstay of treatment [40]. The extent of surgery depends on imaging findings and the presence and location of associated lymphadenopathy. Total thyroidectomy (prophylactic or therapeutic) and central lymph node dissection is the standard surgical treatment for most patients with MTC. Ultrasound findings and calcitonin levels are helpful in deciding on the need for lateral neck dissection. RET (rearranged during transfection) proto-oncogene testing should be done in all patients with MTC at some stage in the treatment process. If the patient is RET positive, all family members should be offered genetic testing and further appropriate management [34, 37, 41]. As most of the patients without a well-known family history of MTC, has a positive test of inherited RET.

3. Anaplastic Thyroid Cancer (ATC)

Anaplastic thyroid cancer carries a dismal prognosis and is considered as stage IV in the AJCC TNM staging (**Table 1.2**). The disease is aggressive and curative surgery is often unlikely. There are no effective chemo-radiotherapy regimes available [31], but often a combination of various chemotherapeutic agents (including Doxorubicin, Cisplatin and Paclitaxel) and radiotherapy are employed. Research is on-going into the role of tyrosine kinase inhibitors and vascular disrupting agents in improving response to systemic treatment [42] [43].

1.2.3.7 Molecular pathology of thyroid cancer

There are several genetic alterations involved in thyroid cancer progression and development. They have potential as biomarkers as they may help in predicting biological behaviour and may serve as therapeutic targets.

The commonly observed genetic alterations in thyroid cancer tissue include RET/PTC rearrangements, BRAF (B-type raf kinase) mutations, RAS (Rat sarcoma oncogene) mutations, PAX8/PPAR (Paired boxed gene 8/Peroxisome proliferator-activated receptor gamma) rearrangements and genetic abnormality of P53 (tumour suppressor gene) deletion, point mutation and insertion.

RET/PTC

RET is a growth factor receptor tyrosine kinase that plays an important role in kidney development and neuronal differentiation. It is located on chromosome 10q11.2. Chromosomal rearrangements involving the RET gene resulting in a fusion gene can occur by the juxtaposition of a foreign gene at the 5' end of (or proximal to) the RET gene. These are called RET/PTC rearrangements [44]. The first RET/PTC rearrangement was reported in 1987 and since then, 13 different types have been reported. RET/PTC1 and RET/PTC3 are the most common types [44, 45]. RET/PTC rearrangements have been identified in 13-46% of PTC [46-48]. The prevalence of RET/PTC rearrangements vary according to geographical distribution and are more common in radiation-induced PTC [47, 49]. The prognostic significance of RET/PTC is unclear. Some authors have suggested that RET/PTC rearrangements are associated with increased tumour aggressiveness [50] but others suggested that this is associated with slow growth and lack of progression [51, 52].

Point mutations of RET (a genetic abnormality that is different to the RET/PTC rearrangement described above) are identified in 40-50% of MTC [48].

BRAF

BRAF is an intracellular signal transducer that links extracellular signals to cellular effects. BRAF plays an important role in cell differentiation, proliferation, apoptosis and survival [53]. More than 40 BRAF mutations have been identified. BRAF V600E is the most common and accounts for up to 95% of all BRAF mutations [48]. BRAF

V600E mutations have been identified in around 45% of PTC [46-48]. BRAF mutations have been described in 25-50% and 12-17% of ATC and MTC respectively [47]. BRAF V600E mutation is associated with poor prognosis, disease recurrence and disease aggressiveness [48, 54].

RAS

RAS is also an intracellular signal transducer and plays an important role in regulating cell growth. RAS is observed in around 30% of human tumours [53]. There are three members of RAS oncogene family - Hras, Kras and Nras (located on chromosome 11p11, 12p12 and 1p13 respectively) [47-49]. Point mutations account for 40-50% of FTC tumours [46]. RAS point mutations have also been identified in ATC [55] and MTC [47]. RAS mutations are associated with poor prognosis and tumour aggressiveness in FTC, MTC and ATC [56].

PAX8-PPARγ1

Paired boxed gene 8 (PAX8) is a transcription factor and plays an important role in kidney organogenesis. Peroxisome proliferator-activated receptor gamma (PPARγ1) is a nuclear hormone receptor and is involved in the metabolism of differentiated adipocytes. PAX8-PPARγ1 rearrangements [at(2;3)(q13;p25) translocation] have been identified in around 36% of FTC [48] and are associated with favourable prognosis [57].

P53

P53 gene acts as a tumour suppressor gene. It is involved in cell cycle control and apoptosis and is altered in most human cancer cells. It is located on chromosome 17p13. Genetic abnormalities of P53 (point mutations, deletions and insertions) are identified in 67-88% of ATC [47]. P53 mutations are also described in 17-38% of MTC [47], but only in 10% of PTC [58]. P53 mutations in thyroid cancer are associated with increased tumour aggressiveness [59].

1.3 Metformin

Metformin (N', N' -dimethybiguanide) is an oral anti-diabetic drug of the biguanide class and one of the most commonly prescribed drugs worldwide [3]. It is the first drug of choice in patients with type 2 diabetes and has been licensed for use in in UK since 1958 [4-6].

1.3.1 Metformin structure

The molecular formula of Metformin is $C_4H_{11}N_5$ and molecular weight is 129.167 g/mol and the structure formula shown as below [60]. (**Figure 1.5**)

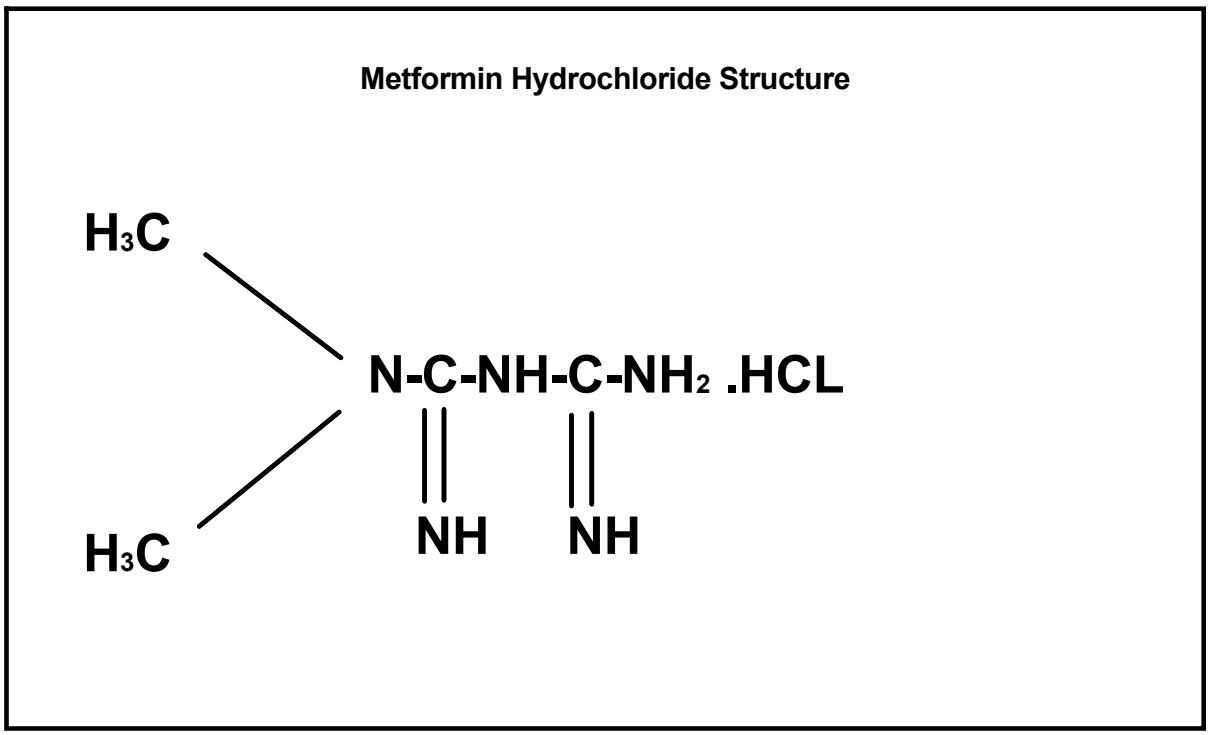

Figure 1.5: Structural formula of Metformin hydrochloride [60].

Metformin is also referred to as Dimethylbiguanidine, Dimethylguanylguanidine, glucophage and Metformin hydrochloride.

1.3.2 Metformin indications dose and side effects

Metformin has been licensed to use in type 2 diabetes mellitus and polycystic ovarian syndrome (PCOS).

- Diabetic mellitus: The initial dose of Metformin in diabetic patients (adult and child over 10 years old) is 500 mg with breakfast for at least 1 week, followed by 500 mg twice daily for a week. Subsequent increases may be up to 2 gm daily in divided doses [61].
- Polycystic ovary syndrome: The doses used for PCOS are similar to that for diabetes; but the maximum recommended dose is up to 1.7 gm daily in 2-3 divided doses [62].

The side effects of Metformin include nausea, vomiting, anorexia, diarrhoea, abdominal pain, taste disturbance, erythema, pruritus, urticaria, decreased vitamin B12 absorption and rarely lactic acidosis [63, 64].

1.3.3 Pharmacokinetics of Metformin

Metformin is administrated orally. The bioavailability of 500 mg Metformin is 40 to 60% and the absorption is complete within six hours of ingestion [65]. Metformin is not metabolized in humans [66] and this distinguishes it from other biguanides. Metformin undergoes renal excretion, largely unchanged in the urine by active tubular process, with a mean plasma elimination half-life after oral administration of approximately 6.2 hours and blood elimination half-life approximately 17.6 hours [65, 67, 68]. Approximately 90% of the absorbed Metformin is eliminated in the kidney within 24 hours and 10% of unabsorbed Metformin excreted in the faeces [68]. Metformin is distributed into body tissues via several transporters such as Organic Cation Transports 1-3 (OCTs 1-3), Plasma membrane Monoamine Transporter (PMAT) and multidrug and toxin extrusion protein 1-2 (MATE 1-2) [69]. In the intestine PMAT, OCT1 and OCT3 has been identified to facilitate in Metformin uptake; PMAT localized to the tips of the mucosal epithelial layer [70], OCT1 and OCT3 are localized to the basolateral membrane [67, 71]. In the liver, Metformin uptake is mediated by OCT1 and probably by OCT3 and both transporters are expressed on the basolateral membrane of hepatocytes [67, 72-74]. However, Metformin uptake from the circulation into renal epithelial cells is facilitated by OCT2; expressed in the basolateral membrane of the cells [72]. The renal excretion of Metformin from tubule cells to the lumen is mediated through MATE1 and MATE2 [75-78]. Both these transporters are expressed in the apical membrane of the renal proximal tubule cells [79]. OCT1 may also play an important role in Metformin reabsorption in the kidney tubules, which is expressed on the apical and sub-apical

domain side of both the proximal and the distal tubules in the kidney [80]. PMAT may play a role in the renal reabsorption of Metformin, which expressed on the apical membrane of renal epithelial cells [81].

1.3.4 Mechanism of action of Metformin

The action of Metformin within the body is initiated in the liver and peripheral tissues and includes decreasing liver glucose production by liver and increasing glucose utilization by the peripheral tissues (muscle) [4]. Unlike other anti-diabetic drugs such as Sulfonylureas, Metformin does not produce hypoglycemia in either patients with type 2 diabetes or normal subjects and also does not cause hyperinsulinemia [82]. Metformin activates Adenosine Monophosphate-activated Protein Kinase (AMPK), which is a ubiquitously expressed sensor of cellular energy status [83]. AMPK reduces hepatic gluconeogenesis and fatty acid synthesis, whilst also increasing glucose uptake and fatty acid oxidation by peripheral tissues [84]. Furthermore, Metformin down regulates mitochondrial metabolism [85, 86].

Metformin has recently been investigated for its possible anti-cancer effects in several types of cancer either directly via the AMPK pathway or indirectly via its known ‘anti-diabetic’ effects. By reducing blood glucose, Metformin results in a reduction in circulatory insulin [87]. Insulin can act as a growth factor through stimulation of Insulin and insulin-like growth factor 1 (IGF-1) receptors (**Figure 1.6**) [88-90].

Although the molecular mechanism by which Metformin acts appears to be complex and is the topic of substantial debate, there is common agreement that Metformin administration induces phosphorylation and activation of AMP-activated protein kinase (AMPK) in the liver, which may lead to diverse pharmacological effects such as inhibition of lipid and glucose synthesis [91, 92]. The route of AMPK phosphorylation by Metformin remains unclear. The molecule LKB1 (liver kinase B1) has been shown to play important role in phosphorylation of AMPK in the presence of Metformin [92]. However, LKB1 and AMPK are not the direct targets of Metformin [93]. In a study using liver specific AMPK-knockout mice, Metformin was shown to

inhibit hepatic glucose production, suggesting that Metformin inhibits hepatic gluconeogenesis by LKB1 and AMPK in an independent manner [94]. Metformin inhibits complex 1 of the mitochondrial respiratory chain, suggesting activation of AMPK by increasing cellular AMP: ATP ratio [93, 95].

Although AMPK is a major cellular regulator of glucose and lipid metabolism, up-regulation of AMPK results in inactivation of many targets including mammalian target of rapamycin (mTOR), 3-hydroxy-3-methyle-glutargl-coenzyme A reductase (HMG-CoA reductase), acetyl-CoA carboxylase (ACC), and glycerol-3-phosphate acyltranferase 1 mitochondrial (GPAM) [92, 96]. Furthermore, AMPK increases glucose uptake in skeletal muscle by increasing glucose transporter type 4 (GLUT4) translocation activity [97]. The overall effect of AMPK activation in the liver includes inhibition of cholesterol and triglyceride synthesis with stimulation of fatty acid oxidation. The peripheral effects are stimulation of glucose uptake in skeletal muscles and fatty acid oxidation and also systemic increase in insulin sensitivity [95].

The detailed mechanism of action of Metformin in cancer is not well understood; however, studies on Metformin-mediated effects on gene/pathways in many cancer types are increasing with interesting findings. In breast cancer, Metformin has been shown to induce cell cycle arrest and activate AMPK and down-regulate cyclin D1 [98, 99]. Metformin has also been shown to suppress overexpression of human epidermal growth factor receptor 2 (HER2) oncoprotein through inhibition of mTOR effector p70S6K1 in breast cancer cells [100]. Recently, a study on bladder cancer cells found that Metformin down-regulated cyclooxygenase-2 (COX2) and also signal transducer and activator of transcription 3 (STAT3) pathway, subsequently decreasing the expression of cyclin D1 and B-cell lymphoma 2 (Bcl-2) resulting in inhibition of cell proliferation and induction of apoptosis [101]. Metformin also has shown to have anti-cancer effects in ovarian cancer cells by the down-regulation of genes that associated with apoptosis regulation such as vascular endothelial growth factor (VEGF), Bcl-2, Bcl-2-associated X (Bax) and caspase-3 [102]. Furthermore, Metformin inhibited cell proliferation and induced apoptosis through the activation of AMPK and down-regulation of mTOR, protein kinase B (Akt) and P53 [103].

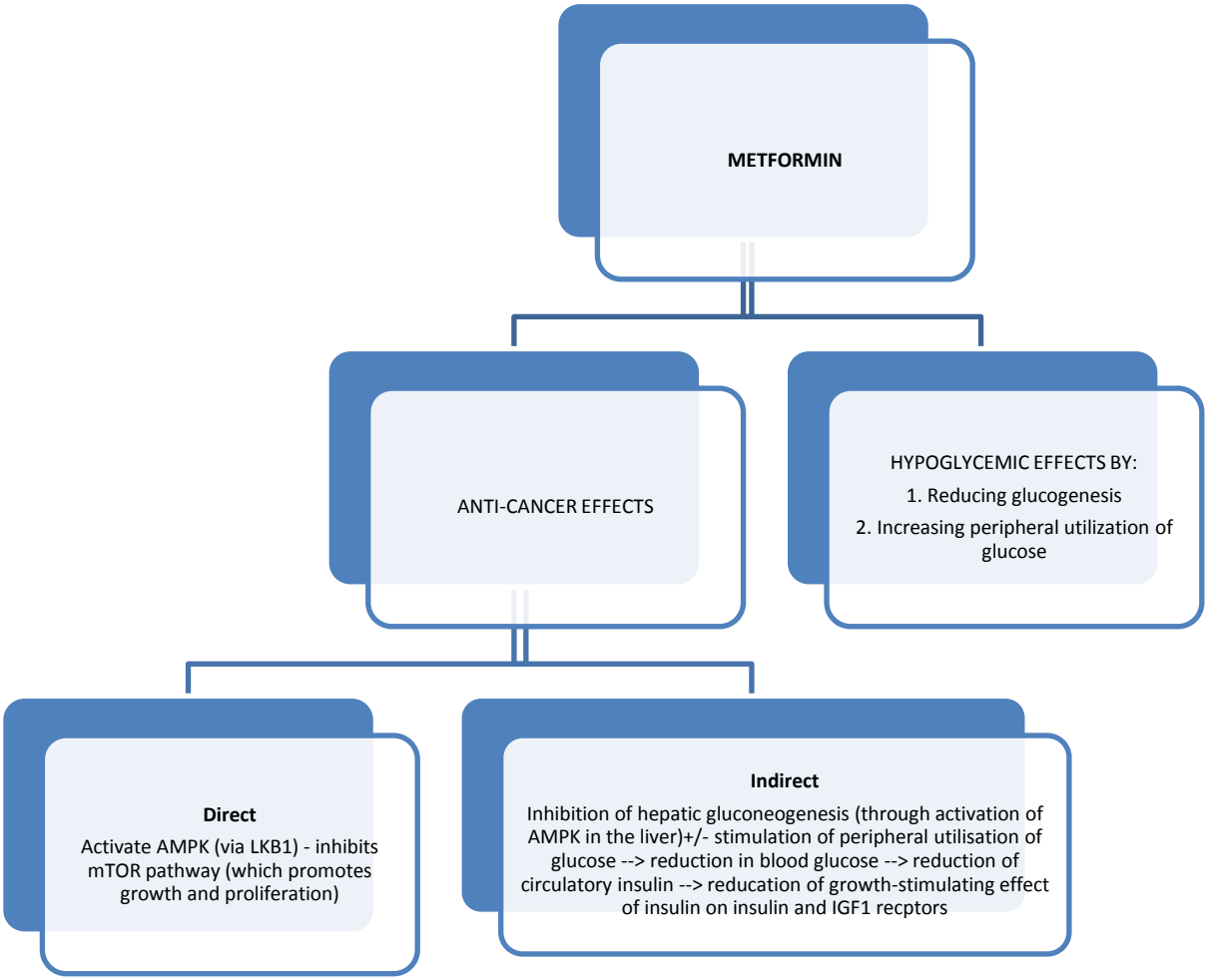

Figure 1.6: The possible modes of action of Metformin.

The molecular pathway of Metformin in thyroid cancer is not clear due to a lack of studies. In the last 5 years studies on thyroid cancer have found that Metformin altered the expression of several genes (**Figure 1.7**) [104-107]. The key findings were activation of AMPK and down-regulation of mTOR pathways resulting in inhibition of cell proliferation, colony formation, cell migration, promotion of apoptosis and induced cell cycle arrest [104-106]. Furthermore, Metformin induced AMPK activation in dose dependent manner and inhibited cyclin D1 and c-Myc expression through inhibition of mTOR pathways [105-107]. Moreover, knockdown of tuberous sclerosis complex 2 (TSC2) abolished the ability of Metformin to inhibit expression of cyclin D1, c-Myc and mTOR pathway [105]. However, loss of AMPK expression did not prevent Metformin from down-regulation mTOR pathway, cyclin D1 and S6K1 [106]. This indicated that several pathways influenced by Metformin actions in thyroid cancer. Additionally, down-regulation of the mTOR pathways dampened the phosphorylation of its downstream effectors (4E-BP1, ribosomal protein S6 kinase beta 1 (S6K1) and cyclin D1), inhibiting cell proliferation and protein synthesis [105, 106]. Furthermore, treatment with Metformin associated with decreased expression of extra cellular signal-regulated kinase (ERK) in thyroid cancer cells resulting in the inhibition of cell proliferation and induced cell cycle arrest [104, 106].

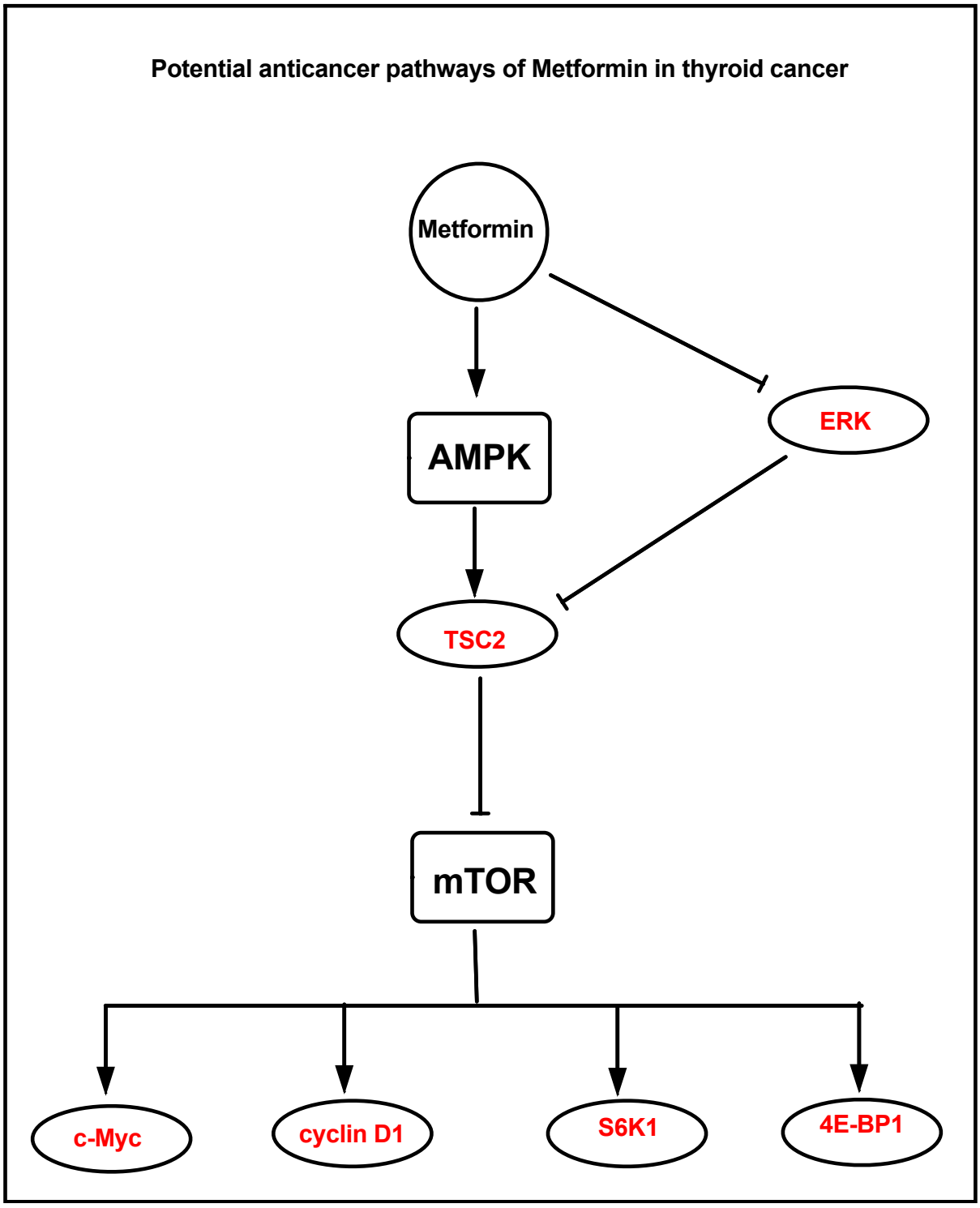

Figure 1.7: Potential anti-cancer pathways of Metformin in thyroid cancer.

This figure shows that Metformin treatment altered the expression of several genes in thyroid cancer. Genes are either down-regulated (marked with inhibition arrow symbol (⊥)) or genes are activated (marked with activation arrow symbol (↓)).

1.3.5 Possible role of Metformin in Cancer

1.3.5.1 Population based studies

Several population-based studies have demonstrated the potential role of Metformin as a chemopreventative agent [108-110] in cancers. Evan et al [108] reported the first population based study demonstrating Metformin use to be associated with low cancer incidence among type 2 diabetic patients. Several other reports have since been published to support the potential role of Metformin as an anti-cancer agent [88, 109, 111-117]. These include studies demonstrating reduced risk of breast cancer [112-114], prostate cancer [113, 118], gastric cancer [113, 119], lung cancer [112, 113, 119], pancreatic cancer [113, 119], and colorectal cancer [113]. There is also observational evidence that cancer-related mortality is reduced in patients on Metformin [111, 115, 117, 120].

In retrospective cohort study of over 62,000 people in the UK, patients were categorized into 4 groups based on the treatment of diabetes. This study shows that patients on Metformin has a reduced risk of cancer such as colorectal and pancreas. Metformin has also been seen to reduce the risk of cancer progression. This study only included patients for whom treatment for diabetes was recently started. It could be that in patients with severe diabetes (requiring insulin treatment or treatment other than Metformin) have a different predisposition to cancer and that the glucose levels influence cancer risk. In addition there is potential in this study for under reporting of cancer [109].

Another study reported by the same group [109], included patients in general practice who were diagnosed with cancer. Patients were categorized by the presence of diabetes and the nature of diabetes treatment. In over 110,000 patients this study demonstrated increased mortality of those with diabetes and also increased mortality in diabetics on sulfonylureas or insulin compared to Metformin therapy. This observation could be related to the diabetes as opposed to cancer and the severity of diabetes as opposed to treatment with non-Metformin therapies. The study did not present cause of death but only described all-causes of mortality [111].

A further study was an observational cohort study of patients with type 2 diabetes who were on Metformin treatment, compared to patients who have never used Metformin in over 9,000 patients. Metformin use was associated with reduced risk of cancer after adjusting for age, sex, BMI, HbA1c, deprivation, smoking and other drug use. It is possible that patients on Metformin had a different cancer risk profile and they may be other confounders such as ethnicity, age of onset that could have influenced the result [112]. Moreover, a study performed in the Netherlands looked at the pharmacy record and linked to hospital discharge data from 2.5 million people. The study found a lower risk of cancer in Metformin users compared to those on sulfonylureas. The study did not included diabetic patients treated with dietary or life style advice. This study also limited by 'reverse causality'. Data on cancer was only obtained from hospital discharge records and this may also have influenced the result. Other risk factors such as smoking and BMI were not adjusted for in this study [113].

Other population based studies focused on specific cancers such as breast cancer. A nested case-control study of type 2 diabetes patients in northern Denmark demonstrated that Metformin users were less likely have of breast cancer diagnosis compared to non-users [114]. This study reported 20% reduction in the risk of cancer for Metformin users and these results are consistent with several other similar studies [121, 122]. The limitation of case-control studies in general would apply to this study; in particularly, selection bias, ascertainment bias and bias due to confounding. In another study of the national Taiwanese database, from which up to half a million female patients with type 2 diabetes were followed up to evaluate breast cancer risk; patients were characterized into never-users and ever-users of Metformin. The study found that the Metformin use reduced breast cancer risk significantly. However, other confounders of cancer risk and details of cancer were not evaluated [123]. Similarly, in another retrospective cohort study of patients with ovarian cancer, patients with type 2 diabetes who used Metformin had a longer progression-free survival. Again, this study is limited by small sample size in the various subgroups categorized by diabetic status and Metformin use and the data on the severity of diabetes was not evaluated [115]. Additionally, a study of 1448 patients who received chemotherapy for triple negative breast cancer, 9% were

diabetic; of these, 48% were on Metformin during chemotherapy. The results of this study demonstrated that Metformin use does not significantly impact on survival, but Metformin users and non-diabetic patients were less likely to have distant diseases. As suggested before, this study has the usual limitations of a retrospective cohort design [116]. Finally, in a study of non-small cell lung cancer patients with pre-existing diabetes, the role of Metformin on response to chemotherapy was studied. The data appeared to show that Metformin improved the response rate and survival. This study is limited by a small sample size and the analysis did not appeared to be adjusted for a number of other patient and disease related influences [117].

More specifically in relation to thyroid cancer, Chin et al. studied the risk of thyroid cancer in patients with type 2 diabetes in Taiwan. Of more than 1.5 million patients included over the three year period, Metformin use in patients with diabetes was associated with a reduced risk of thyroid cancer diagnosis. However, this study has a short follow up period. The details on the type of thyroid cancer and the possibility of cofounding factors such as the severity of diabetes, exposure to ionizing radiation, and reliability of the recorded diagnosis within the databases influencing the results should be considered [124]

1.3.5.2 *In vitro* studies on cancers other than thyroid cancer.

Metformin has also been studied extensively *in vitro* using a number of human cancer cell lines. The cancers studied include breast cancer [125, 126], gastric cancer [127], lung cancer [126], ovarian cancer [128] and thyroid cancer [106, 129].

In a study of ovarian cancer cell lines (OVCAR-3 OVCAR-4); cells were treated with various concentrations of Metformin (1, 5, 10, 15, 20, 50 and 100 mM) at several time points (24, 48,72 and 96 hours). The study showed that Metformin inhibited cell growth of both cell lines in a time-dependant and concentration-dependent manner. The study also shows up-regulation of phosphorylation of AMPK pathway and down-regulation of p70S6K and S6K. The strengths of this study was that cells were exposed for long duration of time and various concentrations of Metformin were used. However, the concentration of Metformin used was supra-physiological [128]. In a study of breast cancer cell lines (MCF-7, MCF-7/713, BT-474 and SKBR-3);

cells were treated with various concentrations of Metformin (2,10 and 50 mM) for 72 hours. Metformin decreased cell proliferation in concentration-dependent manner and reduced expression and activation of erbB2 protein. In addition, reduction in phosphorylation (but not expression) of Mitogen Activated Protein Kinase (MAPK) and Protein Kinase A (Akt) was observed. Metformin reduced levels of both mTOR and P-mTOR. The study limitations were that the concentration of Metformin used was high and cells were studied at one time point only [125]. In another study on breast cancer cell lines (BT474, SKBR3, BT474-HR20, SKBR3-pool2); cells were treated with Metformin concentrations (0.02, 0.1, 1, 5 and 10 mM) for 72 hours. Metformin inhibited cell proliferation in concentration–dependent manner and reduced expression and activation of erbB2/ Insulin-like growth factor-1 receptor (IGF-1R) complexes. These effects were observed in resistant sub-lines only but not in the parental cells. The strength of this study was various concentration of Metformin were used but cells were studied at one time point only [130]. Additionally, in a further study, breast cancer and lung cancer cell lines (MCF-7 and A549 respectively) were treated with Metformin concentrations (1, 5, 10, 25 and 50 mM) for two different durations - 48 and 72 hours. Metformin inhibited cell proliferation of both cell lines. Inhibition was significant at the concentration of 10 mM. Metformin also increased phosphorylation of AMPK but phosphorylation of mTOR, 4EBP1 and P70S6K was reduced [126]. In another study on breast cancer cell lines (MDA-MB-231, MCF-7 and MCF-10A); cells were treated with Metformin (50 and 75 mM) for 12 hours. Metformin inhibited cell proliferation and cell migration and decreased phosphorylation of mTOR and P70-S6K [131]. The last three studies [126, 127, 131] were limited by the fact that only high concentrations of Metformin were used. Finally, in a study on gastric cancer cell lines (MKN1, MKN45, and MKN74); cells were treated with various concentrations of Metformin (1,5 and 10 mM) for several time points (24, 48 and 72 hours). Metformin inhibited cell proliferation, blocked cell cycle in G0-G1 phase and this was associated with a significant reduction of G1 cyclins especially cyclin D1, cyclin-dependent (Cdk) 4 and Cdk6. The phosphorylation of retinoblastoma protein (Rb) and the expression of epidermal growth factor receptor (EGFR) and IGF-1R was reduced [127].

Until recently, there have been few studies of Metformin in thyroid cancer [129]. In a study on Metformin in human anaplastic thyroid cancer cell lines (HTh74, SW1736,

C643), human follicular thyroid cancer cell line FTC 133, doxorubicin-resistant thyroid cancer cell line HTh74Rdox, and a rat thyroid normal epithelial cell line (FRTL-5) [129]; cells were treated with various concentrations of Metformin (0.1, 0.5, 1, 2.5, 5,10, 20 and 40 mmol/L) for different periods of time (24, 48, and 72 hours). The findings of this study showed that Metformin decreased growth of these cell lines in a concentration-dependent and time-dependent manner. The anti-proliferative effect of Metformin was more obvious in HTh74Rdox compared to HTh74. FTC 133 was more sensitive to Metformin compared to other wild types of thyroid cancer cell lines. Further experiments on the same cell lines showed that Metformin induced cell cycle arrest in G_1 phase. In a separate experiment in the same study, insulin significantly enhanced the growth of all human thyroid cancer cell lines described above. When Metformin was added, the insulin-induced increase in cell proliferation was negated. This group have also shown that Metformin enhances the anti-proliferative effect of Doxorubicin and Cisplatin. Moreover, Metformin increased phosphorylation of AMPK at Thr-172 in all human thyroid cancer cell lines. It was noted however that the concentrations of Metformin used are higher than normal human plasma concentrations. It would have been of value to have observed the effects of lower concentrations of Metformin at longer periods of time.

Another study on Metformin in human MTC cell lines (TT and MZ-CRC-1) [106], cells were exposed to various concentrations of Metformin (0.5, 1, 2.5, 5 mmol/L) for different periods of time (24, 48, 72 hours). This study showed that Metformin inhibited cell growth in both cell lines (TT and MZ-CRC-1) in time-dependent and dose-dependent manner and reduced expression of cyclin D1 in dose-dependent manner. Metformin decreased phosphorylation of ERK, p70S6K and pS6 in TT and MZ-CRC-1 cell lines but increased phosphorylation of AMPK in TT cell lines only. In this study, various concentrations of Metformin have been used for three different periods of time, but again the concentration of Metformin is too high compared to normal human plasma concentration.

The findings of the above *in vitro* studies indicate that Metformin inhibits cell growth in a time-dependent and concentration-dependent manner. The concentrations of Metformin used were much higher than normal human plasma concentrations [132]**.**

This therefore limits the extrapolation of these findings to clinical practice. Also, it is not clear from these studies whether the cells were seeded in different concentrations to evaluate the effects of Metformin on factors such as confluence.

1.3.5.3 *In vivo* studies

The possible anti-cancer effect of Metformin has been studied in animal models alongside of population-based study and *in vitro* studies. In a mouse model experimental study, each mouse was inoculated in the flank by human cholangiocarcinoma cells (HuCCT-1). The animals were then divided into two groups (Metformin treated and PBS treated control). The injection was given intraperitoneally (2 mg/kg of Metformin or PBS) five times per week for 4 weeks. The study found that Metformin inhibited tumour growth by 36% compared to control group [133]. In another study of a xenograft model, human pancreatic adenocarcinoma cells (CFAC-1) were subcutaneously injected into the anterior armpit of nude mice. 20 injected mice were subdivided into 4 groups (treated with normal saline, Metformin treated 200 mg/kg/day, Gemcitabine treated and combination therapy of Gemcitabine and Metformin). The study findings show that Metformin and combination therapy were associated with smaller size and weight of xenografts compared to control group [134].

In a more recent study, oesophageal squamous cell carcinoma cells (KYSE450) were injected into mice subcutaneously. After 10 days, 10 mice with the same size of xenograft tumours were selected and divided into two groups. One group was treated with Metformin (35.7 mg/kg/day by intraperitoneal injection) and the other group received normal saline for 15 days. The tumour size was reduced by 70% in the Metformin treated group compared to the control group along with an increase in the area of necrosis and apoptotic rate. Furthermore, Metformin inhibited the expression of S6K1 and 4EBP1 [135]. The anti-tumour effect of Metformin on pancreatic cancer cell growth was also studied in an experimental xenograft model. Mice were divided into two groups (Gemcitabine treated only, Gemcitabine + oral Metformin (20 mg/kg/day diluted in the drinking water) from the time of injection of

pancreatic cancer cells in the flank for 4 weeks. The data show that Metformin treatment inhibited xenograft tumour size [136].

More specifically, the anti-tumour effect of Metformin on papillary thyroid cancer cells was also studied in an experimental xenograft model, BHP10-3SC cells were injected subcutaneously into dorsal skin of mice at 4 different places. Mice were treated with Metformin 0-100 mg/mL in drinking water for four weeks. The study found that Metformin significantly inhibited tumour growth at day 10 for the dose 50 mg/mL and marginally significant at day 30 for the dose 10 mg/mL. Metformin (at a dose of 50 mg/mL) significantly increased the necrotic area, increased AMPK phosphorylation and down regulated mTOR and Akt expression compared to control group [137]. In another xenograft experimental model, mice were implanted with SW579 thyroid cancer cells and then divided into two groups (Metformin treated 100 mg/kg/day orally and vehicle alone control). After tumour size was measured from days 0-45, the study found that Metformin inhibited tumour size in a time-dependent manner [105].

1.3.5.4 Clinical trials of Metformin in chemoprevention and therapy of human cancer

Recently, few clinical trials have been done to investigate the anti-tumour effect of Metformin in patients with breast cancer [138-140]. In a randomised controlled clinical trial, 47 non-diabetic women with operable primary invasive breast cancer were randomised pre-operatively to receiving Metformin (500 mg/day for a week and then 1 g/day until surgery) or no drug. Core biopsies from the breast tumour before randomisation and two weeks later at surgery were done. Ki67 immunohistochemistry, transcriptome analysis on formalin-fixed paraffin-embedded cores and serum insulin levels were performed blinded to treatment. This was considered to be a “window of opportunity” trial, whereby the anti-cancer effects of drugs can be studied in patients who are exposed to the drugs in the period between having a diagnostic tissue biopsy and surgical resection. This study found significant reduction in Ki67 expression in the Metformin group with no change in the control arm; providing evidence for anti-proliferative effects of Metformin [138]. Mean serum insulin levels remained stable in patients receiving Metformin but rose in control patients. One limitation of this study was that the participants were treated with Metformin only for a short period of time; limiting the opportunity to study the effects of Metformin in the longer term. Some would argue that the sample size of this study was relatively small; however the study was not powered to detect differences in clinical outcomes.

In another randomised pre-surgical trial, 200 non-diabetic women with operable breast cancer were divided into two groups of 100 patients – one group received 850mg Metformin twice a day and the other received a placebo for four weeks. There were no significant changes on Ki67 expression in Metformin group compared to the placebo group [139]. The sample size in this study was higher compared to the previous study [138]. Despite no overall differences in the Ki67 expression between the groups, the effects of Metformin seemed to be different when patients were subdivided in accordance with insulin resistance. As the study showed that Metformin decreased cell proliferation in patients with insulin resistance and increased

cell proliferation in patients without insulin resistance.

In a ‘single arm’ clinical trial on 39 non-diabetic women with early stage of breast cancer, Metformin showed anti-proliferative effects and increased apoptosis as reflected by Ki67 and TUNEL assay respectively [140]. The weaknesses of this study are small sample size, absence of control arm and short duration of Metformin treatment. Finally, a double-blind randomised controlled trial study is currently underway to determine the effects of Metformin in the prevention of colorectal polyps [141]. This is based on previous observations that Metformin suppresses polyp formation in a murine model of FAP [142]. Metformin has also been demonstrated to suppress colorectal aberrant crypt foci (ACF) in humans [143]. ACF is thought to be a risk factor for colorectal cancer [144].

From the above studies, it is apparent that Metformin is being increasingly investigated as chemo-preventative as well as adjuvant therapeutic agent in human cancer.

1.3.6 Metformin and its effect on TSH

Another effect of Metformin on thyroid disease is a decrease in Thyroid Stimulating Hormone (TSH) level without change in FT4. The TSH lowering effect of Metformin was reported in a retrospective case study of 4 hypothyroid patients (three patients with type 2 diabetes and one patient with steatohepatitis) [145]. The level of TSH increased again in all patients after Metformin was discontinued. The sample size of this study was too small but the findings can serve as a basis to investigate further the role of Metformin on TSH synthesis and release.

In a pilot study, 11 patients with type 2 diabetes and hypothyroidism on stable thyroxine doses, were treated with Metformin for 6 months [146]. A significantly decreased TSH level was observed after 6 months of treatment. In a second study performed by the same group [146], 29 patients with hypothyroidism on thyroxine (group 1), 18 patients with subclinical

hypothyroidism (group 2) and 54 euthyroid patients (group 3) were treated with Metformin for 1 year. Metformin decreased the TSH level in group 1 and group 2 but not in group 3; without changes in FT4. The sample size of the study was relatively small and there was no information regarding the dose of Metformin used in this study.

The mechanism of TSH lowering effect in patients who received Metformin is not clear and requires further research. In the studies reported so far, the effect of Metformin on TSH level appeared independent of thyroxine treatment [145, 146]. However, Metformin treatment was not associated with major changes in TSH level in patients with an intact thyroid axis [146]. In a single blind randomized clinical trial [147] of 50 non-diabetic patients with DTC (46 patients with papillary thyroid cancer and 4 patients with follicular thyroid cancer); the dose of Metformin was 500 mg/day for 3 months. Thyroid hormones and TSH were measured in the beginning and after 3 months of Metformin treatment. The data indicated that 500 mg/day did not decrease the level of TSH. The study has limitations of small sample size and short administration of Metformin and low dose of Metformin (Metformin dose in diabetic patients 500-2500 mg/day) In another study [148], 66 women with small benign thyroid nodules and insulin resistance were divided in to 4 groups (Group 1 received Metformin alone, group 2 received Metformin + levothyroxine, group 3 received levothyroxine alone and group 4 did not receive either drug) and followed up for 6 months. Patients treated with Metformin showed a decrease in nodule size in association with reduced TSH levels; but this effect was best seen in combination with levothyroxine treatment. In a recent study on patients diagnosed with differentiated thyroid cancer (patients on thyroxine treatment), Metformin treatment was associated with smaller tumour size and low TSH level. These findings were based on clinico-pathological data of 34 diabetic patients treated with Metformin compared to 21 diabetic and 185 non-diabetic patients not treated with Metformin [149].

1.4 Need for this research and implications for patients

In patients with DTC, the prognosis is in general good to excellent. TSH suppression using high doses of thyroxine is an objective of treatment. However, this is associated with side effects [150]. Metformin has a good long term safety profile and may serve a dual role – anti-cancer effect and reduced need for overtreatment with thyroxine – this has potential to significantly reduce treatment-related morbidity in thyroid cancer. The prognosis in certain types of thyroid cancer (such as MTC, and ATC) is poor. New adjuvant treatment options are invaluable for these types of thyroid cancer. Given recent information on the role of Metformin as an anti-cancer agent, there is potential for Metformin to be used as adjuvant treatment in these cancer subtypes.

To facilitate the development of Metformin as a potential clinically useful anti-cancer drug, a detailed understanding of the molecular mechanisms of its effects on thyroid cancer is essential. In addition, its effects on thyroid cancer cell lines at concentrations relevant in the clinical setting, its interactions with TSH and the influence of glucose in the environment needs to be studied. This will be the focus of this research project.

Hypothesis: Metformin inhibits the growth and proliferation of different types of thyroid cancer.

Aims: The aims of this project are to

- Explore the role of Metformin in thyroid cancer cell growth and proliferation
- Compare the effect of Metformin on thyroid cancer cell lines in different environments
  - Glucose-free and glucose-rich media

  - With and without influence of insulin, IGF-1 and TSH
- Investigate the role of Organic Cation Transporter 1 (OCT1) in thyroid cells on the anti-proliferative effect of Metformin on thyroid cancer cells.
- Study the effects of Metformin on gene regulation in thyroid cancer cell lines

CHAPTER TWO

Materials & Methods

2.1 Materials

2.1.1 Basic laboratory equipment

In this section the basic materials used in the research are summarized in the following two tables below (**Table 2.1**).

Table 2.1: Basic laboratory equipment.

Item	Supplier
Hoods (class II microbiological sterile safety cabinet)	UniMAT – BS, medical air technology, Oldham, UK
CO_2 Incubator	Sanyo electric, Japan
Centrifuge	Sanyo harrier 18/80, UK
Micro centrifuge	MSE, UK
Cell viability analyser	Vi-CELL™ XR, Beckman coulter, USA
Light microscope	Olympus optical, Japan
Fluorescent microscope	Zeiss axioscop
Nikon glipse TS100 microscope	Nikon, Japan
Cesium137 irradiator	CIS Bio International
R100/TW rotates shaker	Luckham, UK
Autovortex mixer SA2	Stuart scientific, UK
Dry heating block	Techne
Pipettes (P2, P10, P20, P200 & P1000), pipetting aid	Gilson, France
Pipette tips, sterile eppendrof 1.5 ml tubes, cryogenic vials 1.8 vial	Star lab
Disposable serological 5ml pipettes	Fisherbrand
Disposable serological 10 ml and 25 ml pipettes, Sterile 6 well and 96 well plates	Costar
Specimen tubes (15ml, 20ml, 50ml), cryopure 1.8 ml tubes	Sarstedt
Fluostar Galaxy (Plate reader)	BMG labtech, Germany
NanoDrop™ ND-1000 spectrophotometer	Thermo fisher scientific, Wilmington, USA
PCR	Sensoquest, Germany
TC20™ Automated Cell Counter	BIO RAD, Singapore

Item	Supplier
T25, T75 cm^2 culture flasks, Sterile petri dish 10 cm	Nunc™
2 well silicone insert chambers	Ibidi
Coverslips (22x22/40/50 mm)	Scientific laboratory supplies
Microscope slides	VWR
Aluminium foil	Robinson young, UK
Exam gloves	Micro flex
Distilled water	Gibco
Industrial Methylated Spirit (I.M.S) BP 70% V/V	Adams healthcare, UK
Methanol, absolute ethanol and Acetone	BDH Analar
Effective disinfectant tablets	Presept™

2.1.2 Other materials

In this section the other materials (reagents and antibodies) used in the experiments are summarized (**Table 2.2**).

Table 2.2: Other materials used in the experiments described.

Item	Supplier
Foetal Bovine Serum (FBS) was stored at -20°C in 50 ml aliquots.	Lonza. BioWhittaker
Dulbecco's Phosphate Buffered Saline (DPBS)	
Trypsin/EDTA, Fungizone, Glutamine, Penicillin/streptomycin.	
Dulbecco's Modified Eagle's Medium (DMEM) with 4.5 g/L Glucose, L-glutamine and without Na Pyruvate. The medium was stored at -4°C.	
Dulbecco's Modified Eagle's Medium Ham's F-12 (1.1 MIX) (DMEM F12) with 15 Mm Hepes, L-Glutamine. The medium was stored at -4°C.	
Roswell Park Memorial Institute (RPMI) 1640 medium. The medium was stored at -4°C.	

Item	Supplier
Minimum Essential Medium Eagle (EMEM), Non-Essential Amino Acids (NEAA) solution 100x, Sodium Pyruvate (NaP), Molecular, Cellular and Developmental Biology 105 (MCDB 105) medium, Dimethyl Sulfoxide (DMSO) and Triton X-100 (Sigma-Aldrich, UK).	Sigma-Aldrich
Primary antibody anti-SLC22A1 (OCT1) and secondary antibody (goat anti-rabbit, biotinylated).	
D-(+)-Glucose solution (45%), human TSH (T8785), human Insulin (I2643-50MG).	
Agarose powder, Ethidium bromide, Thiazolyl blue tetra zolium bromide, >= 97.5% TLC, 1g stored at 4°C and Triton-X-100.	Sigma
FITC Annexin V Apoptosis Detection Kit I (Cat. 556547): The kit contents were; FITC Annexin V, Propidium Iodide (PI), 10X Annexin V Binding Buffer	BD Biosciences
DNeasy blood and tissue kit: The kit contents were; Proteinase K, buffer AL, buffer AW, buffer AW2, buffer AE, 2 ml collection tubes and DNeasy mini spin columns	QIAGEN, Germany
RNeasy Mini Kit (50) Rneasy mini kit (50): 50 RNeasy Mini Spin Columns, Collection Tubes (1.5 ml and 2 ml), RNase-free Reagents and buffers	
Trypan Blue Dye 0.4% solution (Cat. 145-0013), counting slides, dual chamber for cell counter (Cat. 145-0011)	BIORAD, USA
Mounting medium with 4',6-DiAmidino-2-Phenylindol (DAPI), normal goat serum and VECTASTAIN ABC kit	Vector laboratories Inc.
Metformin (1,1-Dimethylbiguanide. Hydrochloride, 5g stored at 4°C.	Enzo
Propidium iodide 1 mg/ml (ab14083)	Abcam
Methylene blue 70% alcohol (I.M.S)	BDH, England
Human IGF-1 (Cat. AF-100-11)	Peprotech
BRAF forward and BRAF reverse	Eurofins genomics

Item	Supplier
Immolase DNA polymerase kit	BIOLINE
Paraformaldehyde (PFA)	Fisher scientific, UK
Primary antibody (Phospho-Histone H2A.X (Ser139) (20E3) rabbit mAb)	Cell signalling technology
Secondary antibody (Cy3 goat anti-rabbit IgG)	Invitrogen™ USA

2.1.3 Cell lines and medium

The cell lines used in the projects included:

1. **Nthy-ori 3-1** (human thyroid follicular epithelium immortalised by transfection with a plasmid containing an origin-defective SV40 genome (SV-ori))
2. **K1E7** (a subclone of K1 cell line from primary papillary thyroid cancer)
3. **FTC-133** (derived from primary follicular thyroid cancer)
4. **RO82-W-1** (derived from metastases of follicular thyroid cancer)
5. **8305C** (derived from primary anaplastic thyroid cancer)
6. **TT** (derived from primary medullary thyroid cancer)
7. **MCF7** (established from pleural effusion in patient with metastatic breast adenocarcinoma)
8. **h-TERT-RPE-1** (retinal pigmented epithelial cells immortalized with hTERT)

Nthy-ori 3-1, FTC-133, K1E7, MCF7 and h-TERT RPE-1 were obtained from department of Oncology, University of Sheffield. RO82-W-1, 8305C and TT were authenticated and purchased from the European Collection of Cell Culture (ECACC).

These cell lines were sub-cultured in specific media. The media used for the different cell lines were as follows:

1. Nthy-ori 3-1 - DMEM supplemented with 10% FBS, 1% fungizone and 1% penicillin/streptomycin.
2. K1E7 and FTC-133 - DMEM F-12 supplemented with 10% FBS, 1% fungizone and 1% penicillin/streptomycin and 1% glutamine.

3. RO82-W-1 – DMEM:Ham's F12:MCDB 105 (2:1:1) supplemented with 10% FBS, 1% fungizone and 1% penicillin/streptomycin and 1% glutamine.
4. 8305C – EMEM (HBSS) supplemented with 10% FBS, 1% fungizone and 1% penicillin/streptomycin, 1% Non-Essential Amino Acids and 1% glutamine.
5. TT – Ham's F12 supplemented with 10% FBS, 1% fungizone and 1% penicillin/streptomycin, 1% Non-Essential Amino Acids, 1% Sodium Pyruvate (NaP) and 1% glutamine.
6. MCF7 and h-TERT-RPEI – RPMI supplemented with 10% FBS, 1% fungizone, 1% penicillin/streptomycin and 1% glutamine.

DMEM with 2 gm/L (10 mM) of glucose was chosen for all experiments as standardized medium (see section 3.2.2).

Morphology of thyroid cells: The morphology of K1E7, FTC-133, RO82-W-1 and TT cell lines are similar to normal thyroid cell line (Nthy-ori 3-1). These are all differentiated cells and resemble normal thyroid follicular epithelium. The shapes are variable and ranged from spindle to polygonal. The 8305C cell line is much more undifferentiated; the nucleo-cytoplasmic ratio is high and there is significant variability in the shape of these cells.

2.2 Methods

2.2.1 Cell culture

2.2.1.1 General cell culture

All tissue culture procedures were carried out in a class II microbiological safety sterile cabinet (UniMAT – BS, Medical Air Technology Ltd., UK). Before commencing work, the cabinet was switched on and sterilized with 70% Industrial Methylated Spirit I.M.S (Adams healthcare, UK) and left for 15 minutes. All necessary reagents and equipment were cleaned and sterilized with 70% I.M.S during work.

2.2.1.2 Defrosting and recovery of cells from liquid nitrogen

Cells were taken from liquid Nitrogen storage and quickly defrosted in a water bath at 37°C. Cells were then transferred to a universal tube and 9 ml of medium was added. The pellet was obtained by centrifuging the universal tube at 1000 rpm for 5 minutes. The pellet was cultured in T75 flasks and incubated at 37 °C in a humidified atmosphere of 95% and 5% CO_2 for approximately 3-5 days. The medium was renewed twice a week (until the cells were 70-80% confluent).

2.2.1.3 Subculture/cell split

Cells were observed under the light microscope (Olympus optical, Japan) until they were 70-80% confluent. They were then washed twice with 5 ml of PBS and incubated with 5 ml of trypsin for 2 minutes. The detached cells were observed under the light microscope and the process of trypsinization was halted by adding 5 ml of medium. Cells were collected in a sterile universal tube and centrifuged at 1000 rpm for 5 minutes (at 21 °C). The supernatant was discarded and the cells were re-suspended as pellet in 10 ml of medium. The re-suspended cells were cultured in T75 flasks at 37°C in a humidified atmosphere of 95% and 5% CO_2.

2.2.1.4 Frozen storage of the cells

The cells were frozen between experiments to maintain cell integrity. After the cells were 70-80% confluent, they were washed twice with PBS and then 5 ml of trypsin added for 2 minutes. 5 ml of medium was added to stop the action of trypsin and centrifuged at 1000 rpm for 5 minutes (21°C). The pellet was re-suspended in 1 ml of freezing solution (10% DMSO and 90% foetal bovine serum) and transferred to 1.8 ml cryogenic vial. The cells were labelled and placed in ultra-low temperature freezers at -80°C (Sanyo, Japan) for 24 hours before being stored in liquid nitrogen for long periods of time.

2.2.1.5 Authentication of cell lines

There are several methods to identify and authenticate cell lines such as Short Tandem Repeat (STR), karyotyping, Human Leukocyte Antigen (HLA) typing and isoenzyme analysis. Karyotyping analysis is used to investigate the number and structure of the chromosomes. It is able to detect numerical chromosomal abnormalities, genomic instability and chromosomal rearrangements including deletions, translocations, duplications and inversions. Isoenzyme analysis is a simple, rapid method that is able to define a range of intracellular enzymes from species to species [151]. Both isoenzyme analysis and karyotyping are able to confirm species of origin and detect cross-contamination of cell lines in the early stages [152]. HLA typing is another method to authenticate cell lines and is able to detect variation in human leukocyte antigen genes. Short Tandem Repeat (STR) profiling is now commonly used to authenticate cell lines and it is now an internationally approved and recommended method [153, 154]. Short tandem repeats are repeat sequences of 2-7 base pair nucleotides found in the particular regions (loci) of the genome [155] . These can be amplified by Polymerase Chain Reaction (PCR) and detected. A number of STRs specific to an individual or cell line is referred to as their 'STR profile'. The principle of STR profiling is to be able to determine the genetic identity by determining the STR at various loci of an individual cell line. The numbers of loci at which the STRs are identified and detected vary, but typically include the following: THO1, D21S11, D5S818, D13S317, D7S820, D16S539, CSFIPO, AMEL, vWA and TPOX. STR profiling has many advantages over the other methods such as reliability, accuracy, sensitivity [156, 157], rapidity and cost [155, 157]; however the disadvantage of STR is that it does not provide information on the origin of tissue [156]. In this study Short Tandem Repeat (STR) profiling has been used to authenticate three human thyroid cell lines (FTC-133, K1E7 and Nthy-ori 3-1) that were being maintained in house. This was to ensure that the results of our study of these cell lines would be reliable. The other cell lines with a known STR profile; RO82-W-1, 8305C and TT were purchased from the European Collection of Cell Culture (ECACC) and were not subject to STR profiling.

2.2.1.5.1 DNA extraction for STR profiling

The cell lines Nthy-ori 3-1, K1E7 and FTC were sub-cultured in T75 flask and cell confluence were checked frequently under the microscope. Cells were centrifuged again at 1000 rpm for 5 minutes and re-suspended in 200 µl of PBS. 20 µl of 'proteinase K' and 200µl of 'Buffer AL' were added, mixed by vortexing and incubated at 56°C for 10 minutes. 200 µl of 100% ethanol was added. This was left for 1 minute before being mixed by vortexing and transferred to a mini spin column placed in 2 ml collection tube. This was spun at 8000 rpm for 1 minute and the 2ml collection tube was discarded. A mini spin column was placed in a new 2 ml collection tube before adding 500 µl of 'Buffer AW1'. This was centrifuged at 8000 rpm for 1 minute. The 2 ml collection tube was then discarded. The mini spin column placed in a new 2 ml collection tube. 500 µl of 'Buffer AW2' was added and then centrifuged at 14000 rpm for 3 minutes before transferring the filter with the DNA to a 1.5 ml or 2 ml microcentrifuge tube. 200 µl of 'Buffer AE' was added and incubated at room temperature for 1 minute. The solution was centrifuged for 1 minute at 8000 rpm. The pellet containing the extracted DNA was sent to core genomic facility, University of Sheffield for STR profiling. The concentrations of DNA extracted from the Nthy-ori 3-1, K1E7 and FTC-133 cell lines and estimated using NanoDropTM ND-1000 Spectrophotometer method was 157.35 ng/µl, 84.37 ng/µl and 79.23 ng/µl respectively and considered as a good concentration.

2.2.1.5.2 STR profiling

STR profiling was done by the picogreen method. This is briefly described. The picogreen reagent was warmed up at room temperature before use. TE buffer solution (its components 10 mM Tris-HCL and 0.1 mM Ethylenediaminetetraacetic acid (EDTA) 8.0 PH) was used to dilute DNA samples and quantify picogreen reagent. The working concentration of 1x TE buffer was prepared by diluting 20x TE buffer stock concentration in distilled water. The aqueous working solution of the picogreen reagent was prepared by diluting picogreen reagent 200 fold in TE buffer (200 µl of Picogreen reagent diluted in 39.8 ml of TE buffer) in a plastic container and protected

from light by an aluminium foil cover. 2 µg/mL DNA was mixed and incubated at room temperature with 1.0 ml of the aqueous working solution of picogreen reagent for 5 minutes in plastic test tube covered by foil. The fluorescence was read via microplate reader at emission 520 nm and excitation 480 nm. Following this, 0.84 ng DNA was added to each reaction (the reaction also contains a primer pair mix and an enzyme mix (one-step addition of Taq DNA polymerase, dNTPs, MgCl2) plus water to final volume) before PCR cycling. The amplified DNA was then subjected to fragment analysis on a 3730 DNA analyser. The results were analysed using Genemapper 4.0 software to give genotyping results that can be matched to information in an STR database for cell identification.

2.2.2 Cell proliferation assay (MTT assay)

2.2.2.1 Principles of MTT assay

MTT (3-(4, 5-dimethylthiazol-2-yl)-2,5-diphenyldetrazolium bromide is a colorimetric metabolic activity assay that assesses the viability of cells. The yellow tetrazolium MTT dye in living cells is reduced by cellular reductive enzymes to form insoluble formazan, which is purple in colour [158]. Insoluble purple formazan is dissolved to form a coloured solution by DMSO. The absorbance of the colour solution can be measured by spectrophotometer by using 500-600 nm wavelengths.

In this study, the effect of Metformin on thyroid cancer cell growth at time periods ranging from 1 to 6 days was investigated via MTT assay; all experiments were repeated in triplicate. The concentration of Metformin used ranged between 0.03 mM to 20 mM; this includes therapeutic concentrations of Metformin in humans [132]. The effect of Metformin on breast cancer cells (MCF7) and retinal pigmented epithelial cells (h-TERT RPE-1) was also studied and compared to thyroid cells.

2.2.2.2 Methodology of MTT assay

Cell line preparation: Cells were defrosted and cultured for 3 days in T75 flasks. Cells were seen attached to the base of the flask and were dividing. The target was 70% confluence but if this target was not achieved in 3 days, the culture media was changed and the cells left for a few more days. The medium was aspirated with a Pasteur pipette (new for each flask), and then washed twice with 5 ml of PBS. The PBS was aspirated and 5 ml of trypsin added. This was then incubated for 2 minutes to completely detach the cells. The solution was then pipetted up and down and transferred to a falcon tube before being centrifuged at 1000 rpm for 5 minutes. The supernatant was aspirated and 10.5 ml of medium added. 500µl was aspirated for counting cells with a cell viability analyser (vi-cell XR, Beckman coulter, USA).

As initial standardisation procedure, cells were seeded into a 96 well plate in 3 different concentrations ($1.5x10^4$, $1x10^4$ and $0.5x10^4$ cells per well in 100 µl of medium – 15 wells each). The concentrations were chosen to reflect the optimal growth for up to 144 hours. We decided to choose $0.5x10^4$ cells per well as they showed optimum growth yet still retained space for further growth in the 96 well plate.

Day 1: Cells were seeded into a 96 well plate using $0.5x10^4$ cells per well in 100 µl of medium. They were then incubated at 37°C in a humidified atmosphere of 95% and 5% CO_2 for 24 hours.

Day 2: The cells were treated with various concentrations of Metformin (0.03 mM, 0.1 mM, 0.15 mM, 0.3 mM, 1 mM, 5mM, 10 mM and 20 mM) in triplicate; they were then incubated for certain time points (24, 48, 72, 96,120 and 144 hours) at 37°C in a humidified atmosphere of 95% and 5% CO_2.

Day3: At each time point, 100 µl of MTT (1 mg/ml) was added to each well and incubated for 3 hours at 37°C in a humidified atmosphere of 95% and 5% CO_2 and protected from light by foil. MTT and the media were aspirated and 100 µl of DMSO added to each well. This was incubated for 30 minutes at 37°C in a humidified atmosphere of 95% and 5% CO_2.

The absorbance was read via plate reader (Fluostar Galaxy, BMG labtech, Germany) at 570 nM.

2.2.2.2.1 Cell proliferation assay (MTT) to study the interaction of Metformin with glucose, TSH, IGF-1 and insulin.

The principles and methodology of MTT assay have been described previously. The following modifications were made to study the effects of glucose, TSH, IGF-1 and insulin.

1. **Glucose:**

Day 2: Cells were treated with Metformin concentrations (0.3 mM and 10 mM) in the DMEM glucose free medium and DMEM medium containing 10 mM of glucose; they were then incubated for 6 days at 37°C in a humidified atmosphere of 95% and 5% CO_2.

2. **TSH:**

Day 2: Cells were treated with various concentrations of Metformin (0.3 mM and 10 mM) in triplicate with and without 5 mIU/ml of TSH in the medium; they were then incubated for 6 days at 37°C in a humidified atmosphere of 95% and 5% CO_2.

3. **IGF-1**

Day 2: Cells were treated with Metformin concentrations (0.3 mM and 10 mM) in triplicate with and without 100 ng/ml of IGF-1 in the medium; they were then incubated for 6 days at 37°C in a humidified atmosphere of 95% and 5% CO_2.

4. **Insulin**

Day 2: Cells were treated with Metformin concentrations (0.3 mM and 10 mM) in triplicate with and without 10 µg/ml of insulin in the medium; they were then incubated for 6 days at 37°C in a humidified atmosphere of 95% and 5% CO_2.

2.2.3 Cell proliferation assay (trypan blue assay)

2.2.3.1 Principles of trypan blue assay

This assay was used to validate the results of MTT assay. Trypan blue solution (0.4%) is prepared in 0.81% sodium chloride and 0.06% potassium

phosphate dibasic. Trypan blue solution is a traditional technique, which is used in proliferation assays and cytotoxicity. Trypan blue is a vital stain, which is absorbed by dead cells but is not absorbed by live cells. Live cells are excluded from the staining and the method is referred to as the dye exclusion method. The dead cells are stained blue in colour while the live cells are colourless and bright under the microscope. Trypan blue has been used for years in academic research and laboratory-based work. Traditionally, in trypan blue exclusion method the cells are routinely counted manually via haemocytometer but in recent research, the trypan blue method has been replaced by a quick modern automated method of high quality image and ability of sample handling. The automated cell counter (BIO RAD TC20) counted the percentage of viable cells.

2.2.3.2 Methodology of trypan blue assay

Cell preparation: Similar to that described previously in MTT assay.

Day 1: Cells were seeded into a 24 well plate using $0.5x10^4$ cells per well in 1 ml of medium then they were incubated at 37°C in a humidified atmosphere of 95% and 5% CO_2 for 24 hours.

Day 2: The cells were treated with various concentrations of Metformin (0.03 mM, 0.1 mM, 0.15 mM, 0.3 mM, 1 mM, 5 mM, 10 mM and 20 mM) in triplicate; they were then incubated for 6 days at 37°C in a humidified atmosphere of 95% and 5% CO_2.

Day 3: At each time point, 10 µl of cell-trypan blue mixture solution (10 µl of cell suspension was mixed with 10 µl of trypan blue to make 20 µl of cell-trypan blue solution) was added to the one side of outer opening slide chambers. The percentage of viable cells on the slide chambers was counted via automated cell counter BIO RAD TC20.

2.2.4 Clonal formation assay

2.2.4.1 Principles of Clonal formation assay

This is a proliferation assay that is used to assess the ability of single cells to form a colony. Cells may grow and divide to form a few cells counted as a colony or remain as a single cell, which was counted as a dead cell. The aim of this assay was to investigate the number and the morphology of colonies after cells were treated with various concentrations of Metformin.

Cells were treated with concentrations between 0-5 mM, which include the normal therapeutic concentration of Metformin. The other toxic concentrations of Metformin 10 mM and 20 mM were used in the pilot study but the cells unable to form colonies due to the high toxicity of Metformin. In the previous published study similar concentrations of Metformin were used but different thyroid cancer cell lines were investigated [104].

2.2.4.2 Methodology of clonal formation assay

Cell preparation: Cells were cultured in T75 flasks and constantly checked under the microscope for confluence until the cells were approximately 70% confluent.

Day 1: When the cells approximately were 70% confluent, they were washed twice with 5 ml PBS and trypsinised with 5 ml of trypsin. The cells were suspended in medium and trypsin in a universal tube. Cells were centrifuged at 1000 rpm for 5 minutes and re-suspended as a pellet in 10 ml of medium. The total number of viable cells was counted via cell viability analyser (Vi-CELL^{TM} XR, Beckman coulter, USA). Cells were seeded 500 cells per 10 cm petri dishes and incubated with 10 ml of medium for 24 hours at 37°C, humidified atmosphere of 95% and 5% CO_2.

Day 2: Cells were treated with various concentrations of Metformin in triplicate (control, 0.03 M, 0.1 mM, 0.3 mM, 1 mM and 5 mM) and incubated for 14 days at 37°C, humidified atmosphere of 95% and 5% CO_2.

Day 14: After this period, cells were washed twice with PBS and then fixed with 5 ml of a solution of methanol/acetone solution at a ratio of 1:1. The

dishes were washed again with PBS, colonies stained with methylene blue 70% alcohol (I.M.S) and incubated at room temperature for 40 minutes. After a final wash with distilled water, the dishes were left to dry overnight.

Day 15: Formed colonies were counted by using an inverted microscope for FTC-133, K1E7, RO82-W-1 and Nthy-ori 3-1 cell lines in three independent experiments for each concentration of Metformin (control, 0.03 M, 0.1 mM, 0.3 mM, 1 mM and 5 mM) in triplicate.

2.2.5 Cell migration or scratch assay

2.2.5.1 Principles of Scratch assay

This assay investigated the movements of cell growth under the effect of an anti-proliferative agent. The process of movement of cells in a particular direction is known as cell migration. The assay helps to determine if drugs such as Metformin stop or enhance cell migration *in vitro.*

Two concentrations of Metformin were used in this experiment, the therapeutic concentration 0.3 mM and one toxic concentration 10 mM, which was previously studied [105].

2.2.5.2 Methodology of Scratch assay

Cells were cultured with silicone inserts to ensure a defined cell-free gap in each chamber. The cells were then incubated for 24 hours at 37°C, humidified atmosphere 95% and 5% CO_2. After 24 hours, the silicone insert was removed and the medium changed with medium containing Metformin (control, 0.3 mM and 10 mM) and incubated for 24 hours. This experiment was repeated three times independently and in triplicate at different Metformin concentrations. After 24 hours, pictures were taken of untreated cells and cells treated with Metformin (0.3 mM and 10 mM) using the Nikon glipse TS100 microscope at 4x magnification.

ImageJ software was used to measure the gap closure and to calculate the remaining separation gap between two populations of cells on removal of the partition in control cells and Metformin treated cells (0.3 mM and 10 mM). About 20 horizontal lines were drawn across the edge of the cells and the

measurements of the length of the drawn lines were taken and the percentage of the closed area was calculated. These steps were repeated for each cell line.

2.2.6 Flow cytometric analysis for apoptosis assay

2.2.6.1 Principle of apoptosis

Apoptosis also called programmed cell death is a biochemical consequence resulting in cell characteristic changes (morphology). Annexin V is a family of calcium-dependent phospholipid-binding proteins, which bind to phosphatidylserine (PS) on the cell membrane of apoptotic cells, as PS translocates to the extracellular membrane in apoptotic cells. This assay is able to characterize cells into three populations: - The viable cells (annexin V negative, propidium iodide (PI) negative), necrotic cells (annexin V positive, PI positive) and early apoptotic cells (annexin V positive, PI negative).

In this study both low concentrations of Metformin including therapeutic concentrations of Metformin and high concentrations of Metformin, similar to those used as in the previous study were investigated [104].

2.2.6.2 Methodology of apoptosis assay

10X Annexin V Binding Buffer: 0.1 M Hepes/NaOH (pH 7.4), 1.4 M NaCl, 25 mM CaCl2. For a 1X working solution, dilute 1 part of the 10X Annexin V Binding Buffer to 9 parts of distilled water.

Cell preparation: Cells were cultured in T75 flasks and constantly checked under the microscope for confluence until the cells were approximately 70% confluent.

Day 1: When the cells were 70% confluent, they were washed twice with 5 ml PBS, trypsinised with 5 ml of trypsin and suspended in medium in a universal tube. Cells were centrifuged at 1000 rpm for 5 minutes and re-suspended as a pellet in 10 ml of medium. The total number of viable cells was counted via cell viability analyser (Vi-CELLTM XR, Beckman coulter, USA). Cells were seeded 4 x 10^5 cells per 6 cm dishes and incubated with 10 ml of medium for 24 hours at 37°C, humidified atmosphere of 95% and 5% CO2.

Day 2: Cells were treated with various concentrations of Metformin (control, 0.1, 0.3 mM, 1 mM and 10 mM) in triplicate and incubated for 144 hours at 37°C, humidified atmosphere of 95% and 5% CO2.

Day 3: The medium was transferred from 6 cm dishes to labelled tubes. Cells were washed with PBS twice and then incubated with 2 ml of trypsin for 2 minutes at 37°C, humidified atmosphere of 95% and 5% CO2. Cells were collected in correspondence labelled tubes and centrifuged at 1000 rpm for 5 minutes (at 21°C). The supernatant was discarded and the cells were re-suspended as pellet in 5 ml of ice PBS. Cells were centrifuged again at 1000 rpm for 5 minutes (at 21°C) and the cells were re-suspended as pellet in 10% buffer (2 ml of buffer + 18 ml of distilled water) to get a concentration of 2 x 10^6 cells per ml (by dilution of cells in buffer). 100 µl of cells were transferred into FACS tubes (2 X 10^6 cells). 5 µl of FITC anexin V and 5 µl of propidium iodide (PI) were added to each FACS tubes and incubated at room temperature for 15 minutes. 400 µl of 10% buffer added to each samples and then the percentage of apoptotic cells analysed with flow cytometer (FACS) (BD Biosciences) via Cell Quest Pro software (**Figure 2.1**).

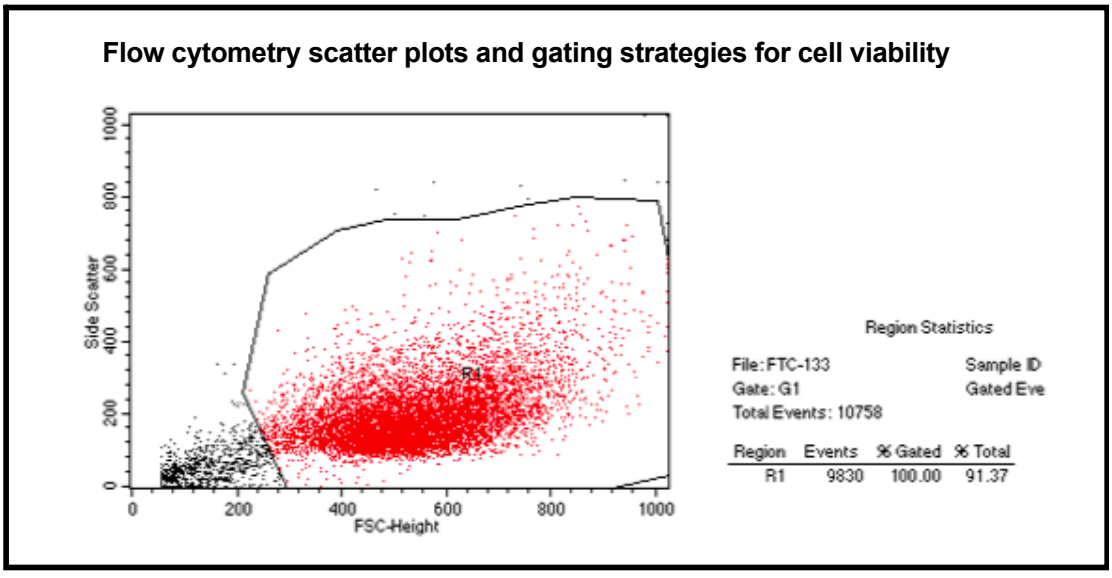

Figure 2.1: Flow cytometry gating strategies for apoptosis assay.

This figure shows the selection of FTC-133 cell population (R1 which is red in colour) used for analysis of the apoptosis assay.

2.2.7 Flow cytometric analysis for cell cycle assay

2.2.7.1 Principles of cell cycle assay

In this assay flow cytometry can differentiate cells in various cell cycle phases. Cells were treated with fluorescent dye (propidium iodide), which stains DNA. The certain wavelengths of fluorescent intensity in stained cells associated with the amount of DNA in the cells. Based on the amount of DNA, flow cytometry identified the percentage of cell population in cell cycle phases.

2.2.7.2 Methodology of cell cycle assay

Cells were cultured in 6 well plates (4 x 10^5 cells per well) and incubated for 24 hours. Cell were treated with different concentrations of Metformin (control, 0.3 mM, 1 mM and 10 mM) and incubated for 6 days, fixed with 70% ethanol and left overnight at 4°C. 50 µl of ribonuclease (100 µg/mL solution) was added to the cells for 15 minutes at room temperature, followed by 200 µl of propidium iodide (PI) and left for 2 hours at 4°C. The samples were analysed with flow cytometer (FACS) (BD LSRII) using FACSDiva 7.0 software (**Figure 2.2**). For each cell line, the experiment was performed in one well and on 3 occasions.

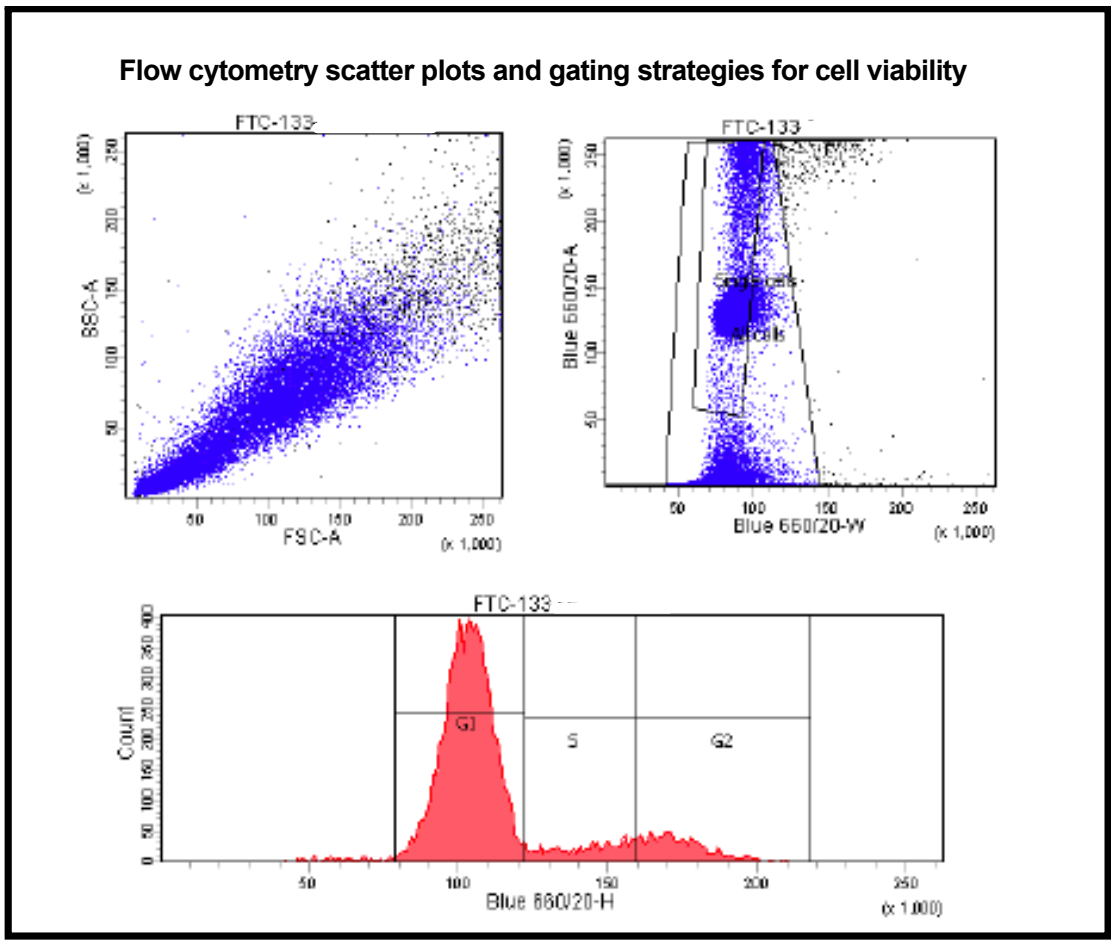

Figure 2.2: Flow cytometry scatter plots and gating strategies for cell cycle analysis.

This shows the gating strategy for the flow cytometry cell cycle assay and shows the population of cells in different phases of the cell cycle (G1, S &G2). The side scatter (SSC) shows the granularity of the cells and forward scatter (FSC) shows the size of the cells.

2.2.8 γH2AX assay for DNA repair

2.2.8.1 Principles of γH2AX assay

Histone proteins are alkaline proteins. H2A.X is a member of the H2A histone protein family and is packed along with DNA to form the subunit of the chromatid (nucleosome).

H2A.X protein (gamma-H2A.X) phosphorylation in cells is a sensitive target for looking at double-strand breaks (DSBs) [159]. In response to double strand breaks-DNA (DSBs-DNA), ataxia telangiectasia mutated (ATM) and DNA dependent protein kinase (DNA-PK) are activated and play an essential role in phosphorylation of H2A.X protein (γH2AX) [160]. Subsequently, nuclear microscopically visible foci in the nucleus form as a result of DSBs.

These therefore can be used as biomarkers of DNA damage and repair [161] (**Figure 3.11**). The γH2AX foci can be visualised with an immunofluorescence microscope after staining with specific primary antibody (Phospho-Histone H2A.X (Ser139) (20E3) Rabbit mAb). In order to induce DNA-DSBs in FTC-133, K1E7 and Nthy-ori 3-1, cells were irradiated (IR) or treated with Metformin or treated with both. The quantitative assessment of γH2AX foci were used to assess DNA damage and repair in thyroid cancer cell lines treated with and without radiation and/or Metformin and Metformin alone.

2.2.8.2 Methodology of γH2AX assay

Cell preparation: Cells were cultured into T75 flasks and checked under the microscope daily until they were approximately 70% confluent.

Day 1: Cover slips 22 X 22mm were immersed in absolute methanol and left for 10 minutes until they were dried. The cover slips were then placed in the 6 well plates. Cells were trypsinised with 5 ml of trypsin and incubated for 2 minutes. Cells were re-suspended in 5 ml of medium and collected in universal tube. The cells in the universal tube were centrifuged for 5 minutes at 1000 rpm. A cell viability analyser (Vi-CELL^{TM} XR, Beckman coulter, USA) was used to count viable cells. Viable cells were seeded (5 x 10^4 cells per coverslip) in each well and 2 ml of medium was carefully added to each well without disturbing cells on the coverslips. The plates were incubated for 24 hours at 37°C, 95% humidification and 5% CO_2.

Day 2: The wells were labelled for different combinations of treatments for each cell lines:-

a) Metformin (20 mM) + radiation (2 Gy IR).
b) Metformin (0.1 mM) + radiation (2 Gy IR).
c) Radiation (2 Gy IR).
d) Metformin (20 mM).
e) Metformin (0.1 mM).
f) Control (not treated with either Metformin or IR)

Cells labelled with Metformin were treated with medium containing Metformin (0.1 mM and 20 mM) for 144 hours prior to radiation.

Day 8: Cells labelled with IR were irradiated with 2 Gy IR using Cesium137 irradiator (CIS Bio International). The cells were incubated for certain time points (0.5 hour, 1 hour and 2 hours) which allowed the recovery of cells after DNA damage. The medium was discarded at each time point (0.5 hour, 1 hour and 2 hours) and washed twice with PBS. The cells were fixed by adding 1.5 ml of 4% PFA to each well and incubated for 10 minutes at room temperature. After incubation, the 4% PFA was discarded and the cells were washed twice with PBS. After this, 2 ml of 0.2% Triton X-100 in PBS was added to each washed well, incubated for 5 minutes at room temperature (for permeation of primary antibody) and then washed twice with PBS. Cells were blocked by adding 1.5 ml of blocking buffer (10% normal goat serum in PBS) to each well and incubated for 1 hour at room temperature and then washed twice with PBS. 100 µl of phospho-histone rabbit anti-y-H2A.X was added on each coverslip and incubated for 24 hours at 4°C in a humidity chamber.

Day 9: Cells were washed 3 times with PBS (5 minutes wash on the rotate shaker). They were incubated with 100 µl of Cy3 goat anti-rabbit IgG in the dark for 1 hour at room temperature. Following incubation, the cells were washed 3 times with PBS (5 minute wash on the shaker and protected from light). The coverslips were then placed with 4',6-DiAmidino-2-Phenylindol (DAPI) (Vector laboratories Inc., USA) onto the centre of microscope slides. The edges of coverslips were fixed with a small drop of nail varnish and the slides were left to dry before being stored at 4°C in the dark.

Day 10: The numbers of γH2AX foci were counted using Cytovision software (Newcastle upon Tyne, UK) in 100 cells per slide via fluorescent microscope with CCD camera at 100x magnification. The foci were detected as red fluorescent signals inside the blue background stained DAPI cells.

This experiment was performed in triplicate and the entire experiment was repeated in three independent experiments. The rationale for using the 2 Gy IR radiation dose in this experiment was that is considered as a therapeutic dose of radiotherapy [162]. In addition, the 2 Gy radiation-induced high DNA damage previously reported by the Rare Tumour Research Group (RTRG) within the department of Oncology, University of Sheffield.

2.2.9 Immunocytochemistry for OCT1 expression

2.2.9.1 Principles of immunocytochemistry

Immunocytochemistry is a common technique used in the laboratory to detect and localize a specific antigen or protein. In order to visualize protein under the fluorescent microscope, a specific primary antibody were used and then treated with a secondary antibody to bond with the primary antibody. Immunocytochemistry was used to investigate the expression of OCT1 in thyroid cancer cells.

2.2.9.2 Methodology of Immunocytochemistry

In a pilot study a serial dilution for the primary antibody as tested (1:25, 1:50, 1:100 and 1:200) and 1:50 20 µl of SLC22A1 in 1000 µl of 2% goat sera was chosen as this distinguished OCT1 staining in HepG2 cells-the positive control.

Cell preparation: Slides were soaked in absolute ethanol for at least 10 minutes. Slides removed with forceps and leant against the side of a large petri dish to allow the ethanol to completely evaporate. Once dried, forceps were used to place the slides into the petri dish so they were completely flat and the lid is replaced. Cells were then prepared for counting. Cells were then seeded at a concentration of between 10,000-15,000/0.5 ml of media and placed onto each slide. After 24 hours, 25 ml of media containing different concentrations of Metformin (0-10 mM) added and incubated for two time points (24 and 48 hours). Once the cells were ready, the media was removed and the slides were washed in the petri dish with PBS 4 times. Slides were transferred to a slide rack and submerged into ice-cold methanol/acetone 50:50 for 10 minutes. The methanol/acetone was prepared 1 hour before use and stored in a – 20 °C freezer. Slides were removed from methanol/acetone and left to dry in fume cupboard. Once completely dry, the slides were stored in a container in the – 20 °C freezer until further use.

SLC22A1 antibody stain for OCT1: The slides were removed from the – 20 °C freezer and allowed to warm up to room temperature. The ImEdge hydrophobic barrier pen was used to mark an area on the slides by drawing

around the cells and washed in PBS for 5 minutes. Slides were soaked in H2O2/methanol at room temperature (30 ml H2O2 + 270 ml methanol) for 5 minutes and then washed on the shaker very gently for 5 minutes and repeated twice. After this, 10% blocking serum (400 µl goat sera in 4 ml of PBS) was added, left for 20 minutes and then tipped off. Cells were incubated with 200 µl of primary antibody (SLC22A1) at 4°C overnight (using the dilution of 1:50 of primary antibody; 20 µl of SLC22A1 in 1000 µl of 2% goat sera). The next day, cells were washed with PBS on a shaker very gently for 5 minutes and repeated twice. Cells were incubated at room temperature with 200 µl of secondary antibody (goat anti-rabbit, Biotinylated) for an hour. Secondary antibody was diluted 1:200 in 2% goat sera (10 µl to 2 ml 2% goat sera). Cells were washed again with PBS 3 times (each time for 5 minutes) and then incubated with ABC reagent (for 5 ml of reagent, 2 drops A, 2 drops B and 5 ml PBS were mixed well and allowed to stand for 30 minutes before being used) for 30 minutes. Cells were washed again with PBS 3 times, each for 5 minutes. The sections were incubated in peroxidase substrate (DAB) solution (for 5 ml of DAB, 2 drops buffer, 4 drops DAB, 2 drop H2O2 are mixed with 5 ml distilled water; this is usually only prepared immediately before use) until desired stain intensity developed; usually around 10 minutes. Slides were washed in tap water for 2 minutes and then counterstain in haematoxylin gills for 30 seconds. Slides were then rinsed in tap water until the water ran clear and washed in Scott's tap water substitute for 10 seconds.

Dehydrate, clear and mount: Slides were soaked in increasing concentrations of ethanol - 70% ethanol for 3 minutes, 90% ethanol for 3 minutes, 95% ethanol for 3 minutes, 100% ethanol for 3 minutes and 100% ethanol for 3 minutes. This was followed by mounting on Xylenel1 for 3 minutes and Xylenel2 for 3 minutes (or until wax from the wax pen has cleared). The slides were mounted and dried overnight. The proportion and intensity of OCT1 expression were estimated using the Allred score. Allred score is a scoring method to estimate the percentage of cells that are stained (on the scale of 0-5) and then to determine the intensity of that stain (on the scale of 0-3) and the total scoring will be ranged 0-8.

This experiment was repeated once for each concentration of Metformin but the entire experiment was repeated in three independent experiments. In this experiment a breast cancer cell line (MDA-MB-231) were used as a control because the MCF7 cells had issues with recovery.

2.2.10 Affymetrix assay

2.2.10.1 Principles of Affymetrix assay

The Affymetrix gene chip microarray is to detect a wide range of genomic expression of each sample (high quality extracted RNA) by using specific probes. The genomic expression profile can be then translated to understanding specific diseases, molecular diagnostic tests and improving therapeutic targets.

2.2.10.2 Methodology of Affymetrix assay

Prior to starting: Preparing Buffer RPE working solution by adding 4 volume of 96-100% ethanol to Buffer RPE.

RNA extraction: Cells were harvested to a maximum 1x 10^7 cells then 600 µl of buffer RLT was added and mixed with 600 µl of 70% ethanol. 700 µl of the sample was transferred to RNeasy Mini spin column and placed in a 2 ml collection tube then centrifuged at ≥8000 x g for 15 seconds. After that 700 µl of Buffer RW1 added to the RNeasy spin column and centrifuged at ≥8000 x g for 15 seconds. 500 µl of Buffer RPE added to the RNeasy spin column and centrifuged at ≥8000 x g for 15 seconds then 500 µl of Buffer RPE added to the RNeasy spin column and centrifuged at ≥8000 x g for 2 minutes. The RNeasy spin column were placed in a new 1.5 ml collection tube and 50 µl RNase-free water was added before centrifuged at ≥8000 x g for 1 minute to elute the RNA. The quality of RNA samples was checked by the microarray core facility, University of Sheffield, UK before proceedings to analysis on the Agilent Bioanalyser.

2.2.11 Statistical analyses

All the data was non-parametric (not normally distributed) and the statistical analyses were performed using Graphpad Prism software v. 6 for Mac. Kruskal-Wallis test was used for multiple comparisons of more than two groups for example to compare the results of the experiments for the treated (cells treated with different concentrations of Metformin) and untreated (cells not treated with Metformin) groups. Mann-Whitney test was used to compare two groups for example cells treated with single concentration of Metformin and cells not treated with Metformin (control). P value < 0.05 was considered as a statistically significant.

CHAPTER THREE

Effect of Metformin on thyroid cancer cell growth and behaviour

3.1 Introduction

Several population-based studies have demonstrated the potential of Metformin as a chemo-preventative agent in cancer (including breast cancer [112-114], prostate cancer [113, 118], gastric cancer [113, 119], lung cancer [112, 113, 119], pancreatic cancer [113, 119], and colorectal cancer [113]). Recently, a few clinical trials have been done to investigate the anti-tumour effect of Metformin in patients with breast cancer [138-140]. These showed significant reduction in Ki67 expression in the Metformin group and changes in the control arm; providing evidence for anti-proliferative effects of Metformin and increased apoptosis as reflected using the TUNEL assay.

Furthermore, investigations of the anti-cancer effects of Metformin in *vitro,* using a number of human cancer cell lines (including breast cancer [125, 126], gastric cancer [127], lung cancer [126], ovarian cancer [128] and thyroid cancer [104, 106]) have shown that Metformin inhibited cancer cell proliferation and induced apoptosis. The response to Metformin has been shown in these studies to be dependent on duration of exposure and concentration of drug in the media. In relation to thyroid cancer, Metformin has been suggested to have anti-cancer effect on anaplastic thyroid cancer cell line HTh74 by inducing cell cycle arrest and apoptosis and also Metformin inhibited cell proliferation on anaplastic (HTh74, C643 and SW1736) and follicular thyroid cancer cell lines (FTC-133) [104]. In another study, Metformin inhibited medullary thyroid cancer cell proliferation (TT and MZ-CRC-1 cell lines) and also Metformin up-regulated the AMPK pathway (TT cell line) [106]. The anti-cancer effects of Metformin are in dose and time dependent manner in thyroid cancer cell lines [104, 106]. The concentrations of Metformin used in these studies were much higher than normal human plasma concentrations (0.01-0.3 mM) [132, 163], limiting the extrapolation of these findings to clinical practice.

Metformin in thyroid cancer has also been investigated *in vitro* in combination with other agents such as Doxorubicin and Cisplatin [129]. The anti-proliferative effect when Metformin was given in combination with either Doxorubicin or Cisplatin was more effective than single agent treatment. In a study of Metformin in combination

treatment with Paclitaxel in breast and lung cancer cell lines (MCF7 and A549) [126], there was significant inhibition of cell proliferation (MCF7 and A549) compared to Paclitaxel treatment only. Furthermore, Metformin boosts the anti-cancer effects of Paclitaxel by increasing AMPK phosphorylation and inhibited mTOR, p70S6K and 4E-BP1 [126]. The findings of these studies showed that Metformin amplified the effect of anti-cancer agents on some types of cancer in laboratory studies. In this study the effect of Metformin on DSBs was investigated as a single agent and in combination with radiotherapy. Radioiodine ablation is recommended in most patients following surgery to decrease the risk of recurrence of differentiated thyroid cancer [24]. However, radiation is also a risk factor to induce thyroid cancer because it causes DSBs-DNA [164]. γH2AX plays an essential role in DNA repair by the recruitment and activation of DNA repair proteins, chromatin remodelling and check points around the site of DNA damage that might cause DNA repair or cell cycle arrest and apoptosis [165]. DNA is repaired by one of two pathways - homologous recombination (where the DNA is accurately repaired by using the sister chromatid as template) and non homologous end joining pathway (where the DNA is repaired without a template) [166]. To facilitate the development of Metformin as a potential clinically useful anti-cancer drug for thyroid cancer, a detailed understanding of its effects on different types of thyroid cancer and the underlying mechanisms are required. The aim of this study is to determine its effects on the growth and proliferation of several thyroid cancer and normal cell lines at concentrations relevant to clinical settings.

In this chapter the effects of Metformin on the growth of normal thyroid follicular epithelium (Nthy-ori 3-1) and cancerous thyroid cell lines (K1E7, FTC-133, RO82-W-1, 8305C and TT) were studied. The cells were exposed to low concentrations of Metformin that are relevant to clinical practice for longer periods of time (up to 14 days). In order to understand the mechanism of any observed effects, a number of different experiments including cell apoptosis, cell cycle arrest and cell migration were performed.

3.2 Results

3.2.1 Cell line authentication

The three thyroid cell lines (Nthy-ori 3-1, K1E7 and FTC-133) were recovered from liquid Nitrogen, and were then checked for STR profiling in order to validate the cell lines. The other cell lines (RO82-W-1, 8305C and TT) were purchased from the European Collection of Cell Culture (ECACC) with a known STR profile; hence a repeat authentication experiment was not performed.

The original STR profile for each cell line was available from ECACC general cell collection, which was recorded on 9 loci. The observed STR profiles for Nthy-ori 3-1, K1E7 and FTC-133 cell lines were matched with the expected STR profiles. Table 3.1 shows expected (black) and observed (red) STR profiles at the 10 loci (THO1, D21S11, D5S818, D13S317, D7S820, D16S539, CSFIPO, AMEL, vWA and TPOX). The number of STRs at each locus is represented as one or two peaks. The number of observed STRs was equivalent to the expected STR profiles for all cell lines. For example the table shows that at the THO1 loci for Nthy-ori 3-1, STR occured 7 times on one chromosome 11 and 9.3 times on the other chromosome 11. At the D21S11 loci, the STR was 29 on one chromosome 21 and 30 on the other chromosome 21.

3.2.2 Thyroid cells growth (MTT assay)

In order to determine the most appropriate growth medium for the cell lines, cells were grown in various media. Figure 3.1 demonstrates the growth curves of K1E7, FTC-133, RO82-W-1, 8305C, TT and Nthy-ori 3-1 cell lines in the different media. Tested all cell lines demonstrated more robust growth in DMEM with 2 gm/L and RMPI medium, compared to DMEM without glucose and DMEM F-12 medium. DMEM with 2 gm/L (10 mM) glucose was chosen for all further experiments, ensuring consistency of the growth environment across the various experiments. In the chapter four (section 4.2.1) the effects of glucose concentrations in the medium on cell proliferation were studied. In each cell lines, there were significant statistical differences of cell growth between different mediums. The significant differences of cell growth among different mediums was DMEM with glucose vs DMEM F-12 ($p = 0.01$) at day 3 and DMEM with glucose vs DMEM without glucose ($p = 0.01$) at day 4 in K1E7 cells, RPMI vs DMEM F-12 ($P = 0.03$) at day 1 and DMEM with glucose vs

DMEM without glucose ($p = 0.01$) at day 3 in FTC-133 cells, DMEM F-12 vs DMEM with glucose ($p = 0.02$) at day 2 and DMEM with glucose vs DMEM without glucose ($p = 0.01$) at day 4 in RO82-W-1 cells, DMEM with glucose vs DMEM without glucose ($p = 0.03$) at day 3 in 8305C cells, RPMI vs DMEM without glucose ($p = 0.03$) at day 4 and DMEM with glucose vs DMEM without glucose ($p = 0.01$) at day 5 in TT cells, RPMI vs DMEM without glucose ($p = 0.03$) at day 3 and DMEM with glucose vs DMEM without glucose ($p = 0.01$) at day 4 in Nthy-ori 3-1 cells.

Table 3.1: STR profiling for Nthy-ori 3-1, K1E7 and FTC-133 thyroid cancer cell lines.

		TH01	D21S11	D5S818	D13S317	D7S820	D16S539	CSFIPO	AMEL	vwA	TPOX
Chromosome number		**11**	**21**	**5**	**13**	**7**	**16**	**5**	**X, Y**	**12**	**2**
Nthy-ori 3-1	Expected	7, 9.3		11	11	7, 12	12, 13	12	X	16, 18	9
	Observed	7, 9.3	29, 30	11	11	7, 12	12, 13	12	X	16, 18	9
K1E7	Expected	6, 9		10, 11	11, 14	11	11, 12	11, 12	X, Y	17, 18	8
	Observed	6, 9	30, 31.2	10, 11	11, 14	11	11, 12	11, 12	X, Y	17, 18	8
FTC-133	Expected	9.3		12	11	9, 10	11	10	X	15, 18	9
	Observed	9.3	32.2	12	11	9, 10	11	10	X	15, 18	9

The observed STR profile was performed by the sequencing core facility, University of Sheffield on 10 loci as shown in red. The expected STR profile is shown in black, which is recorded on 9 loci (available on ECACC website).

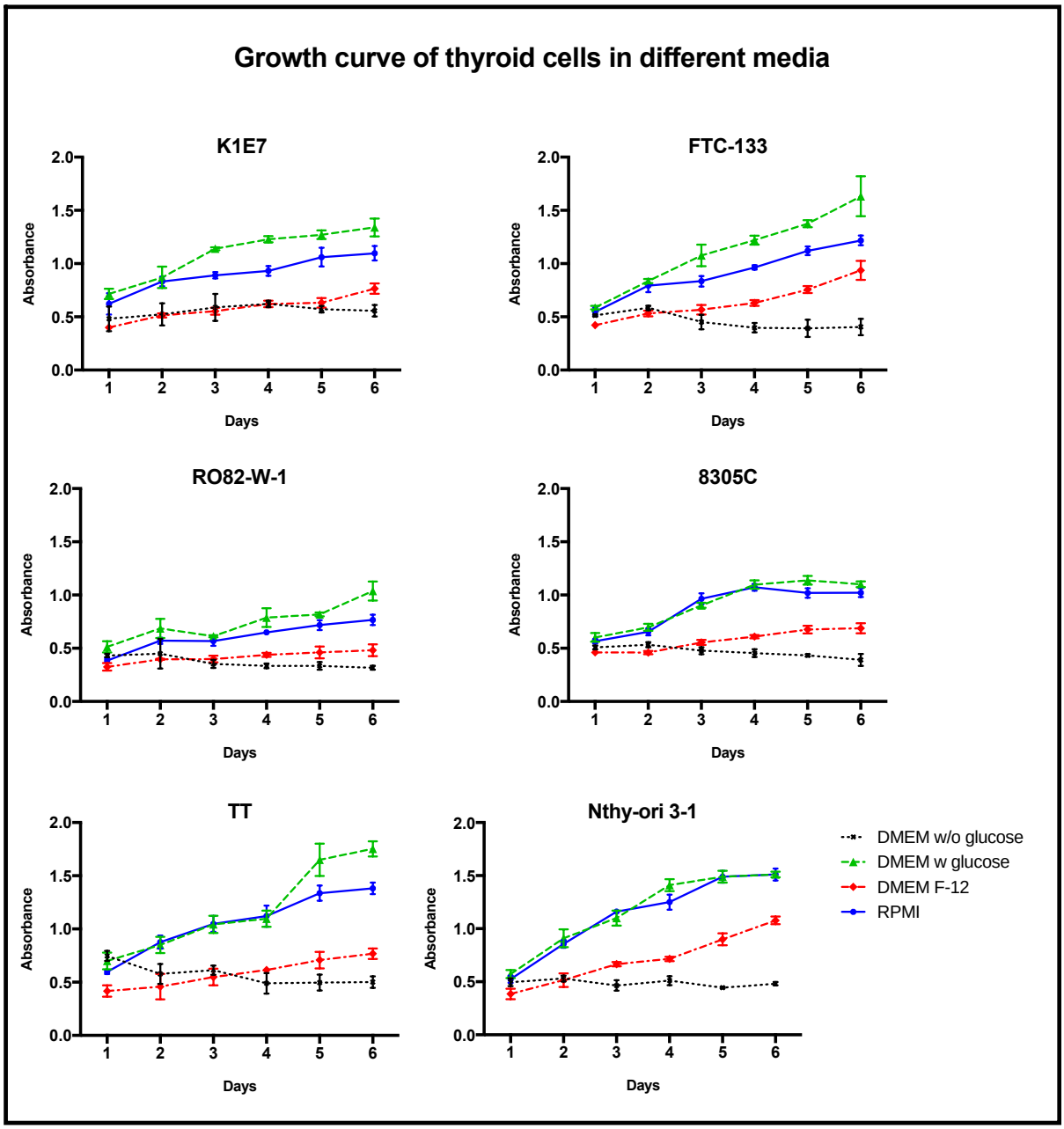

Figure 3.1: The growth curve of thyroid cell lines.

Each data point represents the mean of three independent experiments performed in triplicate for each cell line. In each experiment, cells were cultured in various media (DMEM without glucose, DMEM with glucose 2 g/L (10 mM), DMEM F-12 and RPMI) for 6 time points (1-6 days). At each time point, the absorbance of cells in the medium was recorded. Error bars show the standard error of mean (SEM). Kruskal-Wallis test were used for multiple comparisons of more than two groups. Statistics are not included on the figure due to noise but are included in text. Each thyroid cell line is shown in a separate graph

3.2.3 Cell proliferation assay (MTT assay)

As this study was the first detailed investigation undertaken in the study of thyroid cancer cells. Metformin was used in wide dose range and included doses used in previously published studies [104-106, 149]. In order to assess the cell proliferation by the MTT assay, cells were cultured with various concentrations of Metformin for a number of different time points (section 2.2.2.2). For each time evaluated (1-6 days), the percentage of cell proliferation for Metformin concentrations was determined by using Fluostar Galaxy (plate reader).

This assay evaluated thyroid cancer cell growth and proliferation of 5 thyroid cancer cell lines (K1E7, FTC-133, RO82-W-1, 8305C and TT) and a 'normal' thyroid follicular epithelial cell line (Nthy-ori 3-1). Other cell lines including a breast cancer cell line (MCF7) and a normal retinal pigmented epithelial cells (h-TERT-RPE-1) were also studied. MCF7 was used as a positive control in this study because it has shown a good response to treatment with Metformin in previous studies [125, 126, 131]. The h-TERT-RPE-1 cells were used alongside of Nthy-ori 3-1 cells to boost accuracy of the control arm in this study.

The results showed that Metformin inhibited K1E7 cell proliferation from the day 1 for all concentrations (0.03 mM, 0.1 mM, 0.15 mM, 0.3 mM, 1 mM, 5 mM, 10 mM and 20 mM) but the inhibition did not reach statistical significance (p value > 0.05). On day 2, the inhibition approached marginal significance at 20 mM (p value = 0.05). Increasing the duration of incubation of K1E7 cells with Metformin decreased the minimum concentration of Metformin required to inhibited K1E7 cell proliferation significantly. The minimum significant concentration of Metformin that inhibited K1E7 cell proliferation was 5 mM on day 3, 4, 5 and 6 (p values were 0.019, 0.031, 0.009 and 0.008 respectively) (**Figure 3.2**).

In FTC-133 cells, the minimum significant concentration of Metformin that inhibited FTC-133 cell proliferation was 5 mM (p = 0.044) after an incubation period of 3 days. Following longer periods of incubation, the minimum significant concentration of Metformin remained at 5 mM at days 4, 5 and 6 (p values were 0.044, 0.044 and 0.05 respectively) (**Figure 3.2**).

At day 1 Metformin did not appear to significantly inhibit RO82-W-1 cell proliferation at any concentration. At day 2, Metformin inhibited RO82-W-1 cell proliferation significantly at a minimum concentration of 20 mM ($p = 0.027$). After cells were incubated with Metformin for longer periods of time, Metformin significantly inhibited RO82-W-1 cells at minimum concentrations of 5 mM at days 4, 5 and 6 (p values were 0.037, 0.027 and 0.019 respectively) (**Figure 3.2**).

In 8305C cells, Metformin did not result in significant inhibition of cell proliferation from days 1 to 3 ($p > 0.05$). However, cell proliferation was significantly inhibited at a minimum Metformin concentration of 5 mM at day 4, 5 and 6 (p values were 0.027, 0.008 and 0.022 respectively) (**Figure 3.2**).

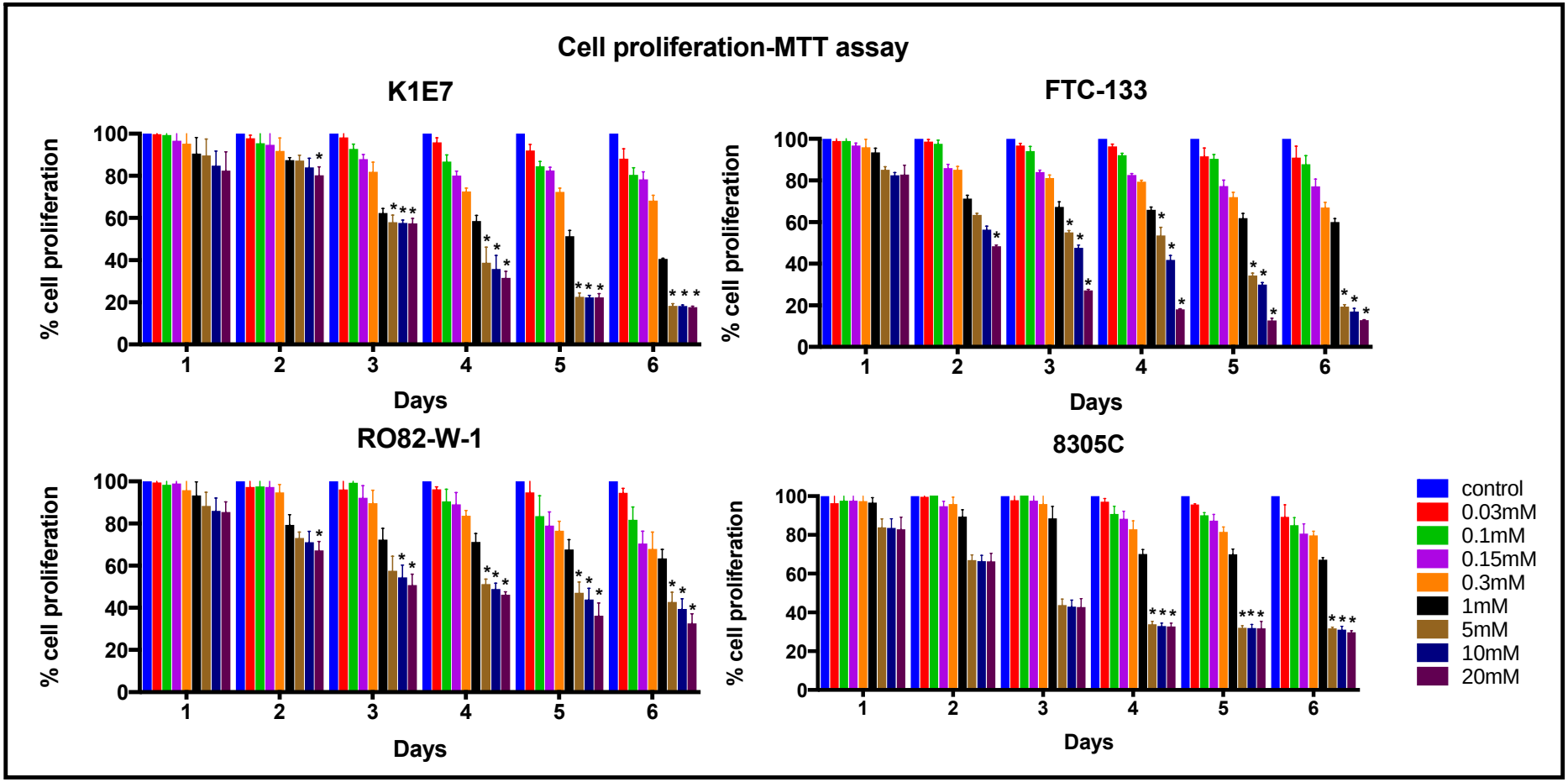

Figure 3.2: Cell proliferation assay (MTT assay)

Each bar represented the mean of three independent experiments (each done in triplicate). Error bars show the standard error of mean (SEM). In each experiment, cells were treated with various concentrations of Metformin (control, 0.03mM, 0.1 mM, 0.15 mM, 0.3 mM, 1 mM, 5 mM, 10 mM and 20 mM as shown in different colours) and incubated for different periods (horizontal axis). Statistical analysis was performed by Graphpad Prism software v. 6 for Mac, Kruskal-Wallis test were used for multiple comparisons of more than two groups. * P value < 0.05 vs control.

The TT cells results show that Metformin inhibited TT cell proliferation from day 1 and this reached statistical significance at minimum concentration of 10 mM at day 2 ($p = 0.027$). After further incubation of TT cells with Metformin for longer period of time, minimum significant concentration of Metformin decreased to 5 mM that inhibited TT cell proliferation at days 3, 4, 5 and 6 (p values were 0.019, 0.021, 0.032 and 0.011 respectively) (**Figure 3.3**).

The normal thyroid cell lines (Nthy-ori 3-1) also showed response to the anti-proliferative effect of Metformin. Metformin inhibited Nthy-ori 3-1 cell proliferation from the day 1 and this reached statistical significance at minimum concentration of 20 mM at day 2 ($p = 0.014$). The minimum significant concentration of Metformin decreased when Nthy-ori 3-1 cells were incubated with Metformin for longer periods of time. The minimum significant concentration of Metformin was 5 mM at days 4, 5 and 6 (p values were 0.029, 0.014 and 0.044 respectively) (**Figure 3.3**).

The other non-thyroid cell lines (MCF7 and h-TERT RPE-1) also responded to anti-proliferative effects of Metformin. The results showed that Metformin inhibited MCF7 cells proliferation significantly at minimum concentration of 5 mM from day 1 ($p = 0.037$). Metformin also inhibited h-TERT RPE-1 cell proliferation significantly from day 1 at minimum concentration of 10 mM ($p = 0.044$) and 5 mM at day 2 ($p = 0.032$) (**Figure 3.3**).

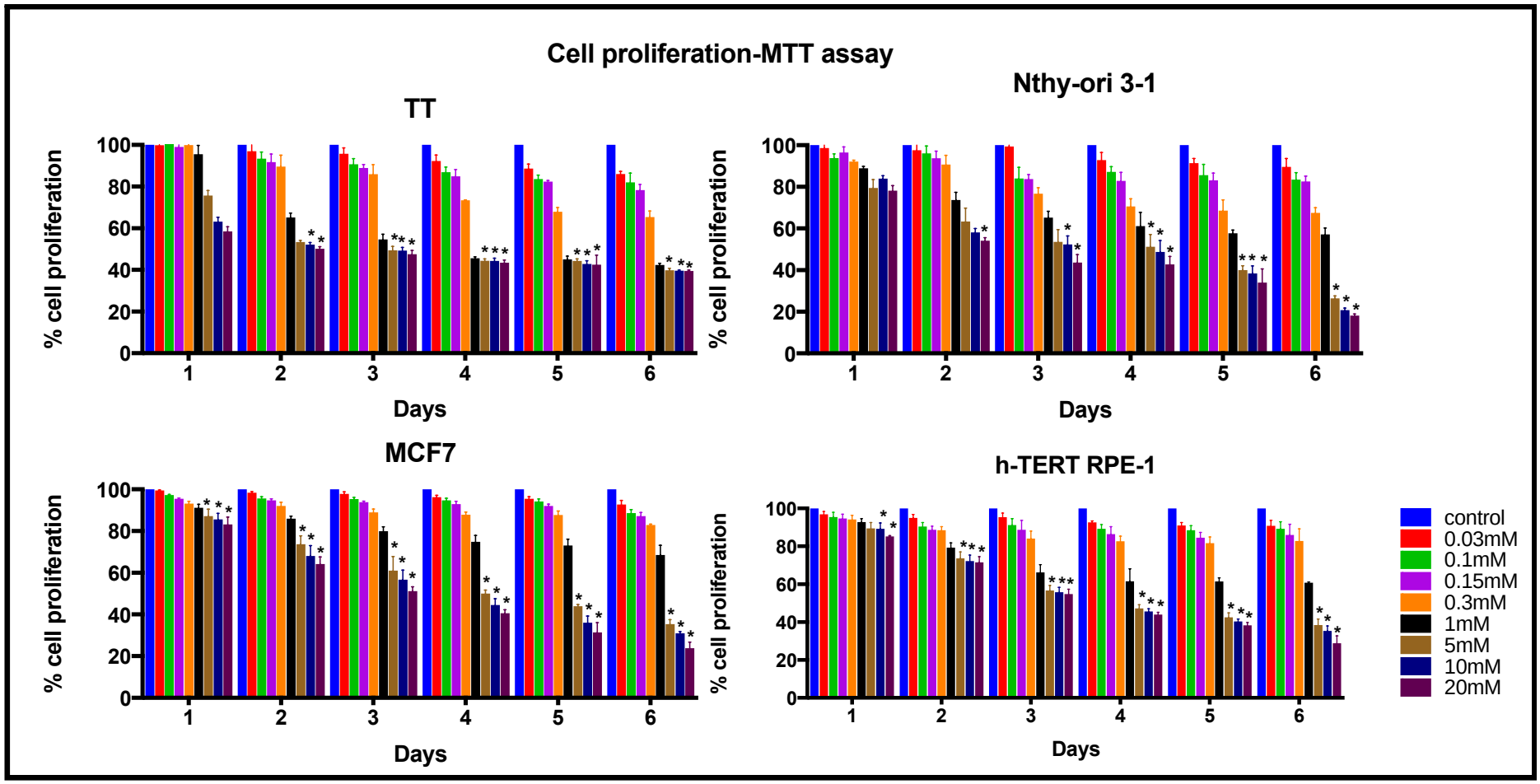

Figure 3.3: Cell proliferation assay (MTT assay).

Each bar represented the mean of three independent experiments (each done in triplicate). Error bars show the standard error of mean (SEM). In each experiment, cells were treated with various concentrations of Metformin (control, 0.03mM, 0.1 mM, 0.15 mM, 0.3 mM, 1 mM, 5 mM, 10 mM and 20 mM as shown in different colours) and incubated for different periods (horizontal axis). Statistical analysis was performed by Graphpad Prism software v. 6 for Mac, Kruskal-Wallis test were used for multiple comparisons of more than two groups. * , p value < 0.05 vs control.

The anti-proliferative effects of Metformin on all cell lines were enhanced at higher concentrations (**Figure 3.2, Figure 3.3 & Figure 3.4**). Even at low physiological doses (0.3 mM), longer exposure reduced proliferation, although this was not shown to be statistically significant (**Figure 3.4**). There were some differences between cell lines in their response to Metformin. As shown, the minimum statistically significant concentration of Metformin that inhibited cell proliferation was 5 mM, at day 3 for K1E7 ($p = 0.01$), FTC ($p = 0.04$) and TT ($p = 0.01$); 5 mM at day 4 for 8305C ($p = 0.02$), Nthy-ori 3-1 ($p = 0.02$) and RO82-W-1 ($p = 0.02$); 5 mM at day 1 for MCF7 ($p = 0.03$); and 5 mM at day 2 for h-TERT RPE-1 ($p = 0.03$).

In all thyroid cancer cell lines Metformin inhibited cell proliferation in a concentration dependent manner with small differential effects of Metformin between cell lines (**Figure 3.4**). The differential effects of Metformin was only significant at concentrations of 1 mM and 5 mM in K1E7 vs RO82-W-1 cells ($p = 0.02$ and $p = 0.04$ respectively) and at concentration of 20 mM FTC-133 vs TT ($p = 0.01$).

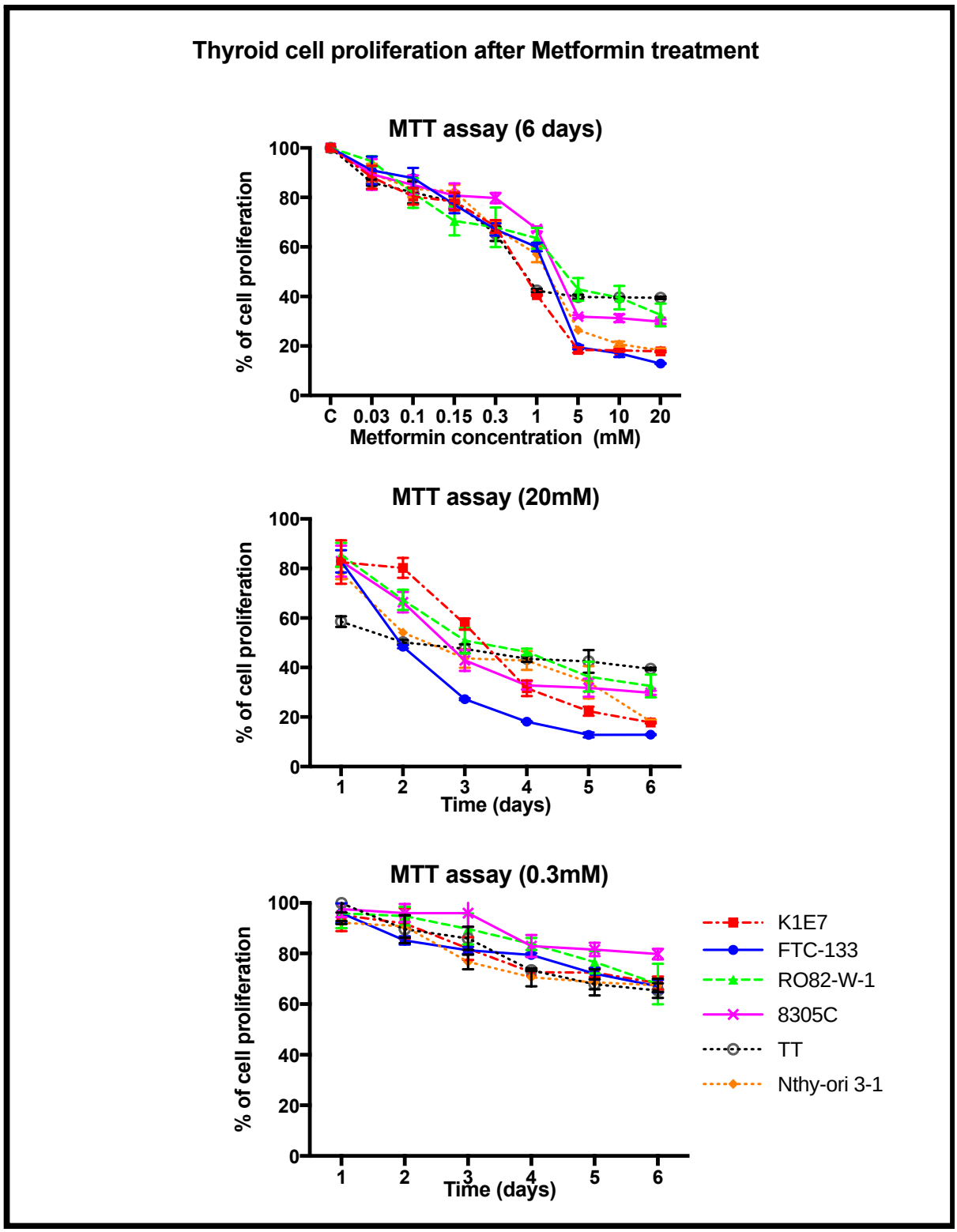

Figure 3.4: Cell proliferation assay (MTT assay).

Each data point represents the mean of three independent experiments performed in triplicate for each cell line (shown in different colours). Panel A shows thyroid cell proliferation after six days with various concentrations of Metformin (horizontal axis). Panel B and C show cell proliferation at supra-physiological concentration (20 mM) and physiological concentrations (0.3 mM) of Metformin at several time points (horizontal axis). Kruskal-Wallis test were used for multiple comparisons of more than two groups.

The growth inhibitory effect of Metformin on two of the above thyroid cancer cells was also studied by the trypan blue cell viability assay. The results are comparable to the MTT assay (**Figure 3.5**). After cells treated with Metformin for 6 days, Metformin inhibited cell viability of K1E7 and FTC-133 cells in a concentration dependent manner. The other thyroid cell lines were not studied. In FTC-133 cells, Metformin inhibited cell proliferation in a concentration dependent manner and reached borderline significance at 1 mM Metformin ($p = 0.051$). The minimum concentration of Metformin that significantly inhibited cell proliferation was 10 mM ($p = 0.02$). In K1E7 cells Metformin inhibited cell proliferation in a concentration dependent manner and reached borderline significant level at concentration 10 mM ($p = 0.06$). However, at 20 mM Metformin cells were significantly inhibited ($p = 0.02$). Furthermore, the statistical analysis shows that there are no differential effects of Metformin in FTC-133 vs K1E7 cell proliferation for the same concentrations of Metformin.

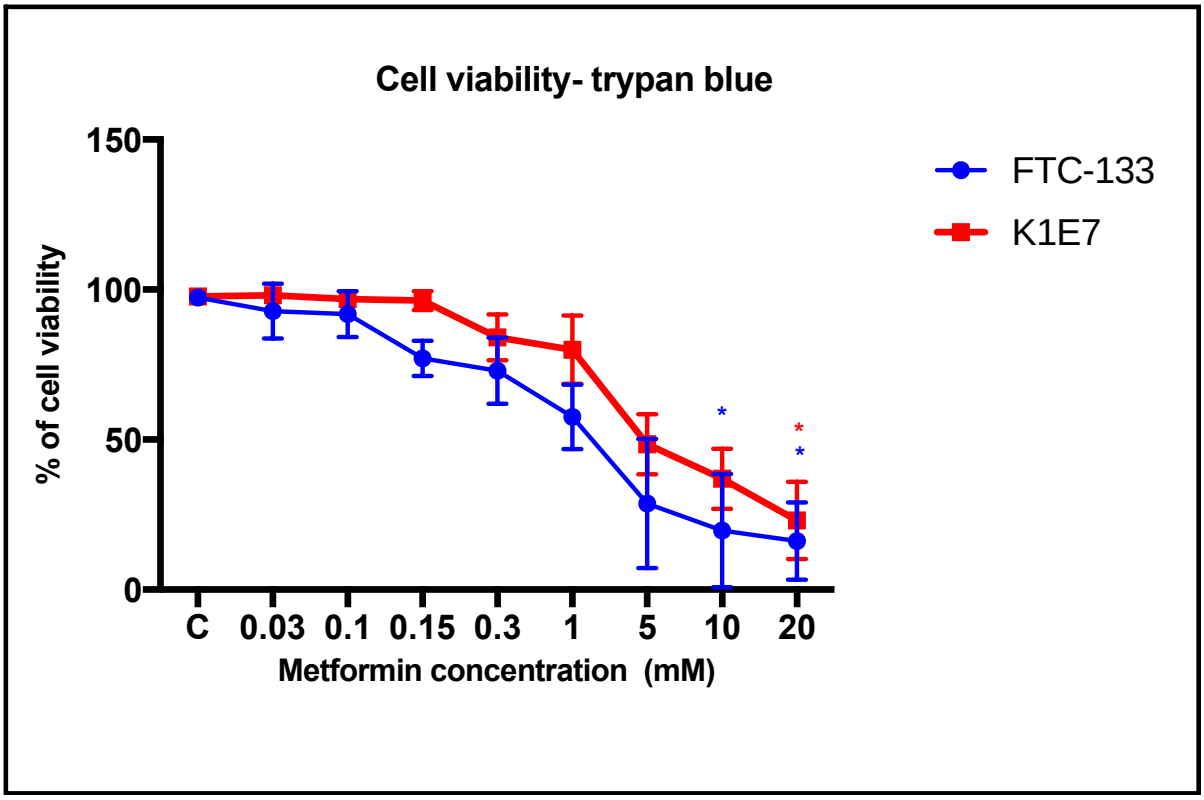

Figure 3.5: Cell viability assay (trypan blue).

Each data point represents the mean of three independent experiments for FTC-133 and K1E7 cells (shown in blue and red colours respectively). In each experiment, cells were treated with various concentrations of Metformin (as shown in the horizontal axis) in triplicate for 6 days. Error bars show the standard error of mean (SEM). Kruskal-Wallis test were used for multiple comparisons of more than two groups. * , P value < 0.05 vs control.

3.2.4 Clonal formation assay

Clonal formation assay was chosen to observe the anti-cancer effect of various concentrations of Metformin on cell growth and ability to form colonies over longer periods of time (14 days) compared to the MTT assay. The toxic concentrations of Metformin 10 mM and 20 mM were also studied in the pilot study, but the cells were unable to form colonies, due to the highly toxic effects of Metformin.

Cells were treated with concentrations of 0-5 mM Metformin, which include the therapeutic concentration of Metformin. The rationale for Metformin concentrations used in this clonal formation assay were discussed in the method and materials (section 2.2.4.1). The cells were cultured in petri dishes for 14 days then the number of colonies was counted. Inhibition of colony formation was evident at Metformin concentrations of 0.03 mM. The minimum statistically significant concentration of Metformin that was demonstrated to inhibit colony formation was 1 mM for K1E7 ($p = 0.02$), FTC-133 ($p = 0.02$), RO82-W-1 ($p = 0.03$) and 8305C ($p = 0.02$) and 5 mM for Nthy-ori 3-1 cells ($p = 0.005$) (**Figure 3.6a & Figure 3.7**). Colony formation was further decreased by increasing the concentration of Metformin and almost abolished at concentration of 5 mM (**Figure 3.6b**). The study also found significant differential effects of Metformin on colony formation between FTC-133 vs 8305C cells at concentrations of 0 mM ($p = 0.01$), 0.03 mM ($p = 0.01$), 0.1 mM ($p = 0.02$) and 0.3 mM ($p = 0.03$). The differential effects of Metformin on colony formation also were demonstrated in K1E7 vs 8305C cells reaching statistical significance at 0.3 mM concentration ($p = 0.04$). The clonogenic assay was also studied on the TT cell line but the TT cells did not form colonies.

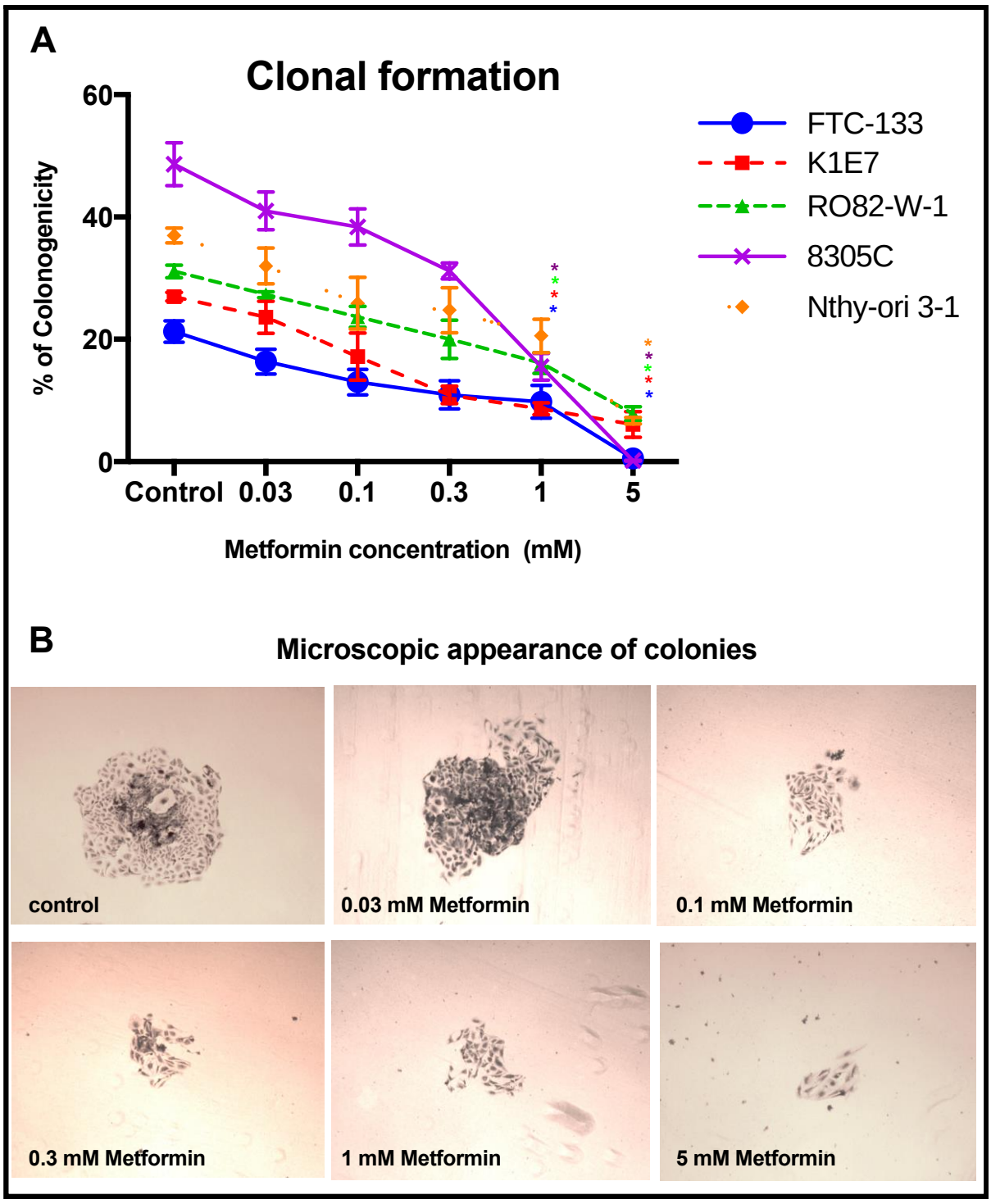

Figure 3.6: Clonal formation assay.

Panel A demonstrates percentage of cells that formed colonies (y-axis) in various thyroid cancer cell lines at 14 days over a range of concentrations of Metformin (x-axis). Panel B shows microscopic morphology of colony formation of FTC-133. After 14 days, pictures of colonies were taken of untreated cells and cells treated with Metformin (5 mM) using the Nikon glipse TS100 microscope at 4x magnification. Error bars show the standard error of mean (SEM). Kruskal-Wallis test were used for multiple comparisons of more than two groups. * , P value < 0.05 vs control.

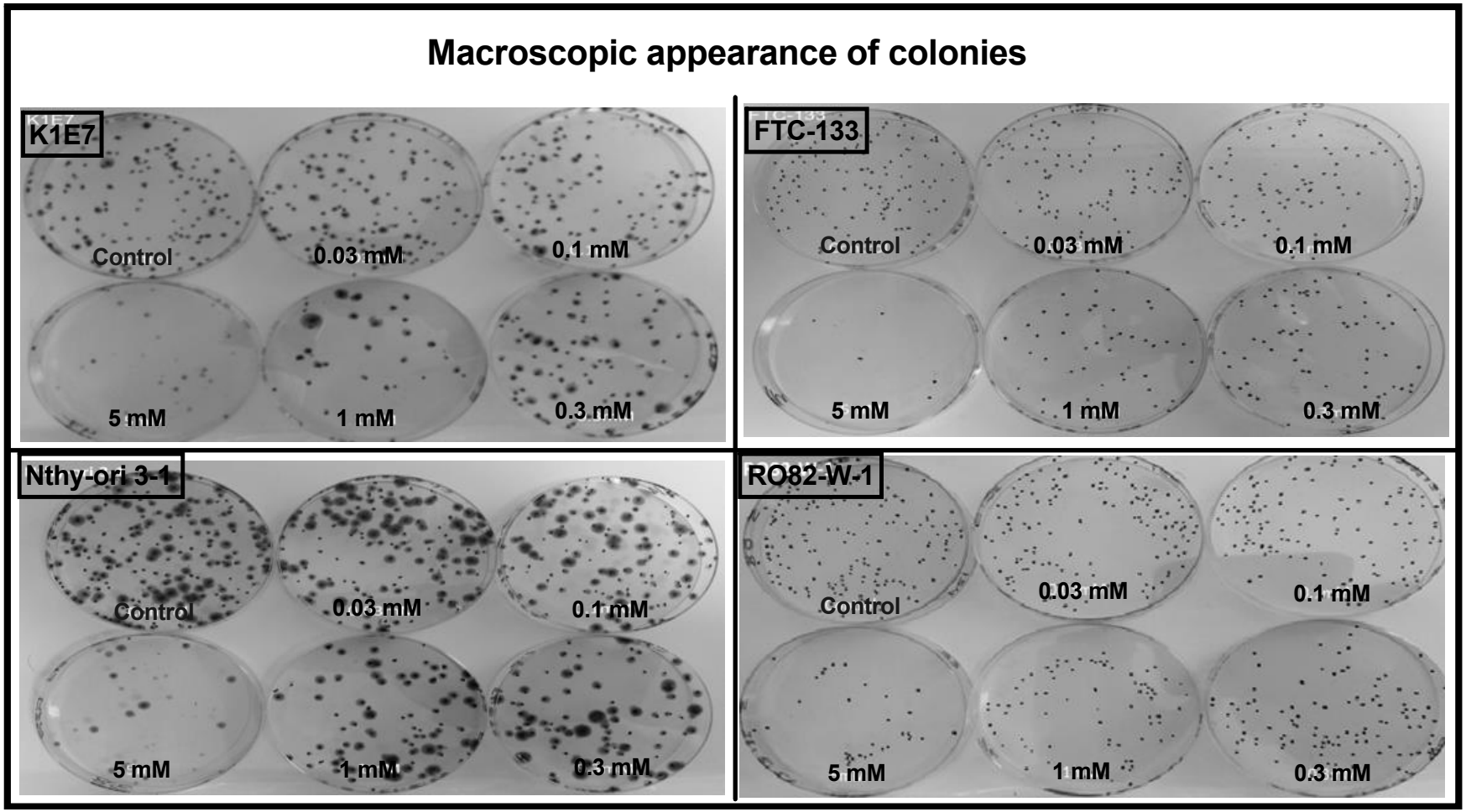

Figure 3.7: Clonal formation assay.

This figure shows the macroscopic morphology of colonies after cells were treated with various concentrations of Metformin for 14 days. 8305c cell line (not shown).

3.2.5 Cell migration (Scratch assay)

The effects of Metformin on cell migration were observed in five thyroid cell lines (K1E7, FTC-133, RO82-W-1, 8305C and Nthy-ori 3-1). Cells were cultured with silicone inserts to ensure a defined cell-free gap in each chamber. The cells were then treated with two concentrations of Metformin (0.3 mM and 10 mM) and incubated for 24 hours to provide a snap shot with therapeutic and toxic doses (section 2.2.5.1).

After 24 hours of exposure of thyroid cancer cells to Metformin at concentration of 0.3 mM, cell migration was inhibited (**Figure 3.8 & Figure 3.9**). At high concentration of Metformin (10 mM), there was further inhibition of cell migration. All cell lines responded to Metformin in concentration dependent manner. Metformin has shown similar anti migration effect on all cell lines. Metformin significantly inhibited cell migration at minimum concentration of 0.3 mM in FTC-133 ($p = 0.01$), K1E7 ($p = 0.004$), 8305C ($p = 0.001$) and Nthy-ori 3-1 ($p = 0.0001$) cell lines. In RO82-W-1 cells the anti migration effect of Metformin was not significant at concentration of 0.3 mM ($p = 0.12$). However, all cell lines significantly responded to anti-migration effect of Metformin at concentration of 10 mM ($p \leq 0.0001$). The process of quantification for migration assay was done by ImageJ software as discussed in section 2.2.5.2.

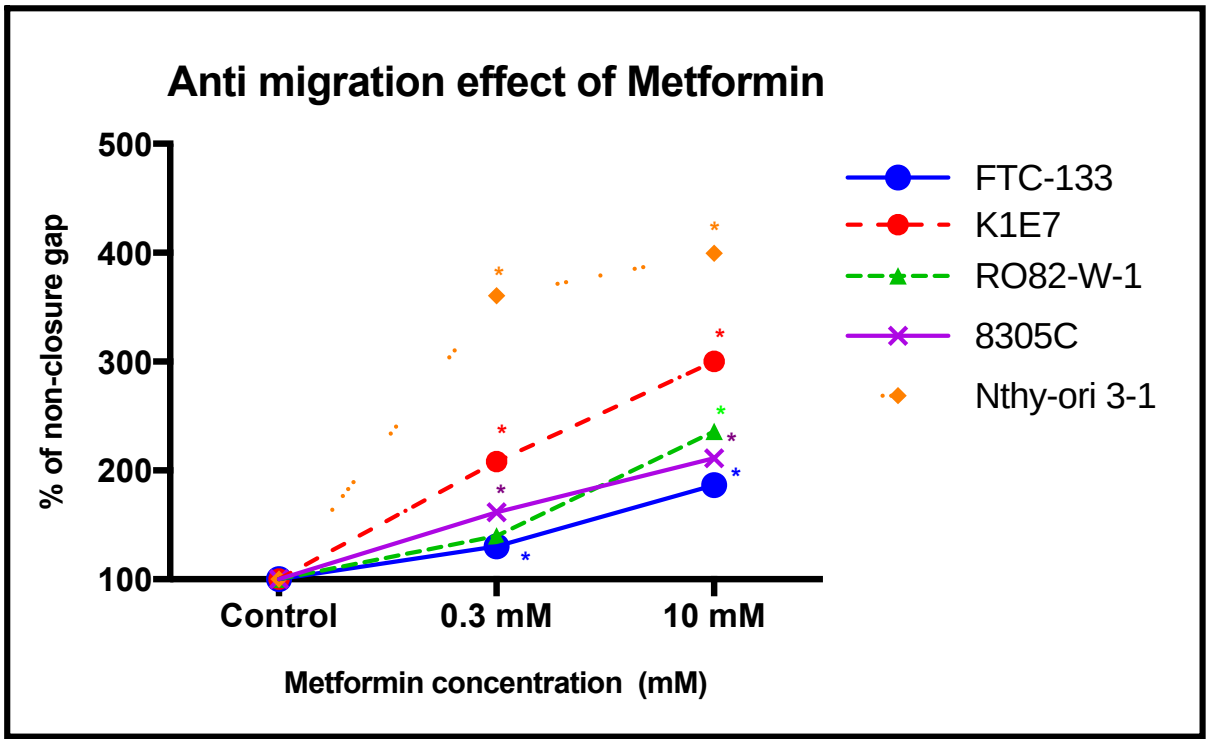

Figure 3.8: Quantification of scratch assay (migration assay).

This figure shows the percentage of remaining gap between the edges of control cells and Metformin treated cells. In all cell lines ImageJ software (using 20 repeatitive) was used to measure the gap closure and to calculate the remaining clear area after 24 hours time point. Kruskal-Wallis test were used for multiple comparisons of more than two groups. * , P value < 0.05 vs control.

K1E7 cells demonstrated cell migration in the control, but in the presence of Metformin cell migration was decreased in a concentration dependent manner and with fewer cells seen at 10 mM (**Figure 3.9**). In contrast to the other cell lines, FTC-133 cell growth was slow with minimal cell migration observed in control cells whilst Metformin inhibited the growth at 0.3 mM and cell death was seen at 10 mM. RO82-W-1 cells were also able to migrate to fill the gap in the control cells, but Metformin inhibited cell migration at 0.3 mM with less cells observed in the cells treated with 10 mM Metformin. In 8305C cells, cell migration was observed within the gap in the control group, but Metformin inhibited cell migration at 0.3 mM and 10 mM with fewer cells after treatment with Metformin. For Nthy-ori 3-1 cells, migration was observed in control cells but migration decreased in Metformin treated cells with cell death at 10 mM.

Therefore for all lines, migration was inhibited by 10 mM and there was visual evidence of toxicity.

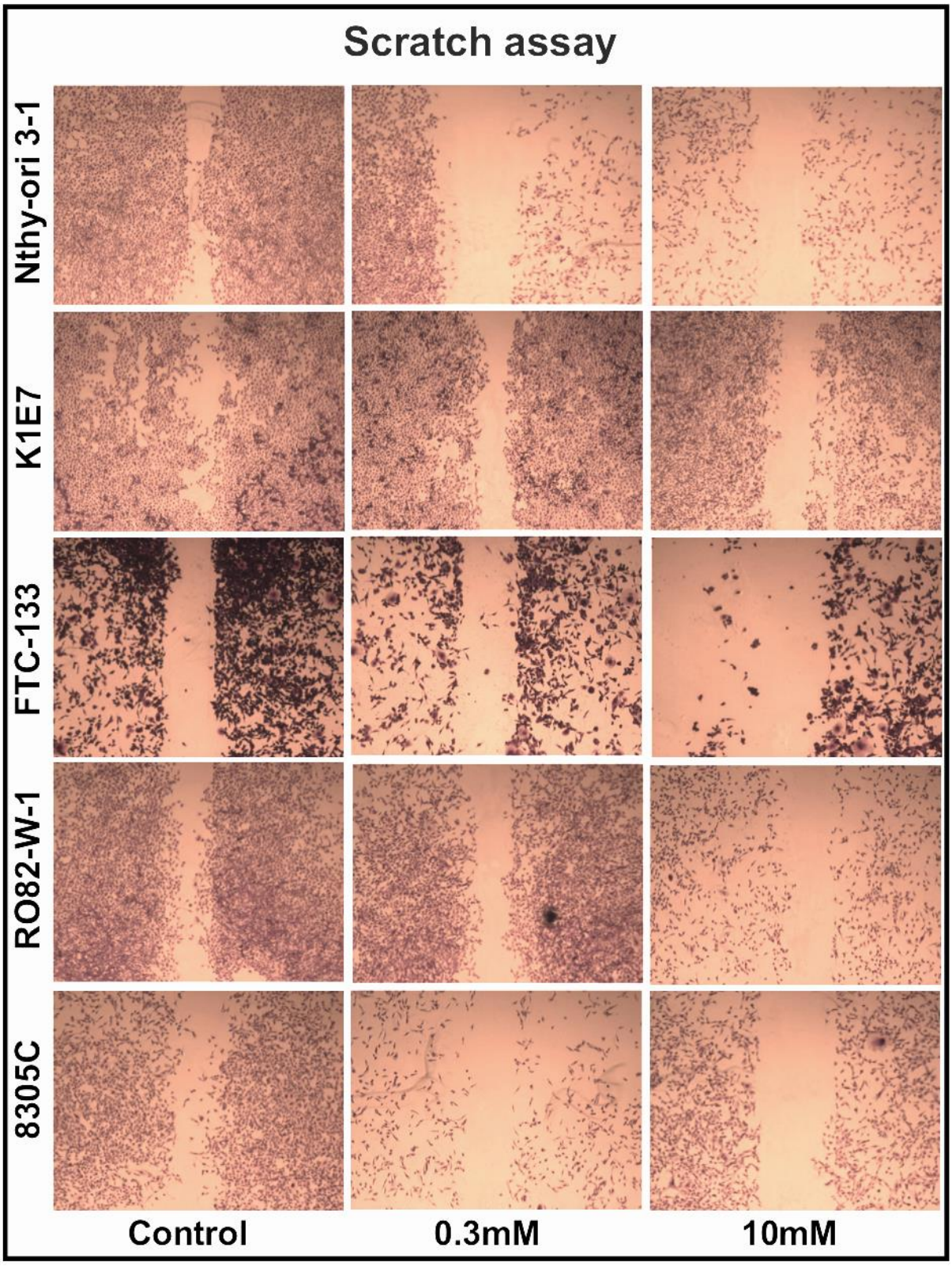

Figure 3.9: Scratch assay (migration assay)

After 24 hours, pictures of cells were taken of untreated cells and cells treated with Metformin (0.3 mM and 10 mM) using the Nikon glipse TS100 microscope at 4x magnification.

3.2.6 Flow cytometric analysis for apoptosis assay

Figure 3.10 & 3.11 shows that at concentrations of 0.1 mM and above, apoptosis was observed in all cell lines (K1E7, FTC-133, RO82-W-1, 8305C, TT & Nthy-ori 3-1) and this increased in a dose dependent manner.

In K1E7 cells, Metformin significantly promoted apoptosis at 10 mM and the percentage of viable cells, apoptosis and necrotic cells was 74.2 ± 3.38, 24.25 ± 3.24 & 1.55 ± 0.31 respectively ($p = 0.01$). In FTC-133 cells, the significant effect of Metformin-induced apoptosis was observed at concentration of 10 mM and the percentage of viable cells, apoptosis and necrotic cells was 24.21 ± 16.4, 68.09 ± 14.45 & 7.68 ± 2.12 respectively ($p = 0.007$). In RO82-W-1 cells, Metformin slightly induced apoptosis but not reached significant level and at 10 mM the percentage of viable cells, apoptosis and necrotic cells was 92.35 ± 4.5, 5.87 ± 3.0 & 1.77 ± 1.48 respectively ($p > 0.9$). In 8305C cells, Metformin significantly induced apoptosis at concentration of 10 mM and the percentage of viable cells, apoptosis and necrotic cells was 55.08 ± 23.34, 38.73 ± 24.25 & 6.18 ± 5.07 respectively ($p = 0.01$). The TT cells had higher levels of apoptosis before treatment with Metformin compared to other cells. At TT cell lines Metformin significantly induced apoptosis at minimum concentration of 10 mM and the percentage of viable cells, apoptotic cells and necrotic cells was 19.61 ± 1.42, 79.55 ± 1.57 & 0.83 ± 0.21 respectively ($p = 0.01$).

It is also of interest that the Nthy-ori 3-1 normal thyroid cells appeared less responsive, with apoptosis only marginally significant at 10 mM ($p = 0.04$) and the percentage of viable cells, apoptosis and necrotic cells was 94.22 ± 1.81, 4.46 ± 1.16 & 1.31 ± 0.8 respectively.

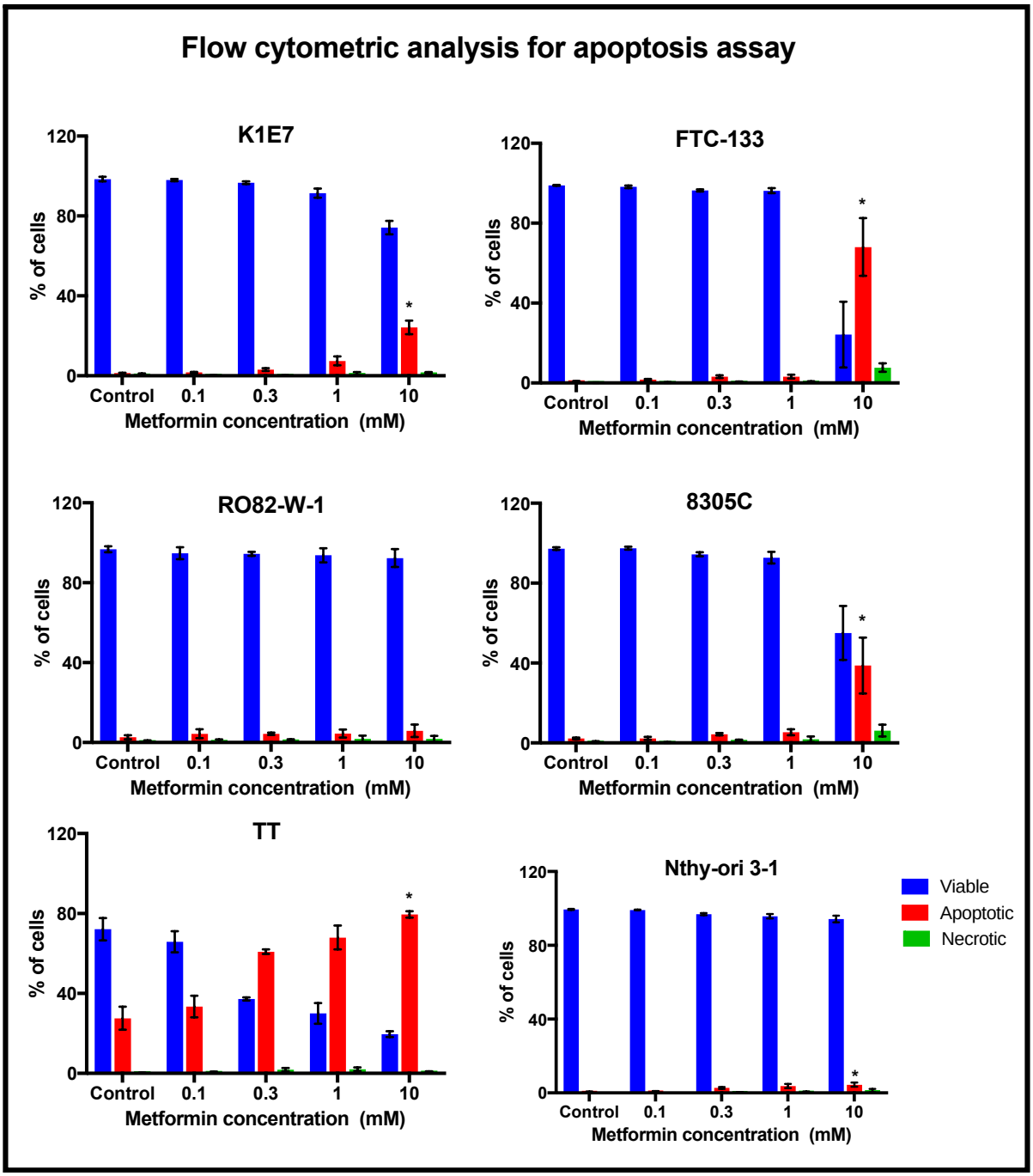

Figure 3.10: Flow cytometric analysis for apoptosis assay.

Each bar represents the mean of three independent experiments (each done in triplicate). In each experiment, cells were treated with various concentrations of Metformin for 6 days (horizontal axis). The % of apoptotic, necrotic and viable cells shown in different patterns. Error bars show the standard error of mean (SEM). Kruskal-Wallis test was used for multiple comparisons of more than two groups. *, p value < 0.05 vs control.

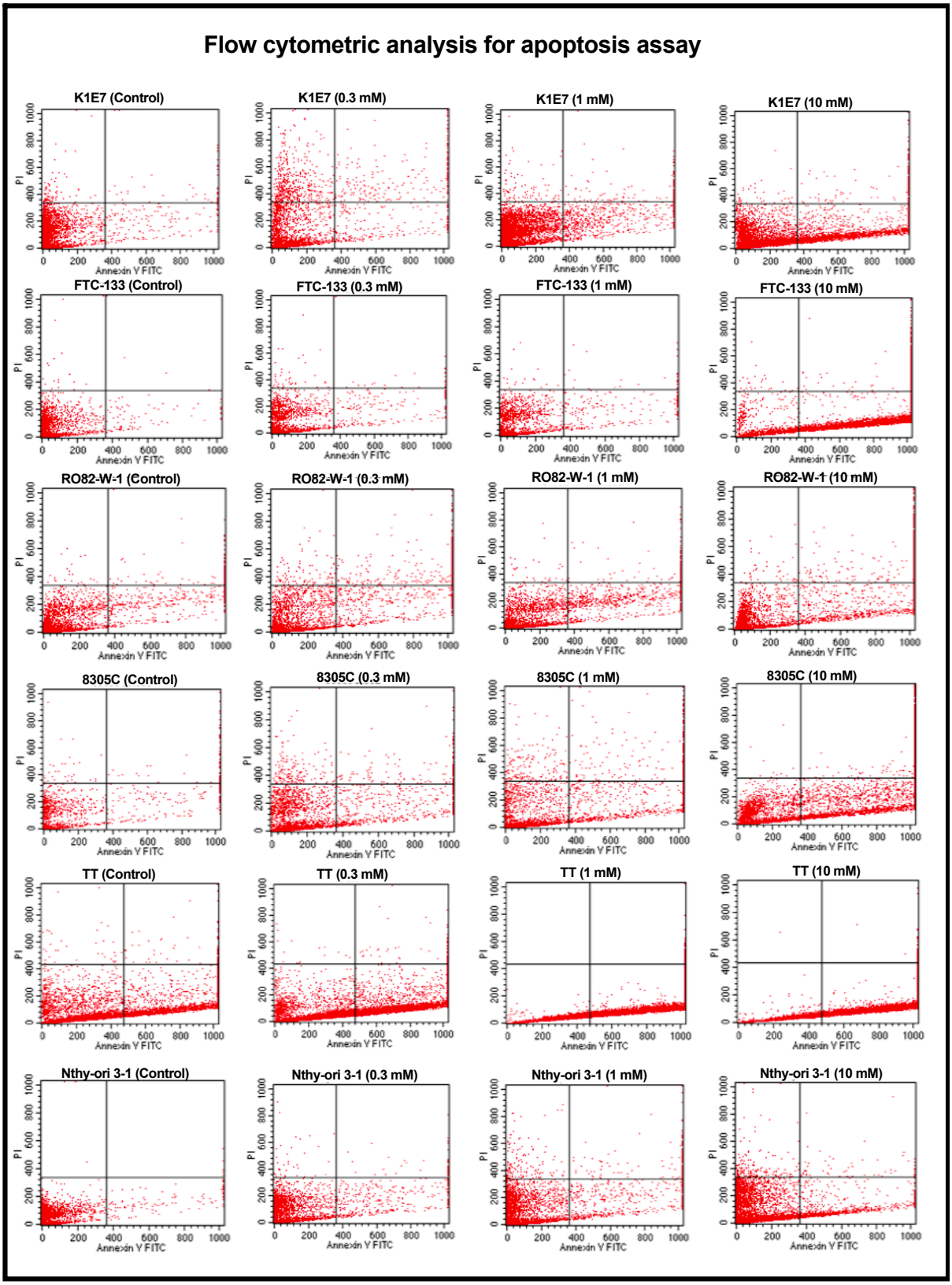

Figure 3.11: Flow cytometry scatter plots for apoptosis assay.

Plot of cells that positive to annexin v FITC against PI. Each square shows population of viable cells (LL), apoptosis (LR), necrotic (UL) & a mix of apoptotic and necrotic cells (UR).

3.2.7 Flow cytometric analysis for cell cycle assay

Figure 3.12 and 3.13 shows that Metformin increased the percentage of cells in G0/G1 phase in a concentration dependent manner. This is probably due to cell cycle arrest in G0/G1 phase. The results were statistically significant at concentrations of 10 mM in all thyroid cell lines except Nthy-ori 3-1. The percentage of thyroid cells in G0/G1 phase for the concentrations of Metformin used in the study (control, 0.3 mM, 1 mM and 10 mM) was 34.4%, 43.3%, 43.3% and 51.3% respectively in K1E7 cells, 57.9%, 65.5%, 72.7% and 74.3% respectively in FTC-133 cells, 56.5%, 62.5%, 70% and 77.3% respectively in RO82-W-1 cells, 56.7%, 63.9%, 69.8% and 71.4% in 83O5C cells and 58.8%, 69.8%, 95.3% and 95.6% respectively in TT cells

In Nthy-ori 3-1 cells, the percentage of G0/G1 cells remained unchanged with Metformin treatment. The percentage of Nthy-ori 3-1 cells following treatment with Metformin ((control, 0.3 mM, 1 mM and 10 mM) was 53.4%, 53.9%, 55.3% and 56.2% respectively.

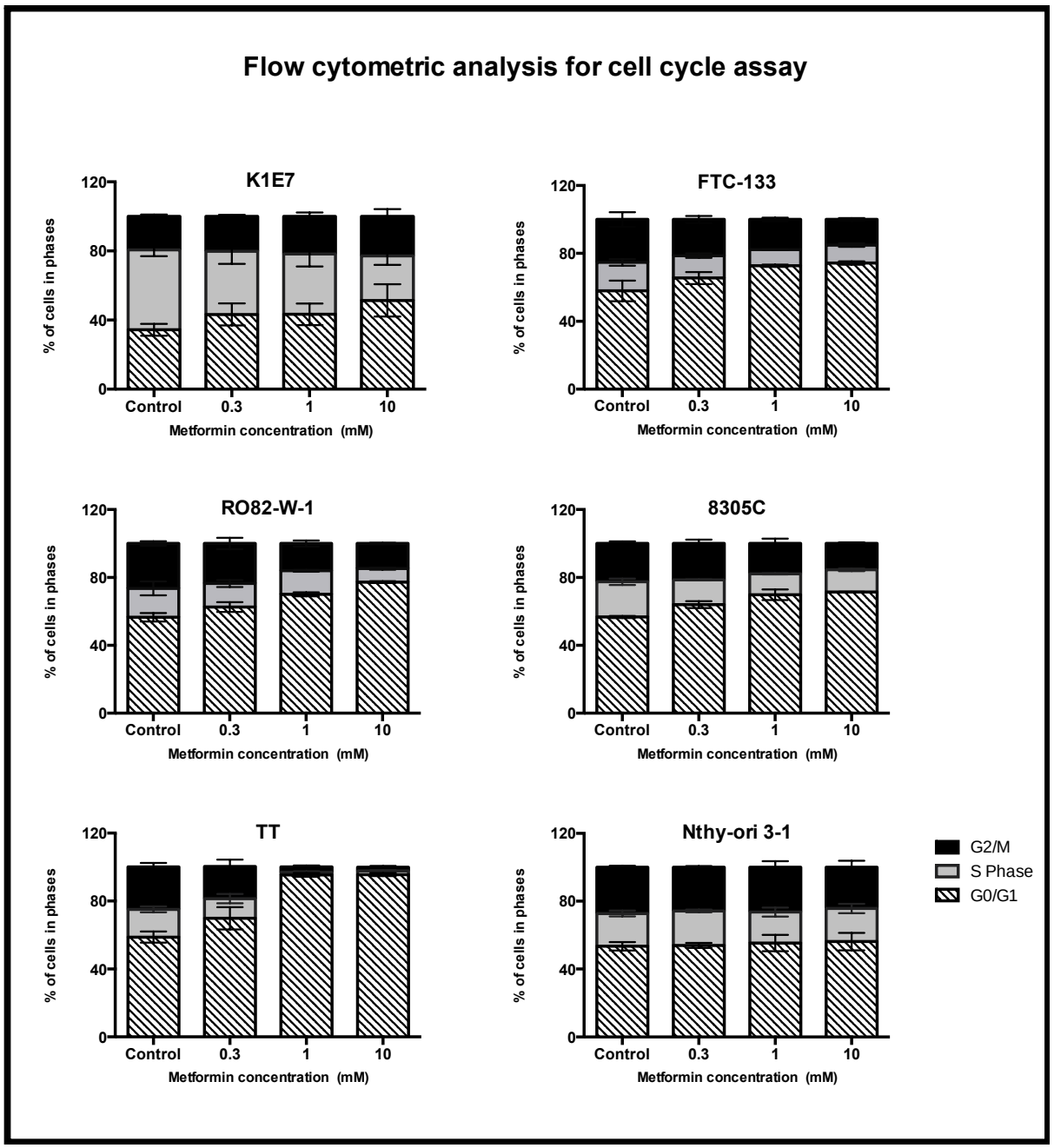

Figure 3.12: Flow cytometric analysis for cell cycle assay.

Each bar represented the mean of three independent experiments (each done in triplicate). In each experiment, cells were treated with various concentrations (as shown in horizontal axis). The percentage of viable cells in different phases shown in different patterns and colors. Error bars show the standard error of mean (SEM).

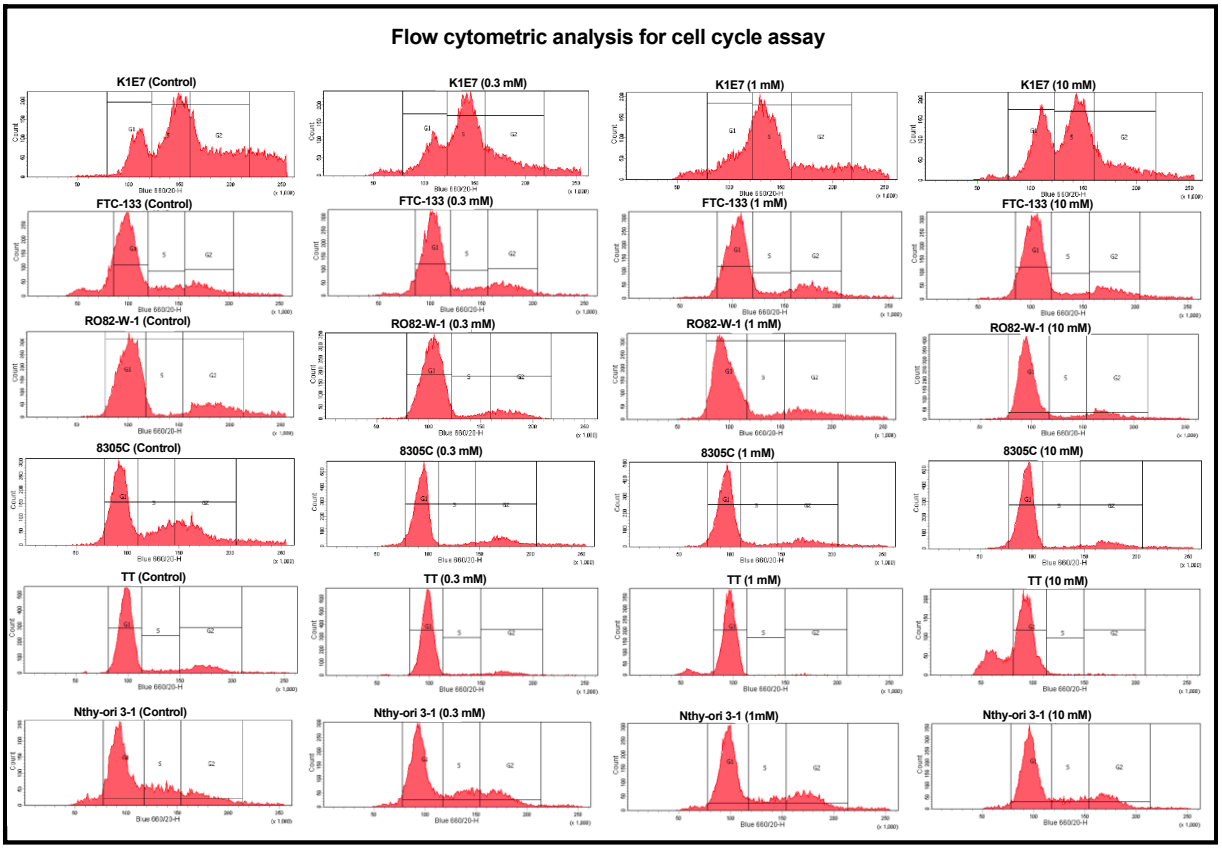

Figure 3.13: Flow cytometry plots for cell cycle assay.

This figure shows number of cells in different phases of cell cycle (G1, S and G2)

3.2.8 γH2AX assay for DNA repair

Previous studies reported that Metformin induced double strand breaks and could affect DNA repair in nasopharyngeal carcinoma cells and mammalian cells [167, 168]. To confirm if Metformin had any DNA-damaging properties, its effects in combination with radiation have been explored. Radiation is used to treat some thyroid cancers and other thyroid cancers may arise due to radiation exposure. Metformin treatment could increase the effectiveness of radiation or produce damaging side effects if DSB occurs.

In untreated cells (control), and cells treated with Metformin (0.1 mM and 20 mM) very low levels of phosphorylation of γH2AX foci were detected at the comparable post irradiation time points for all cell lines (**Figure 3.14 & 3.15**). Following radiation for the K1E7 cell line, the percentage of cells with more than 10 γH2AX foci was

99.6% at 30 minutes, 83% at 1 hour and 76% at 2 hours. Similar results were observed in FTC-133, RO82-W-1, 8305C and TT; In FTC-133 cell line, 97.66% at 30 minutes, 85.33% at 1 hour and 74% at 2 hours; In RO82-W-1 cell line, 98.33% at 30 minutes, 88% at 1 hour and 80% at 2 hours; In 8305C cell line, 97.33% at 30 minutes, 85% at 1 hour and 79% at 2 hours; In TT cell line, 97% at 30 minutes, 85.33% at 1 hour and 80% at 2 hours.

Following radiation for the Nthy-ori 3-1 cell line, the percentage of cells with more than 10 γH2AX foci was In Nthy-ori 3-1 cell line, 87% at 30 minutes, 56.33% at 1 hour and 31% at 2 hours.

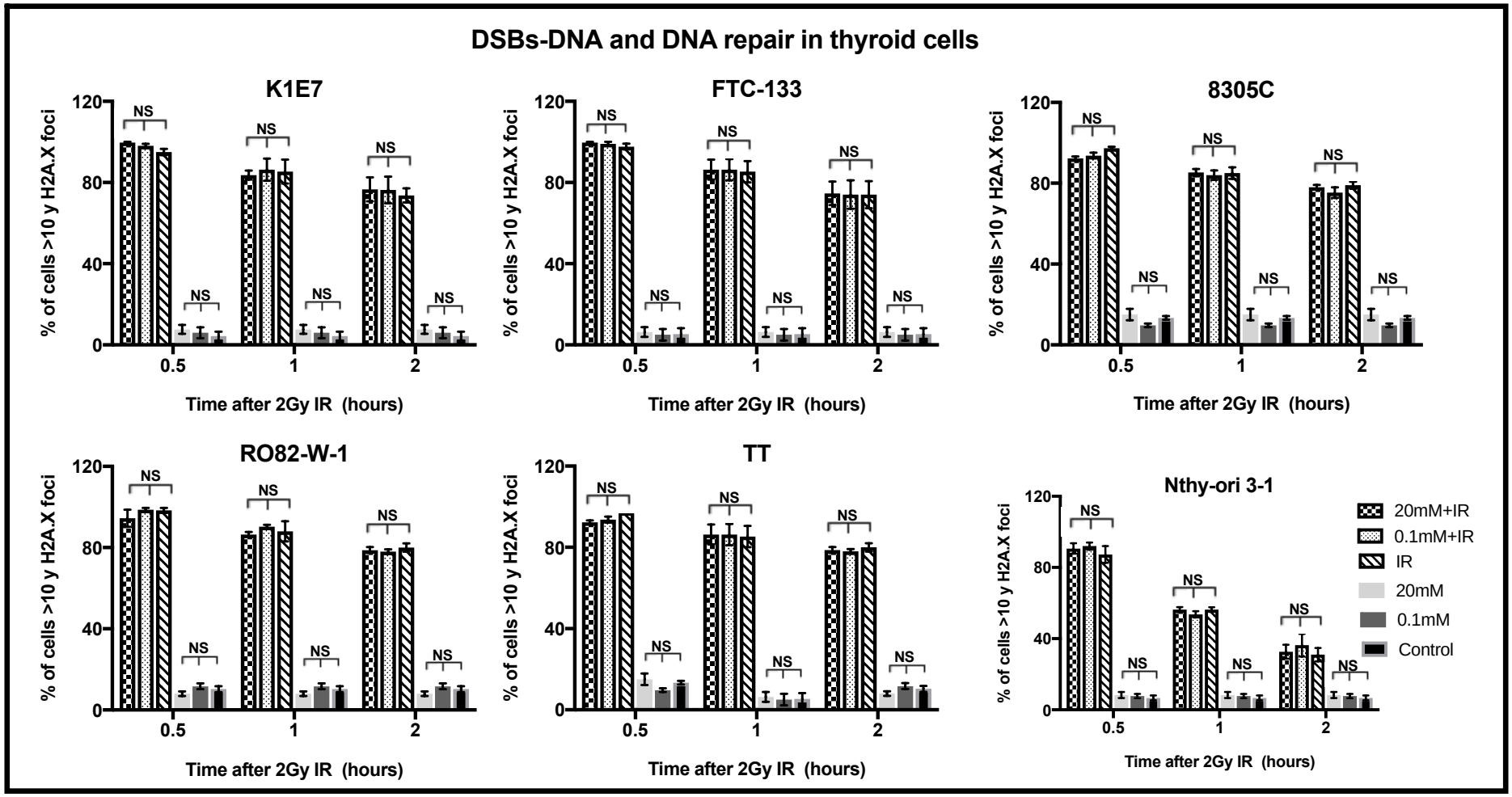

Figure 3.14: The effect of Metformin on DSBs and DNA repair in thyroid cells.

γH2AX assay shows DSBs-DNA and DNA repair in KIE7, FTC-133, RO82-W-1, 8305C, TT and Nthy-ori 3-1 cells. Each bar represented the mean of three independent successful experiments. Cells were either treated with Metformin (0.1 mM and 20 mM) for 144 hours or treated with Metformin for 144 hours and followed by radiation 2 Gy IR (0.1 mM + IR and 20 mM + IR) or cells irradiated with 2Gy IR only (IR). Kruskal-Wallis test was used for multiple comparisons of more than two groups. NS (not significant) P value > 0.05.

Following radiation the γH2AX foci appear as a small immunofluorescence stained red dotted in blue background cell stained with DAPI and by time the number of γH2AX foci was decreased (**Figure 3.15**).

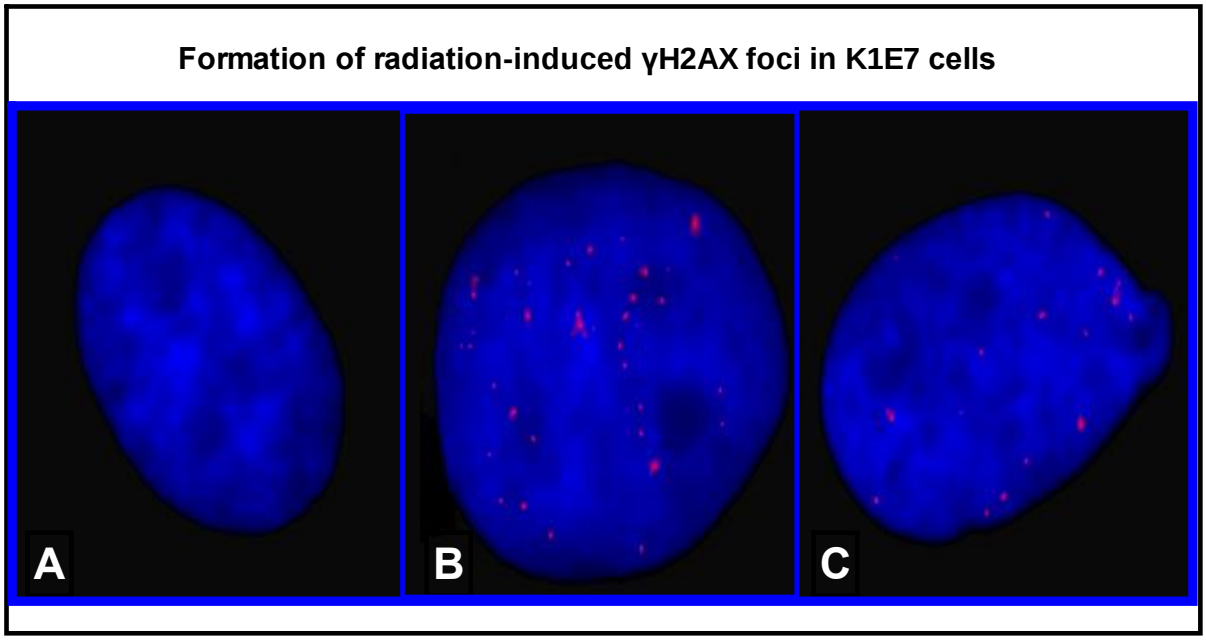

Figure 3.15: Formation of radiation-induced YH2AX foci in K1E7.

γH2AX assay shows formation of radiation-induced γH2AX foci in K1E7 cells. The picture was taken via immunofluorescence microscopy at 100x magnification. Panel A shows no γH2AX foci formation in control cells. Panel B shows > 10 γH2AX foci formation at 0.5 hour after irradiated cells with 2 Gy IR. Panel C shows a decrease the number of γH2AX foci formation at 2 hours after irradiated cells with 2 Gy IR.

Data variability was assessed while training for the γH2AX assay, the γH2AX score was determined in real time a second independent observer did not score the results.

3.3 Discussion

Human cancer cell lines play a critical role in the study of cancer biology and therapy. Historically, HeLa is the oldest established human cell line and was derived from human cervical cancer [144]. Several factors can contribute to cross-contamination and misidentification of human cell lines. These include mislabelling of cell lines during sub-cultures, using same pipettes for different cell lines, unplugged pipettes, sharing reagents and media between cell lines [156, 169], mutations after several passages [155] and incorrect diagnoses by pathologists [157]. HeLa cell line cross-contamination with other cell lines, was first reported in 1960 [170] and 1962 [171]. In a study on 100 human cell lines, 18.8% of cell lines in the national cell bank of Iran were cross-contaminated [155]. The German collection of microorganisms and cell culture reported that misidentification or contamination occurred in 18% of 252 cell lines used [143]. In a study on 6 human adenoid cystic carcinoma cell lines, all 6 cell lines were found to be contaminated with other cell lines [172]. Shweppe et al (2008) evaluated 40 human thyroid cancer cell lines; many of them are commonly used in thyroid cancer studies. The findings of this study showed that 50% of these cell lines were cross-contaminated or misidentified [173]. These misidentified cell lines had been used in a large number of publications thereby raising doubts about the validity of their findings.

In this study, to validate the thyroid cell lines, ten STR loci were studied for Nthy-ori 3-1, K1E7 and FTC-133. The observed STR profiles for the cell lines were then compared with culture collections in Public Health England website (http://www.hpacultures.org.uk) and matched with their specific STR profiling (**Table 3.1**). This demonstrates that these cell lines (Nthy-ori 3-1, FTC-133 and K1E7) are valid and are not cross-contaminated or misidentified. The other cell lines (RO82-W-1, 8305C and TT) were purchased from the European Collection of Cell Culture (ECACC) with a known STR profile; hence a repeat authentication experiment was not performed.

The aim of this study was to investigate the effect of Metformin and explain the observations of the clinical studies where Metformin reduced the risk of cancer. Some of the data presented here repeats an earlier investigation in which high doses of Metformin was used, but this study specifically set out to examine the effects of Metformin within a therapeutic range, and for the first time explore the effect over a longer time frame.

The cell lines evaluated in this project represent different types of thyroid cancer seen in clinical practice. Initially, proliferation of all cell lines (normal thyroid, thyroid cancers and breast cancer cell line MCF-7) was studied following exposure to a broad range of Metformin concentrations ranging from sub-physiological to supra-physiological concentrations (0.3 mM – 20 mM). Our findings demonstrated that Metformin reduced proliferation, supporting earlier investigations on thyroid cancer [106, 129] and the control breast cancer cell line MCF-7 [125, 126]. In previous studies however, cells were treated with high concentrations of Metformin for relatively short periods of up to 3 days [104]. In this study, Metformin was tested at therapeutic doses over a longer time period (1 -14 days). These results suggest that at lower physiological doses (0.01-0.3 mM) [132, 163], Metformin does dampen cell proliferation in cancer and normal cell lines (**Figure 3.4**).

The clonogenic assays demonstrated that Metformin inhibited colony formation from a low concentration of 0.3 mM and almost abolished colony formation at 5 mM. When combining the observations on cell proliferation with those of the clonogenic assays (**Figure 3.6**), the dampening effect appeared enhanced over time, with the lowest significant dose (affecting proliferation) dropping from 5 mM at day 3 to 1 mM Metformin at day 14 (**Figure 3.2, 3.3 & 3.6**). The effects of Metformin on clonogenicity have been intensively investigated in other cancers and also thyroid cancer cell lines. As with these earlier studies [104, 125, 130] we found that supra-physiological concentrations of Metformin (1 mM and 5 mM) virtually obliterated colony formation for some cell lines (8305C and FTC -133) (**Figure 3.6**). Furthermore, we found that at concentrations above 5 mM no colonies were formed and cells were dead at 14 days (data not shown). The action of

Metformin appears wide ranging, and whilst only high doses clearly affect proliferation at 24hrs in MTT assay (**Figure 3.4**) its effect on other processes is evident even at lower doses, with 0.3 mM inhibiting migration in the scratch assay (**Figure 3.8 & 3.9**), suggesting that Metformin targets different pathways to varying degrees. The limitations for the migration assay were that only 1 time point was used to investigate the influence of Metformin on cell migration. The TT cell line was not recovered at that time and so it was not possible to investigate the effects of Metformin on the migration of TT cells. It was clear that high dose Metformin 10 mM affected both viability and proliferation of the cells and far fewer cells were left in the wells after 10 mM treatment; the more highly proliferative lines should potentially be able to fill the gap quicker.

How does Metformin exert its action on thyroid cancer cells? This is unclear but it is thought that the growth inhibitory effect of Metformin on cancer cell proliferation may be through the activation of AMPK (via LKB1). This in turn causes inhibition of mammalian target of rapamcycin (mTOR) pathway (which promotes growth and proliferation) [85, 174]. In numerous human cancers, mTOR is associated with increased cell growth and proliferation [175]. In addition to the above, it has been suggested that the growth inhibitory effect of Metformin on tumour growth may be indirect - by a decrease in circulatory tumour growth factors such as glucose [4, 87], insulin [87] and TSH [145, 146]. Insulin and glucose may play a critical role in tumour growth and malignant transformation through stimulation of insulin and IGF-1 receptors [88-90, 176]. As TSH has been shown to specifically promote thyroid cancer growth in rat [177] and mouse models [178], it may be suggested that Metformin would be specifically effective against thyroid cancers, as previous studies have reported that Metformin decreased TSH level without change in FT4 [145, 146]. In term of Metformin doses is unclear whether higher doses of Metformin may act via a different mechanism but this need further investigations.

This study also demonstrated that Metformin induced apoptosis and cell cycle arrest in thyroid cancer cells, increasing both the percentage of apoptosis

cells and accumulating cells in G0/G1 phase (**Figure 3.10 & 3.12**). Similar findings were reported in other studies on different cancers, including thyroid [104, 179, 180]. It is however of interest that the normal thyroid cell line Nthy-ori 3-1 appeared relatively unaffected by Metformin even at doses of 10 mM at 6 days. These cells only showed low levels of apoptotic cells, negligible necrosis and no change to the percentage of cells in GO/G1 (**Figure 3.10 & 3.12**).

Furthermore, colony formation for all thyroid cancer cell lines was inhibited at 1 mM; but for the Nthy-ori 3-1 cell line, it was significant only at 5 mM. In contrast, TT (medullary thyroid cancer cell line) had naturally high levels of apoptosis, which increased dramatically on exposure to Metformin. At 10 mM, Metformin virtually obliterated TT cell division and stalled the majority of the cells in G0/G1 (**Figure 3.12**). The observations of apoptosis and cell cycle assist in explaining the varying responses of the different thyroid cancers to Metformin. For example it seems that the high natural rate of apoptosis in TT means that it is the most sensitive to low doses (**Figure 3.3 & 3.4**) and that high doses will have a catastrophic effect even at day 1 (**Figure 3.4**) that tips the balance in favour of apoptosis and stalls the remainder of the cells in G0/G1 (**Figure 3.4 and 3.10 & 3.12**). As only one medullary thyroid cancer cell line was studied, it is not possible to say if this subtype is particularly sensitive, or whether the naturally high level of apoptosis affects its response to Metformin. Recently, it has been reported that the *RET* induced medullary thyroid cancers show increased apoptosis in response to therapy targeting the *RET* oncogene [181, 182] with inhibition of the MAPK and mTOR pathways. Another study suggested that Metformin targets these pathways in medullary thyroid cancer [105]. These observations in combination with our findings suggest that some subtypes of thyroid cancer may be more sensitive to Metformin than others. However, it is too early to say if these differences are clinically relevant. Variation in the response to Metformin among the different sub-types of thyroid cancer may explain why a recent study has not found any decreased risk of developing thyroid cancer for Metformin users [183].

How Metformin exerts its action on thyroid cancer cells is unclear, but unlike previous investigations [168] this study did not find that exposure to Metformin induced DNA damage; even treatment with 20 mM of Metformin for 6 days (prior to measuring DNA damage) although significantly reducing proliferation did not increase DSBs-DNA in the absence of IR (**Figure 3.14**). In this study, the kinetics of formation and loss of γH2AX foci were investigated in K1E7, FTC-133, RO82-W-1, 8305C, TT and Nthy-ori 3-1 cells. The findings demonstrated very low DSBs-DNA in non-irradiated cells (with or without Metformin) compared to cells irradiated with 2Gy IR. We found high DNA damage in all cell lines at 30 minutes after cells were irradiated with 2 Gy IR compared to control. In Nthy-ori 3-1 cells, there was a relatively rapid elimination of γH2AX foci at 1 hour and 2 hours after radiation compared to thyroid cancer cells. The results show that Nthy-ori 3-1 was able to repair DSBs faster compared to cancer cell lines. DNA repair is essential to reproduce correct sequences and avoid malignant transformation [184, 185]. Normal cells have low levels of genetic instability as opposed to cancer cells; in addition cancer cell lines are more sensitive to radiation compared to normal cell lines. Ataxia-telangiectasia mutated (ATM) [186] and DNA-dependent protein kinase (DNA-PK) [187] genes are mutated in cancer cell lines; resulting in reduced phosphorylation of H2A.X, thus impairing the ability to repair DSBs. These findings suggest that Metformin neither induces DSBs-DNA nor promotes DNA repair. Similar findings were reported in a study on human lymphocytes, where oxidative stress induced DNA damage and the influence of Metformin was investigated. The findings demonstrated that DNA damage was not prevented by Metformin at concentrations of 0.01 to 0.05 mM [188].

This is the first *in vitro* study that looks at longer-term exposure to low dose Metformin in thyroid cancer. This investigation has demonstrated that the cumulative effects of Metformin increase over time for all types of thyroid cancer, and suggests that even sub-physiological doses alters behaviour and can act to dampen down the proliferative response. In combination, our results possibly explain why prolonged exposure to therapeutic doses, as

occurs in diabetic patients, may account for the observed longer disease free survival from thyroid cancer in these populations [189].

3.4 Is Metformin selectively affecting thyroid cancer over normal thyroid tissues?

The current investigations found that Metformin inhibited cell proliferation in all cell lines in a concentration and time dependent manner. However, some variations were observed in cancer cell lines compared to normal cells in response to Metformin treatment. Metformin inhibited cell proliferation significantly at 5 mM at day 3 in cancer cells and day 4 in normal cells (section 3.2.3). Similar observations were reported in a previous study where normal lines were less sensitive to Metformin treatment compared to cancer lines [104]. The minimum significant concentration of Metformin to inhibit the colony formation was decreased from 5 mM to 1 mM in cancer cells but normal cells remained at 5 mM (section 3.2.4). In addition, Metformin significantly induced apoptosis and cell cycle arrest in cancer cells at 10 mM but normal lines were less sensitive to Metformin in terms of apoptosis and also cell cycle (section 3.2.6 & 3.2.7). Furthermore, the normal lines demonstrated more rapid DNA repair compared to cancer lines following radiation (section 3.2.8). The overall findings suggested that Metformin was selectively affected cancer cells over normal tissues. The findings of this current study are therefore in broad agreement with other investigations on numerous cancer types that suggest normal tissues, although responding to Metformin treatment are overall less sensitive [104, 106].

3.5 Conclusions

In summary, Metformin inhibited cell proliferation in a concentration and time dependent manner. Metformin also inhibited colony formation, cell migration, induced apoptosis and cell cycle arrest in a concentration dependent manner. Metformin does not induce or prevent DSBs-DNA and does not promote DNA repair in thyroid cancer cells. The study demonstrated high level of DSBs-

DNA in thyroid cancer cell lines after radiation followed by a reduction with time. Further work will be aimed at understanding the molecular mechanisms of the above effects of Metformin and its interactions with TSH, insulin, IGF-1 and glucose in the environment.

CHAPTER FOUR

Modulating the anti-cancer effects of Metformin

4.1 Introduction

Metformin is effective in the treatment of diabetes by decreasing blood glucose, through prevention of glucose production in the liver, whilst increasing the sensitivity of muscle and fat cells to insulin [5]. The action of Metformin may be influenced by regulatory factors, which are altered as a consequence of the disease. Indeed, in the previous chapter, the anti-cancer effect of Metformin on a number of different thyroid cancer cell lines was investigated only after standardization of the amount of glucose to be included in the media (section 3.2.2). In this chapter, the effects of glucose and regulators important in controlling diabetes (insulin, IGF-1) were explored in more depth. Furthermore, the modulation by TSH was also studied, as TSH suppression therapy is currently used for the treatment of thyroid cancer post-surgery and the main goal of thyroxine therapy is to reduce the levels of TSH (that may act as a growth factor) in thyroid cancer patients [39], TSH actions may be synergistic or antagonistic to Metformin.

Glucose ($C_6H_{12}O_6$) is a simple monosaccharide that is the main source of energy used by cells within the body, and is metabolized in the cytosol by glycolysis, either aerobically or anaerobically [190]. The importance of glucose on promoting cancer growth and proliferation has been extensively studied in many cancer types for example breast, colon, pancreatic and thyroid [191-199] and universally increases growth. Furthermore, the epidemiological data on several types of cancer has shown that high blood glucose associates with an increased risk of cancer [200, 201]. The effect of glucose on the action of Metformin has also been studied. A recent study on breast cancer cell lines (MDA-MB-231) showed that the anti-cancer effect of Metformin was highly dependent on glucose concentration [192]. The study showed that Metformin inhibited MDA-MB-231 cell growth in the medium containing 5 mM of glucose, but the anti-cancer effect of Metformin was abolished in medium containing 25 mM of glucose, as determined by the MTT assay after 48 and 96 hours incubation. The amount of glucose in the medium may also influence the anti-cancer effect of Metformin on thyroid cancer cells. A recent study on the thyroid cancer cell line (FTC-133) showed that the anti-cancer effects of

Metformin depends on the glucose concentration in the medium [195], with Metformin inhibiting thyroid cancer cells in a dose dependent manner when the medium contained no glucose; but Metformin was less effective when the medium contained 5 mM and 20 mM of glucose.

Glucose levels are regulated by insulin, a hormone, which is secreted from beta cells of the pancreas. Insulin secretion by the pancreas is increased in response to high levels of glucose in the blood, and enhances glucose absorption by various cells in the body such as fat cells, muscle cells and red blood cells. In the case of low levels of glucose in the blood, insulin secretion by the pancreas is decreased to maintain the normal level of glucose in the blood. The effect of insulin on cancer has also been investigated in population based studies; Hemkens and colleagues conducted a cohort study by using records of German health insurance between 1998-2005 of 127,000 patients treated with insulin and noted the incidence for cancer [202]. They found that treatment with insulin is associated with an increased risk of cancer. The findings of this study can be given more weight, because of the large numbers of patients involved. However, the study had limitations as information on the body mass index and duration of diabetes was not available. The effect of insulin on cancer cell proliferation has also been studied *in vitro.* A study on colon cancer cell lines (Caco-2 and HT-29) treated with various concentration of insulin (10^{-14}, 10^{-12}, 10^{-10}, 10^{-8} and 10^{-6} mol/L) for 3 days [203], found that insulin promoted cell proliferation. Similar findings were observed in a study for prostate cancer cell lines (LNCaP, C4-2 and P69), but in contrast insulin has no effect on cell proliferation in other prostate cancer cell lines in the same study (M12 and PC3) [204]. Of more relevance to the current investigation, a study in which anaplastic thyroid cancer cell lines (HTh74 and HTh74Rdox), were treated with insulin in the presence and absence of Metformin (10 µg/ml of insulin only, 5 mM or 10 mM of Metformin only and Metformin + insulin) for 3 days [104], insulin promoted cell proliferation and induced ERK phosphorylation. Furthermore, the study also found that Metformin abolished the effect of insulin on cell proliferation and extra cellular signal-regulated kinase (ERK) phosphorylation. Insulin promotes cancer cell proliferation through the activation of phosphoinositol-3 kinase/Akt (P13K-Akt)

pathway and inhibition of insulin growth factor binding protein 1 and 2 (IGFBP-1 & IGFBP-2), leading to the release of free IGF-1 and activation signalling via IGF1-receptor [205]. P13K/Akt signaling pathways play an important role in cell growth [206] and cell cycle entry at G1/S [207] and inhibition of apoptosis [208, 209].

Insulin-like growth factor 1 (IGF-1) has a similar function and molecular structure to insulin, and equally plays an important role in growth and development. The importance of IGF-1 in cancer was investigated in many studies [210-214]. For example the relationship between IGF-1 and risk of breast cancer has been studied in a case control study [215] on 397 women diagnosed with breast cancer and 620 matched controls, between1989-1990, and found a positive relationship between high IGF-1 plasma concentration and breast cancer in premenopausal women. However, the study demonstrated no relationship between high plasma concentration of IGF-1 and risk of breast cancer in postmenopausal women. The effect of IGF-1 on cancer cell growth and proliferation was also investigated in *in vitro* studies. In a study on colon cancer cell lines (HTC116 cells), cells were treated with the following concentrations of IGF-1 (0, 50, 100 and 200 ng/ml) for 3 days [216] and IGF-1 was associated with increased cell proliferation and decreased apoptosis.

TSH, also known as thyrotropin, is secreted from the pituitary gland and plays an important role in the production and release of T3 and T4 from the thyroid gland [7, 11] as part of the hypothalamo-pituitary-thyroid axis. The relationship of serum TSH concentration and risk of thyroid cancer were studied in a retrospective cohort study [217]. Serum TSH was measured preoperatively for 843 patients with thyroid nodules between 1994-2007. The data showed that increasing the concentration of serum TSH increased the probability of cancer. Furthermore, another study confirmed that the likelihood of cancer diagnosis increased in patients with TSH in the upper three quartiles compared to patients with TSH in the lower quartiles [218]. TSH has also shown to promote thyroid cancer growth in rat [177] and mouse models [178]. The mechanism of TSH promoted cell proliferation in cancer cells remains

unclear. However, the possible effects of TSH on cancer cell growth has been investigated *in vitro*, with follicular thyroid cancer cell lines (HTC TSHr) and hurthle cell (XTC), treated with TSH for 48 hours [219], finding that TSH increased vascular endothelial growth factor (VEGF) mRNA production. In this chapter the focus will be to examine the effect of Metformin on thyroid cancer cell in combination with other modulators (glucose, insulin, IGF-1 & TSH).

4.2 Results

4.2.1 The influence of glucose on Metformin's anti-proliferative and apoptotic effects

Previously it was shown that increasing glucose promoted thyroid cancer growth (section 3.2.2), and the standard for glucose to be included in the media was set at 10 mM, as some cell lines had poor growth in glucose-free media. The action of Metformin has thus been explored against the standard of 10 mM glucose *in vitro* (chapter 3) but here as part of the investigations into factors that could modulate the anti-proliferative action of Metformin the findings in glucose-free and glucose containing medium are presented in more detail (**Figures 4.1 & 4.2**). Higher levels of glucose of more than 10 mM were not included here because the cells over grow and it makes it difficult to measure inhibition of growth in an accurate manner (section 3.2.3). As before, glucose increased mean cell growth in the absence of Metformin (**Figure 4.1 and 4.2**). The addition of Metformin however decreased cell growth not only in the glucose-free medium group but also in the glucose-rich medium group in a concentration (**Figure 4.1**) and time dependent manner (**Figure 4.2**). At six days (**Figure 4.1**) 0.3 mM Metformin reduced growth to a level comparable to that of glucose-free media, but the presence of glucose (10 mM) moderated this effect. No significant differences were seen for 10 mM Metformin in glucose and glucose free medium, but this concentration is toxic (section 3.2.3) and shows that although glucose can modulate the anti-proliferative effects of Metformin it does not overcome its toxic effects at high doses.

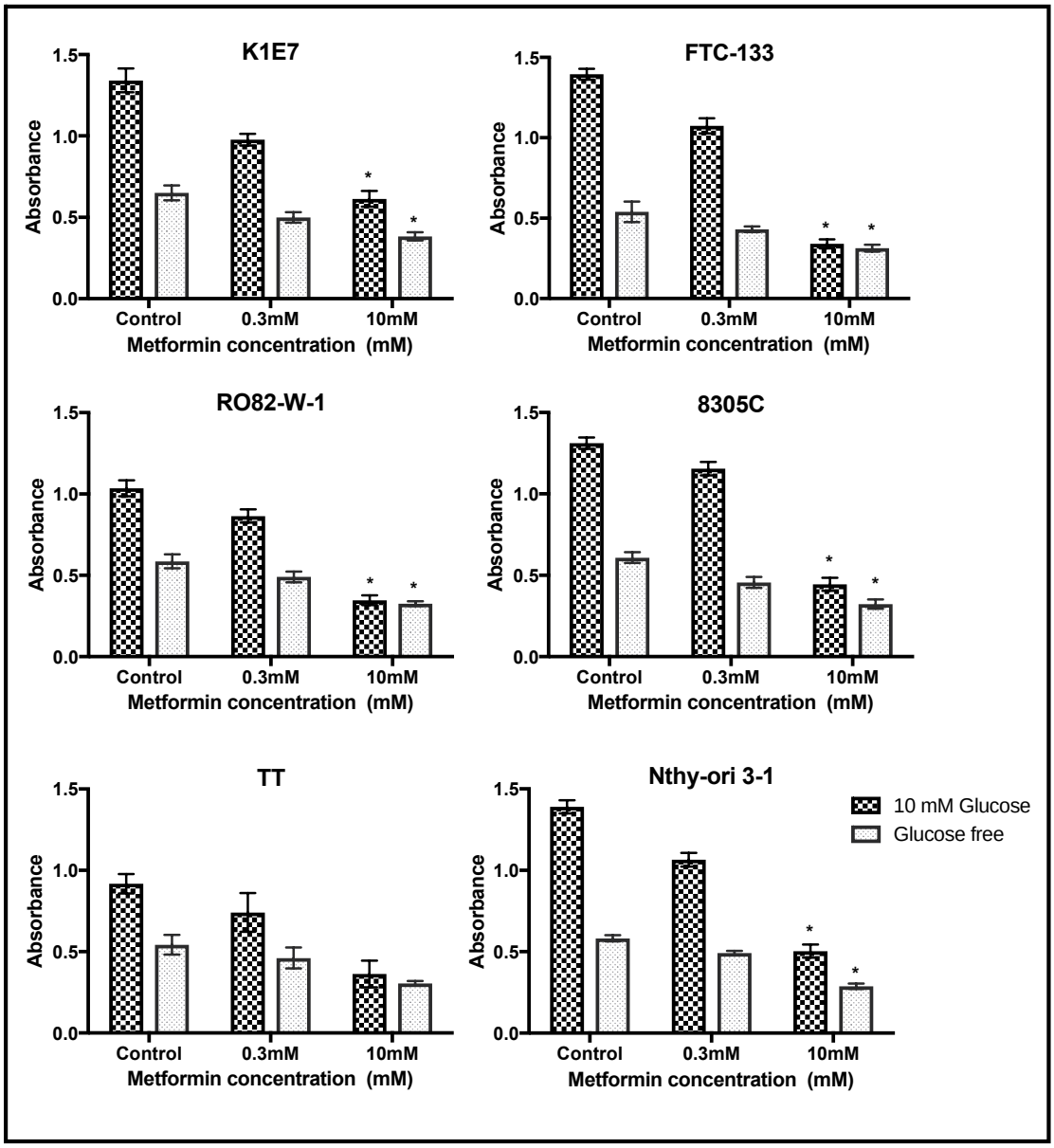

Figure 4.1: The effect of glucose on control of thyroid cancer proliferation by Metformin at 6 days.

This figure shows the absorbance (y-axis) of thyroid cells at day 6 following incubation at different Metformin concentrations (x-axis) in glucose and glucose-free media. The columns represent the mean of three independent experiments, each of which was done in triplicate. Error bars show the standard error of mean (SEM). The different pattern of bars shows the different media (black dotted represented DMEM containing 10 mM of glucose (2 g/L) and white dotted shows glucose-free DMEM) used in the experiments. Kruskal-Wallis test was used for multiple comparisons of more than two groups. * P value < 0.05 vs control within the same medium.

Over 6 days, (**Figure 4.2**) the anti-proliferative effect of 0.3 mM Metformin in glucose-free medium was greater than its effects on medium containing glucose.

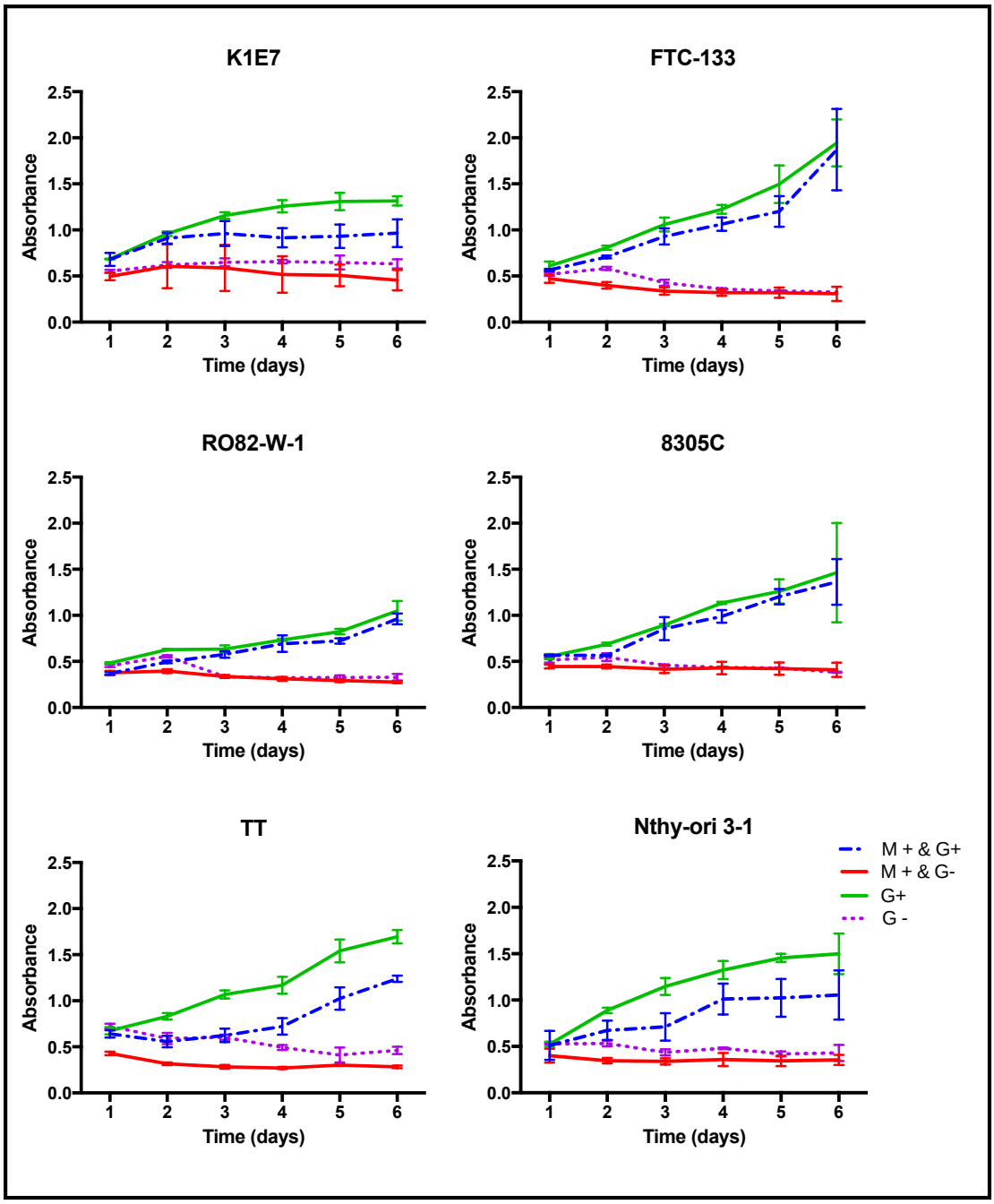

Figure 4.2: The effect of glucose and 0.3 mM Metformin on thyroid cell proliferation over time.

The figure shows the absorbance (y-axis) of cells in different time points (x-axis) after cells were treated with 0.3 mM (M+) of Metformin for 6 days in glucose-free medium (G-) and medium containing 10 mM of glucose (G+). The data points represent the mean of three independent experiments, each of which was done in triplicate. Error bars show the standard error of mean (SEM). Statistics are not included on the figure due to noise but are included in text. Each thyroid cell line is shown in a separate graph.

There were however some differences in response between the thyroid cell lines, with significance at day 3 for K1E7, FTC-133, 8305C and TT ($p < 0.01$,

p = 0.04, p = 0.04 and p = 0.01 respectively) and at day 4 for RO82-W-1 and Nthy-ori 3-1 (p = 0.05 and p < 0.01 respectively). As had been found previously (section 3.2.3) the findings would seem to suggest that thyroid cell lines are more susceptible to the anti-proliferative action of Metformin than the normal control Nthy-ori 3-1, but that in higher concentrations of glucose this effect is reduced.

Metformin was previously shown to promote apoptosis (section 3.2.6), but here, just as was found with proliferation, glucose similarly moderated the induction of apoptosis by Metformin (**Figure 4.3**), in those cell lines where apoptosis was a feature.

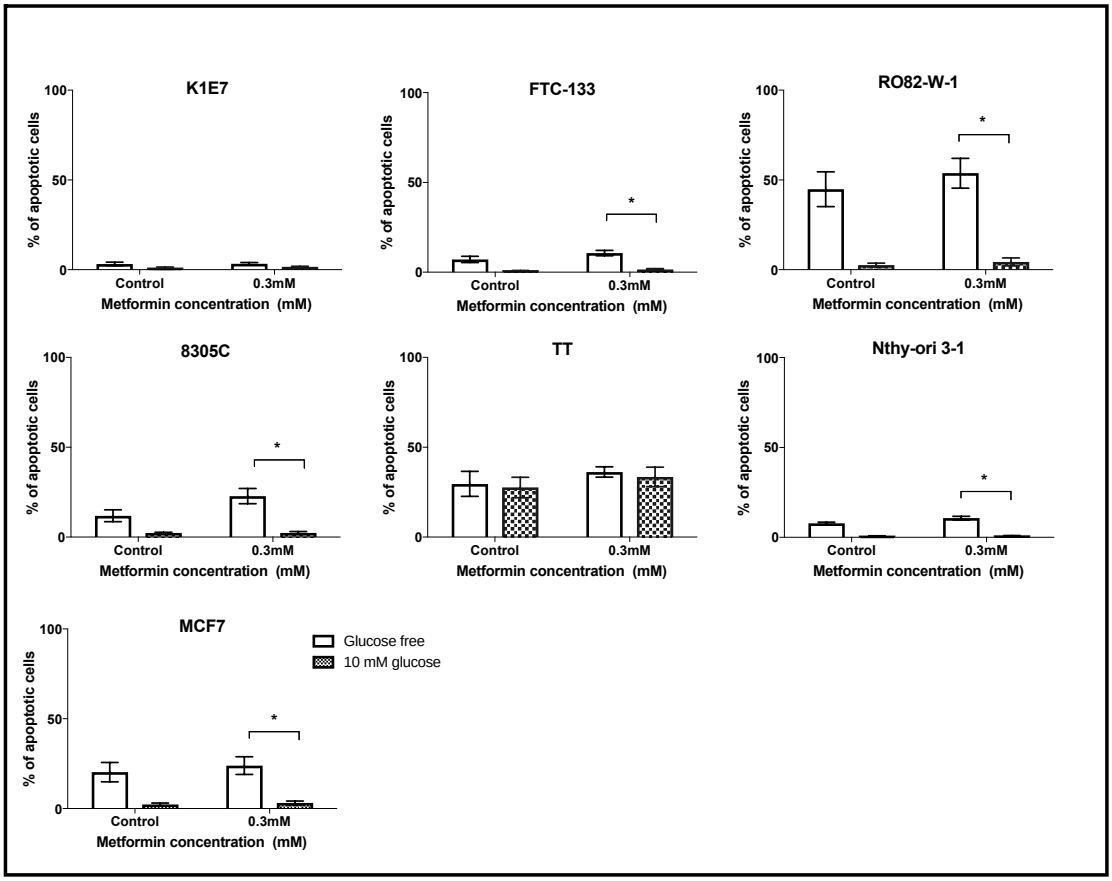

Figure 4.3: The effect of glucose on control of thyroid cell apoptosis by Metformin.

This figure shows the percentage of apoptotic cells (y-axis) for cell lines treated with 0.3 mM of Metformin (x-axis) for 6 days in both glucose-rich (10 mM) and glucose-free media. The columns represent the mean of three independent experiments, each of which was done in triplicate. Error bars show the standard error of mean (SEM). Mann-Whitney test was used to compare two groups. * , P value < 0.05.

The effect of either Metformin or glucose deprivation independently has similar results in terms of both proliferation and apoptosis. But in combination glucose will modulate the effect of Metformin, as seen in the previous chapter (section 3.2.2, 3.2.3, 3.2.6 & 4.2.1).

The difference between the percentages of apoptotic cells in glucose-free medium compared to glucose-rich medium after adding 0.3 mM of Metformin for 6 days was significant for FTC-133, RO82-W-1, 8305C, Nthy-0ri 3-1 and MCF7 cell lines ($p = 0.004$, $p = 0.004$, $p = 0.008$, $p = 0.001$ and $p = 0.029$ respectively) but not significant for K1E7 and TT cell lines ($p = 0.097$ and $p = 0.673$ respectively). TT has high levels of apoptosis anyway, (section 3.2.6), and the same was observed here with apoptosis not significantly altered regardless of the inclusion of glucose. For K1E7, there was no significant difference between induction of apoptosis by Metformin with or without glucose, and these findings mirror those found in chapter 3 (section 3.2.6) whereby only high and toxic levels of Metformin were found to increase apoptosis for K1E7. RO82-W-1 cell line like the TT line also has high apoptosis as a result of Metformin treatment, but unlike TT the addition of glucose blocks the action of Metformin and reduces apoptosis to a lower level. The other cell lines (FTC-133, 8305C, Nthy-ori 3-1 & MCF7) all had a similar response with a high level of apoptosis as a result of Metformin treatment in the glucose-free medium. Hence these findings clearly indicate that the presence of glucose in the media modified the anti-cancer effects of Metformin *in vitro*.

4.2.2 The influence of insulin on the anti-proliferative effects of Metformin on thyroid cancer cell lines

The next studies were carried out in the glucose-rich medium, as the cell lines would not grow in the medium without glucose (section 3.2.2). Increasing concentrations of Metformin in the media without the addition of growth factors inhibits thyroid cancer growth (section 3.2.3). Here, the difference in anti-proliferative action of Metformin on thyroid cells was assessed at 6 days after growth in media containing insulin (10 µg/ml) as a previous study used the same insulin concentration, allowing comparison of our data with Chen et al results [104] and compared to media without insulin. As shown in figures 4.4 and 4.5, the addition of 10 µg/ml of insulin in the medium showed no significant effects on thyroid cell proliferation, and Metformin significantly inhibited cell proliferation in all thyroid cell lines (K1E7, FTC-133, RO82-W-1, 8305C and Nthy-ori 3-1) regardless of the inclusion of insulin. The TT cell line was not tested in this experiment as frozen stocks of the cell line had failed to recover for these investigations.

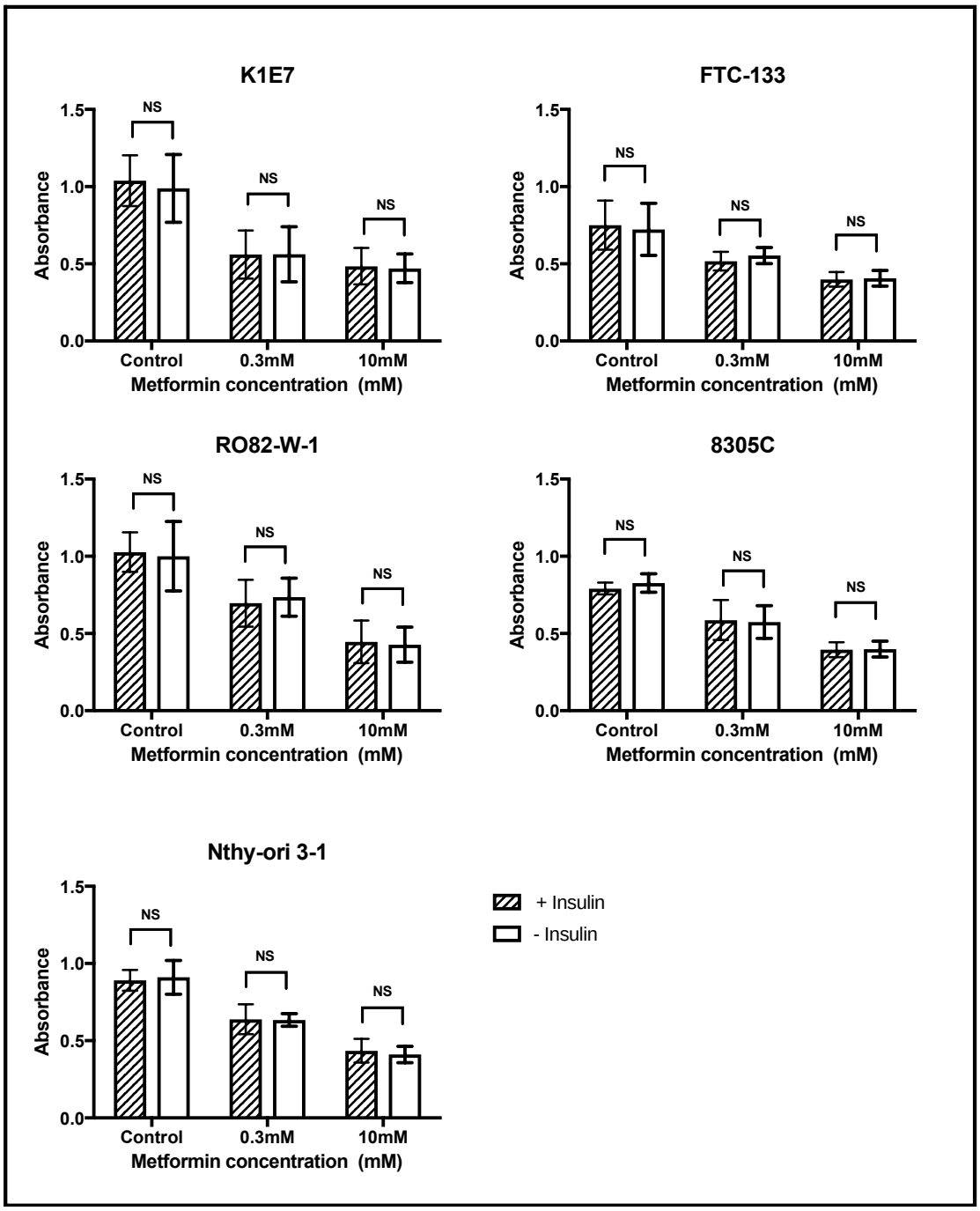

Figure 4.4: The effect of insulin on control thyroid cancer proliferation by Metformin.

MTT assay shows the absorbance (y-axis) of thyroid cells, which were treated for 6 days with different concentrations of Metformin in mM (x-axis). The media either contained 10 µg/ml of insulin (+insulin) or did not contain insulin (-insulin). The columns represent the mean of three independent experiments, each of which was done in triplicate. Error bars show the standard error of mean (SEM). Mann-Whitney test was used to compare two groups. NS (not significant) P value > 0.05. Each thyroid cell line is shown in a separate graph.

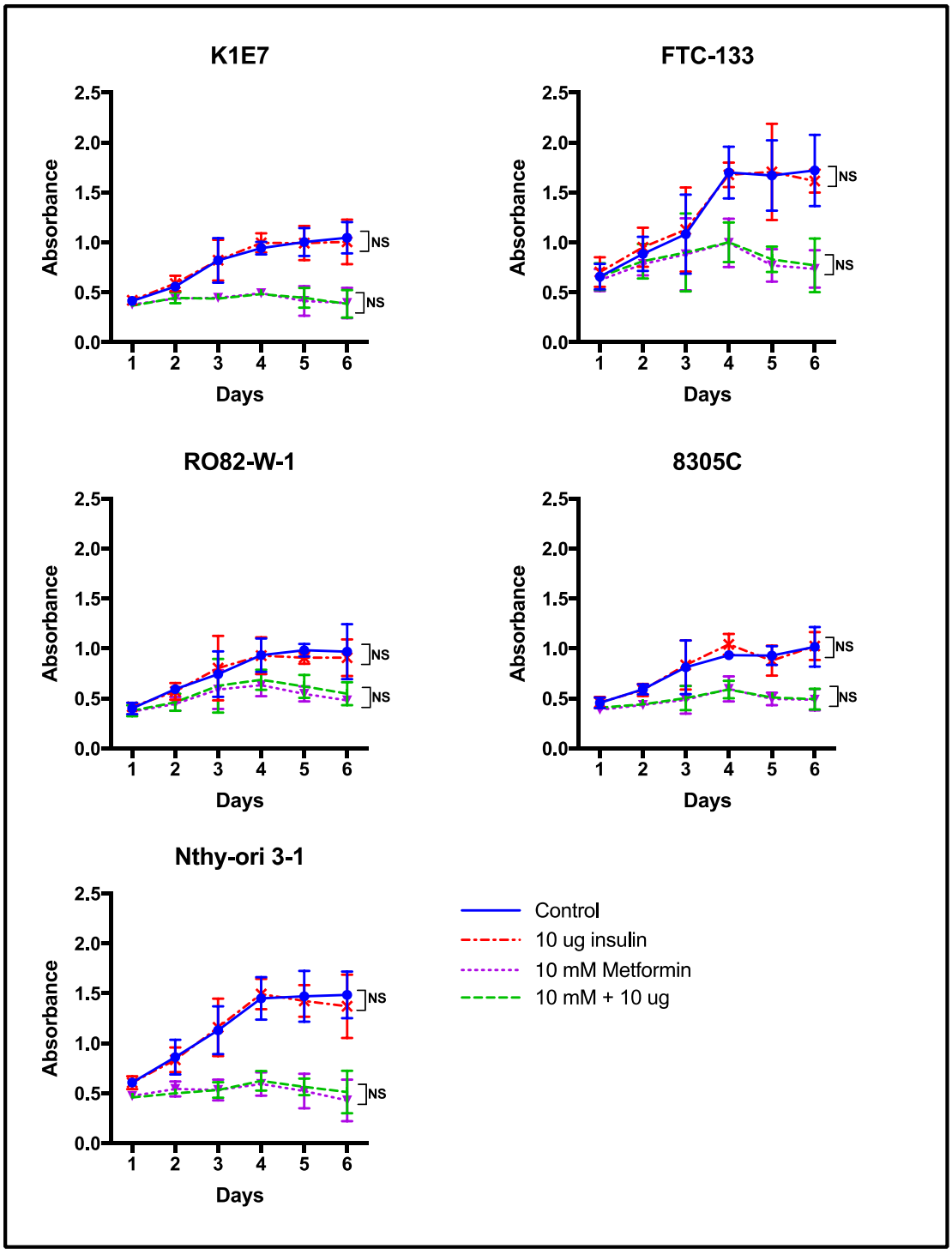

Figure 4.5: The effects of Metformin & insulin on thyroid cell proliferation over a period of 6 days.

MTT assay shows the absorbance /cell proliferations (y-axis) of thyroid cells under different conditions control (blue), 10 µg/ml of insulin (red), 10 mM of Metformin + 10 µg/ml of insulin (green) and 10 mM Metformin (purple), for several time points (x-axis). Each data point represents the mean of three independent experiments done in triplicate. Error bars show the standard error of mean (SEM). Mann-Whitney test was used to compare two groups. NS (not significant) P value > 0.05. Each thyroid cell line is shown in a separate graph.

4.2.3 The influence of IGF-1 on the anti-proliferative effects of Metformin on thyroid cancer cell lines

The importance of IGF-1 on the regulation of cancer growth has been extensively studied in many types of cancer, showing a positive stimulation [210-214]. However, the presence of IGF-1 in combination with Metformin has not previously been investigated and by adding IGF-1 to the media the anti-cancer effects of Metformin on thyroid cancer cells maybe modulated. As shown in figure 4.6 IGF-1 concentrations (50 ng, 100 ng and 200 ng) in the medium for up to 6 days did not affect thyroid cell proliferation in any of the cell lines studied (K1E7, FTC-133, RO82-W-1, 8305C and Nthy-ori 3-1). For all cell lines, similar findings were also obtained overtime on days 0-5 (the data not shown).

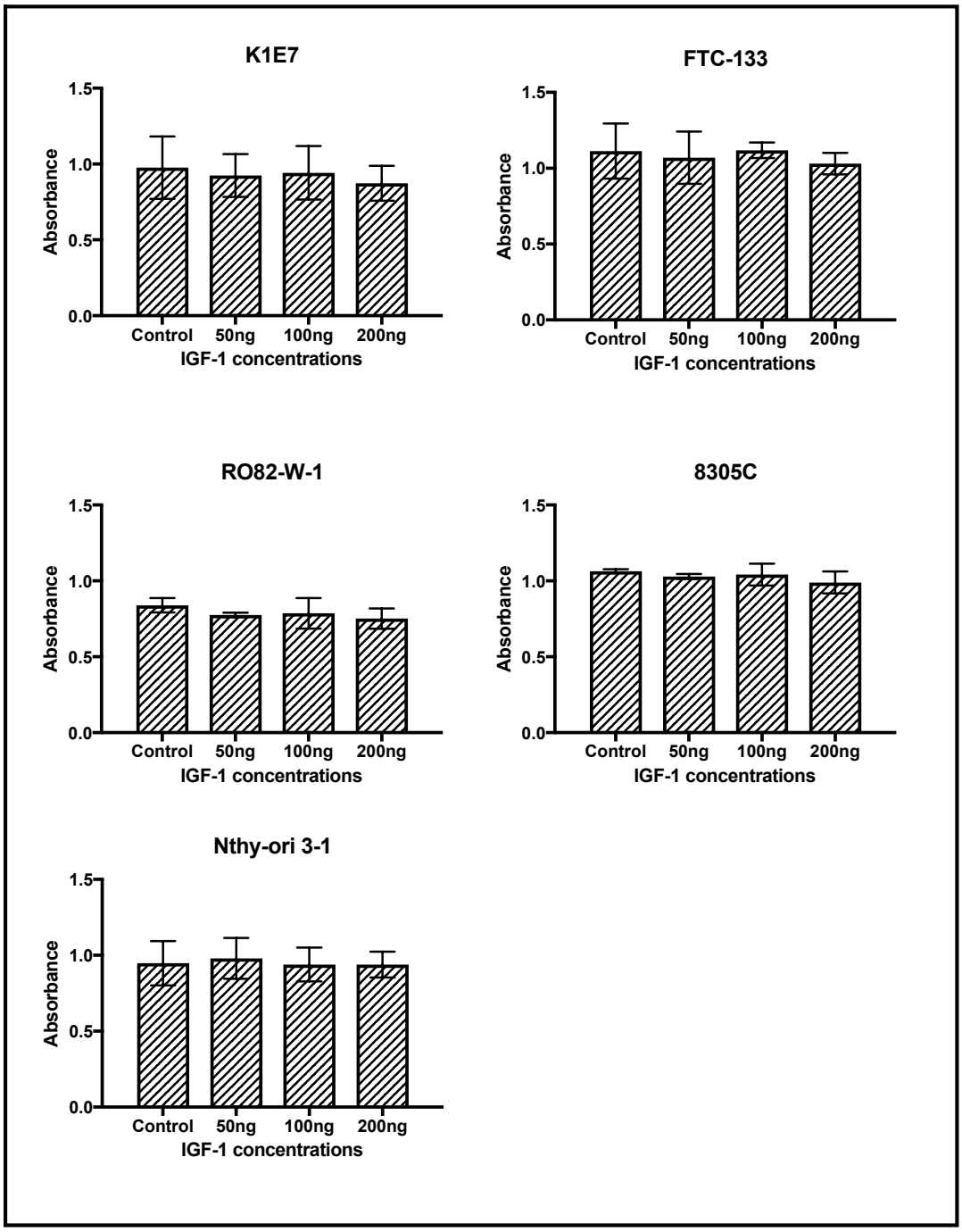

Figure 4.6: Effect of IGF-1 on thyroid cell proliferation.

MTT assay shows the absorbance /cell proliferation of thyroid cells (y-axis) after cells were treated with various concentrations of IGF-1 (x-axis) for 6 days. The columns represent the mean of three independent experiments, each of which was done in triplicate. Error bars show the standard error of mean (SEM). Each cell line is represented by a separate graph.

IGF-1 did not affect the proliferation of all thyroid cancer cell lines (K1E7, FTC-133, RO82-W-1, 8305C and Nthy-ori 3-1), and furthermore did not alter the anti-proliferative action of Metformin figure 4.7, regardless of the presence and absence of 100 ng/ml of IGF-1 in the medium. This IGF-1 concentration

100 ng/ml is within the concentrations used in the previous study [216], so our results are comparable with their findings. All media contained glucose (10 mM) and the TT cell line was not included due to failure to recover.

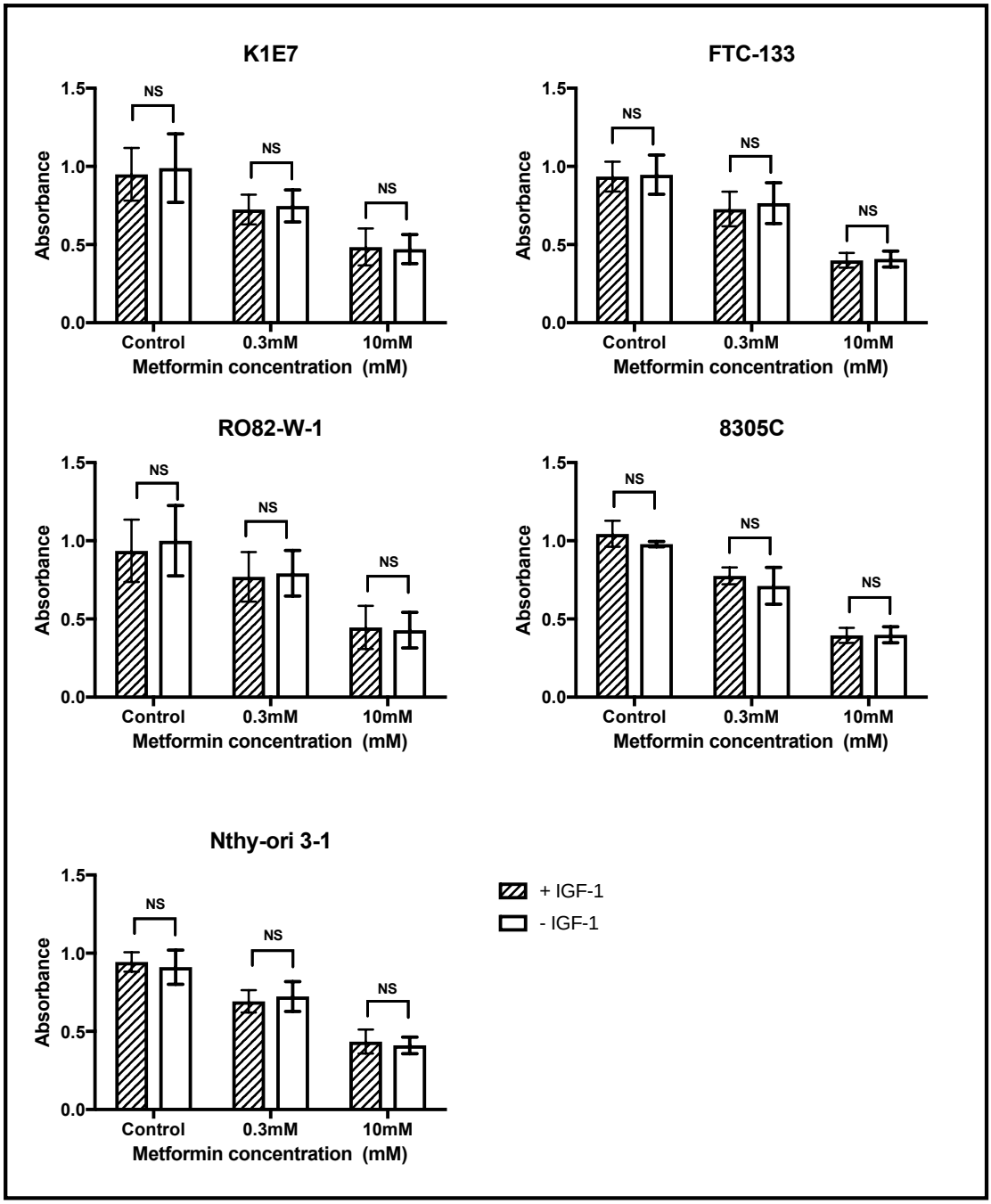

Figure 4.7: The effect of IGF-1 on control of thyroid cancer proliferation by Metformin.

MTT assay shows the absorbance (y-axis) of thyroid cells after cells treated for 6 days with different concentrations of Metformin in mM (x-axis). Growth was in medium with 100 ng/ml of IGF-1 (+IGF-1) or without IGF-1 (-IGF-1). Each column represents the mean of three independent experiments done in triplicate. Error bars show the standard error of mean (SEM). Mann-Whitney test was used to compare two groups. NS (not significant) P value > 0.05. Each thyroid cell line is shown in a separate graph.

4.2.4 The influence of TSH on Metformin's anti-proliferative effects

Previous studies on TSH have shown high serum TSH is associated with cancer growth and risk of cancer [217, 219, 220]. However, its action in the presence of Metformin has not previously been investigated. As shown in figure 4.8 various concentrations of TSH (5 mIU, 10 mIU and 50 mIU) in the media for up to 6 days did not influence cell proliferation for any of the cell lines studied (K1E7, FTC-133, RO82-W-1, 8305C and Nthy-ori 3-1). Similar findings were observed on days 0-5 (the data not shown).

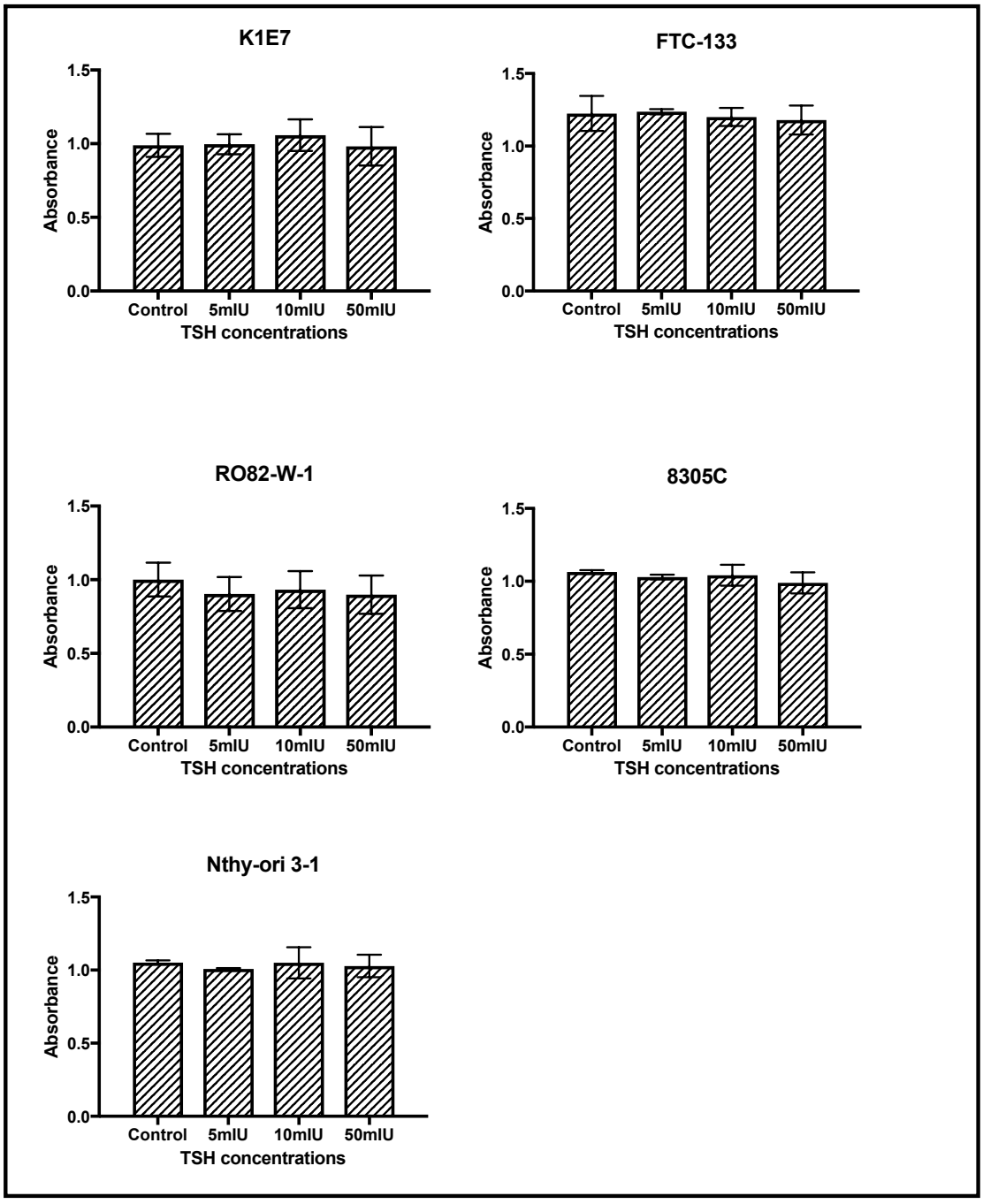

Figure 4.8: Effect of TSH on thyroid cell proliferation.

MTT assay shows the absorbance of thyroid cells (y-axis) after treatment with various concentrations of TSH (x-axis) for 6 days. The columns represent the mean of three independent experiments, each of which was done in triplicate. Error bars show the standard error of mean (SEM).

Furthermore, as shown in figure 4.9 Metformin inhibited cell proliferation in both TSH free medium (-TSH) and TSH rich medium (+TSH) for all thyroid cell lines. This suggests that Metformin has anti-proliferative effects regardless of TSH (5 mIU) in the medium (this TSH concentration is within the concentrations used in the previous study [219]), and all cell lines (K1E7, FTC-133, RO82-W-1, 8305C and Nthy-ori 3-1) had similar responses in the TSH free medium and TSH rich media. All the above observations were performed in medium containing glucose (10 mM) and the TT cell line was not included as it had failed to recover. This data shows that TSH in the medium does not inhibit the action of Metformin on thyroid cancer cell lines over a period of 6 days.

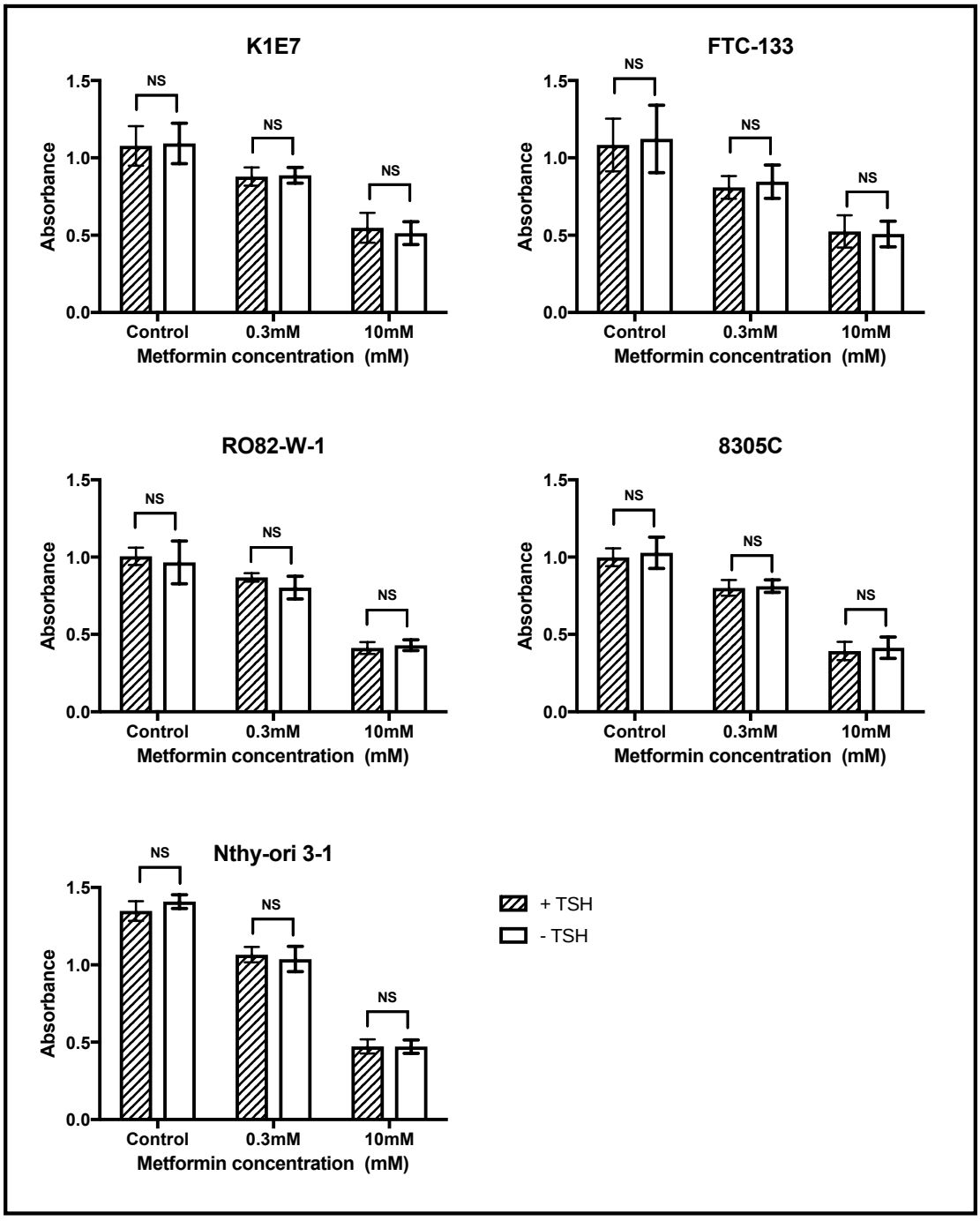

Figure 4.9: The effect of TSH on control of thyroid cancer proliferation by Metformin.

MTT assay shows the absorbance (y-axis) of thyroid cells after treatment for 6 days with different concentrations of Metformin (x-axis) in TSH containing (5 mIU/ml) and TSH free media. The columns represent the mean of three independent experiments, each of which was done in triplicate. Error bars show the standard error of mean (SEM). Mann-Whitney test was used to compare two groups. NS (not significant) P value > 0.05. Each thyroid cell line is shown in a separate graph.

4.3 Discussion

Previous studies on thyroid cancer found that glucose and insulin both modulated the anti-cancer effects of Metformin in thyroid cancer cells [104, 195].

4.3.1 Glucose deprivation promotes the anti-cancer effects of Metformin in thyroid cancer cells.

In the previous chapter, it was demonstrated that Metformin inhibited cell proliferation in the medium containing 10 mM of glucose. Numerous factors may influence the anti-cancer effects of Metformin. Previous studies reported that the anti-cancer effects of Metformin were highly dependent on the glucose concentration in the media [192, 221]. A study on breast cancer cells has shown that increasing concentrations of glucose (0-17 mM) in the media promoted cell proliferation, colony formation, cell migration, up-regulation of pro-oncogenic signalling such as AKT, mTOR and ERK and also reduced cell apoptosis in breast cancer cell lines [221]. Furthermore, the concentrations of glucose at 10 mM or greater abolished the anti-cancer effects of Metformin on breast cancer cell lines [221]. In a study on breast cancer cell line (MDA-MB-231), Metformin inhibited cell proliferation and activated the AMPK pathway in the normoglycemic (5 mM) condition only, while the anti-cancer effects of Metformin on MDA-MB-231 cells was abolished in hyperglycemic condition (25 mM) [192].

In this study the modulation of Metformin by 10 mM glucose in thyroid cancer cells was investigated. Evidence from previous investigations consistently shows that increasing glucose in the medium counteracts the action of Metformin on in thyroid cancer cells [195]. Here lower doses of Metformin (0.3 mM) were used over a longer period of time (6 days), but similarly confirmed that glucose counteracts the inhibitory action of Metformin on thyroid cancer cells (**Figure 4.1 & 4.2**). Whereas Bikas et al study on thyroid cancer, high concentrations of Metformin were used (1 mM and 5 mM) for shorter period time (48 hours), so toxicity maybe an issue [195]. Certainly, the action of

Metformin without glucose in the medium is not useful, as the cells are unable to grow and there cannot be a true measure of Metformin inhibition, hence, as shown in figure 4.2 the absence of glucose has the same results as just treating with Metformin. The normal serum glucose levels in non-diabetic individuals is maintained in between 70 and 100 mg/dl (4 to 5.5 mM) and also in cases of prolonged nutrient deprivation the glucose level dropped to 55 – 65 mg/dl [222]. The amount of glucose used in this study was 10 mM (180 mg/dl). This is within the range of glucose used in the published previous studies (0 mM – 50 mM), and was also shown to maintain the growth of thyroid cell lines, but at lower than 10 mM of glucose, growth was retarded (section 3.2.2).

The data also verifies previously reported findings on breast cancer cell lines demonstrating pro-apoptotic effects of Metformin were observed in low glucose medium but not in the medium containing high glucose [221]. Similarly another study on breast cancer also found that Metformin induced extensive cell-death in the glucose-deprived microenvironment [223].

Consistent with previous reports [221, 223], the current study demonstrated that the pro-apoptotic activity of Metformin on thyroid cancer cells increased in glucose depleted medium (0 mM) compared to the medium containing 10 mM glucose. Furthermore, a recent study on thyroid cancer cells, demonstrated that Metformin induced cellular morphological changes and cell death in low glucose conditions (5 mM) compared to the medium containing high glucose (20 mM) [195]. These findings are also in agreement with the current observations on colony formation, where Metformin treatment associated with changes in the morphology of colonies (section 3.2.4).

The inhibition of Metformin by glucose provides clues to the pathways by which Metformin suppresses thyroid tumour growth, and the various possible mechanisms and molecular pathways whereby glucose counteracts the anti-cancer effects of Metformin have been reported in previous studies. Metformin treatment was observed to become more cytotoxic by decreasing ATP production and increased AMPK phosphorylation in a medium which contained low glucose (2.5 mM) compared to medium which contained 25 mM

of glucose [224]. In another study on ovarian cancer cell lines (HeyA8, Tyk-nu, DOV13 and ID8), Metformin increased AMPK phosphorylation in medium contained 5.5 mM of glucose but this anti-cancer effect of Metformin was again found to be inhibited in medium containing 25 mM of glucose [225]. Of more relevance a recent study on thyroid cancer cells (FTC133) and Metformin found that glucose deprivation also increased AMPK phosphorylation and down-regulated phopho-pS6 [195]. Taken together these findings suggest that Metformin may inhibit up-regulation of the AMPK pathway and that glucose is capable of modulating this response.

4.3.2 The anti-cancer effects of Metformin on thyroid cancer cells in the presence of insulin, IGF-1 and TSH in the media.

Many factors potentially contribute to the development and progression of cancer. These include hyperinsulinemia and insulin-like growth factor I, and hyperglycaemia [221, 226]. Epidemiological studies have shown that hyperinsulinemia and hyperglycaemia associated with type 2 DM are linked to an increased risk of several types of cancer, especially the liver and pancreas [200-202]. Hyperinsulinemia and the exposure of liver to high insulin concentrations in the portal circulation play a major role in cancer development. This is because insulin binds to and activates the related insulin-like growth factor-I (IGF-I) receptor (80% homology with insulin receptor). This leads to more potent mitogenic and transforming activities. Moreover, insulin decreases IGF-I-binding proteins (IGF-BP1) resulting in increased free IGF-I, the biologically active form of the growth factor [227].

In addition to the influence of glucose on the anti-cancer action of Metformin, the effects on thyroid cell proliferation were also investigated in media containing insulin, IGF-1 or TSH. In contrast to evidence from previous studies, that showed increasing insulin in the medium increased cell proliferation [104, 203, 204], here, insulin in the medium (10 µg/ml) did not affect cell proliferation (**Figure 4.4 & 4.5**). It is possible that differences in

these findings reflect the use of the various cell lines used as Cheng et al [104] studied anaplastic thyroid cancer cells (HTh74 & HTh74Rdox), whereas, in this present study, four different thyroid cancer cell lines (K1E7, FTC-133, RO82-W-1 and 8305C) and one normal thyroid cell line (Nthy-ori 3-1) were tested, but one of these lines 8305c is also an anaplastic thyroid cancer, so subtype may not be accountable for the differences. Certainly Doron *et al*. [204] in a previous investigation on prostate cancer found that insulin promoted growth of 3 cell lines (LNCaP, C4-2 & P69) but had no effect on two other cell lines (M12 & PC3) [204]. These variations were found after cells were treated with various concentration of insulin (0, 5, 50, 100, 500 ng/ml) for 48 hours, and measured using the MTT assay and the results were obtained from three independent experiments. In contrast to Doron *et al.* another study on the same prostate cell lines (PC3) found that insulin (3 nM at 48 hours) enhanced cell proliferation [226]. Variations among studies could be explained by the use of different cell lines and different experimental procedures. Despite these variations this investigation did find similar results to Cheng et al where insulin increased cell proliferation, but in the presence of Metformin the increase in phosphorylation of ERK induced by insulin was prevented and thereby reducing growth [104]. In the current study it was found that insulin did not increase growth as such, with growth matching the control. To explain differences in these findings both human and animal insulin was studied but produced the same results. The study by Chen et al had found that insulin increased growth, however the information on the type of insulin and medium was not provided [104], and despite contacting the author differences in insulin could not be confirmed. The findings from this current investigation provide further clues to the pathways whereby Metformin exerts its effects, as both this study and that of Chen et al, found that Metformin inhibited cell growth and proliferation in the presence and absence of insulin. Chen et al indicated that ERK phosphorylation increases with insulin and so the MAPK/ERK pathway may also be targeted by Metformin.

This present study also demonstrated that IGF-1 and TSH had no effects on thyroid cell proliferation and no influence on the anti-cancer effects of Metformin (**Figures 4.7 & 4.9**). This is again in contrast with previous

investigations that reported increasing the concentrations of IGF-1 and TSH increased cell proliferation in breast and colon cancers cell lines [228-230]. In a breast cancer cell line (MCF7) IGF-1 (100 ng/ml) up-regulated P13K/Akt pathway and increased cell proliferation [228]. Koenuma et al [229] found that insulin and IGF-1 (0-100 ng/ml) for 5 days increased colon cancer cell proliferation in a time and concentration dependent manner. Furthermore, Koenuma et al showed that NL-44 cells were less sensitive to growth stimulation of insulin and IGF-1 than NL-17 cells [229]. This provided evidence of variation in the degree of response from different cell lines to the growth stimulatory effects of insulin and IGF-1. It maybe that the concentration of glucose affected the results, here 10 mM of glucose were used for all investigation but in the other studies up to 25 mM of glucose was used [228, 229].

Several epidemiological studies have suggested that higher serum TSH concentrations, even within the normal TSH range, associate with a thyroid cancer diagnosis in patients presenting with thyroid nodules [218, 231, 232]. Furthermore, a study on 843 patients in the United States suggested that the likelihood of thyroid cancer increases, with higher serum TSH levels and also higher serum TSH levels are associated with a more advanced stage of differentiated thyroid cancer [217]. These findings indicated that TSH might play an important role in thyroid cancer progression and/or development. Furthermore, in animal models (tumourigenic clone of papillary thyroid cancer cells were implanted in nude mice), TSH promoted tumour growth by promoting tumour angiogenesis and macrophage recruitment in the microenvironment mediated by overexpression of VEGF [233]. Thus, TSH suppression therapy by administering exogenous thyroid hormone treatment may inhibit the growth and development of thyroid nodules [234]. Additionally, therapy with suppressive doses of thyroxine (T4) are associated with favourable outcomes in differentiated thyroid cancer patients [235] and retrospective studies have shown that a lesser degree of TSH suppression is associated with an increased risk of recurrence of differentiated thyroid cancer [236]. Moreover, prospective studies have suggested that aggressive TSH suppression therapy associated with superior outcomes in thyroid carcinoma-

related death and relapse in high-risk patients [237, 238]. In this current study we found that treatment by TSH had no effect on thyroid cancer proliferation or modulated the effects of Metformin (**Figures 4.9**). Consistent with these observations, a study on 86 newly diagnosed breast cancer patients shows that thyroid hormone (FT3, FT4 and TSH) levels were not found to be correlated to cell proliferation (Ki67) and tumour size [239].

4.3.3 Exploring the differences in observations of Insulin, IGF and TSH on thyroid cancer proliferation.

In the most of the above-mentioned studies, cells were cultured in H6 medium, which is rich with growth factors. The H6 medium is a DMEM medium supplemented with a mixture of six hormones (DMEM medium + 10 µg/ml insulin + 5 µg/ml human transferrin + 10 ng/ml somatostatin + 10 ng/ml glycyl-L histidyl-L-lysine acetate + 10 nm hydrocortisone + 1 nm TSH) [229, 240]. In the present study, we tested the effect of TSH, IGF-1 and insulin on thyroid cells in the DMEM medium without adding growth factors as mentioned. These differences may account for why this investigation is different to previous studies of TSH, insulin and IGF-1 in thyroid cancer cells. In addition, the variation in the current observations on insulin, IGF and TSH could be because of different cell lines and different experimental procedures. As mentioned earlier, in one study three prostate cancer cell lines responded to insulin-induced cell proliferation, whereas the other two cell lines did not respond to insulin [204]. Moreover, insulin-induced proliferation in prostate cancer cell lines (PC3) was reported in one study [226] while in other study no effects were found on the same cell line [204].

This however is the first study that investigated the anti-cancer effect of Metformin (therapeutic dose) with and without modulators (IGF-1 and TSH) in the medium. It is of interest that previous studies on thyroid cancer cells with TSH (1 nm) and IGF-1 (100 ng/ml) were found to decrease the Forkhead box O 1 (FOXO1) protein levels; FOXO1 act as tumour suppressor for thyroid malignancy [240]. The study also found that TSH and IGF-1 activated P13K

pathway via up-regulated of Akt phosphorylation. In this current study no modulation of the action of Metformin was found by either TSH or IGF-1, but it remains to be determined if Metformin exerts its effects by inhibiting pathways such as the P13K and the expression of FOXO1. Finally the data suggests that TSH may be part of the change from differentiated to de-differentiated status, therefore it would be interesting to see if this alters the ability to form colonies or migration. Evidence from an *in vivo* study show that TSH is associated with overexpression of VEGF [233]. However, VEGF activation is associated with promoting growth and invasion of differentiated thyroid cancer cells in culture and in *in vivo* models [241].

The effect of insulin, IGF and TSH on apoptosis was not explored, as time was limited, and as the data from the proliferation assays were essentially negative. It could of course be that any observed effects of insulin, IGF and TSH may relate to an effect on apoptosis, which was not explored here.

4.4 Conclusion

To summarize, the anti-cancer actions of Metformin can be abrogated or reduced in the presence of glucose, but are not modulated by insulin, IGF-1 and TSH. Therefore it could be assumed in patients that treatment with Metformin would work in combination with TSH and would not be affected by other factors in non-diabetic patients. Furthermore the interaction of Metformin with these modulators has provided evidence for the pathways that are up-regulated as part of its anti-cancer response, and these aspects are explored further later.

CHAPTER FIVE

Potential methods of action of Metformin in thyroid cancer

5.1 Introduction

In the previous chapters (chapter 3 & 4) Metformin was shown to have anti-cancer effects on thyroid cancer cells. The possible methods of action of Metformin as an anti-cancer drug in thyroid cancer cell lines are however unclear. This current study aims to understand the mechanism by which Metformin enters into the thyroid cells and then the genes and pathways it modulates. Organic Cation Transporter 1 (OCT1) plays a role in the cellular uptake of Metformin in liver cells and is highly expressed in the kidney and intestine [242, 243]. Similarly OCT1 maybe expressed by thyroid cancer cells and therefore play an important role in facilitating the anti-cancer effect of Metformin. The presence and absence of OCT1 in thyroid cancer cells was investigated via immunocytochemistry in this study.

In addition to the potential importance of OCT1 to the uptake of Metformin by thyroid cancer cells, this study aimed to demonstrate the genes targeted and the pathways involved in the anti-cancer effects of Metformin. Several non-thyroid cancer studies have shown the importance of some genes and pathways that may be targeted as a result of the anti-cancer actions of Metformin, such as in breast cancer [244], ovarian cancer [128], oesophageal squamous cell carcinoma [245], pancreatic cancer [246] and thyroid cancer [104-106].

In a study on breast cancer cells (MCF7) Metformin inhibited proliferation and induced apoptosis via promotion of P53 up-regulation, increasing phosphorylation of AMPK and decreasing phosphorylation of mTOR [125, 244]. Another study on breast cancer cells (MCF7) found that Metformin inhibited cell growth and induced cell cycle arrest via reduced expression and activation of erbB2 protein [125], decreased phosphorylation of a Protein Kinase (Akt) and decreased phosphorylation of mTOR [125]. In addition to breast cancer cells, in oesophageal squamous cell carcinoma cells (OSCC), Metformin induced cell cycle arrest and decreased cell growth via up-regulation of AMPK, p27cip1, p21kip1 and p53 and down-regulation of

cyclinD1 [245]. In other investigations of ovarian cancer cells (OVCAR-3 and OVCAR-4), Metformin up-regulated the AMPK pathway and down-regulated p70S6K and S6K [128]. Finally in pancreatic cancer cells (BxPC3 and PANC-1), Metformin inhibited cell growth through down-regulation of Bcl2 and Mcl-1 (both anti-apoptotic proteins), and also decreased phosphorylation of mTOR, S6K, 4EBP1, ACC and STAT3 whilst increasing phosphorylation of AMPK [246]. The actions of Metformin therefore appear to target a number of pathways, but these studies in others cancers seem to suggest that up-regulation of the AMPK pathway and down-regulation of mTOR are consistent features.

In order to understand the potential methods of action of Metformin, the Affymetrix expression assay was chosen because it provides information on the expression of a large number of genes, including targets (AMPK and mTOR) identified in other investigations. The two thyroid cancer cell lines (K1E7 and FTC-133) and one normal thyroid cell line (Nthy-ori 3-1) were chosen for the Affymetrix array, the other cell lines were not studied because of financial issues.

5.2 Results

5.2.1 Immunocytochemistry assay.

A positive control line (HepG2 liver cancer cell line) and a breast cancer cell line (MDA-MB-231) were also tested in addition to the thyroid cancer cell lines. OCT1 was strongly expressed by the control HepG2 (known expression of OCT1) and equally by all thyroid cell lines (K1E7, FTC-133, RO82-W-1 and 8305C), but was not expressed by the breast cancer cell line MDA-MB-231, which acted as the negative control (**Figure 5.1 & 5.2**). The pattern of staining for OCT1 in thyroid cells showed a robust diffuse staining localized to the plasma membrane (**Figure 5.1 & 5.2**). The proportion and intensity of OCT1 expression was estimated using the Allred score (range 0-8) [247] as detailed in the material and methods chapter in section 2.2.9. Metformin did not influence the proportion and intensity of OCT1 expression in thyroid cells, and all thyroid cancer cell lines strongly expressed OCT1 regardless of treatment with Metformin (**Table 5.1**).

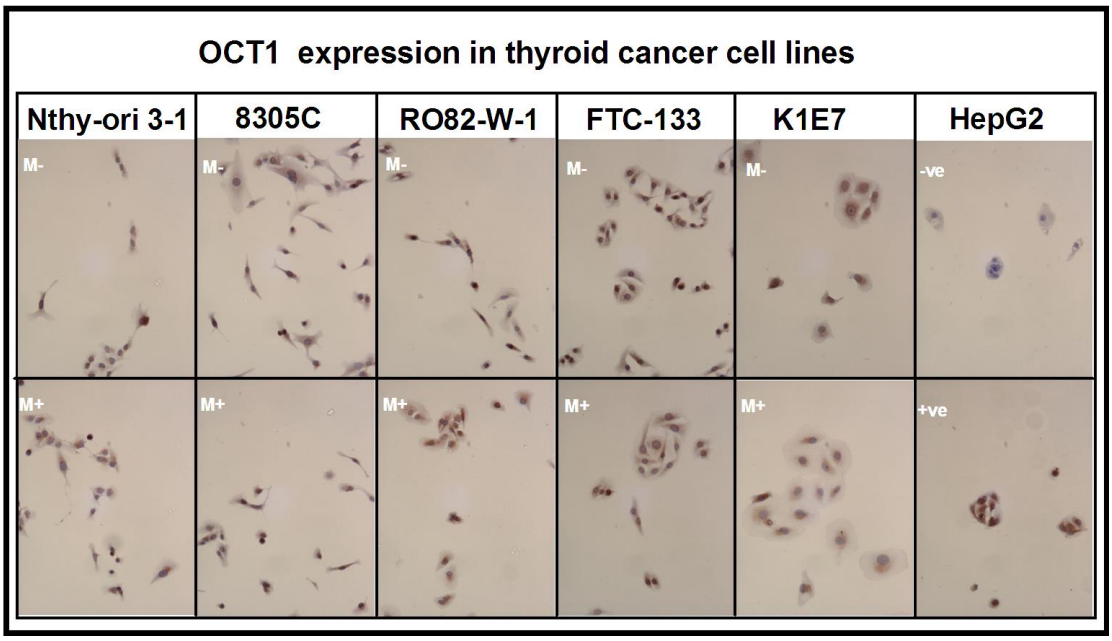

Figure 5.1: OCT1 expression in thyroid cancer cell lines.

Low magnification images using x4 objective of the results of the immunocytochemistry assay showing OCT1 expression in thyroid cancer & normal cells (K1E7, FTC-133, RO82-W-1, 8305C and Nthy-ori 3-1) and compared to HepG2 (positive control & negative control without antibody). The figure only shows thyroid cells treated with 0.3 mM of Metformin for 48 hours (M+) and cells not treated with Metformin (M-).

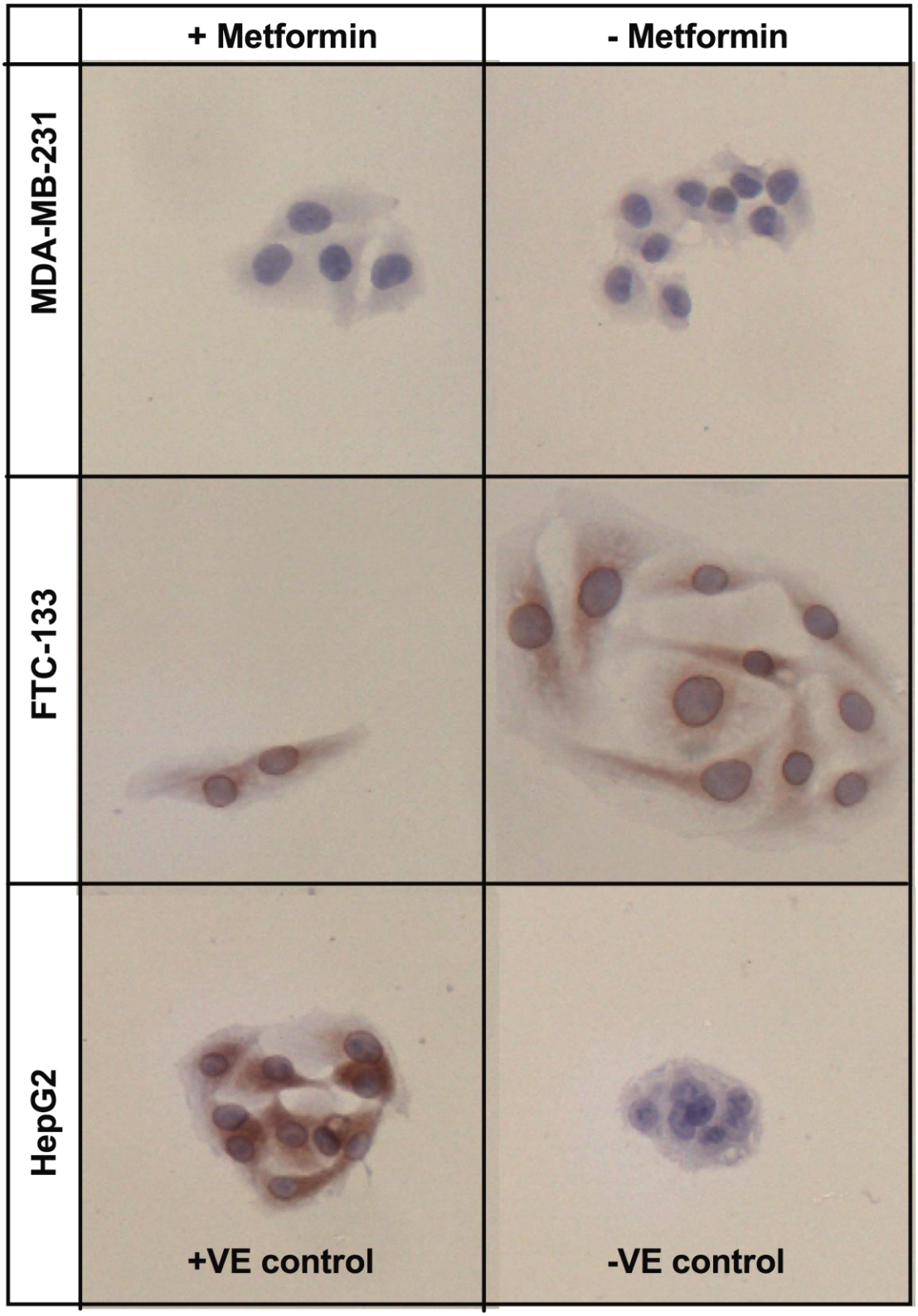

Figure 5.2: OCT1 expression in HepG2, FTC-133 & MDA-MB-231 cells.

Immunocytochemistry assay comparing OCT1 expression in FTC-133, HepG2 and MDA-MB-231 using high magnification images x40. Cells treated with 0.3 mM (+ Metformin) for 48 hours compared to the cells not treated with Metformin (- Metformin). + ve control = HepG2 cells were incubated with 200 µl of primary antibody (SLC22A1) and – ve control = HepG2 cells were not Incubated with primary antibody (SLC22A1).

Table 5.1: Results of the immunocytochemistry assay showing OCT1 expression in thyroid cells with & without Metformin.

OCT 1 expression in thyroid cell lines with and without metformin

Cell line	Metformin concentration and duration of exposure							
	None		0.3mM / 48 hours		1mM / 48 hours		10mM / 48 hours	
	Staining – yes/no	Allred score (PS+IS) (0-8)	Staining – yes/no	Allred score (PS+IS) (0-8)	Staining – yes/no	Allred score (PS+IS) (0-8)	Staining – yes/no	Allred score (PS+IS) (0-8)
K1E7	Yes	6	Yes	5	Yes	6	Yes	6
FTC-133	Yes	7	Yes	6	Yes	6	Yes	6
RO82-W-1	Yes	6	Yes	7	Yes	7	Yes	5
8305C	Yes	6	Yes	5	Yes	5	Yes	5
Nthy-ori 3-1	Yes	6	Yes	6	Yes	6	Yes	6

The Immunocytochemistry assay shows the results of quantification of OCT1 expression in thyroid cells (K1E7, FTC-133, RO82-W-1, 8305C and Nthy-ori 3-1). Cells were treated with different concentrations of Metformin (0 mM, 0.3 mM, 1 mM and 10 mM), for two different time points 24 and 48 hours (Only 48hr time point shown because there was no difference between time points). The Allred score was used to score the proportion and intensity of OCT1 expression.

5.2.2 Results of changes in gene expression using the Affymetrix expression array.

The Affymetrix expression array was only performed using three paired thyroid cancer cell lines (K1E7, FTC-133 and Nthy-ori 3-1) and compared the expression of a total of 53617 genes for all cell lines, before and after Metformin treatment (cells were treated with 0.3 mM Metformin for 6 days). Due to the financial considerations it was not feasible to perform the analysis on all the thyroid cancer cell lines, so only K1E7, FTC-133 and Nthy-ori 3-1 were investigated. Furthermore it was not possible to perform independent repeats. Nthy-ori 3-1 was studied to investigate gene expression in normal cells and the cell lines K1E7 and FTC-133 were selected because they represent the common types of thyroid cancer. Metformin significantly up-regulated and down-regulated a wide range of genes for all cell lines (K1E7, FTC-133 and Nthy-ori 3-1). To evaluate, a targeted approach was taken and the genes with either a 1 fold change up or down in expression, following Metformin treatment, were chosen for further evaluation. This approach is a standard approach established by the core facility in the department of Neuroscience, University of Sheffield (Dr Paul Heath). However, as seen (**Figure 5.3**) this initial screen still found there were a large number of genes altered in response to Metformin treatment.

5.2.3 Overview of the findings on gene expression following Metformin treatment.

Previous studies have taken a more focused approach when assessing the potential targets and pathways that Metformin could regulate. This study found that the effects of Metformin were wide ranging, with 9.3% genes up-regulated in the lines and 8.3% down-regulated. In all these instances there was at least a one-fold change. In previous studies using the Affymetrix array the level considered as relevant for analysis varied among different studies,

but mainly ranged between 1-2 fold [248-252]. In these other investigations (not exploring Metformin but looking at the action of other drugs) a similar approach was taken, but the level of alteration induced was far less than found in this current study as a response to Metformin. Therefore although the fold changes found using the Affymetrix array were comparable between this investigation and others, there was a much higher degree of modulation produced by Metformin than reported for other drugs. Dr Heath (Department of Neuroscience, University of Sheffield), was surprised at how much changed was induced by Metformin treatment particularly for K1E7.

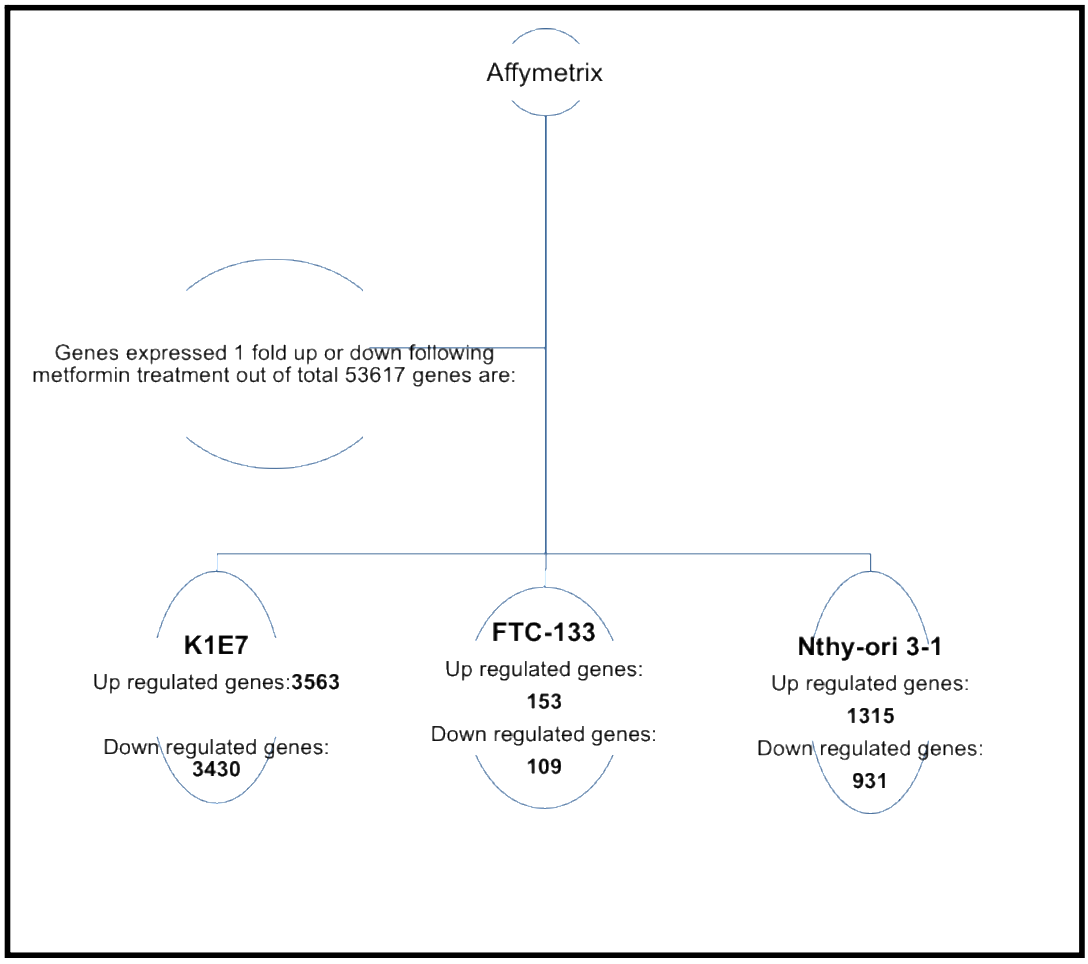

Figure 5.3: Overview of the level of altered genes expression in thyroid cells, following Metformin treatment using the Affymetrix array assay.

The numbers of genes that were up or down-regulated by at least 1 fold, using the Affymetrix assay, after Metformin treatment (0.3 mM) in the K1E7, FTC-133 and Nthy-ori 3-1 cell lines is summarised.

The K1E7 cell line had the most variation in the number of genes that were significantly up-regulated (3563 genes) and down-regulated (3430 genes) following Metformin treatment. The protein phosphatase 1 regulatory subunit 10 gene (*PPP1R10*), was the top up-regulated gene with an increased expression of 18.39 fold compared to the expression of the control. The PPP1R10 gene plays an important role in cellular processes, such as the cell cycle [253]. The small nucleolar RNA, C/D box 115-5 gene (*SNORD115-5*) was the top down-regulated gene and decreased expression by 16.3 fold compared to control (**Table 5.2**).

Table 5.2: Results of the Affymetrix array assay- identification of the top 10 up-regulated and down-regulated genes after K1E7 cells were treated with 0.3 mM of Metformin for 6 days.

Numbers	Gene Symbol	Upregulated Expression	Gene Symbol	Down regulated Expression
1	PPP1R10	18.396358	SNORD115-5	-16.309266
2	IPW	18.180253	LOC100272216	-15.106969
3	HCG8	13.96817	SNORD32B	-9.661779
4	IER3	10.379987	SNORA38	-9.284843
5	FLJ22447	8.675055	SNORD117	-8.509836
6	C6orf47	8.49042	HSPA1A	-7.513288
7	PPT2-EGFL8	8.417027	TAF1D	-7.095325
8	MTRF1L	7.367797	SNORD52	-6.96934
9	LOC100132167	7.181866	SNORD48	-6.498743
10	LINC01000	6.776727	SNORD116-3	-6.014839

Selected up-regulated or down-regulated genes discussed later have been highlighted in the table.

The FTC-133 cell line, demonstrated the fewest altered genes, with 153 up-regulated genes, and 109 down-regulated. The top up-regulated gene was the solute carrier family 18 member A3 (*SLC18A3*), and expression was increased by 2.91 fold compared to the control. The top gene that was down-

regulated was small nucleolar RNA, C/D box 99 (*SNORD99*) decreased by 3.13 fold expression compared to control (**Table 5.3**).

Table 5.3: Results of the Affymetrix array assay- identification of the top 10 up-regulated and down-regulated genes after FTC-133 cells were treated with 0.3 mM of Metformin for 6 days.

Numbers	Gene Symbol	Expression	Gene Symbol	Expression
1	SLC18A3	2.914271	SNORD99	-3.138417
2	SERTAD4	2.912107	SNORA66	-2.819541
3	DIO1	2.60728	DUSP5	-2.722006
4	RP4-791M13.3	2.410873	SNORD75	-2.721084
5	LINC01037	2.3793	SNORD103A	-2.64968
6	LOC102723919	2.288908	RNU6-773P	-2.567926
7	HIST2H4B	2.23496	SNHG12	-2.34524
8	IKBKE	2.166837	HMGN2	-2.241845
9	PARS2	2.159519	CIART	-2.200218
10	BICC1	2.056973	MIR554	-2.149709

Selected up-regulated or down-regulated genes discussed later have been highlighted in the table.

In the Nthy-ori 3-1 cell line acting as the normal thyroid control, 1315 genes were significantly up-regulated and 931 genes down-regulated following Metformin treatment. The top up-regulated gene was the complement component 4 gene (*C4B*) and the expression was increased by 17.13 fold compared to control. The top down-regulated gene was the *SNORD32B* and the expression was decreased by 6.25 fold compared to control (**Table 5.4**).

Table 5.4: Results of the Affymetrix array assay- identification of the top 10 up-regulated and down-regulated genes after Nthy-ori 3-1 cells were treated with 0.3 mM of Metformin for 6 days.

Numbers	Gene Symbol	Expression	Gene Symbol	Expression
1	C4B	17.1382	SNORD32B	-6.252246
2	SNAR-C2	8.260474	SNORD3B-1	-4.47315
3	PPP1R10	8.143419	TAF1D	-4.209673
4	IER3	7.378793	SNORD24	-3.419105
5	PDE4DIP	6.931958	ID3	-3.208322
6	PTPRQ	6.519714	TNC	-2.803944
7	SNORA38	6.10198	CGB8	-2.80279
8	CEACAMP7	5.237918	RNU6-767P	-2.694614
9	LINC00963	4.722674	HIST1H2BM	-2.672788
10	PRKXP1	4.617178	ERVK-7	-2.670674

Selected up-regulated or down-regulated genes discussed later have been highlighted in the table.

5.2.4 Common genes regulated by Metformin treatment of thyroid (normal and cancer cell lines).

It was observed that genes amongst the top 10 significantly up and down-regulated genes were common to both K1E7 and Nthy-ori 3-1 cells. Two up-regulated genes (*IER3* and *PPP1R10*) and two down-regulated genes (*SNORD32B* and *TAF1D*) were common altered in both K1E7 and Nthy-ori 3-1 cells. In fact, other members of the *SNORD* family of non-coding small nucleolar RNAs were altered in all cell lines tested (**Table 5.2, 5.3 & 5.4**).

When comparison of the findings on all cell lines were made (including those genes where expression was altered more than 1 fold, but not among the top candidates), there was also 15 significantly up-regulated genes and 3 significantly down-regulated genes that were shared between all cell lines (K1E7, FTC-133 and Nthy-ori 3-1) (**Table 5.5 & 5.6, Figure 5.4**).

Table 5.5: The commonly up-regulated genes shared between K1E7, FTC-133 & Nthy-ori 3-1 cells, found using the Affymetrix array assay.

Numbers	Gene Symbol	Nthy-ori 3-1	FTC-133	K1E7
1	TOE1	1.113663	1.251928	1.557604
2	S1PR1	1.334568	1.486556	1.304211
3	SLC16A1-AS1	1.307473	1.065338	1.4398
4	LOC102723919	1.174772	2.288908	1.351293
5	C1orf220	1.060775	1.694529	1.026326
6	SERTAD4	1.58121	2.912107	3.696954
7	FBXO28	1.055935	1.083433	1.797531
8	COG2	1.155445	1.513195	1.410165
9	Unknown1	2.05395	1.576519	1.285898
10	TSPAN2	1.150647	1.365549	1.848103
11	Unknown2	1.264119	1.289381	1.613705
12	RP4-791M13.3	1.375516	2.410873	2.561201
13	PIGM	1.27974	1.104949	1.66414
14	BICC1	1.546207	2.056973	1.539705
15	STOX1	1.842854	1.166804	1.462698

Selected up-regulated or down-regulated genes discussed later have been highlighted in the table.

Table 5.6: Affymetrix Array assay- The commonly down-regulated genes shared between K1E7, FTC-133 & Nthy-ori 3-1 cells.

Numbers	Gene Symbol	Nthy-ori 3-1	FTC-133	K1E7
1	RABGGTB	-1.350999	-1.495314	-1.087615
2	Unknown	-1.058718	-1.160969	-1.545412
3	FAM72C	-1.599743	-1.015477	-1.177497

As the expression of these genes was altered in all 3 cell lines, it suggests that common pathways maybe implicated in all thyroid tissues, whether normal or cancer, however the most significantly altered genes shared by the

two cancer cell lines (K1E7 & FTC-133.) were not of significance in the normal Nthy-ori 3-1 control. These findings would therefore suggest that there is a different mode of action by Metformin specifically in thyroid cancer.

A summary of the overview of commonly altered genes in the lines is presented in figure 5.5.

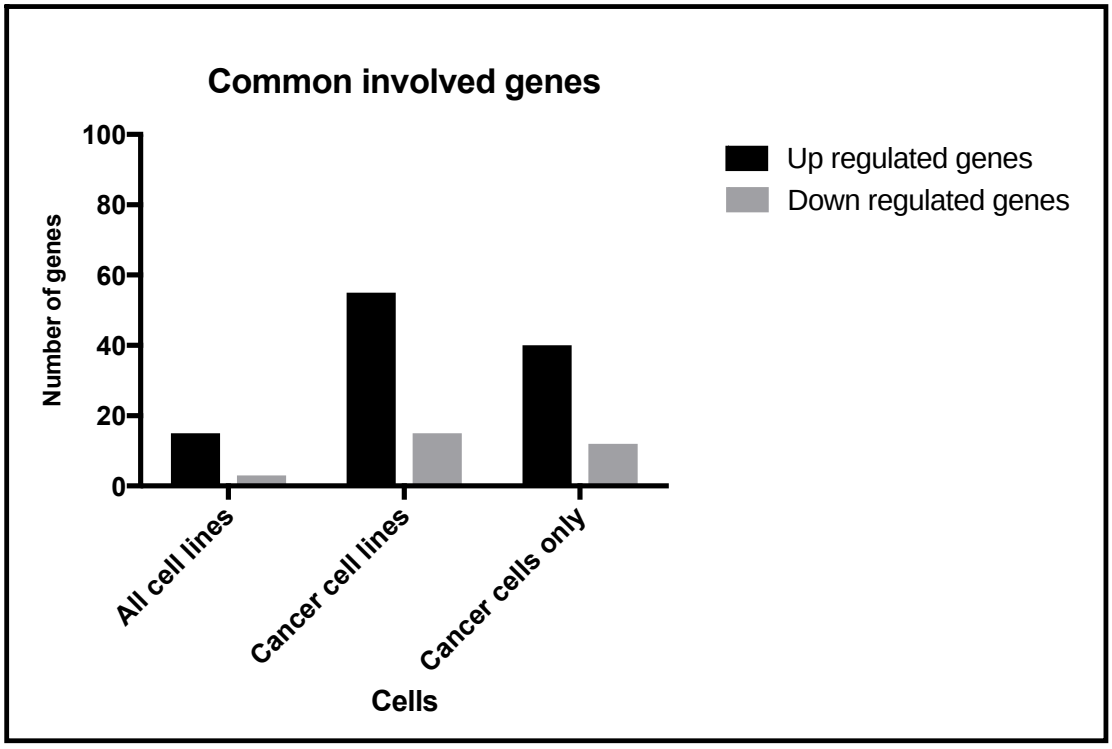

Figure 5.4: Overview of the results of the Affymetrix array assay and the common involved genes in K1E7, FTC-133 & Nthy-ori 3-1 cells.

Results of the Affymetrix array assay showing the number of genes for which changes in expression were shared in all cell lines (K1E7, FTC-133 and Nthy-ori 3-1 cells). Also the genes that were shared between the cancer cell lines (K1E7 and FTC-133), and finally the genes shared by the cancer cells, but unchanged in the normal Nthy-ori 3-1 cells. The findings demonstrate that there is a large amount of change in expression of genes that is specific to the cancer cell lines.

In addition to looking at individual target genes, it is possible to look at what pathways are implicated and show significant change. A large number of genes were identified as potentially of interest from the initial screen. The data produced by the Afffymetrix Array can be refined using the Database for Annotation, Visualization and Integrated Discovery (DAVID) to identify the top 10 significantly involved pathways in K1E7, FTC-133 and Nthy-ori 3-1 cells

following Metformin treatment. DAVID uses a comprehensive set of functional annotation tools, to refine the results for the systematic and integrative analysis of the gene lists (https://david.ncifcrf.gov/summary.jsp). DAVID allows for an integrated approach to be taken to the analysis and identifies any relationship between up and down-regulated genes to reveal pathways implicated by treatment with Metformin.

Following the submission of the results of the expression arrays to DAVID, several involved pathways were found for each of the cell lines. In total 468, 24 and 151 functional annotation clusters (implying linked pathways) were found as a result of the up-regulated genes for K1E7, FTC-133 and Nthy-ori 3-1 respectively. Furthermore 88, 13 and 41 functional annotation clusters were revelaed in relation to the down-regulated genes for K1E7, FTC-133 and Nthy-ori 3-1 respectively. The top 10 fucnctional annotation clusters based on the p-value were selected for K1E7, FTC-133 and Nthy-ori 3-1 (**Table 5.7 & 5.8**). The study did not find any commonly affected pathways between all three cell lines among the top 10 significant either up or down-regulated pathways.

Table 5.7: Findings of analysis with DAVID, to analyse the top 10 functional annotation clusters of up-regulated genes in the cell lines; following treatment with Metformin (0.3 mM) for 6 days.

No.	K1E7 (10 out of 468 clusters)		FTC-133 (10 out of 24 clusters)		Nthy-ori 3-1 (10 out of 151 clusters)	
	Annotation clusters	P-value	Annotation clusters	P-value	Annotation clusters	P-value
1	Transferase	3.6E-10	Lipid metabolism	8.0E-3	Response to hypoxia	8.7E-6
2	Metal-binding	7.4E-9	Mitochondrial part	1.6E-2	Positive regulation of cell migration	4.2E-6
3	Ubl conjugation pathway	4.3E-9	Flavoprotein	1.8E-2	Response to oxygen levels	1.5E-5
4	Zinc	1.8E-8	Golgi membrane	1.9E-2	Domain:Anaphylatoxin-like	3.2E-5
5	Zinc-finger	7.1E-8	Golgi apparatus part	2.2E-2	Anaphylatoxin	9.5E-5
6	Nucleus	2.5E-12	FAD	2.2E-2	Complement C3a/C4a/C5a anaphylatoxin	9.5E-5
7	Serine/threonine protein kinase-related	4.7E-7	Glycoprotein metabolic process	2.3E-2	Antiviral defense	3.3E-5
8	Serine/threonine-protein kinase	5.9E-7	Fatty acid metabolism	3.0E-2	Regulation of cell motion	1.0E-4
9	Apoptosis	1.7E-6	Protein amino acid glycosylation	3.1E-2	Regulation of cell migration	1.0E-4
10	Protein kinase, core	1.2E-6	Glycosylation	3.1E-2	Response to nutrient levels	1.3E-4

The P-value (or EASE score generated by DAVID) examines the significance of the entire gene list and compares altered expression, whether up or down for individual genes, to relate such changes to pathway. On this basis the analysis can detemine which pathways are most altered

Table 5.8: Findings of analysis with DAVID, to analyse the top 10 functional annotation clusters of down-regulated genes in the cell lines; following treatment with Metformin (0.3 mM) for 6 days.

No.	K1E7 (10 out of 88 clusters)		FTC-133 (10 out of 13 clusters)		Nthy-ori 3-1 (10 out of 41 clusters)	
	Annotation clusters	P-value	Annotation clusters	P-value	Annotation clusters	P-value
1	Olfactory receptor	2.2E-9	Cytosolic part	2.7E-4	Metal ion-binding site:Zinc; catalytic	9.6E-4
2	Olfaction	4.6E-9	S_TKc	6.9E-4	Extracellular region	9.1E-3
3	Olfactory receptor activity	6.4E-9	Kinase	8.8E-4	Cell motion	1.2E-2
4	Sensory perception of smell	1.1E-8	Cell cycle	9.9E-4	Secreted	1.3E-2
5	GPCR, rhodopsin-like superfamily	2.0E-8	Binding site:ATP	1.4E-3	Extracellular region part	1.4E-2
6	7TM GPCR, rhodopsin-like	2.0E-8	Serine/threonine protein kinase	3.1E-3	Metalloprotease	1.4E-2
7	Sensory perception of chemical stimulus	8.6E-8	Nucleotide phosphate-binding region:ATP	6.0E-3	Response to organic substance	1.8E-2
8	Olfactory transduction	1.1E-7	Nucleotide binding	9.0E-3	Regulation of protein complex assembly	2.1E-2
9	G-protein coupled receptor	3.7E-7	Serine/threonine protein kinase, active site	9.2E-3	Actin binding	2.1E-2
10	Nucleosome core	6.0E-7	Serine/threonine protein kinase-related	9.6E-3	Signal	3.2E-2

The P-value (or EASE score generated by DAVID) examines the significance of the entire gene list and compares altered expression, whether up or down for individual genes, to relate

such changes to pathway. On this basis the analysis can detemine which pathways are most altered.

Using DAVID, genes up-regulated and down-regulated were highlighted and their expression was clustered to provide relationships that point to the pathways implicated (**Table 5.7 & 5.8**). To verify and further analyse the data, the functional annotation clusters were examined to see if individual genes within the pathways, rather than the pathways, were common targets amongst all cell lines. It was hoped that this analysis might reveal which gene /genes were specifically responsive to Metformin. To do this, targets originally identified without the use of DAVID were crossed referenced with the clustered data. Furthermore genes repeated as part of clusters on more than, or equal to 5, occasions (out of the top ten significant pathways) were identified. For all 3 cell lines the number of genes repeated as part of different clusters were 83 up-regulated and 35 down-regulated. However, there was such a significant cross over, that it was not possible to determine if any particular gene was the target for Metformin action (**data included in the appendix table 7.1, 7.2 & 7.3**). The genes originally identified as most highly up-regulated or down-regulated (**Tables 5.2, 5.3 & 5.4**) were also not identified within the top ten most significant clusters. The findings therefore provide evidence for pathways that are either up-regulated or down-regulated in response to Metformin, such as apoptosis (**Table 5.9**), but equally identifies individual target genes whose action maybe specific, such as *PPP1R10*. Genes such as *PPP1R10,* were not identified as part of the clustering data from DAVID as they do not belong to pathways with a high number of genes that showed commonality of expression changes.

The data overall not perhaps surprisingly found that Metformin modulated several pathways including pathways related to cancer, such as the up-regulation of apoptosis and down-regulation of the cell cycle (**Table 5.9, 5.10 & 5.11**). Other pathways were however highlighted that appeared to have no relationship, in particular the olfactory pathway which appears to have no bearing on the cancer behaviour or modulation of the thyroid cancer cell lines by Metformin.

Table 5.9: The list of involved genes identified using the Affymetrix array present in the apoptosis and cell cycle pathways following Metformin treatment in K1E7 cells.

Pathways	Apoptosis	Cell cycle
Down regulated genes	TPT1, NDUFA13, CASP1, MEF2C, PPP2R2B, ROCK1P1, COL18A1, HSPA1A, HSPA1B, ID3, IFI6, NEUROD1, RPS3A, SNCB, TP53I3	HORMAD1, PRDM9, CNTROB, GFI1, MNS1, MND1, MSH5
Up regulated genes	DHCR24, API5, ALMS1, BCL10, BAG2, BCL2L13, BNIP3L, DFFA, DRAM1, EP300, FASTKD2, FASTKD3, FAF1, GPR65, GSPT1, GULP1, JAK2, KLF11, KCNIP3, NCKAP1, NAIP, PTK2B, ARHGEF6, RASGRF1, RRAGC, ARHGEF12, ARHGEF18, ARHGEF2, SLTM, SH3GLB1, SLK, STEAP3, TIAM1, TIA1, TAX1BP1, AIMP2, AATF, AHR, CASP2, F3, CUL1, DAPK1, DOCK1, DNASE2, ERN1, FEM1B, FGF2, GLRX2, GREM1, GADD45A, HRK, HIPK2, HIPK3, IER3, IL1A, IL1B, IL24, IL6, JUN, LIG4, LITAF, MUL1, MEF2A, NGF, NET1, NME6, NFKB1, PAK2, PTRH2, PMAIP1, PREX1, PEA15, PHLDA1, PDCD4, PDCD6IP, PSME3, PRUNE2, RABEP1, RIPK1, RIPK2, RTN4, RNF144B, SEMA3A, SQSTM1, STK17A, ROCK1, SIRT1, SOS1, SOS2, SGMS1, SGPL1, SGPP1, TCTN3, TRIB3, TNFRSF10D, TNFRSF12A, TP53BP2, UBE4B, KRAS, MYC, ZMAT3	DHCR24, BLM, CDC14A, CSRP2BP, CHTF8, CABLES1, DCLRE1A, EP300, E2F3, E2F8, GPS2, G0S2, GSPT1, HAUS6, KAT2B, LATS1, MPHOSPH8, MIS12, NEK3, NEK4, NIPBL, PDS5A, RAD17, RAD50, RB1CC1, ARHGEF2, SH3BP4, STEAP3, SENP5, TAF2, ZWILCH, ACVR1, APPL2, APBB2, ANAPC13, ANAPC1, AVPI1, AHR, BCAT1, BRCA2, CDC6, CGRRF1, CEP120, SKA3, SKA1, CUL1, CUL3, CUL5, CCND1, CCNT1, CINP, CDK6, CLASP2, DSCC1, DUSP1, DMWD, EML4, EVI5, ERN1, EGFR, ERBB2IP, ESCO1, ESCO2, EIF4G2, FOXN3, GSK3B, GADD45A, HDAC3, INHBA, JMY, LMLN, LIG4, MCM8, MAP3K8, NEDD1, NPAT, PARD3, PARD6B, PHGDH, PKD2, PDCD6IP, PA2G4P4, PSMD11, PSMD5, PSME3, PPM1D, PPP3CA, PPP6C, PTP4A1, PRUNE2, RBBP8, RNF2, SEPT7P2, SESN2, SESN3, SGOL1,, SPAST, SPIN1, STAG1, STAG2, TNKS, TXNL4B, TOP3A, TFDP2, TBRG1, TUBE1, TP53BP2, MYC, VPS4B, ZMYND11

Selected up-regulated or down-regulated genes discussed later have been highlighted in the table.

Table 5.10: The list of involved genes identified using the Affymetrix array present in the apoptosis and cell cycle pathways following Metformin treatment in FTC-133 cells.

Pathways	Apoptosis	Cell cycle
Down regulated genes	NUAK2, GADD45A, IL24, MEF2D, NGF	CDK1, CKS1B, G0S2, NEK2, RAD54L, GADD45A, PHGDH, PLK3, RGS2
Up regulated genes	BCL10, CDKN2C, PAFAH2	CDC14A, NSL1, ASPM, BTRC, CDKN2C, FMN2, ZMYND11

Selected up-regulated or down-regulated genes discussed later have been highlighted in the table.

Table 5.11: The list of involved genes identified using the Affymetrix array present in the apoptosis and cell cycle pathways following Metformin treatment in Nthy-ori 3-1 cells.

Pathways	Apoptosis	Cell cycle
Down regulated genes	CD24, BIRC2, CGB8, LGALS1, SRGN, SGK1, TNFRSF21, BTG2, CD44, GSTP1, ID3, TXNIP	
Up regulated genes	DAPK1, DRAM1, DDIT4, NAIP, PTK2B, RASGRF1, ARHGEF2, AHR, C5, FUS, HRK, IER3, IFI6, IL6, OLR1, RNF144B, SEMA3A, SQSTM1, SGPL1, TRIB3, TNFRSF11B	CSRP2BP, CABLES1, DDIT3, E2F8, KAT2B, ARHGEF2, XRCC2, AHR, BRCA2, DSCC1, DUSP1, EGFR, PARD3B, PKD2, PA2G4P4, BRCC3, CITED2, BMP4, EDN1, HEXIM1

Selected up-regulated or down-regulated genes discussed later have been highlighted in the table.

Among the genes significantly implicated in the apoptosis pathway, one gene was commonly regulated by Metformin in K1E7 and FTC-133 cells (*BCL10*) and 16 genes were shared between K1E7 and Nthy-ori 3-1 (*AHR, ARHGEF2, BCL2, DAPK1, DRAM1, HRK, IER3, IL6, NAIP, PTK2B, RASGRF1, RNF144B, SEMA3A, SGPL1, SQSTM1 and TRIB3*) (**Figure 5.5 & Table 5.9, 5.10 & 5.11**). Metformin also commonly down-regulated one gene in the K1E7 and Nthy-ori 3-1 cell lines (*ID3*) (**Table 5.9 & 5.11**).

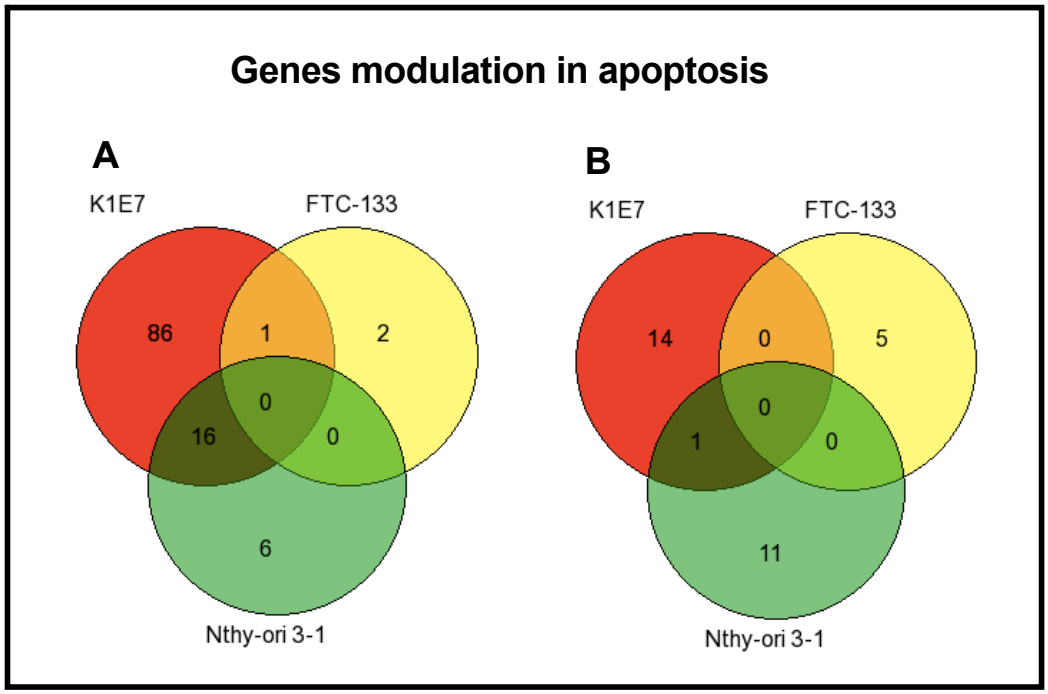

Figure 5.5: Pattern of shared genes involved in the apoptosis pathway identified using the Affymetrix assay in K1E7, FTC-133 & Nthy-ori 3-1 cells.

This figure shows the number of shared genes that were up-regulated (panel A) and down-regulated genes (panel B) in the apoptosis pathway in K1E7 cells (red circle), FTC-133 cells (yellow circle) and Nthy-ori 3-1 cells (green circle).

For the cell cycle pathway, 2 significantly up-regulated genes were shared by K1E7 and FTC-133 (*CDC14A* and *ZMYND11*), but more down-regulated genes were shared between K1E7 and Nthy-ori 3-1 (*AHR, ARHGEF2, BCL2, BRCA2, CABLES1, CSRP2BP, DSCC1, DUSP1, E2F8, EGFR, KAT2B, PA2G4P4 and PKD2*) (**Figure 5.6 & Table 5.9, 5.10 & 5.11**).

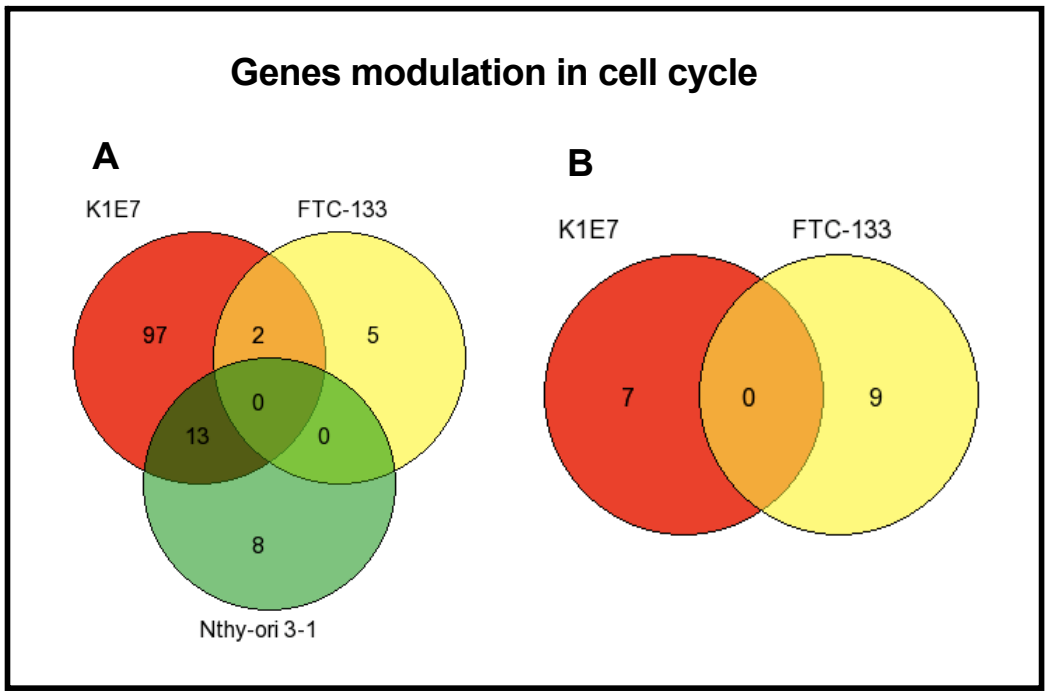

Figure 5.6: Pattern of shared genes involved in the cell cycle pathway identified using the Affymetrix assay in K1E7, FTC-133 & Nthy-ori 3-1 cells.

This figure shows the number of shared genes that were up-regulated (panel A) and down-regulated genes (panel B) in the cell cycle pathway in K1E7 cells (red circle), FTC-133 cells (yellow circle) and Nthy-ori 3-1 cells (green circle).

When looking at the patterns of pathways it appears that more pathways are affected in the thyroid cancer lines compared to the normal Nthy-ori 3-1(**Table 5.9 & Figures 5.5 & 5.6**). These findings would need to be explored further, but seem to validate some of the data from chapter 3 and 4 (sections 3.2.6 & 3.2.7) that suggest Metformin is acting more effectively on thyroid cancer, and that these lines they may be more sensitive.

5.2.5 Does Metformin regulate genes specifically in thyroid cancer but not normal tissue?

In this section specific comparison of the two cancer lines (K1E7 and FTC-133) was undertaken to see identify target was selectively affected in cancer only. The current study found that 55 significantly up-regulated genes and 14 significantly down-regulated genes were common between K1E7 and FTC-

133 cells (**Table 5.12 & 5.13**). Furthermore, It is clear that when the genes were commonly up or down-regulated in the thyroid cancer cell lines, the change in the level of expression was broadly comparable for both lines (**Table 5.12 & 5.13**). These findings may suggest that major pathways modulated by Metformin are essential to all tissues (both normal and cancer), such as cell cycle and apoptosis, whilst other pathways are also implicated in cancer cells and provide additional targets for modulation.

Table 5.12: The commonly up-regulated genes shared between K1E7 and FTC-133 cells, found using the Affymetrix array assay.

Numbers	Gene Symbol	Expression in FTC-133	Expression in K1E7
1	FAM213B	1.074924	1.015541
2	UBE4B	1.11957	1.349833
3	DNAJC16	1.103066	1.879633
4	RAB42	1.152434	1.330498
5	ZMYM4	1.038411	1.423858
6	ZNF691	1.17977	1.159623
7	TOE1	1.251928	1.557604
8	CPT2	1.659833	1.605741
9	ROR1	1.132694	1.557849
10	CACHD1	1.219443	1.104747
11	AGL	1.623054	1.751588
12	CDC14A	1.403379	1.50894
13	S1PR1	1.486556	1.304211
14	SLC16A1-AS1	1.065338	1.4398
15	LOC102723919	2.288908	1.351293
16	MAN1A2	1.086991	1.831226
17	NBPF25P	1.258747	1.229284
18	PRUNE	1.027419	1.078087
19	FLG-AS1	1.424351	1.454022
20	SLC25A44	1.76949	1.08994
21	C1orf220	1.694529	1.026326
22	RGL1	1.21664	1.228333

Numbers	Gene Symbol	Expression in FTC-133	Expression in K1E7
23	SERTAD4	2.912107	3.696954
24	LOC100287497	1.172272	1.949758
25	FBXO28	1.083433	1.797531
26	RAB4A	1.626263	1.572824
27	COG2	1.513195	1.410165
28	Unknown1	1.576519	1.285898
29	C1orf233	1.144269	1.243295
30	SYNC	1.166014	1.006925
31	BCL10	1.063442	1.236285
32	LRIF1	1.432328	1.903429
33	TSPAN2	1.365549	1.848103
34	Unknown2	1.289381	1.613705
35	RP4-791M13.3	2.410873	2.561201
36	THEM4	1.12133	1.238752
37	PIGM	1.104949	1.66414
38	EDEM3	1.494628	1.126477
39	RAB29	1.064365	1.246003
40	ZMYND11	1.225645	1.406281
41	BICC1	2.056973	1.539705
42	TET1	1.079681	1.91316
43	STOX1	1.166804	1.462698
44	KAT6B	1.04286	1.648313
45	LOC642361	1.044005	1.066369
46	TSPAN14	1.073806	1.397822
47	IFIT5	1.312251	1.528192
48	Unknown3	2.191284	1.655302
49	WBP1L	1.135208	1.060112
50	HTRA1	1.166512	1.81714
51	PTPRE	1.704732	1.041017
52	ST8SIA6	1.123277	2.265311
53	CASC10	1.495583	1.222906

Numbers	Gene Symbol	Expression in FTC-133	Expression in K1E7
54	ZNF248	1.172855	1.047531
55	C10orf25	1.318821	1.258493

Selected up-regulated or down-regulated genes discussed later have been highlighted in the table.

The table 5.13 represents those genes that have altered expression in the cancer cell lines (FTC-133 & K1E7), but may still be changed less significantly in normal tissues.

Table 5.13: The commonly down-regulated genes shared between K1E7 and FTC-133 cells, found using the Affymetrix array assay.

Numbers	Gene Symbol	FTC-133	K1E7
1	RNU6ATAC27P	-1.09637	-2.554632
2	RNU11	-1.760812	-3.019247
3	RNU6-753P	-1.286647	-1.703753
4	RNU4-61P	-1.053955	-1.781177
5	RABGGTB	-1.495314	-1.087615
6	Unkown1	-1.160969	-1.545412
7	Unkown2	-2.394764	-1.693968
8	PRAMEF11	-1.036984	-1.573027
9	SNORD103A	-1.32484	-1.361419
10	SNORA55	-1.385548	-1.225207
11	FAM72C	-1.015477	-1.177497
12	NBPF20	-1.737692	-1.206808
13	SNORA14B	-1.933805	-3.893102
14	RNU6-1067P	-1.202275	-2.642413

Selected up-regulated or down-regulated genes discussed later have been highlighted in the table.

The findings suggest that Metformin acts on certain shared targets. In some instances up / down-regulated genes in the cancer lines are modulated at higher levels, but are unaffected in normal thyroid cells. The expression of B-cell lymphoma/leukemia 10 (*BCL10*) decreased by 1.06 & 1.23 fold in FTC-133 and K1E7 cell lines respectively but were unaffected in Nthy-ori 3-1 cell lines (- 0.05 fold change). Small nucleolar RNA, C/D box 103A (*SNORD103A*) was down-regulated at comparable levels in both thyroid cancer lines (1.32 & 1.36 fold down-regulation in FTC-133 & K1E7 respectively), but was unaffected in the Nthy-ori 3-1 cell line (0.12 fold change) (**Table 5.13**).

5.3 Discussion.

5.3.1 OCT1 is ubiquitously expressed and is likely to promote uptake of Metformin by thyroid cancer cells.

Several transporters play an important role in Metformin uptake in the intestine, kidney and liver. In the intestine, the plasma membrane monoamine transporter (PMAT), OCT3 (SLC22A3) and OCT1 (SLC22A1) contribute to Metformin uptake [67, 70, 71]. In the liver Metformin uptake is mediated by OCT1 and probably by OCT3 and both transporters are expressed on the basolateral membrane of hepatocytes [67, 72-74]. In the kidney Metformin uptake from the circulation into renal epithelial cells is facilitated by OCT2 (SLC22A2) [72]. The renal excretion of Metformin from tubule cells to the lumen is mediated through MATE1 (SLC47A1) and MATE2-K (SLC47A2) [75-78], and studies in healthy individuals have suggested that they contribute to the renal excretion of Metformin [79]. Furthermore, OCT1 and PMAT (SLC29A4) may play important roles in the reabsorption of Metformin in the kidney tubules [80] [81].

In the current study, the presence and absence of OCT1 in thyroid cancer cells were examined, because the antibody for OCT1 was already available within the department and the importance of OCT1 in facilitating the anti-cancer effects of Metformin had already been reported in studies on ovarian cancer cell lines [254]. All thyroid cancer cell lines and normal thyroid cells were found to strongly express OCT1 even before treatment with Metformin (**Figure 5.1 & Table 5.1**). Furthermore, the OCT1 expression was not altered in gene expression array data and this is consistent with the OCT1 expression results found by Immunocytochemistry.

Previous studies have reported that Metformin has an anti-cancer effect by activation of the AMPK pathway [105, 245]. The presence of OCT1 in the thyroid cells is maybe essential for Metformin to enter the cells and activate AMPK [97], as previous studies have suggested this maybe the case. In ovarian cancer cell lines (SKOV-3 and OVCAR-3), OCT1 was shown to be

essential for the anti-cancer effects of Metformin in order for the activation of specific targets inside the cells such as activation of AMPK [254]. The study also found that Metformin induced-activation of AMPK decreased when the expression of OCT1 was blocked in both ovarian cell lines. Unlike, previous studies the expression data here on thyroid cancer did not show clear evidence for the activation of AMPK and mTOR pathways (**section 5.2.3**). It is possible that this is because the cells were treated with low doses (therapeutic dose) of Metformin, whilst previous studies have used toxic concentrations of Metformin. Due to time and financial constraints blocking of OCT1 expression or investigation of other previously studied transporters was not undertaken.

It is of course possible that other transporters are important in the uptake of Metformin by the cells, as here the expression data identified clear up-regulation of both the solute carrier family 18 member A3 (SLC18A3) in FTC-133 and SLC16A1-AS1 in all 3 lines tested (**Tables 5.3 & 5.5**). Consistent with current observations, Metformin treatment associated with overexpression of SLC18A3 in an animal study, where Metformin was investigated as a promising therapeutic agent for stroke therapy [255]. In addition to considerations about Metformin treatment, a study on chronic myeloid leukemia patients found that OCT1 expression was a useful biomarker for Imatinib therapy [256]. Patients failed to respond to Imatinib therapy, due to OCT1 down-regulation, and it is possible that OCT1 expression by all thyroid cancer cell lines in this study may equally prove of value as a therapeutic biomarker.

5.3.2 Metformin modulated a large number of genes that point to the pathways implicated in thyroid cancer.

This is the first study that has used the Affymetrix array to investigate the anti-cancer effect of Metformin in thyroid cancer. In this study, after Metformin treatment a large number of genes were modulated in thyroid cells (**Figure 5.3**). In the literature, several genes (cyclin D1, c-Myc, AKT, ERK, TSC2, 4E-BP1 and S6K1) have already been reported as associated with the role of

Metformin in thyroid cancer [104-106, 149]. There is consistent evidence in thyroid cancer to suggest that the AMPK pathway is up-regulated and the mTOR is down-regulated. A study on thyroid cancer cell lines found that Metformin inhibited cell growth and cell migration via up-regulation of the AMPK pathway and down-regulation of mTOR pathway, resulting in decreased expression of cyclinD1 and c-myc, subsequently decreasing the phosphorylation of S6K and 4E-BP1 [105]. However, the dose of Metformin was much higher than used here in these expression studies. In 2 studies using different thyroid cancer lines, found that Metformin increased AMPK and down-regulated mTOR, as well as decreasing the phosphorylation of P70S6K, PS6, cyclin D1 and ERK [106, 149]. Furthermore, Chen, in a study on anaplastic thyroid cancer cells (HTh74), found that Metformin inhibited thyroid cell growth, by increasing phosphorylation of AMPK and decreasing phosphorylation of mTOR and ERK [104].

As previously mentioned this current investigation did not show any evidence for the activation of AMPK and mTOR pathways (**section 5.2.3**). For all 3 cell lines no fold changes for AMPK and mTOR were detected by Affymetrix. The molecular mechanisms behind the anti-cancer effects of Metformin in thyroid cancer are not clear, as there has been limited study. In this investigation thousands of genes were up and down-regulated following Metformin treatment of the 3 different thyroid cell lines (Nthy-ori 3-1, K1E7 and FTC-133) (**Figure 5.3**). The top up-regulated genes in K1E7, FTC-133 and Nthy-ori 3-1 cells were *PPP1R10*, *SLC18A3* and *C4B* respectively (**Table 5.2, 5.3 and 5.4**). The *PPP1R10* gene is thought to play an important role in cellular process such as cell cycle [253]. Whereas *SLC18A3* encodes vesicular acetyl-choline (Ach transporter), and may represent an alternative transporter for the uptake of Metformin as discussed previously [257]. *SLC18A3* has been associated with recessive congenital myasthenic syndrome [258]. The complement component 4 gene (*C4B*), is involved in the complement system and assists with important functions such as immunity, tolerance and autoimmunity in combination with the other numerous components [259]. Its importance in the context of this study is not yet clear. What however was

clear was the evidence implicating the *SNORD* family as most commonly regulated genes across all lines (**Table 5.2, 5.3 and 5.4**). Among the top 10 significantly up-regulated or down-regulated genes, mutual genes were found in K1E7 and Nthy-ori 3-1 cells; two up-regulated genes (*IER3* and *PPP1R10*) and two down-regulated genes (*SNORD32B* and *TAF1D*) (**Table 5.2 & 5.4**). Furthermore from the initial screen members of the *SNORD* family were consistently down-regulated across all lines. The *SNORD* family has been found to be over expressed in tumour cells [260], but there is very limited data on the family in cancer. In relation to *SNORD32B* it is a small nucleolar RNA a member of SNORD family and with little information available on the databases. *TAF1D* (TATA-box binding protein associated factor), plays a role in RNA polymerase 1 transcription) [261] but again with very little evidence for its role in cancer. Of particular interest is *IER3* (Immediate early response 3), also known as *IEX-1* (Immediate early gene X-1). *IER3* plays an important role in cell growth control and acts as a negative regulation of apoptosis [262]. *IER3* is activated to protect cells from stimuli induced cell apoptosis such as stress, radiation and viral infection or therapies such as Metformin [263]. The *IER3* cell survival function is in response to stimuli inducing cell death and is obtained upon ERK activation pathway [264]. As *IER3* is a top gene up-regulated in this study it suggests that there is ERK activation as a response to Metformin, which may mean that indeed there is some modulation of the AMPK and mTOR pathways here, but that there are so many other potentially more important findings it was not identified in this study as significant. The protein phosphatase 1 regulatory subunit 10 (*PPP1R10*) plays an important role in cellular process such as cell cycle, by protecting chromosome de-condensation [253], and links into the current findings by suggesting that the stalling of the cell cycle observed here (**Figure 3.12**) may require increased expression of *PPP1R10* to maintain chromosome integrity whilst stalled and slowed by Metformin.

Although mutual genes were shared by all 3 cell lines, the study found no shared mutual genes in the top 10 significantly up and down-regulated genes between FTC-133 and the other two cell lines. However, among all significant

genes approximately 15 mutual genes were observed to be up-regulated and 3 genes to be down-regulated in K1E7, FTC-133 and Nthy-ori 3-1 cells (**Table 5.5 & 5.6**). The effect of some of these genes is not known, and for all these genes there is no evidence to suggest a possible role in thyroid cancer or for treatment by Metformin.

Using DAVID, the most significant of the pathways modulated by Metformin can be identified. It is however, important to remember that in these pathways indicated genes maybe up or down-regulated. But the overall effect is a down-regulation or up-regulation of the pathways. The selected pathways provide a better understanding of the findings in chapter 3 related to apoptosis and cell cycle (**section 3.2.6 & 3.2.7**) as here (**Table 5.9, 5.10 & 5.11**) there is evidence to show up-regulation of apoptosis and down-regulation of the cell cycle, and thus confirming that the anti-cancer effects of Metformin in thyroid cancer result in increased apoptosis and stalling of the cell cycle. This study shows several genes that were up-regulated and down-regulated in apoptosis and cell cycle pathways that were not previously reported in thyroid cancer [104-106, 149] and these targets (cyclin D1, c-Myc, AKT, ERK, TSC2, 4E-BP1 and S6K1) have already been discussed.

There was however some confusing evidence relating to data on the olfactory clusters, which was a top target among the down-regulated genes (**section 5.2.4 & Table 5.8**). The modulation of the olfactory clusters was found only in the K1E7 cell line, and comprises 26 down-regulated genes. It is possible that this was a bystander change brought about because of the large number of other pathways altered in the K1E7 cell line (556 pathways), and there is no evidence for a possible role in the Metformin regulation of thyroid cancer in the literature. Furthermore, as Metformin modulation of K1E7 produced so much more alteration than for the other cell lines, it is possible that the results for this line are less robust when specifically compared to the other annotated clusters, and may suggest that was unreliability of the data for these clusters. The experiments would need to be repeated to confirm these possible pathways as implicated.

5.3.2.1 Metformin-induced regulation of apoptosis and cell cycle arrest in thyroid cells.

The current study found that Metformin modulated several genes that play an important role in apoptosis and cell cycle (**Table 5.9, 5.10 & 5.11**), Metformin decreased the expression of Cyclin-dependent kinase 1 also known as *CDK1* by 1.04 fold in FTC-133 cells (**section 5.2.4 & Table 5.10**). *CDK1* plays an important role in cell cycle regulation [265]. More recently, a study on non-small cell lung cancer cells found that knockdown of *CDK1* resulting inhibition of cell proliferation, cell migration, and induced cell cycle arrest and enhanced cell apoptosis [266].

In addition to *CDK1*, Metformin altered the expression of the *NUAK2* gene. *NUAK2* expression decreased by 1.39 fold following Metformin treatment of FTC-133 cells. *NUAK2* is known as SNF1-like kinase 2 and plays an important role in cell cycle regulation and growth of melanoma cells [267]. A study on melanoma cells found that knockdown *NUAK2* resulting inhibition of cell proliferation, cell migration, and also induced apoptosis and cell cycle arrest [268]. Furthermore, knockdown of *NUAK2* decreased the expression of cyclin D1, cyclin D3, cyclin-dependent kinase 2 and down-regulated the expression of mTOR [268].

Recently, a study reported that the tumour suppressor p53 is required for Metformin-inhibited cell proliferation [269] and Metformin-induced apoptosis in breast cancer [244]. In this investigation, Metformin modulated the expression of the *TP53BP2* gene in K1E7 cells increasing its expression by 1.45 fold (**section 5.2.4 & Table 5.9**). *TP53BP2* gene, also known as tumour suppressor p53-binding protein 2 (*TP53BP2*) or apoptosis-stimulating p53 protein 2 (ASPP2) [270], is a tumour suppressor gene which promotes damage-induced apoptosis through activation with p53 [271]. *TP53BP2* controls p53 by boosting the DNA binding and transactivation function of p53, on the promoters of pro-apoptotic genes *in vivo* [272]. Moreover, the down-

regulation of *TP53BP2* associates with increased cell proliferation, tumour metastasis and poor prognosis in human cancers [273, 274], and can result in increased resistance to gemcitabine treatment [275]. *TP53BP2* expression however enhanced sensitivity of chemotherapy-induced apoptosis in colon cancer cells [276].

In this current study, tumour protein translationally-controlled 1 (*TPT1*) also known as *TCTP*, was found to decrease by 1.62 in K1E7 (**section 5.2.4 & Table 5.9**) Metformin treated cells compared to control (non-Metformin treated cells). It is thought that *TCTP* plays an important role in cell growth and protects cells from apoptosis. In other studies, the expression of *TCTP* decreased during tumour suppression associated with the activation of the tumour suppression gene (p53) in human monocytic leukemia cells [277]. The knockdown of *TCTP,* in primary mammary tumour cells from ErbB2 transgenic mice, results in activation of p53 and inhibits cancer cell growth [278]. More recently, *in vivo* and *in vitro* data shows that the knockdown of *TCTP* in lung cancer cells results in the inhibition of cell proliferation, colony formation and cell migration and also induces apoptosis (by altering apoptosis regulatory proteins such caspase-3, p53 and BCL2) and cell cycle arrest [279]. The findings here on *TCTP* in K1E7 mirror those discussed on *TP53BP2*, and suggest that down-regulation of an inhibitor of p53 matched with up-regulation of an activator are related and ultimately through p53 increase apoptosis.

In this study, Metformin treatment increased the expression of Caspase 2 (*CASP2*) by 1.14 fold in K1E7 cells compared to non-treated cells (**section 5.2.4 & Table 5.9**). CASP2 is an enzyme encoded by the *CASP2* gene in humans and is one of the hallmarks of apoptotic cell death [280]. A study on prostate cancer cell lines (PC-3 and LNCaP) and the anti-cancer effects of Ferulic acid, found that Ferulic acid inhibited cell proliferation and induced cell apoptosis as reflected by activation of *CASP2* [281]. Alternatively, knock down of *CASP2,* inhibited Docetaxel-induced apoptosis in prostate cancer cells (PC3), the data indicated that premitochondrial activation of *CASP2* was required for Docetaxel-induced apoptosis in prostate cancer cells [282].

Similar to the current findings on thyroid cancer, a previous study using Metformin found that it inhibited cell proliferation and induced apoptosis through activation of the caspase family and AMPK in cholangiocarcinoma cells [269]. In addition, overexpression of *CASP2* in the current study might be through the potential activation of the AMPK pathway, as previous reports suggest that the AMPK pathway is involved in CASP2-modulated autophagy [283, 284].

In the current study, the expression of the death associated protein kinase 1 (*DAPK1*) gene increased following Metformin treatment in K1E7 and Nthy-ori 3-1 cells by 2 and 1.49 fold respectively (**section 5.2.4, Table 5.9 & 5.11**). DAPK1 is a calcium/calmodulin (Ca^{2+}/CaM)-dependent serine/threonine kinase encoded by *DAPK1* gene in humans [285]. *DAPK1* acts as a tumour suppressor gene and plays an important role in apoptosis and cell cycle arrest [286]. A study on human neuroblastoma cell lines (U251) shows that overexpression of *DAPK1* induces apoptosis and G2/M cell cycle arrest; whilst knockdown of *DAPK1* inhibited apoptosis and cell cycle arrest [287]. In another study on pancreatic cancer cells (BxPC-3), overexpression of *DAPK1* in BxPC-3 cells significantly inhibited cell proliferation, cell migration and activation of caspase-3, which was followed by down-regulation of AKT and ERK phosphorylation [288]. The study suggested that overexpression of *DAPK1* in pancreatic cancer cells inhibited cell proliferation through P13K/AKT and ERK pathway. Furthermore, as previously mentioned Chen, reported that Metformin inhibited ERK phosphorylation and the mTOR pathway in thyroid cancer cells [104]. The overexpression of *DAPK1* in the current study suggests that Metformin could be targeting the MAPK/ERK pathway in thyroid cancer cells, but needs further investigation.

The regulation of other genes in this investigation also supports the potential of Metformin to induce apoptosis and regulate the cell cycle. The expression of B-cell lymphoma/leukemia 10 gene (*BCL10*) increased by 1.23 and 1.06 fold in K1E7 and FTC-133 cells respectively but no changes was observed in Nthy-ori 3-1 cells (**section 5.2.4, Table 5.9 & 5.10**). B-cell

lymphoma/leukemia 10 protein is encoded by the *BCL10* gene [289] and wild type BCL10 expression acts as a tumour suppressor with *BCL10* overexpression inducing apoptosis [290]. A study using breast cancer cell lines (MCF7 and T47D) shows that an anti-cancer agent, Benzene-poly-carboxylic acid complex, induced cell apoptosis, as determined by over expression of *BCL10* [291]. The expression of HORMA domain containing protein 1 (*HORMAD1*) was decreased by 1.13 fold in K1E7 cells following Metformin treatment (**section 5.2.4 & Table 5.9**). (HORMAD1) is a protein encoded by the *HORMAD1* gene in humans and play an important role in cell cycle regulation [292, 293]. *In vitro* and *in vivo* studies on ovarian cancer cells found that silencing *HORMAD1* gene enhanced Docetaxel-induced apoptosis and reduced tumour weight [294].

The specific gene regulation following Metformin treatment clearly indicates that Metformin treatment is associated with cell cycle arrest and induces apoptosis (**Figure 5.7**).

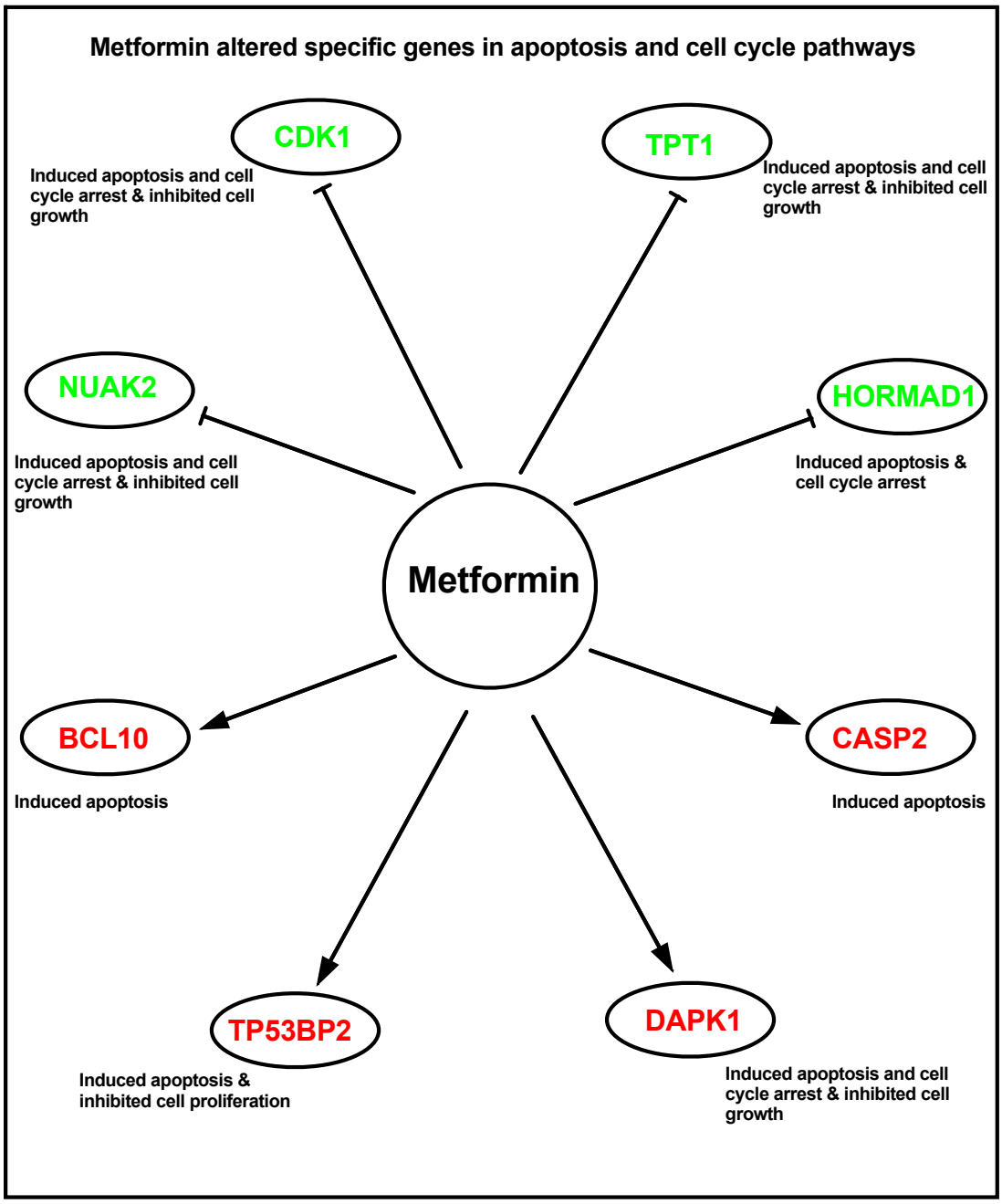

Figure 5.7: Metformin alters specific genes in the apoptosis and cell cycle pathways.

The findings here of the expression array all serve to support the previous findings of Metformin inhibiting cell proliferation, induced cell cycle arrest, and accelerated apoptosis presented in chapter 3 (**section 3.2.3, 3.2.6 and 3.2.7 respectively**).

5.3.2.2 Evidence for modulation of the action of Metformin by other regulators.

In this study, presented in chapter 4, TSH and IGF-1 had no effect on the ability of Metformin to control cell proliferation of the thyroid cell lines (**section 4.2.3 & 4.2.4**). It has been previously reported that TSH and IGF-1 activate the P13K/Akt signaling pathway and show down-regulation of FOXO1 (act as a tumour suppressor) in thyroid cancer cells [240]. Examination of the array data here (**section 5.2.3**) only found a slight increase in the expression of *FOXO1* in K1E7 cells by 0.42 fold. Of course as the study was not performed with TSH and IGF-1 it is not possible to say if their inclusion would affect the regulation of *FOXO1* by Metformin. Furthermore, in a study on endometrial cancer cells, Metformin inhibited cell growth via *FOXO1* and AMPK activation [295]. In the current study, FOXO1 was slightly up-regulation by Metformin suggesting another way of controlling thyroid cancer cells. It remains to be determined if Metformin exerts its effects by inhibiting pathways such as the P13K/Akt pathway and the expression of *FOXO1*.

5.3.2.3 Specific gene expression in thyroid cancer cell lines, is BCL10 induced by Metformin?

As previously mentioned expression of the *BCL10* gene, involved in apoptosis, was increased by 1.06 and 1.23 fold in FTC-133 and K1E7 (thyroid cancer cells) but not normal cells (**section 5.2.5**). This may suggest that although apoptosis is up-regulated in all thyroid cells its action may be increased in thyroid cancer specifically. Unfortunately the TT cell line, which had the highest level of apoptosis, was not investigated by the array, and it would have been interesting to make a comparison with the expression of *BCL10* post Metformin treatment.

Finally the data suggests that Metformin action in cancer is wide ranging and targets multi-signalling pathways and further investigation is required to

understand the molecular action of Metformin in depth. The thyroid cancer cell lines showed variation in the number of genes modulated, as did the normal control, potentially reflecting characteristics of the subtypes of thyroid cancer responding to modulation by Metformin in a different manner.

5.3.2.4 Other regulatory pathways associated with Metformin.

The gene expression data detailed above included many targets of interest as part of the pathways that are possibly modulated by Metformin. However other targets have previously been suggested to be the focus for the action of Metformin in cancer. These include GLUT4, COX-2, ACC, STAT3, GPAM, Bax, Ki67, RET [101, 102, 181, 182]. Unfortunately although the array included information on over almost 54,000 genes the above were not part of the array, and it was not possible to confirm if they were the subject of modulation by Metformin.

5.4 Conclusions

OCT1 was ubiquitously expressed in thyroid cells even prior to treatment with Metformin, suggesting it can facilitate the anti-cancer effects of Metformin and possibly that thyroid cancer may be more responsive than other cancers. Metformin treatment significantly modulated thousands of genes and hundreds of pathways in thyroid cell lines, but findings confirmed the importance of both apoptosis and cell cycle regulation by low dose Metformin.

In the current study the gene expression data was obtained from medium containing 10 mM of glucose, as this had been shown to produce good growth of all the cell lines. The level of glucose chosen here could however prevent / reduce AMPK activation, in favour of alternative pathways. Metformin treatment has been shown to become more cytotoxic by decreasing ATP production and increasing AMPK phosphorylation in a medium which contained low glucose (2.5 mM) compared to medium which contained 25 mM of glucose [224]. AMPK pathway activation induces p53 up-regulation [296],

and the current study found Metformin-induced activation of *TP53PB2* (P53 activator) in K1E7 cells (**Table 5.9**) suggesting the potential activation of the AMPK pathway. In this study the lower doses of Metformin present in a higher concentration of glucose is different to previous investigations, and it is possible that the response to Metformin in this investigation still activates AMPK but that other pathways maybe more important.

CHAPTER SIX

General discussion

6.1 Background to project and summary of findings.

At the start of this project, a literature search found population-based studies that suggested the potential anti-cancer effects of Metformin in several types of cancer [109, 111, 112]. Furthermore, other studies found that Metformin treatment in type 2 diabetes patients was associated with a reduced risk of cancer, decreased cancer recurrence and reduced cancer mortality [111, 115, 117, 120]. Metformin had also been studied *in vitro* [125, 128], with investigations confirming Metformin's anti-cancer properties on different cancer cells such as breast, pancreatic, ovarian, colorectal, lung, oesophageal, and specifically on thyroid cancer [104-106, 149]. At the beginning of the current study, there were few studies on the anti-cancer effects of Metformin in thyroid cancer; but currently, there are in excess of more than 20 studies on thyroid cancer [104-107, 124, 137, 147, 149, 183, 189, 195, 297-305] including our own based on the results of chapter 3. These include investigations based on *in vitro*, *in vivo* and clinical data.

Despite the evidence supporting the anti-cancer action of Metformin, the molecular mechanisms through which it modulates cancers have not been well characterized. Although both the AMPK and mTOR pathways are targeted in a number of cancers [85, 105, 174, 306], this study has not found clear evidence from the gene expression data, that in thyroid cancer the AMPK and the mTOR pathways are modulated by Metformin (**section 5.2.2**). The current study did however find strong evidence in favour of the anti-cancer effects of Metformin in thyroid cancer, and the main findings are summarized in figure 6.1.

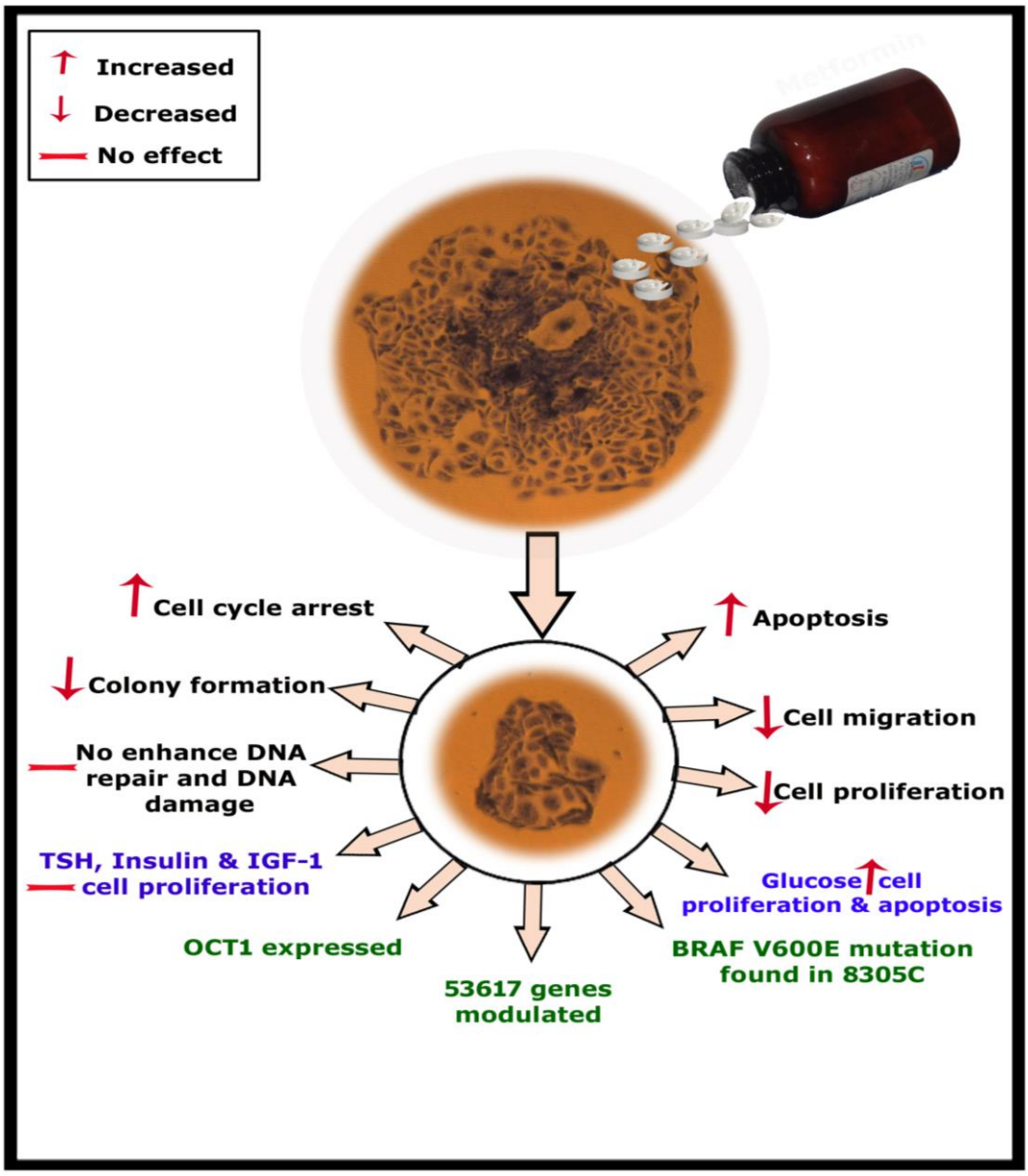

Figure 6.1: Summary of the anti-cancer findings of Metformin in thyroid cancer cell lines.

This figure shows the anti-cancer effects of Metformin in chapter 3 (black), chapter 4 (blue) and chapter 5 (green).

Consistent with the previous reports, Metformin inhibited thyroid cancer cell proliferation and clonal formation as analysed by MTT assay and clonal formation assay (chapter 3) [104, 195]. At the doses of Metformin considered to be within normal therapeutic concentrations in diabetic patients (< 0.3 mM) [132, 163], the effects were not statistically significant over 6 days on thyroid cells. However, the relationship could explain the significant anti-cancer

effects when Metformin is used for longer periods, as with diabetic patients. This investigation standardized all tests in 10 mM glucose, as the growth for all cell line was good. However previous studies on thyroid cancer have used other concentrations of glucose in a variety of media with different additives. Thereby the action of Metformin could be modulated in these studies by the higher glucose used or the additional additives [240].

6.2 How modulation of the anti-cancer action of Metformin may alter patient response.

The anti-cancer effects of Metformin on thyroid cell proliferation were modulated by the amount of glucose in the medium (section 4.2.1). Without glucose, cells did not grow and the action of Metformin was strongest. High levels of glucose (10 mM) however abrogated the action of Metformin. It is important to consider that the oxidation of 1 molecule of glucose under aerobic conditions can produce 38 molecules of ATP, whilst in anaerobic conditions only 2 molecules of ATP are produced [190]. The findings in an earlier study that Metformin treatment decreased ATP production and increased AMPK phosphorylation in a low glucose medium may also help with the translation of the use of Metformin to the clinic [224]. Since, glucose metabolism in cancer cells occurs mainly under anaerobic conditions; cancer cells need more glucose to grow and replicate. In this study the thyroid cancer cells were cultured in aerobic conditions and it can be counted as one of the limitations of this study, but if Metformin does decrease ATP production its anti-proliferative effects, as reported in this study, may be augmented in the patient under hypoxic conditions and with a low glucose diet, by further restricting the production of ATP. Unfortunately it was not possible during this current investigation to look at the effect of Metformin in hypoxic conditions. The action of other possible modulators affecting the response in patients was also studied. Investigation into the role of TSH, Insulin and IGF on cell proliferation under defined circumstances demonstrated no effect (chapter 4). Further studies are required to investigate the influence of other modulators in more detail. Once again differences between this study and past

investigations may reflect variation in other factors included in the media that may have additionally modulated the findings [240].

6.3 The uptake of Metformin by thyroid cancer cells.

All the effects as a consequence of treatment with Metformin have yet to be determined. Unlike previous investigations [168], this study found that exposure to Metformin did not induce DNA damage (**section 3.2.8**); even at high concentrations of Metformin for prolonged periods (up to 20 mM of Metformin for up to 6 days). Another recent study has confirmed our findings [188]. It is thought that the growth inhibitory effect of Metformin on cancer cell proliferation may be through the activation of AMPK via activation of LKB1 [85], which causes inactivation of mTOR pathway [174]. In ovarian cancer lines, OCT1 was shown to facilitate uptake of Metformin and when knocked down AMPK was inactivated, suggesting this is the method whereby Metformin is internalized [254]. All thyroid cancers (and the normal thyroid cell line) in this study expressed OCT1, which may indicate that they are involved in the action of Metformin. Furthermore, as OCT1 expression appears to be linked to Metformin activating AMPK [254], it suggests that in thyroid cancers, the AMPK would be activated and mTOR down-regulated. The findings in chapter 5 found unclear evidence for the modulation of the common target genes in the AMPK and mTOR pathways. Why this should be is unclear, but this study used therapeutic doses, whilst others studies used doses known to be toxic, and this may be the explanation for different responses. The activation of AMPK may therefore be a response to toxic conditions. Alternatively, as mentioned in chapter 4 (section 4.2.1) it may be down to the fact that in this current study glucose was used in the medium and OCT1 modulation of AMPK may be under situations of low glucose only [254].

Unfortunately because of time constraints blocking OCT expression or investigation of other previously studied transporters was not undertaken. It is of course possible that other transporters are important in cellular uptake of Metformin, as here the expression data identified clear up-regulation of both solute carrier family 18 member A3 (*SLC18A3*) in FTC-133 and *SLC16A1*-

AS1 in all 3 lines tested (**Tables 5.3 & 5.5**). Consistent with current observations, Metformin treatment was associated with overexpression of *SLC18A3* in an animal study investigating Metformin as a promising therapeutic agent in stroke therapy [255]. However, the expression array was performed only once and repeats are important to validate the data and undertake further research on the genes that are consistently up or down-regulated.

6.4 What pathways does Metformin act on to produce its anti-cancer effect in thyroid cancer?

As mentioned before, evidence in this study did not find direct up-regulation of the AMPK pathway. Importantly however, the current study has found that low dose of Metformin treatment (0.3 mM) for 6 days altered the expression of several specific genes that previously have not been identified in studies of Metformin and thyroid cancer, such as *TP53BP2*, *NUAK2*, *CASP2*, *DAPK1*, *TCTP*, *BCL10* and *HORMAD1* (**Table 5.9, 5.10 & 5.11**). Additionally, some of these specific genes have been investigated before as targets for therapy in several types of cancer [267, 268, 275, 276, 279, 281, 282, 287, 288, 290, 294], and in the context of this study they can help to improve the understanding of the mechanisms by which Metformin produces its anti-cancer actions.

It has been previously reported that p53 is required for Metformin to inhibit cell growth and induce apoptosis [244]. AMPK pathway activation induces p53 up regulation [296], and the current study found Metformin induced activation of *TP53PB2* (P53 activator) in K1E7 cells (**Table 5.9**), suggesting the potential activation of AMPK pathways. In the current study, low dose of Metformin increased the expression of *TP53BP2* by 1.45, 0.36 and 0.37 fold in K1E7, FTC-133 and Nthy-ori 3-1 cells respectively. *TP53BP2* expression has been shown to enhance sensitivity of chemotherapy-induced apoptosis in colon cancer cells [276]. If TP53BP2 were increasing sensitivity to chemotherapy-

induced apoptosis, then maybe treatment with Metformin to up-regulate TP53BP2 before giving chemotherapy in thyroid cancer would be a possibility. Furthermore, Metformin inhibited cell proliferation and induced apoptosis through activation of the caspase family and AMPK in cholangiocarcinoma cells [269]. Overexpression of *CASP2* in the current study might be through the potential activation of AMPK pathway, as it has been previously reported that AMPK is involved in CASP2-modulated autophagy [283, 284].

This study suggests that the potential activation of AMPK pathways at low dose (non-toxic) Metformin in thyroid cancer cell lines is through the activation of other AMPK-target genes, that are linked to and interact with this pathway. Similarly, although there was no direct evidence that the mTOR pathway was down-regulated by Metformin, the current study did find that Metformin decreased the expression of *NUAK2* in FTC-133 cells (**Table 5.10**). Evidence suggests that knockdown of *NUAK2* decreases the expression of cyclin D1, and down-regulates the expression of mTOR [268]. The MAPK/ERK pathway is another pathway that may be targeted by Metformin. As previously mentioned, Chen, reported that Metformin inhibited ERK phosphorylation and mTOR pathways in thyroid cancer cells [104]. The overexpression of *DAPK1* in pancreatic cancer cells inhibited cell proliferation through P13K/AKT and ERK pathway [288]. The overexpression of *DAPK1* in the current study suggests that Metformin could be targeting the MAPK/ERK pathway in thyroid cancer cells, but needs further investigation.

However, although direct activation of AMPK and down-regulation of the mTOR pathways was not found in this study, importantly there was consistency of findings between those of chapter 3 and the experimental data in chapter 5, that suggests Metformin induces apoptosis and stalls cell cycle (**section 3.2.6, 3.2.7**). Observations from chapter 3 on the up-regulation of apoptosis and blocking of the cell cycle were confirmed in section 5.2.4 with both thyroid cancer and normal cell lines demonstrating modulation of the expression of genes in these pathways. Importantly the expression data from this study shows that Metformin has a wide-ranging action (chapter 5). 0.3

mM of Metformin was enough to significantly modulate 53617 genes in K1E7, FTC-133 and Nthy-ori 3-1.These findings suggest that there is still much to learn about how Metformin acts in cells and the pathways and targets of its actions. There is consistency in this study however between genes up or down-regulated for all cell lines, and there are also genes targeted specifically in the thyroid cancers compared to the normal Nthy-ori 3-1 cell line (section 5.2.5). Differences between the top genes and pathways altered between Nthy-ori 3-1 and the thyroid cancer lines suggest that there are genuine differences in response to Metformin. This mirrors and support the observations of chapter 3 where apoptosis and cell cycle arrest was more evident in the thyroid cancer lines (section 3.2.6 & 3.2.7) Why certain genes and pathways are targeted needs to be explored further. The *SNORD*s family looks a promising angle, and there have been links to cancer but the relationship is unclear [260]. Other pathways such as the members of olfactory pathways in KE17 are so far unrelated to the Metformin use or cancer, so the relevance of these findings warrants further exploration.

Furthermore, the differences in the expression of the transporters could explain increased uptake in the thyroid cancer lines resulting in more apoptosis than Nthy-ori 3-1 cells. In addition, as mentioned in section 5.2.4 Metformin modulates more genes in cancer lines (120 & 133 genes modulated in apoptosis and cell cycle pathways respectively) compared to Nthy-ori 3-1 cells (34 & 21 genes modulated in apoptosis and cell cycle pathways respectively), consistent with the finding that cancer cell lines demonstrated more apoptosis and cell cycle arrest (section 3.2.6 & 3.2.7).

The *CDK1* expression was increased in FTC-133 cells following Metformin treatment. *CDK1* plays an important role in cell cycle progression and itself is activated by A-type cyclins and is in complex with cyclin B1 to facilitate the onset of mitosis [265]. The exquisite control of CyclinB1/Cdk1 activity peaking at metaphase is necessary for a successful G2/M transition. Previous studies on thyroid cancer cells found that Metformin induced AMPK activation in a dose dependent manner and inhibited cyclin D1 through inhibition of mTOR

pathways [105, 106]. Cyclin D1 plays an important role in cell cycle progression through the G1/S phase via binding to the cyclin dependent kinase 4 (cdk4), acting to phosphorylate and inactivate the retinoblastoma protein, and release E2F transcription factors to transcribe genes required for entry into S phase of cell cycle [307]. Comparison of the findings from this and other studies suggests that Metformin treatment is associated with arrest in different phases of the cell cycle; since the data presented here, indicates that the action of Metformin is wide ranging and affects different targets acting on other phases of the cell cycle. Alternatively the action of Metformin could vary among different types of cell lines in terms of cell cycle arrest, as a response to the cells own biology.

6.5 Study limitations

The main limitations to this current study were the logistical and financial constraints. More cell lines could have been studied with the Affymetrix expression array to identify patterns across all 5 thyroid cancer lines. Furthermore, the Affymetrix assay was done on the 3 thyroid cell lines only once (not triplicate), potentially affecting results and allow variability. Repetition of the expression data would hopefully narrow the targets by confirming genuine changes in expression that are consistent rather than as a result of variability in the quality of the array data. Such findings would confirm if there are real differences in the way thyroid cancers and normal thyroid tissues respond to Metformin. Finally, evidence also suggests that hypoxia may influence the response to Metformin, so it would have been good to look at the effect of hypoxia at low doses. Another limitation in the current study was the TT cell line was not tested for the influence of insulin, IGF-1 and TSH. This was due to technical issues limiting the recovery of the cell line for further investigation. Insulin, IGF-1 and TSH were also only studied in the proliferation assay and not in the assays investigating apoptosis, cell migration and colony formation. Despite the array being detailed and including many targets of interest, as part of the pathways possibly modulated by Metformin, the array was not however totally inclusive of some interesting targets e.g. RET, so other potential targets could not be studied.

6.6 Study strengths

This study clearly demonstrated the anti-cancer effects of Metformin on different thyroid cancer subtypes *in vitro*. Several thyroid cell lines (5 thyroid cancer cell lines and 1 normal thyroid cell line) were chosen to represent the different thyroid cancer types and study the anti-cancer effects of Metformin. Unlike other studies, the study used a wide range of Metformin concentrations including its therapeutic dose in diabetic patients (0.3 mM). In this study all experiments were performed in the same medium (DMEM contained 10 mM of glucose) because this study observed that the growth patterns were different in different media such as DMEM 4.5g/L, DMEM F-12 and RPMI. As such the different investigations undertaken here can be compared in a manner that is not always possible when relating to previous published work.

Furthermore, this is the first study, to my knowledge, that investigated the modulatory effects of IGF-1 and TSH on the Metformin treatment of thyroid cancer. In addition, the consistent expression of OCT1 by thyroid cancer cells suggested that Metformin could be readily up-taken in thyroid cancer, a novel finding that has previously not been reported elsewhere.

The Affymetrix data has shown the wide-ranging effects of Metformin on the thyroid cancer cell lines. Low dose Metformin modulated thousands of genes including several important genes that play key roles in cancer therapy. The data also implicated specific genes for further investigation that might help in gaining a better understanding of the molecular pathways influenced by Metformin, but these require further investigation.

6.7 On-going and future work

In order to better understand the role of Metformin in thyroid cancer, further research may involve one or more of the following components:

- Repetition of the results of the expression array on the same cell lines in triplicate to confirm which targets were consistently up and down-regulated following Metformin treatment. Study of other cell lines to identify common genes and variations across cancer types would also be valuable.
- Study of cation transporters other than OCT1 such as OCT2 (SLC22A2), OCT3 (SLC22A3), PMAT (SLC29A4), MATE1 (SLC47A1) and MATE2-K (SLC47A2) would be useful. SLC18A3 expression has been demonstrated in FTC-133 cells. Additionally, blocking of OCT1 expression to study its influence on the anti-cancer effect of Metformin is also important.
- TSH, IGF-1 and insulin did not alter the proliferation of the cells in the cell proliferation assay (MTT assay). Their role on apoptosis could also be explored.
- Human thyroid cancer tissue obtained from bio-banks could also be investigated for the expression of markers involved in pathways affected by Metformin should be done.
- The role of Metformin on animal models of thyroid and other cancers could also be investigated. In addition to observing the effects of Metformin on the tumours *in vivo*, changes in expression of relevant proteins with treatment as investigated in other *in vitro* and *in vivo* studies that could be studied (S6K1 and 4EBP1 [135]).

6.8 Conclusion

This *in vitro* study confirmed that Metformin has anti-cancer effects on thyroid cancer cell lines. Based on these findings, it is important to undertake further research along the lines described above. These could subsequently lead to clinical trials of Metformin treatment in the management of thyroid cancer.

References

References

1. Vanderpump, M., *The epidemiology of thyroid disease.* British medical bulletin, 2011. **99**: p. 39.
2. Middendorp, M. and F. Grunwald, *Update on recent developments in the therapy of differentiated thyroid cancer.* Semin Nucl Med, 2010. **40**(2): p. 145-52.
3. Sahra, I.B., et al., *Metformin in cancer therapy: a new perspective for an old antidiabetic drug?* Molecular Cancer Therapeutics, 2010. **9**(5): p. 1092-1099.
4. Nicholson, G. and G. Hall, *Diabetes mellitus: new drugs for a new epidemic.* British journal of anaesthesia, 2011. **107**(1): p. 65-73.
5. Micic, D., et al., *Metformin: its emerging role in oncology.* Hormones (Athens), 2011. **10**(1): p. 5-15.
6. Dowling, R.J., P.J. Goodwin, and V. Stambolic, *Understanding the benefit of metformin use in cancer treatment.* BMC medicine, 2011. **9**(1): p. 33.
7. Sinnatamby, C.S. and R.J. Last, *Last's Anatomy: Regional and Applied*. 2011, GB: Churchill Livingstone.
8. Bliss, R.D., P.G. Gauger, and L.W. Delbridge, *Surgeon's approach to the thyroid gland: surgical anatomy and the importance of technique.* World J Surg, 2000. **24**(8): p. 891-7.
9. Ellis, H., *Anatomy of the thyroid and parathyroid glands.* Surgery (Oxford), 2007. **25**(11): p. 467-468.
10. Burr, W.A., et al., *Serum triiodothyronine and reverse triiodothyronine concentrations after surgical operation.* Lancet, 1975. **2**(7948): p. 1277-9.
11. Johnson, J.L., *Diabetes Control in Thyroid Disease.* Diabetes Spectrum, 2006. **19**(3): p. 148-153.
12. Kim, B., *Thyroid hormone as a determinant of energy expenditure and the basal metabolic rate.* Thyroid, 2008. **18**(2): p. 141-144.
13. Epstein, F.H., et al., *Maternal and fetal thyroid function.* New England Journal of Medicine, 1994. **331**(16): p. 1072-1078.
14. Vanderpump, M.P., *The epidemiology of thyroid disease.* Br Med Bull, 2011. **99**: p. 39-51.
15. Kamijo, K., et al., *A novel bioreporter assay for thyrotropin receptor antibodies using a chimeric thyrotropin receptor (mc4) is more useful in differentiation of Graves' disease from painless thyroiditis than conventional thyrotropin-stimulating antibody assay using porcine thyroid cells.* Thyroid, 2010. **20**(8): p. 851-856.
16. Iglesias, P., et al., *Severe hyperthyroidism: aetiology, clinical features and treatment outcome.* Clinical endocrinology, 2010. **72**(4): p. 551-557.
17. Abraham, P., et al., *A systematic review of drug therapy for Graves' hyperthyroidism.* European Journal of Endocrinology, 2005. **153**(4): p. 489-498.

18. Hausmann, W., *Treatment of hyperthyroidism.* Hormone Research in Paediatrics, 2008. **3**(6): p. 313-331.
19. Grodski, S., et al., *Surgery versus radioiodine therapy as definitive management for Graves' disease: the role of patient preference.* Thyroid, 2007. **17**(2): p. 157-160.
20. Schüssler-Fiorenza, C.M., C.M. Bruns, and H. Chen, *The surgical management of Graves' disease.* Journal of Surgical Research, 2006. **133**(2): p. 207-214.
21. Hueston, W.J., *Treatment of hypothyroidism.* American family physician, 2001. **64**(10): p. 1717-1724.
22. Liénart, F., *Thyroid nodule: benign or malignant?].* Revue médicale de Bruxelles, 2012. **33**(4): p. 254.
23. Sipos, J.A. and E.L. Mazzaferri, *Thyroid cancer epidemiology and prognostic variables.* Clin Oncol (R Coll Radiol), 2010. **22**(6): p. 395-404.
24. Cooper, D.S., et al., *Revised American Thyroid Association management guidelines for patients with thyroid nodules and differentiated thyroid cancer.* Thyroid, 2009. **19**(11): p. 1167-1214.
25. Hundahl, S.A., et al., *Initial results from a prospective cohort study of 5583 cases of thyroid carcinoma treated in the United States during 1996.* Cancer, 2000. **89**(1): p. 202-217.
26. Kilfoy, B.A., et al., *International patterns and trends in thyroid cancer incidence, 1973–2002.* Cancer Causes & Control, 2009. **20**(5): p. 525-531.
27. Davies, L. and H.G. Welch, *Increasing incidence of thyroid cancer in the United States, 1973-2002.* JAMA: the journal of the American Medical Association, 2006. **295**(18): p. 2164-2167.
28. McNally, R.J., et al., *Increasing incidence of thyroid cancer in Great Britain, 1976–2005: age-period-cohort analysis.* European journal of epidemiology, 2012. **27**(8): p. 615-622.
29. Cramer, J.D., et al., *Analysis of the rising incidence of thyroid cancer using the Surveillance, Epidemiology and End Results national cancer data registry.* Surgery, 2010. **148**(6): p. 1147-1153.
30. Sipos, J. and E. Mazzaferri, *Thyroid cancer epidemiology and prognostic variables.* Clinical Oncology, 2010. **22**(6): p. 395-404.
31. Nagaiah, G., et al., *Anaplastic thyroid cancer: a review of epidemiology, pathogenesis, and treatment.* Journal of oncology, 2011. **2011**.
32. Bucsky, P. and T. Parlowsky, *Epidemiology and therapy of thyroid cancer in childhood and adolescence.* Experimental and Clinical Endocrinology & Diabetes, 2009. **105**(S 04): p. 70-73.
33. McTiernan, A.M., N.S. Weiss, and J.R. Daling, *Incidence of thyroid cancer in women in relation to previous exposure to radiation therapy and history of thyroid disease.* J Natl Cancer Inst, 1984. **73**(3): p. 575-81.
34. Rapkin, L. and F.D. Pashankar, *Management of Thyroid Carcinoma in Children and Young Adults.* Journal of Pediatric Hematology/Oncology, 2012. **34**: p. S39.

35. González-González, A., et al., *New guidelines for the management of thyroid nodules and differentiated thyroid cancer.* Minerva Endocrinologica, 2011. **36**(1): p. 7-12.
36. Popoveniuc, G. and J. Jonklaas, *Thyroid nodules.* The Medical clinics of North America, 2012. **96**(2): p. 329.
37. Shaha, A.R., *Controversies in the management of thyroid nodule.* The Laryngoscope, 2009. **110**(2): p. 183-183.
38. Milas, Z., J. Shin, and M. Milas, *New guidelines for the management of thyroid nodules and differentiated thyroid cancer.* Minerva Endocrino1, 2011. **36**: p. 53-70.
39. Haymart, M.R., et al., *Higher serum TSH in thyroid cancer patients occurs independent of age and correlates with extrathyroidal extension.* Clin Endocrinol, 2009. **71**(3): p. 434-9.
40. Kebebew, E., et al., *Medullary thyroid carcinoma.* Cancer, 2000. **88**(5): p. 1139-1148.
41. Ahmed, S.R. and D.W. Ball, *Clinical review: Incidentally discovered medullary thyroid cancer: diagnostic strategies and treatment.* J Clin Endocrinol Metab, 2011. **96**(5): p. 1237-45.
42. Podtcheko, A., et al., *The selective tyrosine kinase inhibitor, STI571, inhibits growth of anaplastic thyroid cancer cells.* J Clin Endocrinol Metab, 2003. **88**(4): p. 1889-96.
43. Podtcheko, A., et al., *Inhibition of ABL tyrosine kinase potentiates radiation-induced terminal growth arrest in anaplastic thyroid cancer cells.* Radiat Res, 2006. **165**(1): p. 35-42.
44. Ciampi, R. and Y.E. Nikiforov, *RET/PTC rearrangements and BRAF mutations in thyroid tumorigenesis.* Endocrinology, 2007. **148**(3): p. 936-41.
45. Romei, C. and R. Elisei, *RET/PTC Translocations and Clinico-Pathological Features in Human Papillary Thyroid Carcinoma.* Front Endocrinol, 2012. **3**(54): p. 00054.
46. Greco, A., et al., *Molecular pathology of differentiated thyroid cancer.* The Quarterly journal of nuclear medicine and molecular imaging, 2009. **53**(5): p. 440-454.
47. Fagin, J.A. and N. Mitsiades, *Molecular pathology of thyroid cancer: diagnostic and clinical implications.* Best Practice & Research Clinical Endocrinology & Metabolism, 2008. **22**(6): p. 955-969.
48. Cassol, C.A. and S.L. Asa, *Molecular pathology of thyroid cancer.* Diagnostic Histopathology, 2011. **17**(3): p. 124-139.
49. Scopa, C., *Histopathology of thyroid tumors. An overview.* Hormones (Athens, Greece), 2004. **3**(2): p. 100.
50. Jhiang, S.M., et al., *Detection of the PTC/retTPC oncogene in human thyroid cancers.* Oncogene, 1992. **7**(7): p. 1331-7.
51. Nikiforova, M.N., et al., *RAS point mutations and PAX8-PPAR gamma rearrangement in thyroid tumors: evidence for distinct molecular pathways in thyroid follicular carcinoma.* J Clin Endocrinol Metab, 2003. **88**(5): p. 2318-26.
52. Tallini, G., et al., *RET/PTC oncogene activation defines a subset of papillary thyroid carcinomas lacking evidence of progression to poorly differentiated or undifferentiated tumor phenotypes.* Clin Cancer Res, 1998. **4**(2): p. 287-94.

53. Couto, J.P., et al., *How molecular pathology is changing and will change the therapeutics of patients with follicular cell-derived thyroid cancer.* Journal of clinical pathology, 2009. **62**(5): p. 414-421.
54. Xing, M., *BRAF mutation in papillary thyroid cancer: pathogenic role, molecular bases, and clinical implications.* Endocrine reviews, 2007. **28**(7): p. 742-762.
55. Yeung, S.-C.J. and M.A. Habra, *Solid Tumour Section.* http://AtlasGeneticsOncology. org, 2008: p. 477.
56. Garcia-Rostan, G., et al., *ras mutations are associated with aggressive tumor phenotypes and poor prognosis in thyroid cancer.* J Clin Oncol, 2003. **21**(17): p. 3226-35.
57. Reddi, H.V., et al., *Expression of the PAX8/PPARgamma Fusion Protein Is Associated with Decreased Neovascularization In Vivo: Impact on Tumorigenesis and Disease Prognosis.* Genes Cancer, 2010. **1**(5): p. 480-492.
58. Hunt, J.L., *Molecular mutations in thyroid carcinogenesis.* Am J Clin Pathol, 2002. **118**(27): p. S116-27.
59. Donghi, R., et al., *Gene p53 mutations are restricted to poorly differentiated and undifferentiated carcinomas of the thyroid gland.* J Clin Invest, 1993. **91**(4): p. 1753-60.
60. Kalariya, N.M., *Antidiabetic Drug Metformin Suppresses Endotoxin-Induced Uveitis in Rats.* 2012. **53**(7): p. 3431-40.
61. Ji, L., et al., *Efficacy and Safety of Linagliptin Co-Administered with Low-Dose Metformin Once Daily Versus High-Dose Metformin Twice Daily in Treatment-Naïve Patients with Type 2 Diabetes: a Double-Blind Randomized Trial.* Adv Ther, 2015. **32**(3): p. 201-15.
62. Harborne, L., et al., *Descriptive review of the evidence for the use of metformin in polycystic ovary syndrome.* The Lancet, 2003. **361**(9372): p. 1894-1901.
63. Dunn, C.J. and D.H. Peters, *Metformin. A review of its pharmacological properties and therapeutic use in non-insulin-dependent diabetes mellitus.* Drugs, 1995. **49**(5): p. 721-49.
64. Bolen, S., et al., *Systematic review: comparative effectiveness and safety of oral medications for type 2 diabetes mellitus.* Ann Intern Med, 2007. **147**(6): p. 386-99.
65. Scheen, A.J., *Clinical pharmacokinetics of metformin.* Clin Pharmacokinet, 1996. **30**(5): p. 359-71.
66. Hardie, D.G., *AMP-activated protein kinase as a drug target.* Annu Rev Pharmacol Toxicol, 2007. **47**: p. 185-210.
67. Graham, G.G., et al., *Clinical pharmacokinetics of metformin.* Clin Pharmacokinet, 2011. **50**(2): p. 81-98.
68. Moses, R.G., *Repaglinide/metformin fixed-dose combination to improve glycemic control in patients with type 2 diabetes: an update.* Diabetes Metab Syndr Obes, 2010. **3**: p. 145-54.
69. McCreight, L.J., C.J. Bailey, and E.R. Pearson, *Metformin and the gastrointestinal tract.* Diabetologia, 2016. **59**: p. 426-35.
70. Zhou, M., L. Xia, and J. Wang, *Metformin transport by a newly cloned proton-stimulated organic cation transporter (plasma membrane monoamine transporter) expressed in human intestine.* Drug Metab Dispos, 2007. **35**(10): p. 1956-62.

71. Muller, J., et al., *Drug specificity and intestinal membrane localization of human organic cation transporters (OCT).* Biochem Pharmacol, 2005. **70**(12): p. 1851-60.
72. Takane, H., et al., *Polymorphism in human organic cation transporters and metformin action.* Pharmacogenomics, 2008. **9**(4): p. 415-22.
73. Chen, L., et al., *Role of organic cation transporter 3 (SLC22A3) and its missense variants in the pharmacologic action of metformin.* Pharmacogenet Genomics, 2010. **20**(11): p. 687-99.
74. Nies, A.T., et al., *Expression of organic cation transporters OCT1 (SLC22A1) and OCT3 (SLC22A3) is affected by genetic factors and cholestasis in human liver.* Hepatology, 2009. **50**(4): p. 1227-40.
75. Tsuda, M., et al., *Involvement of human multidrug and toxin extrusion 1 in the drug interaction between cimetidine and metformin in renal epithelial cells.* J Pharmacol Exp Ther, 2009. **329**(1): p. 185-91.
76. Sato, T., et al., *Transcellular transport of organic cations in double-transfected MDCK cells expressing human organic cation transporters hOCT1/hMATE1 and hOCT2/hMATE1.* Biochem Pharmacol, 2008. **76**(7): p. 894-903.
77. Tsuda, M., et al., *Targeted disruption of the multidrug and toxin extrusion 1 (mate1) gene in mice reduces renal secretion of metformin.* Mol Pharmacol, 2009. **75**(6): p. 1280-6.
78. Ito, S., et al., *Competitive inhibition of the luminal efflux by multidrug and toxin extrusions, but not basolateral uptake by organic cation transporter 2, is the likely mechanism underlying the pharmacokinetic drug-drug interactions caused by cimetidine in the kidney.* J Pharmacol Exp Ther, 2012. **340**(2): p. 393-403.
79. Kusuhara, H., et al., *Effects of a MATE protein inhibitor, pyrimethamine, on the renal elimination of metformin at oral microdose and at therapeutic dose in healthy subjects.* Clin Pharmacol Ther, 2011. **89**(6): p. 837-44.
80. Tzvetkov, M.V., et al., *The effects of genetic polymorphisms in the organic cation transporters OCT1, OCT2, and OCT3 on the renal clearance of metformin.* Clin Pharmacol Ther, 2009. **86**(3): p. 299-306.
81. Xia, L., et al., *Membrane localization and pH-dependent transport of a newly cloned organic cation transporter (PMAT) in kidney cells.* Am J Physiol Renal Physiol, 2007. **292**(2): p. F682-90.
82. Pryor, R. and F. Cabreiro, *Repurposing metformin: an old drug with new tricks in its binding pockets.* Biochem J, 2015. **471**(Pt 3): p. 307-22.
83. Hardie, D.G. and D.R. Alessi, *LKB1 and AMPK and the cancer-metabolism link - ten years after.* BMC Biol, 2013. **11**(36): p. 1741-7007.
84. Kahn, B.B., et al., *AMP-activated protein kinase: ancient energy gauge provides clues to modern understanding of metabolism.* Cell Metab, 2005. **1**(1): p. 15-25.
85. Shaw, R.J., et al., *The kinase LKB1 mediates glucose homeostasis in liver and therapeutic effects of metformin.* Science, 2005. **310**(5754): p. 1642-6.

86. Faure, P., et al., *An insulin sensitizer improves the free radical defense system potential and insulin sensitivity in high fructose-fed rats.* Diabetes, 1999. **48**(2): p. 353-7.
87. Dowling, R.J., et al., *Metformin in cancer: translational challenges.* Journal of molecular endocrinology, 2012. **48**(3): p. R31-R43.
88. Lee, J.H., et al., *The effects of metformin on the survival of colorectal cancer patients with diabetes mellitus.* International Journal of Cancer, 2012. **131**(3): p. 752-759.
89. Hardie, D.G., *AMP-activated protein kinase—an energy sensor that regulates all aspects of cell function.* Genes & development, 2011. **25**(18): p. 1895-1908.
90. Bo, S., et al., *Cancer mortality reduction and metformin: a retrospective cohort study in type 2 diabetic patients.* Diabetes, Obesity and Metabolism, 2012. **14**(1): p. 23-29.
91. Viollet, B., et al., *Cellular and molecular mechanisms of metformin: an overview.* Clin Sci (Lond), 2012. **122**(6): p. 253-70.
92. Foretz, M. and B. Viollet, *Regulation of hepatic metabolism by AMPK.* J Hepatol, 2011. **54**(4): p. 827-9.
93. Hardie, D.G., *Neither LKB1 nor AMPK are the direct targets of metformin.* Gastroenterology, 2006. **131**(3): p. 973; author reply 974-5.
94. Foretz, M., et al., *Metformin inhibits hepatic gluconeogenesis in mice independently of the LKB1/AMPK pathway via a decrease in hepatic energy state.* J Clin Invest, 2010. **120**(7): p. 2355-69.
95. Shackelford, D.B. and R.J. Shaw, *The LKB1-AMPK pathway: metabolism and growth control in tumour suppression.* Nat Rev Cancer, 2009. **9**(8): p. 563-75.
96. Kawaguchi, T., et al., *Mechanism for fatty acid "sparing" effect on glucose-induced transcription: regulation of carbohydrate-responsive element-binding protein by AMP-activated protein kinase.* J Biol Chem, 2002. **277**(6): p. 3829-35.
97. Shu, Y., et al., *Effect of genetic variation in the organic cation transporter 1 (OCT1) on metformin action.* J Clin Invest, 2007. **117**(5): p. 1422-31.
98. Zhuang, Y. and W.K. Miskimins, *Cell cycle arrest in Metformin treated breast cancer cells involves activation of AMPK, downregulation of cyclin D1, and requires p27Kip1 or p21Cip1.* J Mol Signal, 2008. **3**: p. 18.
99. Ben Sahra, I., et al., *The antidiabetic drug metformin exerts an antitumoral effect in vitro and in vivo through a decrease of cyclin D1 level.* Oncogene, 2008. **27**(25): p. 3576-86.
100. Vazquez-Martin, A., C. Oliveras-Ferraros, and J.A. Menendez, *The antidiabetic drug metformin suppresses HER2 (erbB-2) oncoprotein overexpression via inhibition of the mTOR effector p70S6K1 in human breast carcinoma cells.* Cell Cycle, 2009. **8**(1): p. 88-96.
101. Liu, Q., et al., *Metformin represses bladder cancer progression by inhibiting stem cell repopulation via COX2/PGE2/STAT3 axis.* Oncotarget, 2016. **7**(19): p. 28235-46.
102. Dang, J.H., et al., *Metformin in combination with cisplatin inhibits cell viability and induces apoptosis of human ovarian cancer cells by inactivating ERK 1/2.* Oncol Lett, 2017. **14**(6): p. 7557-7564.

103. Lee, J.E., et al., *High-Dose Metformin Plus Temozolomide Shows Increased Anti-tumor Effects in Glioblastoma In Vitro and In Vivo Compared with Monotherapy.* Cancer Res Treat, 2018.
104. Chen, G., et al., *Metformin inhibits growth of thyroid carcinoma cells, suppresses self-renewal of derived cancer stem cells, and potentiates the effect of chemotherapeutic agents.* J Clin Endocrinol Metab, 2012. **97**(4): p. E510-20.
105. Han, B., et al., *Metformin inhibits thyroid cancer cell growth, migration, and EMT through the mTOR pathway.* Tumour Biol, 2015. **36**(8): p. 6295-304.
106. Klubo-Gwiezdzinska, J., et al., *Metformin inhibits growth and decreases resistance to anoikis in medullary thyroid cancer cells.* Endocrine-related cancer, 2012. **19**(3): p. 447-456.
107. Shen, C.T., et al., *Metformin reduces glycometabolism of papillary thyroid carcinoma in vitro and in vivo.* J Mol Endocrinol, 2017. **58**(1): p. 15-23.
108. Evans, J.M., et al., *Research Pointers: Metformin and reduced risk of cancer in diabetic patients.* BMJ: British Medical Journal, 2005. **330**(7503): p. 1304.
109. Currie, C., C. Poole, and E. Gale, *The influence of glucose-lowering therapies on cancer risk in type 2 diabetes.* Diabetologia, 2009. **52**(9): p. 1766-1777.
110. Monami, M., et al., *Sulphonylureas and cancer: a case–control study.* Acta diabetologica, 2009. **46**(4): p. 279-284.
111. Currie, C.J., et al., *Mortality after incident cancer in people with and without type 2 diabetes impact of metformin on survival.* Diabetes Care, 2012. **35**(2): p. 299-304.
112. Libby, G., et al., *New Users of Metformin Are at Low Risk of Incident Cancer A cohort study among people with type 2 diabetes.* Diabetes Care, 2009. **32**(9): p. 1620-1625.
113. Ruiter, R., et al., *Lower Risk of Cancer in Patients on Metformin in Comparison With Those on Sulfonylurea Derivatives Results from a large population-based follow-up study.* Diabetes Care, 2012. **35**(1): p. 119-124.
114. Bosco, J.L.F., et al., *Metformin and incident breast cancer among diabetic women: a population-based case–control study in Denmark.* Cancer Epidemiology Biomarkers & Prevention, 2011. **20**(1): p. 101-111.
115. Romero, I.L., et al., *Relationship of type II diabetes and metformin use to ovarian cancer progression, survival, and chemosensitivity.* Obstetrics and gynecology, 2012. **119**(1): p. 61-67.
116. Bayraktar, S., et al., *Effect of metformin on survival outcomes in diabetic patients with triple receptor‐negative breast cancer.* Cancer, 2012. **118**(5): p. 1202-1211.
117. Tan, B.X., et al., *Prognostic influence of metformin as first‐line chemotherapy for advanced nonsmall cell lung cancer in patients with type 2 diabetes.* Cancer, 2011. **117**(22): p. 5103-5111.

118. Wright, J.L. and J.L. Stanford, *Metformin use and prostate cancer in Caucasian men: results from a population-based case–control study.* Cancer Causes & Control, 2009. **20**(9): p. 1617-1622.
119. Monami, M., et al., *Metformin and cancer occurrence in insulin-treated type 2 diabetic patients.* Diabetes Care, 2011. **34**(1): p. 129-131.
120. Landman, G.W., et al., *Metformin Associated With Lower Cancer Mortality in Type 2 Diabetes ZODIAC-16.* Diabetes Care, 2010. **33**(2): p. 322-326.
121. Libby, G., et al., *New users of metformin are at low risk of incident cancer: a cohort study among people with type 2 diabetes.* Diabetes Care, 2009. **32**(9): p. 1620-5.
122. Bodmer, M., et al., *Long-term metformin use is associated with decreased risk of breast cancer.* Diabetes Care, 2010. **33**(6): p. 1304-8.
123. Tseng, C.H., *Metformin may reduce breast cancer risk in Taiwanese women with type 2 diabetes.* Breast Cancer Res Treat, 2014. **145**(3): p. 785-90.
124. Tseng, C.H., *Metformin reduces thyroid cancer risk in Taiwanese patients with type 2 diabetes.* PLoS One, 2014. **9**(10): p. e109852.
125. Alimova, I.N., et al., *Metformin inhibits breast cancer cell growth, colony formation and induces cell cycle arrest in vitro.* Cell Cycle, 2009. **8**(6): p. 909-915.
126. Rocha, G.Z., et al., *Metformin amplifies chemotherapy-induced AMPK activation and antitumoral growth.* Clinical Cancer Research, 2011. **17**(12): p. 3993-4005.
127. Kato, K., et al., *The antidiabetic drug metformin inhibits gastric cancer cell proliferation in vitro and in vivo.* Molecular Cancer Therapeutics, 2012. **11**(3): p. 549-560.
128. Gotlieb, W.H., et al., *< i> In vitro</i> metformin anti-neoplastic activity in epithelial ovarian cancer.* Gynecologic oncology, 2008. **110**(2): p. 246-250.
129. Chen, G., et al., *Metformin inhibits growth of thyroid carcinoma cells, suppresses self-renewal of derived cancer stem cells, and potentiates the effect of chemotherapeutic agents.* Journal of Clinical Endocrinology & Metabolism, 2012. **97**(4): p. E510-E520.
130. Liu, B., et al., *Potent anti-proliferative effects of metformin on trastuzumab-resistant breast cancer cells via inhibition of erbB2/IGF-1 receptor interactions.* Cell Cycle, 2011. **10**(17): p. 2959-2966.
131. Alalem, M., A. Ray, and B.K. Ray, *Metformin induces degradation of mTOR protein in breast cancer cells.* Cancer Med, 2016.
132. Schulz, M. and A. Schmoldt, *Therapeutic and toxic blood concentrations of more than 800 drugs and other xenobiotics.* Die Pharmazie-An International Journal of Pharmaceutical Sciences, 2003. **58**(7): p. 447-474.
133. Fujimori, T., et al., *Antitumor effect of metformin on cholangiocarcinoma: In vitro and in vivo studies.* Oncol Rep, 2015. **34**(6): p. 2987-96.
134. Shi, Y., et al., *Inhibitory effect of metformin combined with gemcitabine on pancreatic cancer cells in vitro and in vivo.* Mol Med Rep, 2016. **14**(4): p. 2921-8.

135. Wang, F., et al., *Metformin inhibited esophageal squamous cell carcinoma proliferation in vitro and in vivo and enhanced the anti-cancer effect of cisplatin.* PLoS One, 2017. **12**(4): p. e0174276.
136. Chai, X., et al., *Metformin Increases Sensitivity of Pancreatic Cancer Cells to Gemcitabine by Reducing CD133+ Cell Populations and Suppressing ERK/P70S6K Signaling.* Sci Rep, 2015. **5**: p. 14404.
137. Cho, S.W., et al., *Therapeutic potential of metformin in papillary thyroid cancer in vitro and in vivo.* Mol Cell Endocrinol, 2014. **393**(1-2): p. 24-9.
138. Hadad, S., et al., *Evidence for biological effects of metformin in operable breast cancer: a pre-operative, window-of-opportunity, randomized trial.* Breast cancer research and treatment, 2011. **128**(3): p. 783-794.
139. Bonanni, B., et al., *Dual effect of metformin on breast cancer proliferation in a randomized presurgical trial.* Journal of clinical oncology, 2012. **30**(21): p. 2593-2600.
140. Niraula, S., et al., *Metformin in early breast cancer: a prospective window of opportunity neoadjuvant study.* Breast cancer research and treatment, 2012. **135**(3): p. 821-830.
141. Higurashi, T., et al., *Metformin efficacy and safety for colorectal polyps: a double-blind randomized controlled trial.* BMC cancer, 2012. **12**(1): p. 118.
142. Gartler, S.M., *Genetic markers as tracers in cell culture.* National Cancer Institute Monograph, 1967. **26**: p. 167.
143. MacLeod, R.A., et al., *Widespread intraspecies cross‐contamination of human tumor cell lines arising at source.* International Journal of Cancer, 1999. **83**(4): p. 555-563.
144. Gey, G., W. Coffman, and M.T. Kubicek, *Tissue culture studies of the proliferative capacity of cervical carcinoma and normal epithelium.* Cancer res, 1952. **12**(4): p. 264-265.
145. Vigersky, R.A., A. Filmore-Nassar, and A.R. Glass, *Thyrotropin suppression by metformin.* Journal of Clinical Endocrinology & Metabolism, 2006. **91**(1): p. 225-227.
146. Cappelli, C., et al., *TSH-Lowering Effect of Metformin in Type 2 Diabetic Patients Differences between euthyroid, untreated hypothyroid, and euthyroid on L-T4 therapy patients.* Diabetes Care, 2009. **32**(9): p. 1589-1590.
147. Mousavi, Z., et al., *Effects of short-term metformin therapy associated with levothyroxine dose decrement on TSH and thyroid hormone levels in patients with thyroid cancer.* Minerva Endocrinol, 2014. **39**(1): p. 59-65.
148. Rezzónico, J., et al., *Metformin treatment for small benign thyroid nodules in patients with insulin resistance.* Metabolic syndrome and related disorders, 2011. **9**(1): p. 69-75.
149. Klubo-Gwiezdzinska, J., et al., *Treatment with metformin is associated with higher remission rate in diabetic patients with thyroid cancer.* J Clin Endocrinol Metab, 2013. **98**(8): p. 3269-79.
150. Reverter, J.L. and E. Colome, *[Potential risks of the adverse effects of thyrotropin suppression in differentiated thyroid carcinoma].* Endocrinol Nutr, 2011. **58**(2): p. 75-83.

151. Steube, K.G., D. Grunicke, and H.G. Drexler, *Isoenzyme analysis as a rapid method for the examination of the species identity of cell cultures.* In Vitro Cell Dev Biol Anim, 1995. **31**(2): p. 115-9.
152. Nims, R.W., et al., *Sensitivity of isoenzyme analysis for the detection of interspecies cell line cross-contamination.* In Vitro Cellular & Developmental Biology-Animal, 1998. **34**(1): p. 35-39.
153. Masters, J.R., et al., *Short tandem repeat profiling provides an international reference standard for human cell lines.* Proceedings of the National Academy of Sciences, 2001. **98**(14): p. 8012-8017.
154. Oldroyd, N.J., et al., *A highly discriminating octoplex short tandem repeat polymerase chain reaction system suitable for human individual identification.* Electrophoresis, 1995. **16**(1): p. 334-337.
155. Azari, S., et al., *Profiling and authentication of human cell lines using short tandem repeat (STR) loci: Report from the National Cell Bank of Iran.* Biologicals, 2007. **35**(3): p. 195-202.
156. Nims, R.W., et al., *Short tandem repeat profiling: part of an overall strategy for reducing the frequency of cell misidentification.* In Vitro Cellular & Developmental Biology-Animal, 2010. **46**(10): p. 811-819.
157. Barallon, R., et al., *Recommendation of short tandem repeat profiling for authenticating human cell lines, stem cells, and tissues.* In Vitro Cellular & Developmental Biology-Animal, 2010. **46**(9): p. 727-732.
158. Mosmann, T., *Rapid colorimetric assay for cellular growth and survival: application to proliferation and cytotoxicity assays.* J Immunol Methods, 1983. **65**(1-2): p. 55-63.
159. Foster, E.R. and J.A. Downs, *Histone H2A phosphorylation in DNA double-strand break repair.* Febs J, 2005. **272**(13): p. 3231-40.
160. Modesti, M. and R. Kanaar, *DNA repair: spot(light)s on chromatin.* Curr Biol, 2001. **11**(6): p. R229-32.
161. Rogakou, E.P., et al., *DNA double-stranded breaks induce histone H2AX phosphorylation on serine 139.* J Biol Chem, 1998. **273**(10): p. 5858-68.
162. Fasola, C.E., et al., *Low-dose radiation therapy (2 Gy x 2) in the treatment of orbital lymphoma.* Int J Radiat Oncol Biol Phys, 2013. **86**(5): p. 930-5.
163. Lalau, J.D., A.S. Lemaire-Hurtel, and C. Lacroix, *Establishment of a database of metformin plasma concentrations and erythrocyte levels in normal and emergency situations.* Clin Drug Investig, 2011. **31**(6): p. 435-8.
164. Hess, J., et al., *Gain of chromosome band 7q11 in papillary thyroid carcinomas of young patients is associated with exposure to low-dose irradiation.* Proc Natl Acad Sci U S A, 2011. **108**(23): p. 9595-600.
165. Stucki, M. and S.P. Jackson, *Tudor domains track down DNA breaks*. Nat Cell Biol. 2004 Dec;6(12):1150-2.
166. Xie, A., et al., *Control of sister chromatid recombination by histone H2AX.* Mol Cell, 2004. **16**(6): p. 1017-25.
167. Li, H., et al., *Metformin inhibits the growth of nasopharyngeal carcinoma cells and sensitizes the cells to radiation via inhibition of the DNA damage repair pathway.* Oncol Rep, 2014. **32**(6): p. 2596-604.
168. Amador, R.R., et al., *Metformin (dimethyl-biguanide) induced DNA damage in mammalian cells.* Genet Mol Biol, 2012. **35**(1): p. 153-8.

169. Capes‐Davis, A., et al., *Check your cultures! A list of cross‐contaminated or misidentified cell lines.* International Journal of Cancer, 2010. **127**(1): p. 1-8.
170. Defendi, V., et al., *Immunological and karyological criteria for identification of cell lines.* Journal of the National Cancer Institute, 1960. **25**(2): p. 359-385.
171. Brand, K. and J. Syverton, *Results of species-specific hemagglutination tests on "transformed," nontransformed, and primary cell cultures.* Journal of the National Cancer Institute, 1962. **28**(1): p. 147-157.
172. Phuchareon, J., et al., *Genetic profiling reveals cross-contamination and misidentification of 6 adenoid cystic carcinoma cell lines: ACC2, ACC3, ACCM, ACCNS, ACCS and CAC2.* PLoS ONE, 2009. **4**(6): p. e6040.
173. Schweppe, R.E., et al., *Deoxyribonucleic acid profiling analysis of 40 human thyroid cancer cell lines reveals cross-contamination resulting in cell line redundancy and misidentification.* Journal of Clinical Endocrinology & Metabolism, 2008. **93**(11): p. 4331-4341.
174. Dowling, R.J., et al., *Metformin inhibits mammalian target of rapamycin-dependent translation initiation in breast cancer cells.* Cancer res, 2007. **67**(22): p. 10804-12.
175. Wullschleger, S., R. Loewith, and M.N. Hall, *TOR signaling in growth and metabolism.* Cell, 2006. **124**(3): p. 471-484.
176. Frasca, F., et al., *The role of insulin receptors and IGF-I receptors in cancer and other diseases.* Arch Physiol Biochem, 2008. **114**(1): p. 23-37.
177. Goldberg, R.C., et al., *Induction of Neoplasms in Thyroid Glands of Rats by Subtotal Thyroidectomy and by the Injection of One Microcurie of I-131.* Cancer res, 1964. **24**: p. 35-43.
178. Brewer, C., N. Yeager, and A. Di Cristofano, *Thyroid-stimulating hormone initiated proliferative signals converge in vivo on the mTOR kinase without activating AKT.* Cancer res, 2007. **67**(17): p. 8002-6.
179. Malki, A. and A. Youssef, *Antidiabetic drug metformin induces apoptosis in human MCF breast cancer via targeting ERK signaling.* Oncol Res, 2011. **19**(6): p. 275-85.
180. Queiroz, E.A., et al., *Metformin induces apoptosis and cell cycle arrest mediated by oxidative stress, AMPK and FOXO3a in MCF-7 breast cancer cells.* PLoS One, 2014. **9**(5): p. e98207.
181. Gild, M.L., et al., *Targeting mTOR in RET mutant medullary and differentiated thyroid cancer cells.* Endocr Relat Cancer, 2013. **20**(5): p. 659-67.
182. Gild, M.L., et al., *Destabilizing RET in targeted treatment of thyroid cancers.* Endocr Connect, 2016. **5**(1): p. 10-9.
183. Becker, C., et al., *No evidence for a decreased risk of thyroid cancer in association with use of metformin or other antidiabetic drugs: a case-control study.* BMC Cancer, 2015. **15**: p. 719.
184. Bohr, V.A., D.H. Phillips, and P.C. Hanawalt, *Heterogeneous DNA damage and repair in the mammalian genome.* Cancer res, 1987. **47**(24 Pt 1): p. 6426-36.

185. Schipler, A. and G. Iliakis, *DNA double-strand–break complexity levels and their possible contributions to the probability for error-prone processing and repair pathway choice.* Nucleic acids research, 2013. **41**(16): p. 7589-7605.
186. Ban, S., et al., *Radiation sensitivities of 31 human oesophageal squamous cell carcinoma cell lines.* Int J Exp Pathol, 2005. **86**(4): p. 231-40.
187. Chan, D.W., et al., *Autophosphorylation of the DNA-dependent protein kinase catalytic subunit is required for rejoining of DNA double-strand breaks.* Genes Dev, 2002. **16**(18): p. 2333-8.
188. Onaran, I., et al., *Metformin does not prevent DNA damage in lymphocytes despite its antioxidant properties against cumene hydroperoxide-induced oxidative stress.* Mutat Res, 2006. **611**(1-2): p. 1-8.
189. Jang, E.K., et al., *Metformin Is Associated with a Favorable Outcome in Diabetic Patients with Cervical Lymph Node Metastasis of Differentiated Thyroid Cancer.* Eur Thyroid J, 2015. **4**(3): p. 181-8.
190. Gatenby, R.A. and R.J. Gillies, *Why do cancers have high aerobic glycolysis?* Nature Reviews Cancer, 2004. **4**(11): p. 891-899.
191. Okumura, M., et al., *Leptin and high glucose stimulate cell proliferation in MCF-7 human breast cancer cells: reciprocal involvement of PKC-α and PPAR expression.* Biochimica et Biophysica Acta (BBA) - Molecular Cell Research, 2002. **1592**(2): p. 107-116.
192. Zordoky, B.N., et al., *The anti-proliferative effect of metformin in triple-negative MDA-MB-231 breast cancer cells is highly dependent on glucose concentration: implications for cancer therapy and prevention.* Biochim Biophys Acta, 2014. **1840**(6): p. 1943-57.
193. Volkova, E., et al., *Marginal effects of glucose, insulin and insulin-like growth factor on chemotherapy response in endothelial and colorectal cancer cells.* Oncol Lett, 2014. **7**(2): p. 311-20.
194. Han, L., et al., *High glucose promotes pancreatic cancer cell proliferation via the induction of EGF expression and transactivation of EGFR.* PLoS ONE, 2011. **6**(11): p. e27074.
195. Bikas, A., et al., *Glucose-deprivation increases thyroid cancer cells sensitivity to metformin.* Endocrine-related cancer, 2015. **22**(6): p. 919-932.
196. Salamon, S., et al., *Glucose Metabolism in Cancer and Ischemia: Possible Therapeutic Consequences of the Warburg Effect.* Nutr Cancer, 2017. **69**(2): p. 177-183.
197. Zhang, X., et al., *ETS-1: A potential target of glycolysis for metabolic therapy by regulating glucose metabolism in pancreatic cancer.* Int J Oncol, 2017. **50**(1): p. 232-240.
198. Wang, L., et al., *Diabetes mellitus stimulates pancreatic cancer growth and epithelial-mesenchymal transition-mediated metastasis via a p38 MAPK pathway.* Oncotarget, 2016. **7**(25): p. 38539-38550.
199. Zou, Z.W., et al., *LncRNA ANRIL is up-regulated in nasopharyngeal carcinoma and promotes the cancer progression via increasing proliferation, reprograming cell glucose metabolism and inducing side-population stem-like cancer cells.* Oncotarget, 2016. **7**(38): p. 61741-61754.

200. Jee, S.H., et al., *Fasting serum glucose level and cancer risk in Korean men and women.* Jama, 2005. **293**(2): p. 194-202.
201. Rapp, K., et al., *Fasting blood glucose and cancer risk in a cohort of more than 140,000 adults in Austria.* Diabetologia, 2006. **49**(5): p. 945-952.
202. Hemkens, L.G., et al., *Risk of malignancies in patients with diabetes treated with human insulin or insulin analogues: a cohort study.* Diabetologia, 2009. **52**(9): p. 1732-44.
203. Ayiomamitis, G.D., et al., *Effects of octreotide and insulin on colon cancer cellular proliferation and correlation with hTERT activity.* Oncoscience, 2014. **1**(6): p. 457-67.
204. Weinstein, D., et al., *Insulin receptor compensates for IGF1R inhibition and directly induces mitogenic activity in prostate cancer cells.* Endocr Connect, 2014. **3**(1): p. 24-35.
205. Lee, P.D., et al., *Insulin-like growth factor binding protein-1: recent findings and new directions.* Proc Soc Exp Biol Med, 1997. **216**(3): p. 319-57.
206. Zong, C.S., et al., *Stat3 plays an important role in oncogenic Ros- and insulin-like growth factor I receptor-induced anchorage-independent growth.* J Biol Chem, 1998. **273**(43): p. 28065-72.
207. Grimberg, A. and P. Cohen, *Role of insulin-like growth factors and their binding proteins in growth control and carcinogenesis.* J Cell Physiol, 2000. **183**(1): p. 1-9.
208. Hahn, W.C. and R.A. Weinberg, *Rules for making human tumor cells.* N Engl J Med, 2002. **347**(20): p. 1593-603.
209. Resnicoff, M. and R. Baserga, *The role of the insulin-like growth factor I receptor in transformation and apoptosis.* Ann N Y Acad Sci, 1998. **842**: p. 76-81.
210. Xu, L., et al., *IGF1/IGF1R/STAT3 signaling-inducible IFITM2 promotes gastric cancer growth and metastasis.* Cancer Lett, 2017. **393**: p. 76-85.
211. Ter Braak, B., et al., *Insulin-like growth factor 1 receptor activation promotes mammary gland tumor development by increasing glycolysis and promoting biomass production.* Breast Cancer Res, 2017. **19**(1): p. 14.
212. Bohlke, K., et al., *Insulin-like growth factor-I in relation to premenopausal ductal carcinoma in situ of the breast.* Epidemiology, 1998. **9**(5): p. 570-3.
213. Burtscher, I. and G. Christofori, *The IGF/IGF-1 receptor signaling pathway as a potential target for cancer therapy.* Drug Resist Updat, 1999. **2**(1): p. 3-8.
214. Armakolas, N., et al., *The role of the IGF-1 Ec in myoskeletal system and osteosarcoma pathophysiology.* Crit Rev Oncol Hematol, 2016. **108**: p. 137-145.
215. Hankinson, S.E., et al., *Circulating concentrations of insulin-like growth factor-I and risk of breast cancer.* Lancet, 1998. **351**(9113): p. 1393-6.
216. Yang, S., et al., *Insulin-Like Growth Factor-1 Modulates Polycomb Cbx8 Expression and Inhibits Colon Cancer Cell Apoptosis.* Cell Biochem Biophys, 2015. **71**(3): p. 1503-7.

217. Haymart, M.R., et al., *Higher Serum Thyroid Stimulating Hormone Level in Thyroid Nodule Patients Is Associated with Greater Risks of Differentiated Thyroid Cancer and Advanced Tumor Stage.* J Clin Endocrinol Metab, 2008. **93**(3): p. 809-14.
218. Jonklaas, J., H. Nsouli-Maktabi, and S.J. Soldin, *Endogenous thyrotropin and triiodothyronine concentrations in individuals with thyroid cancer.* Thyroid, 2008. **18**(9): p. 943-52.
219. Hoffmann, S., et al., *Thyrotropin (TSH)-induced production of vascular endothelial growth factor in thyroid cancer cells in vitro: evaluation of TSH signal transduction and of angiogenesis-stimulating growth factors.* J Clin Endocrinol Metab, 2004. **89**(12): p. 6139-45.
220. Deleu, S., et al., *IGF-1 or insulin, and the TSH cyclic AMP cascade separately control dog and human thyroid cell growth and DNA synthesis, and complement each other in inducing mitogenesis.* Mol Cell Endocrinol, 1999. **149**(1-2): p. 41-51.
221. Wahdan-Alaswad, R., et al., *Glucose promotes breast cancer aggression and reduces metformin efficacy.* Cell Cycle, 2013. **12**(24): p. 3759-69.
222. Haymond, M.W., et al., *Differences in circulating gluconeogenic substrates during short-term fasting in men, women, and children.* Metabolism, 1982. **31**(1): p. 33-42.
223. Menendez, J.A., et al., *Metformin is synthetically lethal with glucose withdrawal in cancer cells.* Cell Cycle, 2012. **11**(15): p. 2782-92.
224. Zhuang, Y., et al., *Mechanisms by Which Low Glucose Enhances the Cytotoxicity of Metformin to Cancer Cells Both In Vitro and In Vivo.* PLoS One, 2014. **9**(9).
225. Litchfield, L.M., et al., *Hyperglycemia-induced metabolic compensation inhibits metformin sensitivity in ovarian cancer.* Oncotarget, 2015. **6**(27): p. 23548-60.
226. Heidegger, I., et al., *Diverse functions of IGF/insulin signaling in malignant and noncancerous prostate cells: proliferation in cancer cells and differentiation in noncancerous cells.* Endocrinology, 2012. **153**(10): p. 4633-43.
227. Sandhu, M.S., D.B. Dunger, and E.L. Giovannucci, *Insulin, insulin-like growth factor-I (IGF-I), IGF binding proteins, their biologic interactions, and colorectal cancer.* J Natl Cancer Inst, 2002. **94**(13): p. 972-80.
228. Sarkissyan, S., et al., *IGF-1 regulates Cyr61 induced breast cancer cell proliferation and invasion.* PLoS One, 2014. **9**(7): p. e103534.
229. Koenuma, M., T. Yamori, and T. Tsuruo, *Insulin and insulin-like growth factor 1 stimulate proliferation of metastatic variants of colon carcinoma 26.* Jpn J Cancer Res, 1989. **80**(1): p. 51-8.
230. Tian, L., et al., *TSH stimulates the proliferation of vascular smooth muscle cells.* Endocrine, 2014. **46**(3): p. 651-8.
231. Boelaert, K., et al., *Serum thyrotropin concentration as a novel predictor of malignancy in thyroid nodules investigated by fine-needle aspiration.* J Clin Endocrinol Metab, 2006. **91**(11): p. 4295-301.
232. Polyzos, S.A., et al., *Serum thyrotropin concentration as a biochemical predictor of thyroid malignancy in patients presenting with thyroid nodules.* J Cancer Res Clin Oncol, 2008. **134**(9): p. 953-60.

233. Cho, S.W., et al., *Thyroid Stimulating Hormone Promotes Tumor Growth By Modulating Angiogenesis and Macrophage Recruitment in Papillary Thyroid Cancer Microenvironment*, in *Thyroid Hormone Action, Cancer and Clinical Thyroid*. 2016, Endocrine Society. p. OR11-3-OR11-3.
234. Papini, E., et al., *Long-term changes in nodular goiter: a 5-year prospective randomized trial of levothyroxine suppressive therapy for benign cold thyroid nodules.* J Clin Endocrinol Metab, 1998. **83**(3): p. 780-3.
235. Mazzaferri, E.L. and S.M. Jhiang, *Long-term impact of initial surgical and medical therapy on papillary and follicular thyroid cancer.* Am J Med, 1994. **97**(5): p. 418-28.
236. Pujol, P., et al., *Degree of thyrotropin suppression as a prognostic determinant in differentiated thyroid cancer.* J Clin Endocrinol Metab, 1996. **81**(12): p. 4318-23.
237. Jonklaas, J., et al., *Outcomes of patients with differentiated thyroid carcinoma following initial therapy.* Thyroid, 2006. **16**(12): p. 1229-42.
238. Hovens, G.C., et al., *Associations of serum thyrotropin concentrations with recurrence and death in differentiated thyroid cancer.* J Clin Endocrinol Metab, 2007. **92**(7): p. 2610-5.
239. Mourouzis, I., et al., *Are Thyroid Hormone and Tumor Cell Proliferation in Human Breast Cancers Positive for HER2 Associated?* Int J Endocrinol, 2015. **2015**: p. 765406.
240. Zaballos, M.A. and P. Santisteban, *FOXO1 controls thyroid cell proliferation in response to TSH and IGF-I and is involved in thyroid tumorigenesis.* Mol Endocrinol, 2013. **27**(1): p. 50-62.
241. Hoelting, T., et al., *Epidermal growth factor enhances proliferation, migration, and invasion of follicular and papillary thyroid cancer in vitro and in vivo.* J Clin Endocrinol Metab, 1994. **79**(2): p. 401-8.
242. Nies, A.T., et al., *Organic cation transporters (OCTs, MATEs), in vitro and in vivo evidence for the importance in drug therapy.* Handb Exp Pharmacol, 2011(201): p. 105-67.
243. Sogame, Y., et al., *A comparison of uptake of metformin and phenformin mediated by hOCT1 in human hepatocytes.* Biopharm Drug Dispos, 2009. **30**(8): p. 476-84.
244. Li, P., et al., *p53 is required for metformin-induced growth inhibition, senescence and apoptosis in breast cancer cells.* Biochem Biophys Res Commun, 2015. **464**(4): p. 1267-74.
245. Cai, X., et al., *Metformin Induced AMPK Activation, G0/G1 Phase Cell Cycle Arrest and the Inhibition of Growth of Esophageal Squamous Cell Carcinomas In Vitro and In Vivo.* PLoS One, 2015. **10**(7): p. e0133349.
246. Yue, W., et al., *Metformin combined with aspirin significantly inhibit pancreatic cancer cell growth in vitro and in vivo by suppressing anti-apoptotic proteins Mcl-1 and Bcl-2.* Oncotarget, 2015. **6**(25): p. 21208-24.
247. Qureshi, A. and S. Pervez, *Allred scoring for ER reporting and it's impact in clearly distinguishing ER negative from ER positive breast cancers.* J Pak Med Assoc, 2010. **60**(5): p. 350-3.

248. Hughes-Large, J.M. and N.M. Borradaile, *Gene expression microarray data from human microvascular endothelial cells supplemented with a low concentration of niacin.* Data Brief, 2016. **6**: p. 899-902.
249. Grell, A.S., et al., *Cerebrovascular gene expression in spontaneously hypertensive rats.* PLoS One, 2017. **12**(9): p. e0184233.
250. Sun, Q.S., et al., *[Hypothalamic Transcription Profiles Associated with Twirling-reducing Needling in Rats with Stress-induced Prehypertension].* Zhen Ci Yan Jiu, 2017. **42**(3): p. 209-16.
251. Wang, G., et al., *Validation of whole-blood transcriptome signature during microdose recombinant human erythropoietin (rHuEpo) administration.* BMC Genomics, 2017. **18**(Suppl 8): p. 817.
252. Hage-Sleiman, R., et al., *Genomic alterations during p53-dependent apoptosis induced by gamma-irradiation of Molt-4 leukemia cells.* PLoS One, 2017. **12**(12): p. e0190221.
253. Landsverk, H.B., et al., *PNUTS enhances in vitro chromosome decondensation in a PP1-dependent manner.* Biochem J, 2005. **390**(Pt 3): p. 709-17.
254. Segal, E.D., et al., *Relevance of the OCT1 transporter to the antineoplastic effect of biguanides.* Biochem Biophys Res Commun, 2011. **414**(4): p. 694-9.
255. Guo, J.M., et al., *Involvement of arterial baroreflex and nicotinic acetylcholine receptor alpha7 subunit pathway in the protection of metformin against stroke in stroke-prone spontaneously hypertensive rats.* Eur J Pharmacol, 2017. **798**: p. 1-8.
256. Ben Hassine, I., et al., *hOCT1 gene expression predict for optimal response to Imatinib in Tunisian patients with chronic myeloid leukemia.* Cancer Chemother Pharmacol, 2017. **79**(4): p. 737-745.
257. Eiden, L.E., *The cholinergic gene locus.* J Neurochem, 1998. **70**(6): p. 2227-40.
258. Aran, A., et al., *Vesicular acetylcholine transporter defect underlies devastating congenital myasthenia syndrome.* Neurology, 2017. **88**(11): p. 1021-1028.
259. Li, N., et al., *Association between C4, C4A, and C4B copy number variations and susceptibility to autoimmune diseases: a meta-analysis.* Sci Rep, 2017. **7**: p. 42628.
260. Liao, J., et al., *Small nucleolar RNA signatures as biomarkers for non-small-cell lung cancer.* Mol Cancer, 2010. **9**: p. 198.
261. Wang, L., et al., *A novel nuclear protein, MGC5306 interacts with DNA polymerase beta and has a potential role in cellular phenotype.* Cancer Res, 2004. **64**(21): p. 7673-7.
262. Jin, H., et al., *IER3 is a crucial mediator of TAp73beta-induced apoptosis in cervical cancer and confers etoposide sensitivity.* Sci Rep, 2015. **5**: p. 8367.
263. Kruse, M.L., et al., *Immediate early gene X1 (IEX-1) is organized in subnuclear structures and partially co-localizes with promyelocytic leukemia protein in HeLa cells.* J Biol Chem, 2005. **280**(26): p. 24849-56.
264. Garcia, J., et al., *IEX-1: a new ERK substrate involved in both ERK survival activity and ERK activation.* Embo j, 2002. **21**(19): p. 5151-63.

265. Oh, H.R., J. Kim, and J. Kim, *Critical roles of Cyclin D1 in mouse embryonic fibroblast cell reprogramming.* Febs j, 2016. **283**(24): p. 4549-4568.
266. Pu, S., et al., *Effect of CDK1 shRNA on proliferation, migration, cell cycle and apoptosis in non-small cell lung cancer.* J Cell Physiol, 2017.
267. Yamamoto, H., et al., *Identification of a novel substrate for TNFalpha-induced kinase NUAK2.* Biochem Biophys Res Commun, 2008. **365**(3): p. 541-7.
268. Namiki, T., et al., *AMP kinase-related kinase NUAK2 affects tumor growth, migration, and clinical outcome of human melanoma.* Proc Natl Acad Sci U S A, 2011. **108**(16): p. 6597-602.
269. Zhu, H.Q., et al., *Metformin potentiates the anticancer activities of gemcitabine and cisplatin against cholangiocarcinoma cells in vitro and in vivo.* Oncol Rep, 2016. **36**(6): p. 3488-3496.
270. Iwabuchi, K., et al., *Two cellular proteins that bind to wild-type but not mutant p53.* Proc Natl Acad Sci U S A, 1994. **91**(13): p. 6098-102.
271. Sullivan, A. and X. Lu, *ASPP: a new family of oncogenes and tumour suppressor genes.* Br J Cancer, 2007. **96**(2): p. 196-200.
272. Samuels-Lev, Y., et al., *ASPP proteins specifically stimulate the apoptotic function of p53.* Mol Cell, 2001. **8**(4): p. 781-94.
273. Lossos, I.S., et al., *Apoptosis stimulating protein of p53 (ASPP2) expression differs in diffuse large B-cell and follicular center lymphoma: correlation with clinical outcome.* Leuk Lymphoma, 2002. **43**(12): p. 2309-17.
274. Cobleigh, M.A., et al., *Tumor gene expression and prognosis in breast cancer patients with 10 or more positive lymph nodes.* Clin Cancer Res, 2005. **11**(24 Pt 1): p. 8623-31.
275. Song, B., et al., *Downregulation of ASPP2 in pancreatic cancer cells contributes to increased resistance to gemcitabine through autophagy activation.* Mol Cancer, 2015. **14**.
276. Shi, Y., et al., *ASPP2 enhances Oxaliplatin (L-OHP)-induced colorectal cancer cell apoptosis in a p53-independent manner by inhibiting cell autophagy.* J Cell Mol Med, 2015. **19**(3): p. 535-43.
277. Cans, C., et al., *Translationally controlled tumor protein acts as a guanine nucleotide dissociation inhibitor on the translation elongation factor eEF1A.* Proc Natl Acad Sci U S A, 2003. **100**(24): p. 13892-7.
278. Amson, R., et al., *Reciprocal repression between P53 and TCTP.* Nat Med, 2011. **18**(1): p. 91-9.
279. Wang, L., et al., *Knockdown of translationally controlled tumor protein inhibits growth, migration and invasion of lung cancer cells.* Life Sci, 2018. **193**: p. 292-299.
280. Krumschnabel, G., *The enigma of caspase-2: the laymen's view.* 2009. **16**(2): p. 195-207.
281. Eroglu, C., et al., *Assessment of the anticancer mechanism of ferulic acid via cell cycle and apoptotic pathways in human prostate cancer cell lines.* Tumour Biol, 2015. **36**(12): p. 9437-46.
282. Luo, Y., et al., *Docetaxel loaded oleic acid-coated hydroxyapatite nanoparticles enhance the docetaxel-induced apoptosis through activation of caspase-2 in androgen independent prostate cancer cells.* J Control Release, 2010. **147**(2): p. 278-88.

283. Liu, J., et al., *BECN1-dependent CASP2 incomplete autophagy induction by binding to rabies virus phosphoprotein.* Autophagy, 2017. **13**(4): p. 739-53.
284. Tiwari, M., et al., *A nonapoptotic role for CASP2/caspase 2: Modulation of autophagy.* Autophagy, 2014. **10**(6): p. 1054-70.
285. Feinstein, E., et al., *Assignment of DAP1 and DAPK--genes that positively mediate programmed cell death triggered by IFN-gamma--to chromosome regions 5p12.2 and 9q34.1, respectively.* Genomics, 1995. **29**(1): p. 305-7.
286. Singh, P., P. Ravanan, and P. Talwar, *Death Associated Protein Kinase 1 (DAPK1): A Regulator of Apoptosis and Autophagy.* Front Mol Neurosci, 2016. **9**: p. 46.
287. Wu, B., et al., *DAPK1 modulates a curcumin-induced G2/M arrest and apoptosis by regulating STAT3, NF-kappaB, and caspase-3 activation.* Biochem Biophys Res Commun, 2013. **434**(1): p. 75-80.
288. Qin, Y., et al., *Effect of DAPK1 gene on proliferation, migration, and invasion of carcinoma of pancreas BxPC-3 cell line.* Int J Clin Exp Pathol, 2014. **7**(11): p. 7536-44.
289. Willis, T.G., et al., *Bcl10 is involved in t(1;14)(p22;q32) of MALT B cell lymphoma and mutated in multiple tumor types.* Cell, 1999. **96**(1): p. 35-45.
290. Zhang, Q., et al., *Inactivating mutations and overexpression of BCL10, a caspase recruitment domain-containing gene, in MALT lymphoma with t(1;14)(p22;q32).* Nat Genet, 1999. **22**(1): p. 63-8.
291. Fares, F., et al., *Benzene-poly-carboxylic acid complex, a novel anti-cancer agent induces apoptosis in human breast cancer cells.* PLoS One, 2014. **9**(2): p. e85156.
292. Chen, Y.T., et al., *Identification of CT46/HORMAD1, an immunogenic cancer/testis antigen encoding a putative meiosis-related protein.* Cancer Immun, 2005. **5**: p. 9.
293. Aravind, L. and E.V. Koonin, *The HORMA domain: a common structural denominator in mitotic checkpoints, chromosome synapsis and DNA repair.* Trends Biochem Sci, 1998. **23**(8): p. 284-6.
294. Shahzad, M.M.K., et al., *Biological Significance of HORM-A Domain Containing Protein 1 (HORMAD1) in Epithelial Ovarian Carcinoma.* Cancer Lett, 2013. **330**(2): p. 123-9.
295. Zou, J., et al., *Metformin inhibits estrogen‐dependent endometrial cancer cell growth by activating the AMPK–FOXO1 signal pathway.* Cancer Sci, 2016. **107**(12): p. 1806-17.
296. He, G., et al., *AMP-activated protein kinase induces p53 by phosphorylating MDMX and inhibiting its activity.* Mol Cell Biol, 2014. **34**(2): p. 148-57.
297. Tseng, C.H., *Thyroid cancer risk is not increased in diabetic patients.* PLoS One, 2012. **7**(12): p. e53096.
298. Abdulrahman, R.M., et al., *Impact of Metformin and compound C on NIS expression and iodine uptake in vitro and in vivo: a role for CRE in AMPK modulation of thyroid function.* Thyroid, 2014. **24**(1): p. 78-87.
299. Moon, H.S. and C.S. Mantzoros, *Regulation of cell proliferation and malignant potential by irisin in endometrial, colon, thyroid and esophageal cancer cell lines.* Metabolism, 2014. **63**(2): p. 188-93.

300. Chen, G., et al., *Synergistic anti-proliferative effect of metformin and sorafenib on growth of anaplastic thyroid cancer cells and their stem cells.* Oncol Rep, 2015. **33**(4): p. 1994-2000.
301. Hanly, E.K., et al., *mTOR inhibitors sensitize thyroid cancer cells to cytotoxic effect of vemurafenib.* Oncotarget, 2015. **6**(37): p. 39702-13.
302. Anil, C., et al., *Metformin Decreases Thyroid Volume and Nodule Size in Subjects with Insulin Resistance: A Preliminary Study.* Med Princ Pract, 2016. **25**(3): p. 233-6.
303. Bikas, A., et al., *Metformin Attenuates 131I-Induced Decrease in Peripheral Blood Cells in Patients with Differentiated Thyroid Cancer.* Thyroid, 2016. **26**(2): p. 280-6.
304. Park, J., et al., *Metformin blocks progression of obesity-activated thyroid cancer in a mouse model.* Oncotarget, 2016. **7**(23): p. 34832-44.
305. Kheder, S., et al., *Effects of prolonged exposure to low dose metformin in thyroid cancer cell lines.* J Cancer, 2017. **8**(6): p. 1053-1061.
306. Cheng, K. and M. Hao, *Metformin Inhibits TGF-beta1-Induced Epithelial-to-Mesenchymal Transition via PKM2 Relative-mTOR/p70s6k Signaling Pathway in Cervical Carcinoma Cells.* Int J Mol Sci, 2016. **17**(12).
307. Hanse, E.A., et al., *Cdk2 plays a critical role in hepatocyte cell cycle progression and survival in the setting of cyclin D1 expression in vivo.* Cell Cycle, 2009. **8**(17): p. 2802-9.

Appendices

Table 7.1: Affymetrix assay- genes repeated in ≥ 5 top 10 significant pathways for K1E7 cells.

Grand Total: 269 Number of repeated genes: 26	**Repeat**	Grand Total: 2096 Number of repeated genes: 72	**Repeat**
Down regulates genes		**Up regulated genes**	
OR10A2, OR10G8, OR10H2, OR11H12, OR13C2, OR1D2,OR1D5, OR1L4, OR2T4, OR3A1, OR3A3, OR4M1, OR4N5, OR51A4, OR51B4, OR52M1, OR52N2, OR5AC2, OR5AN1, OR5AP2, OR5D18, OR5F1, OR5H2, OR6T1, OR9A2	**9**	ACVR1, ACVR2A, ASH1L, BAZ1B, BMP2K, BMPR1A, BMPR2, CASK, CDK8, CDK9, CDKL5, CHUK, CNOT4, CREBBP, DAPK1, ESCO1, ESCO2, HIPK1, HLTF, KLF11, LATS1, MAP3K15, MAP3K8, MUL1, MYCBP2, NEK3, NEK7, NSD1, NUAK1, OXSR1, PIAS2, PLK4, POLR1B, POLR3B, PRKAA1, PRKAA2, PRKACB, PSKH1, RCHY1, RIPK1, RIPK2, RNF111, RNF144B, RNF2, RPS6KA3, RPS6KB1, SIK2, SIK3, SLK, SQSTM1, TESK1, TRIM33, TSSK3, ZMAT3, ZRANB1	**8**
OR6P1	**7**	CDC42BPA, PRKD3, ROCK2	**7**
		EP300, ERN1, HIPK2, HIPK3, MAP3K2, MKNK2, NEK4, NLK,	**6**

Grand Total: 269 Number of repeated genes: 26	**Repeat**	Grand Total: 2096 Number of repeated genes: 72	**Repeat**
Down regulates genes		**Up regulated genes**	
		PAK2, RPS6KA5, STK17A, STK38	
		PRKCI, ROCK1	**8**

Table 7.2: Affymetrix assay- genes repeated in ≥ 5 top 10 significant pathways for FTC-133 cells.

Grand Total: 70 Number of repeated genes: 5	**Repeat**	Grand Total: 49 Number of repeated genes: 6	**Repeat**
Down regulates genes		**Up regulated genes**	
CDK1, NEK2, PLK3	**9**	ACADM, ACADSB, COG2, MAN1A2, ST6GALNAC5, ST8SIA6	**5**

Table 7.3: Affymetrix assay- genes repeated in top 10 significant pathways for Nthy-ori 3-1 cells.

No.	Grand Total: 125 Number of repeated genes: 4	**Repeat**	Grand Total: 105 Number of repeated genes: 5	**Repeat**
	Down regulates genes		**Up regulated genes**	
1	ADAMTS6	6		
2	ADAM12, CD44, CPA4	5	EDN1, PDGFB, PTK2B,	5

Table 7.4: List of genes that 1 fold down regulated in Nthy-ori 3-1 cells following Metformin treatment (0.3 mM) for 6 days.

Gene Symbol	Expression	Gene Symbol	Expression	Gene Symbol	Expression	Gene Symbol	Expression
SNORD32B	-6.252246	RNA5SP25	-1.652925	FSCN1	-1.395712	RNU6-1125P	-1.239692
SNORD3B-1	-4.47315	AOX1	-1.649277	CD24	-1.392565	RAP1GAP2	-1.236415
TAF1D	-4.209673	SNORA23	-1.64583	DPYSL3	-1.388522	SMAGP	-1.232379
SNORD24	-3.419105	APOBEC3C	-1.64251	RPSAP52	-1.386029	RP11-91H12.4	-1.227397
ID3	-3.208322	SNORD65	-1.637415	MT-TN	-1.385114	SNORD36C	-1.217121
TNC	-2.803944	RNU6-577P	-1.631045	RNU7-12P	-1.37752	SNORD4B	-1.216727
CGB8	-2.80279	SNORD114-3	-1.625387	RP11-171A24.3	-1.369992	RP11-3G21.1	-1.21596
RNU6-767P	-2.694614	SLC16A14	-1.619389	SRGN	-1.368837	TRPM4	-1.214193
HIST1H2BM	-2.672788	MIR130B	-1.611842	SNORD114-22	-1.367522	RNA5SP309	-1.211722
ERVK-7	-2.670674	TSPAN13	-1.600066	SNHG24	-1.367469	RNA5SP46	-1.211372
RNU5D-1	-2.66551	FAM72C	-1.599743	DDB2	-1.367435	TRBJ2-4	-1.210529
ABHD17A	-2.526654	SLC16A2	-1.593783	RNA5SP228	-1.36172	SNORD14A	-1.208134
SNORD80	-2.504472	SNORD114-14	-1.567084	SNORD47	-1.351289	RNU4ATAC	-1.20542
SNORD50A	-2.453068	RNU5F-1	-1.566105	RABGGTB	-1.350999	SNORD42A	-1.202428
RNY4P19	-2.434782	SNORD72	-1.56458	RNU6-741P	-1.348792	DNAPTP3	-1.198375
RNA5SP221	-2.432818	SPACA5 // SPACA5B	-1.564578	HIST1H2AJ	-1.339102	RNU6ATAC14P	-1.193569
KRTAP2-3	-2.313304	RNVU1-14	-1.536307	FAM219A	-1.338774	SERINC2	-1.193263
CD44	-2.282199	CLCA2	-1.535355	MIR3136	-1.336508	ZNF843	-1.187885
SNORD70	-2.275284	LINC00842	-1.534089	SH3BGRL3	-1.332106	AC012593.1	-1.186309
SNORD114-1	-2.21372	SNORD58A	-1.53365	SNORD59B	-1.322598	RNU7-18P	-1.185012
SNORD114-9	-2.194289	SAT1	-1.528811	FKBP11	-1.316025	EMB	-1.184947
RNU5A-8P	-2.174159	LOC101927501	-1.526218	MSMO1	-1.315332	SNORD74	-1.183046
IL23A	-2.171254	TUBB4A	-1.524568	RNU6-219P	-1.310385	CCDC112	-1.178864
SNORD60	-2.088342	EBPL	-1.51845	SNORD27	-1.307994	COX6B1	-1.1733
SNORD91B	-2.085502	RNU6-1075P	-1.507815	HMGCS1	-1.297247	ZNF415	-1.172944
RNU6-900P	-2.074324	SNORA18	-1.496646	LGALS1	-1.293349	SNORD3D	-1.169899
ID1	-2.071566	SMAD9	-1.490794	PSTPIP2	-1.292115	LOC101928947	-1.167635
SNORD41	-2.061413	RNU6-57P	-1.490772	SNORD104	-1.289459	RP11-400D2.2	-1.16599
RNVU1-15	-2.059525	SNORD114-16	-1.485214	PLIN3	-1.288176	QSOX1	-1.162317
SNORD114-13	-2.051996	TAGLN	-1.482171	LOC100507316	-1.285146	MIR1253	-1.157783
SNORD14C	-1.997306	NPPB	-1.480666	CBR3	-1.281856	GLIPR1	-1.157032
FGF5	-1.994547	SEC24D	-1.480282	MIR197	-1.279294	TRDJ3	-1.151964
TGFBI	-1.985938	SNORD45C	-1.47149	PCAT6	-1.277143	RNU6-387P	-1.148672
SNORD3C	-1.963041	SNORD114-12	-1.469167	RN7SKP185	-1.274226	GCNT1	-1.146185
CTB-151G24.1	-1.957957	SNORD15B	-1.463465	RNA5SP265	-1.27123	RPS4Y2	-1.143632
SNORD14B	-1.957166	MIR4290	-1.463122	SNORD1C	-1.27009	LTA4H	-1.142623
SNORD114-11	-1.926553	PLAUR	-1.459269	RNU6-1286P	-1.269935	PRAMEF2	-1.140896

Gene Symbol	Expression	Gene Symbol	Expression	Gene Symbol	Expression	Gene Symbol	Expression
RNU2-63P	-1.875984	CD68	-1.446662	RP11-897M7.1	-1.269924	SNORD95	-1.14074
LINC00707	-1.868693	SNORD100	-1.445072	RP11-410L14.2	-1.269278	LINC01314	-1.138541
SEPW1	-1.866265	RNU6-564P	-1.434174	SNORD57	-1.264677	HSPA6	-1.138181
RNA5SP465	-1.846296	RNU6-778P	-1.434112	RNA5SP193	-1.264175	MIRLET7A1	-1.134684
TIMP1	-1.829922	SNORA21	-1.427784	RNU6-60P	-1.263645	GSTA1	-1.133967
ADAMTS6	-1.815131	MSN	-1.41933	RP11-501C14.5	-1.258491	SNORD15A	-1.133651
SNORD114-10	-1.796657	SNORA76C	-1.416062	RNU12	-1.257208	MIR4420	-1.131832
CPA4	-1.761465	SNORD11	-1.41123	PSMB3	-1.251856	SNORD46	-1.13183
SNORD68	-1.72812	RNU6-986P	-1.408445	MIR1302-6	-1.249674	RNU1-122P	-1.130378
RNU1-59P	-1.701769	ADAM12	-1.400133	RNU1-46P	-1.249095	MIR29B1	-1.127195
SNORA24	-1.658283	SNAI2	-1.399514	TRIM55	-1.248619	RNA5SP174	-1.12266
LCE1F	-1.653459	KRT34	-1.395766	SNORD121A	-1.243922	DPP3	-1.118481
NDUFA1	-1.117683	RNU6-916P	-1.051538	NCEH1	-1.005179	SH3RF2	-1.02471
SGK1	-1.117636	BCAS4	-1.050713	MT1L	-1.004677	UQCRB	-1.023579
MVD	-1.117347	RNU6-102P	-1.050657	RNU7-103P	-1.00413	RNU6-176P	-1.020438
MT-TA	-1.117114	BIRC2	-1.050645	SNORD101	-1.003045	PPA1	-1.020201
SNORD21	-1.114064	RN7SKP33	-1.050285	MTRNR2L10	-1.002552	MIR4781	-1.019665
CTB-140J7.2	-1.11212	NR1D1	-1.049781	WASF3-AS1	-1.002114	MIR520C	-1.019203
SNORD22	-1.110616	ENPP1	-1.048843	HBG2	-1.001469	GSTP1	-1.019073
RNU6ATAC11P	-1.104427	C12orf75	-1.046191	TPM4	-1.00108	SNORD81	-1.017243
DCXR	-1.100228	SEC61G	-1.045251	LMBR1L	-1.000677	IDH1-AS1	-1.017094
AC006262.4	-1.100128	RNU6-612P	-1.042316	RNU6-1191P	-1.067299	AC124944.3	-1.016199
CORO1A	-1.0987	SCARNA18	-1.041066	EML1	-1.066192	AC011284.3	-1.015702
SPRYD3	-1.098458	KRTAP10-5	-1.039706	PRSS50	-1.064648	RP11-124N14.3	-1.015572
MIR302D	-1.096536	ZNF563	-1.038518	RP1-288L1.4	-1.063974	TMED9	-1.015388
SUMO1P3	-1.096453	C6orf205	-1.03714	RNF122	-1.062042	CASC22	-1.014826
AC005324.7	-1.095319	SNORD55	-1.036882	RP11-550C4.6	-1.060734	TMEM158	-1.012336
MIR4461	-1.094127	SNORD99	-1.033106	BEX1	-1.059926	CST5	-1.012302
SCARNA9L	-1.093795	TXNIP	-1.030712	SIX4	-1.058897	SCARNA5	-1.012038
OSTF1	-1.093734	ROMO1	-1.030542	RNA5SP22	-1.058702	GPI	-1.01147
RNU2-25P	-1.093671	SNORD114-20	-1.030133	ARPC3	-1.057886	LOC101928119	-1.011192
C4orf48	-1.092101	SNORD35A	-1.029789	CCBE1	-1.054383	TNFRSF21	-1.009372
P4HA1	-1.09009	ABHD17AP3	-1.029186	RNU4-80P	-1.052953	SDF2L1	-1.00838
RNA5SP495	-1.089334	IFFO2	-1.029036	VIM-AS1	-1.052454	ZFC3H1	-1.006191
AC079354.5	-1.087107	RRAS	-1.029031	RNA5SP476	-1.051857	MPP4	-1.005939
HOMER2	-1.086766	SNORD58C	-1.028742	RNA5SP214	-1.080108	RNA5SP505	-1.07442
RP11-14I17.2	-1.086715	LOC101928271	-1.026824	BTG2	-1.078784	KRT18P39	-1.072027
ALMS1P	-1.086406	SNORD45A	-1.026324	CIART	-1.076079	MGC12916	-1.067621
RNU2-24P	-1.083184	TRBV5-6	-1.081456	RNU6-110P	-1.081668		

Table 7.5: List of genes that 1 fold up regulated in Nthy-ori 3-1 cells following Metformin treatments (0.3 mM) for 6 days.

Gene Symbol	Expression	Gene Symbol	Expression	Gene Symbol	Expression	Gene Symbol	Expression
C4B	17.1382	RNU6-294P	2.591221	EEF1DP3	1.985241	KCTD16	1.746045
SNAR-C2	8.260474	AC104135.3	2.589646	PLEKHS1	1.979516	BMP4	1.744037
PPP1R10	8.143419	ANKRD20A9P	2.583029	OLR1	1.976276	IL18	1.742196
IER3	7.378793	RNU6-433P	2.573448	NSAP11	1.972319	SPG20OS	1.739636
PDE4DIP	6.931958	LINC01293	2.569288	RN7SKP103	1.969026	RP11-465N4.4	1.73358
PTPRQ	6.519714	FTX	2.554234	RN7SKP198	1.964488	RNU6-789P	1.731081
SNORA38	6.10198	NCOA5	2.521023	CTB-147C13.1	1.958482	RP11-110I1.12	1.720515
CEACAMP7	5.237918	KCNH1	2.514307	FJX1	1.955495	MIR3189	1.717637
LINC00963	4.722674	DHRS3	2.511312	SNORA38B	1.946578	ITGB4	1.715645
PRKXP1	4.617178	DLGAP1-AS2	2.435514	FRY	1.946477	CXCL8	1.715208
ZBTB12	4.56794	ANKRD30B	2.433121	MT-TL2	1.939348	PDE1A	1.714236
LOC100132167	4.448485	PPIP5K1	2.416842	RTKN2	1.938739	TAS2R14	1.71316
LOC100506870	4.094731	RP11-34P13.7	2.408226	FZD1	1.930788	ACKR3	1.710937
PROS1	3.726661	C7orf69	2.400004	RNU6-1316P	1.923258	IFIT1	1.709172
PIEZO2	3.724022	AC005392.13	2.387354	PTX3	1.914646	MAMDC2	1.690717
PLCE1-AS1	3.641091	RNU6-957P	2.3866	MUC1	1.912818	RASEF	1.687939
LINC01111	3.556213	RASGRP3	2.357029	DKK1	1.909815	LOC285500	1.683698
DUXAP10	3.555711	CD177P1	2.354582	ZNF451	1.902315	ICAM1	1.681669
LOC441956	3.5445	C3	2.316679	MIR554	1.900519	RP11-314N13.3	1.681607
MAT2A	3.511004	MID1IP1-AS1	2.313057	KCNIP1	1.897427	MIR1205	1.675004
RP11-3L8.3	3.369322	TAS2R46	2.304925	LOC102724425	1.870754	LOC100507477	1.674654
PDZK1	3.291508	ADAMTS5	2.290615	NUPR1	1.864618	ZBTB2	1.672993
SNORD62A	3.228056	PSAT1	2.28173	PARD3B	1.864002	CTD-2269F5.1	1.668163
SSX2B	3.22444	RNU6-530P	2.267139	LOC728339	1.861989	RGS7	1.657907
JRKL-AS1	3.214572	FAM86EP	2.252485	HIF1A-AS2	1.855248	CTAGE11P	1.655691
RP11-745L13.2	3.214332	MIR3671	2.232056	LOC100506895	1.849859	RNU6-1255P	1.651551
CLSTN2	3.20284	SORBS2	2.225418	STOX1	1.842854	VLDLR-AS1	1.648177
KCNH7	3.179391	MIR181B2	2.215367	RNA5SP346	1.831347	FAM198B	1.645376
LOC374443	3.161608	ASS1	2.209457	IFI44	1.830416	PDE1C	1.633017
NEAT1	3.154257	LINC00476	2.206139	ZBTB20	1.827317	NPNT	1.63039
LOC284344	3.153381	LOC400743	2.204532	LOC100507577	1.824106	RP11-360F5.3	1.629866
MIR548I2	3.145784	C4A	2.19773	LINC00883	1.823087	RNU6-1147P	1.629023
SNAR-B2	3.111688	MX1	2.190525	RNU6-1287P	1.814964	DDIT4	1.628775
SSX1	3.09608	CLDN1	2.098145	HNRNPH1P1	1.813023	RP11-757O6.1	1.627755
ARHGAP23P1	3.038614	SDHAP2 // LINC00969	2.094141	IFIT3	1.811479	HNRNPA1L2	1.626685
AC093642.4	3.001863	SMA4	2.090716	MIR181A2HG	1.808694	TOB2P1	1.624983
ZNF807	2.965392	MIR616	2.086582	LINC00965	1.805758	IFI44L	1.624648
PROSP	2.947028	SHISA9	2.057963	DDR2	1.803474	HTR1D	1.622015
GPNMB	2.92643	PRICKLE1	2.056931	C5	1.80135	ADAMTS12	1.618574
LOC645553	2.92015	ITGB8	2.053967	MIRLET7F1	1.794816	CHAC1	1.61421
CDKN2B-AS1	2.7412	C4BPB	2.050059	TTC9	1.792215	RP11-70J12.1	1.613685

Gene Symbol	Expression	Gene Symbol	Expression	Gene Symbol	Expression	Gene Symbol	Expression
CLDN16	2.726477	COL8A1	2.039397	RP11-551L14.4	1.775679	LINC00328	1.613244
SLC7A11	2.713641	DRAM1	2.032892	ALPK2	1.772302	NCKAP5	1.612351
NABP1	2.641271	PTGES	2.031756	DAPK1-IT1	1.76844	ZNF75A	1.610115
PA2G4P4	2.639227	MCOLN3	2.022122	TMC3	1.767519	PLAU	1.609967
ARHGAP23	2.622482	MEGF9	2.013654	TMEM178B	1.766052	NPR3	1.609118
VLDLR-AS1	2.59891	RNU7-80P	2.011094	KRCC1	1.758719	RNU4ATAC18P	1.608476
FLJ38717	2.595691	IPO5P1	2.01017	LOC729987	1.757916	IL6ST	1.605092
CTIF	1.000797	MIR421	1.987304	ZNF37BP	1.750578	AC093110.3	1.603878
PIGL	1.598371	RP11-685N10.1	1.44098	LOC728323	1.357176	RNU6-522P	1.30355
LINC01239	1.595554	LOC101928565	1.44056	RNU7-187P	1.354375	MIR644A	1.300386
RP11-154D6.1	1.587637	SMAD2	1.440079	CPA3	1.353976	LOC101929787	1.300114
ZNF252P	1.587553	MIR4668	1.437956	LOC101928324	1.353589	FAM111B	1.298518
RPL23AP32	1.585392	RP11-389O22.1	1.43759	LINC01355	1.353542	LOC100288637	1.297532
SERTAD4	1.58121	KRT80	1.436258	SETBP1	1.352872	DDIT3	1.295563
LOC100130169	1.580202	RP11-818F20.5	1.436252	E2F8	1.351677	MX2	1.293169
RBM26-AS1	1.577715	SRGAP1	1.433345	MIR27B	1.350116	ANKRD20A11P	1.291922
PRSS23	1.563625	NXPH2	1.432957	MEIS3P1	1.347742	ERBB4	1.291726
LIMCH1	1.563526	IL6	1.428327	ZNF337	1.347141	LOC101929475	1.29141
VEGFA	1.559916	GS1-600G8.5	1.425364	TSPY2	1.346743	FAM133CP	1.290896
LOC101927287	1.553069	ZCCHC8	1.424573	FAM66E	1.346103	SCN9A	1.290819
PPARGC1A	1.547066	KCNMB3	1.42302	TNS3	1.345822	RNF157	1.290665
BICC1	1.546207	LOC101930275	1.422015	ERCC6	1.345797	AC007879.7	1.290508
TAS2R20	1.544782	LOC100506929	1.421573	AHR	1.344931	METAP1D	1.289994
NBPF1	1.544242	HRK	1.420232	RNU6-872P	1.344545	LAMP3	1.289594
LOC90784	1.542143	NAIP	1.418763	LOC101927184	1.342217	SLC4A2	1.288211
MIR548H3	1.535778	LOC100129034	1.417076	LOC440028	1.336957	SLC38A1	1.2855
LOC101928020	1.535777	TRAK2	1.416008	TMEM194B	1.336454	FAM66C	1.285029
MAL2	1.532748	TRIB3	1.414132	NMNAT2	1.334855	PKD2	1.284717
PPP3CB-AS1	1.531101	RNU6-215P	1.413309	S1PR1	1.334568	NCOA7	1.284452
ADAMTS15	1.526897	LMBRD2	1.412615	PDGFB	1.334297	ANKRD1	1.282192
RNU6ATAC16P	1.524537	NCKAP5-IT1	1.412572	LOC728613	1.329268	LOC101927097	1.280171
CTNS	1.521223	DSC3	1.410669	ABI3BP	1.329234	DLEU2	1.279964
TTLL1	1.518174	RN7SKP95	1.410293	LOC101928054	1.328904	PIGM	1.27974
RP11-807H7.2	1.51753	LOC101928706 // LOC101929823	1.409177	LINC01004	1.328859	TMSB4X	1.276145
LOC340581	1.515399	EPSTI1	1.40632	GS1-124K5.2	1.3268	BRWD3	1.276118
GEN1	1.514843	IRS1	1.403744	NAV2	1.322888	GCSHP3	1.275784
PARP14	1.51052	MKRN9P	1.401434	ZNF66	1.322301	RP11-152P17.2	1.2734
TIMP3	1.510448	LOC100130691	1.393899	RNU6-82P	1.321761	LOC100129518	1.271978
SRSF6	1.508137	FAM13B	1.393436	MIR570	1.320256	LOC284581	1.271737
SLC16A6P1	1.503976	RNU6-302P	1.392839	LINC00886	1.319909	MIR3621	1.271113
RP3-368A4.5	1.503508	SECTM1	1.386099	TNFRSF11B	1.319753	PSMD5-AS1	1.270698
GAS5-AS1	1.502007	RP11-585F1.10	1.38016	DPY19L3	1.319454	CLEC2D	1.270614

Gene Symbol	Expression	Gene Symbol	Expression	Gene Symbol	Expression	Gene Symbol	Expression
LOC102724851	1.498241	AJUBA	1.379192	CDC42EP3	1.31871	BRCC3	1.268692
DAPK1	1.496929	EPAS1	1.378037	MYLIP	1.317689	PRKAA2	1.267353
DNAJC6	1.490659	RNU6-998P	1.377231	METTL7A	1.31665	RP11-49O14.2	1.26733
HERC2P9	1.490397	RP4-791M13.3	1.375516	TYRP1	1.314589	STON2	1.259321
NOV	1.486634	LOC100289455	1.375117	PTK2B	1.314278	UAP1L1	1.256256
SLC35F6	1.486548	ANK2	1.374528	CIRBP	1.31413	RNA5SP355	1.255741
LOC102724077	1.483174	AC009229.5	1.372961	RNU6-697P	1.312449	IGFBP3	1.255272
AC099850.1	1.47714	TPCN1	1.372098	SLC43A3	1.311266	GPC6	1.25525
AC002117.1	1.458931	DDX58	1.371331	RASSF3	1.309805	LINC00342	1.253275
RNU6-1284P	1.454859	BCL2	1.369705	AP000704.5	1.308858	RPS6KA5	1.253262
WISP2	1.451802	CLGN	1.364957	SLC16A1-AS1	1.307473	RNU6-316P	1.251013
KCNJ2-AS1	1.450935	ZSCAN16	1.363844	SLC35A5	1.306221	PKP2	1.248811
RP11-436H11.5	1.449994	AP001059.5	1.361519	LOC100294341	1.305715	TAS2R31	1.247655
ULBP1	1.447452	RP11-692D12.1	1.36037	ANKRD20A5P	1.305117	CABLES1	1.247532
PTPN21	1.445818	LOC100653515	1.359744	KIF24	1.303892	ZNF620	1.245263
RP4-657D16.3	1.24426	SRSF1	1.188428	RNU4ATAC16P	1.147163	SNORD114-18	1.108048
RNU6-1162P	1.241597	PTGIS	1.187631	MTSS1L	1.144627	CCDC30	1.107174
RNU6-206P	1.241238	LOC100131826	1.18735	HAVCR1P1	1.144284	RP11-94I2.1	1.105633
ABLIM1	1.240065	MIR573	1.186534	LINC00969	1.144153	CHST15	1.105242
ZNF658	1.239775	MIR454	1.185638	DSCC1	1.143246	FOXE1	1.103903
ZNF385B	1.238092	ANKRD36BP2	1.183821	RP6-206I17.1	1.141838	AC138035.1	1.103577
RASGRF1	1.236543	RP11-123O10.4	1.18367	CCDC125	1.14092	POLR3B	1.103326
NALCN	1.236464	RNU7-182P	1.183381	SGPL1	1.140486	TMEM67	1.103295
LINC01285	1.235605	SLC29A2	1.18216	ADAL	1.140351	RNU6-466P	1.102967
ZNF473	1.23508	RP11-1166P10.1	1.178751	ADAM1A	1.140267	RRAGD	1.101206
AC017002.2	1.234908	POLR3C	1.177247	LCMT2	1.138523	MGC27345	1.100245
LOC101929287	1.234455	HSF2BP	1.177016	RAPGEF1	1.137723	RP11-522M21.3	1.099854
LOC441454	1.234383	CHAC2	1.17627	TCEAL3-AS1	1.137535	FLJ43681	1.099529
MTMR8	1.232008	IFIT2	1.176171	LOC101929964	1.137321	RP11-274J7.2	1.099336
TIGD2	1.231396	LOC102723919	1.174772	CTC-325J23.3	1.137082	FUS	1.095798
RP5-1050D4.2	1.228234	ZDHHC21	1.174542	RNA5SP37	1.136595	GBAP1	1.095666
WBP4	1.227558	SERPINB9	1.173427	GNB5	1.136213	MIR4659A	1.095269
PDGFC	1.227168	STC2	1.173369	UCP2	1.136148	CEP128	1.095195
SLC1A4	1.223744	CARF	1.17267	TRAPPC2	1.135638	AP3M2	1.093371
ARNT2	1.222963	SH3YL1	1.172056	RNU7-62P	1.133752	TBL1XR1	1.093213
LOC100132705	1.222601	SLC38A4	1.170982	MIR4258	1.132806	ARHGEF2	1.091631
ZC3H12B	1.22035	LOC100288842	1.170683	BACH1-IT2	1.131931	SNORD18B	1.090821
RP11-50E11.3	1.219928	RRN3P3	1.170477	PSG9	1.130682	SLC16A7	1.090624
SORL1	1.219495	ERCC6L2	1.166397	FOXRED2	1.130378	LOC101929464	1.090259
RNU6-1045P	1.218309	C9orf64	1.166303	RNF144B	1.129961	USP40	1.089867
ZC3HAV1	1.216662	PTN	1.164695	CLCN7	1.128654	FRMD4A	1.088945
POGLUT1	1.215986	LOC102723672	1.162983	RP11-283C24.1	1.128624	CTC1	1.088372

Gene Symbol	Expression	Gene Symbol	Expression	Gene Symbol	Expression	Gene Symbol	Expression
FNDC1	1.213659	PCBD2	1.162312	ZNF230	1.128476	UGCG	1.088124
LOC100131802	1.212476	CREG1	1.16118	RAD51D	1.125235	MAP3K14	1.087469
FRMPD4	1.21002	LRCH3	1.159974	LURAP1L	1.125081	SLC35E2	1.086693
ITFG2	1.206646	EIF5	1.159705	TRIOBP	1.125065	MIR4295	1.086574
AC159540.1	1.206089	RNU6-606P	1.158293	SLC6A9	1.123094	FAM106CP	1.085609
IFI6	1.205403	SEMA3A	1.15753	LOC101927841	1.122726	CTD-2116N20.1	1.084531
FAM49A	1.201638	VDR	1.157512	BST2	1.121072	RP1-239B22.5	1.084103
PATZ1	1.200338	RNU6-817P	1.157008	LOC653513	1.119441	LPAR4	1.083757
KLHL42	1.198931	RN7SKP56	1.155846	EYA4	1.117332	KGFLP1	1.083365
bP-21201H5.1	1.197715	C22orf46	1.155585	CYP4F35P	1.116906	IGFN1	1.083183
PLEKHG7	1.19703	COG2	1.155445	RNU6-834P	1.116729	TNFAIP2	1.082978
RP1-313L4.3	1.195673	LOC102725076	1.154587	SLC27A2	1.116193	MEPCE	1.081599
FHDC1	1.195167	GREB1L	1.153339	ZC3H12C	1.116089	SLC30A6	1.081109
RNU4-31P	1.195081	DAGLA	1.152792	HEXIM1	1.114872	SPPL2A	1.080276
GOLGA1	1.194451	SAMD9L	1.15258	LINC00882	1.114782	LYPD6B	1.079471
IFIH1	1.192943	LRRC8D	1.151838	GLYR1	1.113724	AC017006.2	1.079367
RP11-435D7.3	1.191314	MIR645	1.151708	TOE1	1.113663	MIR924	1.079
ZBED3	1.190627	CLMN	1.150778	ZNF829	1.112881	RN7SKP173	1.07866
B3GALT6	1.190101	TSPAN2	1.150647	LOC101927506	1.112068	LPA	1.07812
CITED2	1.189508	TSTD2	1.149533	TMEM52B	1.111751	MYO1B	1.077404
RP5-864K19.4	1.189368	DGCR8	1.148644	RP11-385D13.1	1.111404	DENND2A	1.077358
ZNF572	1.188757	RNU6-890P	1.147317	TRAM2	1.110926	CYP20A1	1.077031
NUAK1	1.077012	LINC00472	1.054031	PARP12	1.026287	XRCC2	1.055714
RNU6-1163P	1.076513	LOC101928173	1.05343	MTHFD1	1.025802	TRPM7	1.055625
BRCA2	1.075807	C2CD3	1.052163	ZFX	1.025542	RNA5SP511	1.055171
LINC01123	1.075339	OPN3	1.051686	ANKRD36B	1.024849	MIR548V	1.054068
EGFR	1.074873	ING3	1.051417	GAS6-AS2	1.024457	ETS2	1.029904
TMEM220	1.074837	ZDHHC15	1.05035	EXPH5	1.024438	CCL2	1.029158
SLC7A1	1.074488	ARHGEF39	1.050243	KMO	1.023208	ADM	1.029051
RP11-101E14.3	1.074461	SNAR-H	1.050102	EPHA5-AS1	1.023117	ZNF250	1.027561
LOC284926	1.074127	EDN1	1.050019	STX11	1.022692	ZSWIM7	1.056776
RP11-33B1.3	1.073511	RP1-102E24.8	1.049861	PSPH	1.022481	LINC00152	1.056563
HELQ	1.072892	DCLK2	1.049802	LINC-PINT	1.022048	GPX3	1.05611
ELAVL2	1.071984	MYO16-AS1	1.049683	CBS	1.021246	FBXO28	1.055935
DOLK	1.071815	CYTH3	1.048133	LOC101927978	1.021055	PTS	1.055918
RNU6-895P	1.069716	PSPC1	1.047847	TAF15	1.020676	MT1E	1.032474
FAM86MP	1.069264	NOTCH2NL	1.046593	KIAA1217	1.020653	PHF14	1.032414
RN7SKP88	1.068616	HIST1H4H	1.045594	TAS2R50	1.019401	RP11-398K22.12	1.031467
ZNF770	1.068417	NEAT1 // MIR612	1.044994	FAM122A	1.019392	SLC22A5	1.031289
LOC100133315	1.06826	DVL3	1.044985	SNORA10	1.019245	DLGAP1-AS1	1.030452
GUSBP1 //	1.067155	RNU4-9P	1.044216	CSRP2BP	1.018788	FAT3	1.00514

Gene Symbol	Expression	Gene Symbol	Expression	Gene Symbol	Expression	Gene Symbol	Expression
LOC100996497							
TBX20	1.066464	LOC101927533	1.043809	LINC00240	1.017978	HNRNPA0	1.004366
RP11-417O11.5	1.066286	MBTD1	1.040547	RNU6-971P	1.016805	RNU6-301P	1.003262
LOC553103	1.066102	SDCBP2-AS1	1.040532	RP11-344N10.5	1.016626	URB2	1.002368
VEZF1	1.065327	KIAA1614-AS1	1.039552	MIR4298	1.01541	ST7L	1.001178
VGLL3	1.064534	SECISBP2	1.039178	TGFB2-AS1	1.015181	KAT2B	1.007396
TAS2R13	1.063851	MIR761	1.03894	RNU6-1102P	1.014535	OCLN	1.007071
ZNF782	1.063725	SLC16A13	1.038719	POLR1A	1.013486	CLIP4	1.006042
QPRT	1.063629	SQSTM1	1.038667	CYP1B1	1.013136	RNU6-968P	1.034024
RNU6-1263P	1.061946	MGC70870	1.038267	RNU6ATAC18P	1.012234	RNU6-1223P	1.033789
LTBP1	1.061865	ZNF45	1.037896	SASH1	1.011566	RNU6-1029P	1.03366
LOC283140 // LOC100506870	1.061848	DUSP1	1.037756	CREBBP	1.011503	RP11-798M19.3	1.058282
DNMT3B	1.061358	RP11-773D16.1	1.037567	RP11-107M16.2	1.010346	DSE	1.057635
C1orf220	1.060775	HLA-B	1.03721	LPP-AS2	1.009355	LOC101927116	1.0574
AMIGO2	1.060662	RNU6-954P	1.036963	ECM2	1.009253	SLC7A5	1.05874
RNU4-36P	1.06037	GLRB	1.03599	LOC100506325	1.008527	RNU6-923P	1.034229
RNA5SP283	1.059605	CPVL	1.035675	PLSCR1	1.008422	RNA5SP444	1.007597
RP4-633O19__A.1	1.058824	MIR33B	1.035533	RNU6-220P	1.007692		

Table 7.6: List of genes that 1 fold down regulated in FTC-133 cells following Metformin treatments (0.3 mM) for 6 days.

Gene Symbol	Expression	Gene Symbol	Expression	Gene Symbol	Expression
SNORD99	-3.138417	TUFT1	-1.494788	RN7SKP160	-1.15334
SNORA66	-2.819541	ATP6V0B	-1.48684	UCK2	-1.127401
DUSP5	-2.722006	RGS2	-1.486511	MIR3671	-1.125274
SNORD75	-2.721084	NAMPT	-1.48637	RP11-384C4.7	-1.123829
SNORD103A	-2.64968	SLC19A2	-1.392155	NRBF2	-1.123661
RNU6-773P	-2.567926	PFDN2	-1.391322	ENO1	-1.121763
SNHG12	-2.34524	SNORA55	-1.385548	SCARNA1	-1.112795
HMGN2	-2.241845	OTUD1	-1.328859	PPP1R15B	-1.109595
CIART	-2.200218	G0S2	-1.293682	FAM129A	-1.098725
MIR554	-2.149709	RNU6-753P	-1.286647	RNU6-693P	-1.098367
GAS5	-2.142077	DYRK3	-1.283458	THAP3	-1.097863
SNORA14B	-1.933805	OR2L3	-1.27309	RNU6ATAC27P	-1.09637
RPS27	-1.911409	ZBTB18	-1.268312	RNU6-885P	-1.093934
ATF3	-1.906255	TIMM23B	-1.256248	RAD54L	-1.09338
KCNH1-IT1	-1.87971	RNU7-45P	-1.231558	OCLM	-1.076606
IL24	-1.854969	RNU6-946P	-1.215508	TOMM20	-1.076182
MIR1278	-1.7632	RPL21P28	-1.211071	SRGAP2	-1.064688
RNU11	-1.760812	MEF2D	-1.204484	NEK2	-1.058935
GNG5	-1.744586	RNU6-805P	-1.202467	RNU4-61P	-1.053955
NBPF20	-1.737692	RNU6-1067P	-1.202275	CKS1B	-1.052173
HKDC1	-1.70373	GADD45A	-1.201438	NUAK2	-1.051206
RPS24	-1.68706	RNU7-70P	-1.194104	PHGDH	-1.047373
ARL5B	-1.681324	YRDC	-1.188103	RNU6-1274P	-1.043247
MIR4742	-1.65024	PLK3	-1.182211	CDK1	-1.041123
LOC284561	-1.621344	RNA5SP45	-1.181792	PRAMEF11	-1.036984
MIR3115	-1.547067	SLC22A15	-1.176196	FAM72C	-1.015477
RP11-545I10.2	-1.538732	RP11-275I14.4	-1.175123	EMBP1	-1.002409
RABGGTB	-1.495314	NGF	-1.161649	RP11-295G20.2	-1.001638

Table 7.7: List of genes that 1 fold up regulated in FTC-133 cells following Metformin treatments (0.3 mM) for 6 days.

Gene Symbol	Expression	**Gene Symbol**	Expression	**Gene Symbol**	Expression
SLC18A3	2.914271	EPHX4	1.325457	WBP1L	1.135208
SERTAD4	2.912107	C10orf25	1.318821	ROR1	1.132694
DIO1	2.60728	IFIT5	1.312251	IPO13	1.128392
RP4-791M13.3	2.410873	ACADM	1.308962	LOC100133331	1.12656
LINC01037	2.3793	LCE1A	1.302852	ST8SIA6	1.123277

Gene Symbol	Expression	Gene Symbol	Expression	Gene Symbol	Expression
LOC102723919	2.288908	ACP6	1.296792	THEM4	1.12133
HIST2H4B	2.23496	PEX11B	1.295167	UBE4B	1.11957
IKBKE	2.166837	NBPF1	1.292538	ABCB10	1.118556
PARS2	2.159519	LINC01139	1.285893	MAB21L3	1.112222
BICC1	2.056973	INTS3	1.284189	PIGM	1.104949
LRRC39	2.001026	PIK3R3	1.272465	DNAJC16	1.103066
RNU5E-4P	1.904593	CCDC18	1.263084	GNAI3	1.101555
SLC25A44	1.76949	RP5-1061H20.4	1.260614	LOC729970	1.100031
RP11-148B18.4	1.747115	NBPF25P	1.258747	MAN1A2	1.086991
PTPRE 7	1.704732	TOE1	1.251928	FBXO28	1.083433
LOC101927435	1.703138	HMCN1	1.249894	TET1	1.079681
C1orf220	1.694529	RNU7-165P	1.248054	SYT11	1.078852
CPT2	1.659833	RP11-284F21.7	1.243934	RNVU1-19	1.078367
EIF4EBP2	1.629283	MR1	1.237218	RNU1-122P	1.076841
ST6GALNAC5	1.627499	STPG1	1.230525	TCEANC2	1.076051
RAB4A	1.626263	ZMYND11	1.225645	FAM213B	1.074924
AGL	1.623054	MTFR1L	1.222258	TSPAN14	1.073806
ASPM	1.607022	CACHD1	1.219443	SCYL3	1.071649
PER3	1.587773	RGL1	1.21664	SDHC	1.069283
PMVK	1.58397	NPPA-AS1	1.20978	SLC16A1-AS1	1.065338
SLC35E2	1.554891	BTRC	1.206915	RAB29	1.064365
FAM231D	1.5356	GS1-174L6.4	1.201096	BCL10	1.063442
BTBD8	1.530597	FMO4	1.190572	NFYC-AS1	1.047256
COG2	1.513195	ZNF22	1.184752	FAM63A	1.045453
LOC102724425	1.512033	ZNF691	1.17977	LOC642361	1.044005
NSL1	1.507203	ARV1	1.179298	MIR4677	1.043843
CASC10	1.495583	ZNF248	1.172855	KAT6B	1.04286
EDEM3	1.494628	LOC100287497	1.172272	ZMYM4	1.038411
S1PR1	1.486556	SKIDA1	1.168877	RP11-80B9.1	1.034924
FMN2	1.438571	TRMT1L	1.168654	LINC00702	1.031723
ACOT11	1.435883	IPP	1.168561	DLEU2L	1.031639
LRIF1	1.432328	STOX1	1.166804	PRUNE	1.027419
KLHL20	1.429742	HTRA1	1.166512	PAFAH2	1.025468
FLG-AS1	1.424351	SYNC	1.166014	LDLRAP1	1.014443
ZFP69B	1.419879	CDKN2C	1.163997	PRTFDC1	1.013846
CDC14A	1.403379	KCNT2	1.156313	FAM178A	1.013687
KIAA1107	1.394029	MIR4480	1.155348	RCAN3	1.006583
DNAJC11	1.38977	SPAG17	1.153368	TBX15	1.005901
PHTF1	1.38927	RAB42	1.152434	ACADSB	1.00337

Gene Symbol	Expression	**Gene Symbol**	Expression	**Gene Symbol**	Expression
TAF1A-AS1	1.386637	RP11-815M8.1	1.151448	INPP5A	1.002899
ABCD3	1.372124	NMNAT2	1.148806	TARS2	1.001082
TSPAN2	1.365549	C1orf233	1.144269	MTHFR	1.000777
DNM3	1.348495	THNSL1	1.140079		
CFH	1.330521	ZNF436	1.138494		

Table 7.8: List of genes that 1 fold down regulated in K1E7 cells following Metformin treatments (0.3 mM) for 6 days.

Gene Symbol	Expression	Gene Symbol	Expression	Gene Symbol	Expression	Gene Symbol	Expression
SNORD115-5	-16.309266	RNU6-1072P	-3.282342	MIR574	-2.812188	SNORA6	-2.556597
LOC100272216	-15.106969	SNORD41	-3.268312	RNU6-1095P	-2.802889	MIR4481	-2.556056
SNORD32B	-9.661779	SNORD17	-3.266657	RNA5SP415	-2.785281	RNU6ATAC27P	-2.554632
SNORA38	-9.284843	SNORA36B	-3.255055	RNU6-1167P	-2.780826	RNU6-487P	-2.537045
SNORD117	-8.509836	RNU1-14P	-3.241755	RNU1-138P	-2.777218	SNORD116-1	-2.526007
HSPA1A	-7.513288	RNU5D-1	-3.241036	SNORD115-1	-2.770826	RNU6-702P	-2.521976
TAF1D // SNORA8	-7.095325	MIR1185-2	-3.235616	SNORA71D	-2.767418	RNU6-739P	-2.50272
SNORD52	-6.96934	SNORA54	-3.223583	RNA5SP176	-2.765666	RNU5F-2P	-2.502156
SNORD48	-6.498743	ZNF474	-3.197887	RNA5SP87	-2.76331	SNORD84	-2.493576
SNORD116-3	-6.014839	SNORD14C	-3.197487	RNU6-804P	-2.752915	SNORD24	-2.481144
RNU1-13P	-5.679428	RNU1-42P	-3.159696	HIST1H4B	-2.745049	SNORD115-47	-2.475927
RNU6-540P	-5.348021	RNU1-32P	-3.150842	MIR514A1	-2.742492	SNORD83A	-2.474204
HSPA1B	-5.207419	SNORA61	-3.14295	SNORD100	-2.740214	RNU6-279P	-2.46995
ANKRD20A11P	-5.111095	SNORD81 // SNORD79	-3.133315	RNU6-572P	-2.740106	RNU6-60P	-2.468641
SAPCD1	-4.796992	SCARNA7	-3.109645	SCARNA10	-2.739802	SNORD94	-2.468167
RNU1-38P	-4.796858	PTMA	-3.097041	RNA5SP455	-2.733891	SNORA21	-2.467629
MIR933	-4.627214	SNORD115-4	-3.070124	SNORA52	-2.727871	RP13-401N8.1	-2.466919
SNORD3B-1	-4.53475	MICA	-3.067721	MYH16	-2.727384	SNORD58C	-2.465
SNORA72	-4.40927	SNORA37	-3.062438	DDR1-AS1	-2.722995	SNORD9	-2.46127
SNORA60	-4.360123	SNORD92	-3.057987	SNORD103A	-2.722838	RNA5SP132	-2.459834
SNORA75	-4.358876	SCARNA4	-3.03576	RNU6-560P	-2.718242	RNA5SP28	-2.453412
RNU1-41P	-4.32181	HIST1H2BG	-3.031223	RNU6-580P	-2.714142	MIR548A1	-2.450984
RNA5SP221	-4.303338	RNU6-294P	-3.022542	ROCK1P1	-2.71103	MT-TA	-2.43403
LOC102724689	-4.299147	RNU11	-3.019247	RNU6-151P	-2.710437	SPANXA1	-2.430698
SNORD116-5	-4.181892	RNA5SP90	-3.01892	SNORA11	-2.707471	TRAJ59	-2.428491
MIR4650-1	-4.034786	RNU6-816P	-3.014013	MIR4673	-2.69465	RNU6-471P	-2.425134
SNORA1	-4.003489	SNAR-C2	-3.013218	RNU1-136P	-2.673831	HLA-DQB1-AS1	-2.418987
MIR3156-2	-4.002237	RNA5SP106	-3.007132	RNA5SP478	-2.669549	RNU6-412P	-2.41486
SNORA59B	-3.920698	RNU6-363P	-3.003897	MIR4461	-2.666637	SNORA7B	-2.408545
SNORA14B	-3.893102	ABHD17A	-3.002514	KSR2	-2.6537	RNU6-971P	-2.404938
RNU6-407P	-3.871328	RNU4-8P	-2.988792	SCARNA8	-2.65233	RNA5SP399	-2.385912
RNU5E-4P	-3.861107	SNORA46	-2.980917	SCARNA11	-2.651717	SNORA15	-2.38209
RNVU1-15	-3.835796	RNA5SP116	-2.980795	RNU6-801P	-2.643595	RNA5SP432	-2.381482
SNORD115-17	-3.803325	RNU5F-1	-2.975267	RNU6-1067P	-2.642413	LOC388692	-2.370153
RNU6-271P	-3.735883	SCARNA17	-2.933124	MT-TS1	-2.642356	SNORA80E	-2.368253
RASA4	-3.648009	RN7SK	-2.92742	RNU6-392P	-2.632402	RNU1-143P	-2.360234
SNORA71B	-3.64304	SNORA20	-2.922946	SNORA76C	-2.625838	SNORA57	-2.357718
SNORA33	-3.628663	RNU6-1257P	-2.90714	MIR3156-1	-2.624937	SNORD60	-2.354844
RNA5SP361	-3.622943	SNORA11D	-2.887514	SCARNA9	-2.619746	SNORD104	-2.35343
SNORD116-2	-3.602833	HIST1H2BH	-2.883166	RNU6-1005P	-2.612075	SNORA45B	-2.351086

Gene Symbol	Expression	Gene Symbol	Expression	Gene Symbol	Expression	Gene Symbol	Expression
RNA5SP199	-3.536739	RNU6ATAC2P	-2.873024	RNU6-1112P	-2.611464	RN7SKP173	-2.346026
RNU6-1295P	-3.483577	SCARNA6	-2.87094	SCARNA5	-2.611094	SLC25A3	-2.34435
RNU1-95P	-3.45923	RNU6ATAC	-2.86167	SNORA38B	-2.606791	RNU1-83P	-2.339703
RNA5SP233	-3.426408	RNA5SP265	-2.850359	RNU6-431P	-2.60088	RNA5SP473	-2.339101
RNA5SP100	-3.422696	RNU6ATAC10P	-2.847578	SNORA26	-2.58933	RNU6-371P	-2.318944
RNA5SP390	-3.400606	SCARNA3	-2.847194	RNU6-159P	-2.586944	HCG27	-2.310892
RNA5SP150	-3.383379	SNORD3C	-2.84445	RNA5SP234	-2.57822	RNU6-925P	-2.309352
MIR328	-3.351308	RNU6-353P	-2.842194	RNU1-46P	-2.573426	SNORD116-13	-2.304643
SNORD14E	-3.332556	RPS3A	-2.83085	RNU5B-1	-2.572817	RNU1-119P	-2.303358
RNA5SP368	-2.298712	SNORD15A	-2.128625	RPPH1	-1.946808	RNA5SP295	-1.837402
RNU1-18P	-2.294431	VTRNA2-1	-2.127092	SNORA67	-1.944677	RNU6-981P	-1.83449
RNU6ATAC23P	-2.283364	SNORD123	-2.122878	SNORA17	-1.944532	LOC100133050	-1.834378
LOC101926975	-2.282944	RNU6-1270P	-2.113297	SNORD11	-1.944171	RNA5SP484	-1.832296
RNA5SP99	-2.275895	RNU4-80P	-2.100296	SNORD45C	-1.94385	RN7SKP37	-1.831333
SCARNA9L	-2.269301	RNU6-1010P	-2.098603	RNA5SP195	-1.938964	RNU1-56P	-1.827755
RNU6-1071P	-2.265162	SNORD12	-2.096778	RNU6-317P	-1.935518	RNU1-63P	-1.825954
MIR934	-2.26459	SNORD57	-2.096214	MIR4740	-1.934637	RNA5SP282	-1.820687
SNORA36C	-2.260952	SNORA24	-2.085881	AC004070.1	-1.934028	RNA5SP388	-1.819342
RNU4ATAC15P	-2.256292	SNORD38A	-2.081733	SNORA5C	-1.933919	RP1-32B1.4	-1.811797
RNU6-1080P	-2.255347	HERC2	-2.079987	MT-TW	-1.929517	RNU6-732P	-1.808263
RNU6-1230P	-2.252197	SNORD14A	-2.075876	SNORD58A	-1.927008	MT-TP	-1.80595
SNORA41	-2.249595	RNA5SP85	-2.075766	SNORD45B	-1.923262	SCARNA18	-1.805803
RNU6-893P	-2.244721	RNU5E-9P	-2.072398	KRTAP6-2	-1.92287	RNA5SP119	-1.803166
DKC1	-2.24359	RNU6-933P	-2.066228	SCARNA20	-1.922358	RNA5SP363	-1.802836
RNU5A-8P	-2.241657	RNU1-62P	-2.064661	SNORD119	-1.92191	RNU6-959P	-1.801375
SNORD14B	-2.23937	RNU6-1227P	-2.057292	RNU6-544P	-1.918849	RNA5SP441	-1.800967
RNU6-760P	-2.239142	FCGR1C	-2.033002	RNA5SP188	-1.91703	LINC00616	-1.800464
RNU6-223P	-2.23589	SCARNA22	-2.031877	MIR1321	-1.913079	SNORD1B	-1.800157
SNORA32	-2.231905	RNA5SP88	-2.021019	SNORA4	-1.912519	SNORD36C	-1.798092
RNU1-122P	-2.217655	LOC439994	-2.018923	HIST1H3H	-1.912025	RP11-363G2.4	-1.796242
SNORD116-21	-2.208704	RNU6-1181P	-2.018403	SNORD91B	-1.909351	HIST1H4D	-1.795959
RNU6ATAC28P	-2.208457	RNU6-1293P	-2.011114	RNU4-26P	-1.906635	RNU6-613P	-1.794056
MIR2861	-2.200948	RNA5SP405	-2.00633	SNORD35A	-1.905245	RNA5SP54	-1.794046
SNORA9	-2.197746	RNA5SP264	-2.006043	RNA5SP46	-1.905056	RP11-146D12.2	-1.794024
RNU6-906P	-2.197278	RNA5SP51	-2.004032	RNU6-1031P	-1.904337	RNU6-684P	-1.790579
MIR3975	-2.195479	RNU6-200P	-2.003848	RNU6-178P	-1.902775	SNORD115-45	-1.790301
SNORD115-44	-2.190598	RNA5SP428	-2.000271	RNA5SP403	-1.8989	RNA5SP262	-1.785159
RNU6-1286P	-2.188832	RNU6-59P	-1.999345	RNU1-16P	-1.896598	RNA5SP156	-1.782644
SNORA65	-2.180797	SNORD102	-1.998049	SNORA36A	-1.895575	SNORD70	-1.78187
MXD1	-2.180071	SNORA74B	-1.996461	RP11-232D9.2	-1.884806	RNU6-1058P	-1.781547
RNU6-930P	-2.175602	RNU6-1289P	-1.979633	RNU6ATAC25P	-1.883359	RNU4-61P	-1.781177
RNU1-40P	-2.170926	SNORA5A	-1.976612	SNORD4A	-1.88227	RNU6-1122P	-1.778243
SCARNA2	-2.168486	SCARNA21	-1.975441	LOC101928102	-1.880779	LINC01154	-1.777961
SNORD21	-2.167341	RNU6-213P	-1.975388	SNORA80A	-1.875736	SNORD80	-1.764386

Gene Symbol	Expression	Gene Symbol	Expression	Gene Symbol	Expression	Gene Symbol	Expression
SNORD111	-2.161571	SNORD83B	-1.971923	RNA5SP86	-1.87495	SNORA51	-1.762644
RNU1-86P	-2.159854	SNORA14A	-1.970671	SNORA47	-1.874449	LPA	-1.760009
SNORD67	-2.153906	SNORD11B	-1.970083	RNA5SP419	-1.873979	TRAJ23	-1.759962
RNVU1-3	-2.152492	RNU6-876P	-1.969062	MIR520C	-1.873021	RNU6-524P	-1.759008
RNU4-7P	-2.152265	MIR1185-1	-1.968936	RNU6-179P	-1.870824	RP11-436M15.3	-1.757691
RNU6-266P	-2.150576	RNU6-65P	-1.967313	RNU6-219P	-1.86278	SCARNA23	-1.753972
RNU6-878P	-2.150275	SNORA2A	-1.962677	RNA5SP183	-1.860075	RNU1-44P	-1.751182
SNORA25	-2.148306	SNORD38B	-1.961139	SNORD115-25	-1.860027	RP11-384C4.2	-1.751052
SNORD59A	-2.146387	SNORD6	-1.956828	SNORD116-29	-1.85904	RNU6-986P	-1.749525
RNU6-1288P	-2.142437	TERC	-1.956213	SNORD74	-1.852386	RNU1-7P	-1.749484
RNA5SP129	-2.141479	RNU6-444P	-1.95587	RNA5SP471	-1.852178	RNU4ATAC	-1.74758
RNU4ATAC12P	-2.135352	SNORA12	-1.95074	SNORA71C	-1.851086	RNU6-650P	-1.747298
AC008694.3	-2.132194	RNU6-646P	-1.949713	RNA5SP172	-1.850653	RNU6-952P	-1.746967
SNORA10	-2.128812	RNU6ATAC3P	-1.947002	RNU1-74P	-1.84285	SPANXC	-1.745337
MIR4668	-1.745319	MIR4287	-1.654832	SNORD124	-1.592247	RPS4Y2	-1.537847
RNU6-1105P	-1.73486	SNORD71	-1.65438	RNU6-645P	-1.590186	RNU6-249P	-1.537681
RNU6-28P	-1.732488	RNU6-428P	-1.653494	RNU6-669P	-1.58926	SNHG8	-1.536176
MIR520B	-1.728716	TM4SF1	-1.651839	MIR4420	-1.589146	SNORA18	-1.535553
RNA5SP300	-1.728043	RNA5SP215	-1.647872	SNORD35B	-1.589123	RNU7-133P	-1.534627
RNU6-899P	-1.727855	RN7SKP123	-1.647067	RN7SKP1	-1.588341	TCEB3CL2	-1.534605
RNU6-1127P	-1.727765	RNU6-295P	-1.645547	RN7SKP118	-1.587931	MIR548AD	-1.5322
CTD-2340D6.2	-1.727161	DRD4	-1.645524	SNORD32A	-1.586824	RNU6-1123P	-1.531933
LINC00343	-1.725998	OR6P1	-1.644748	MIR4694	-1.583608	SNORD8	-1.52932
RP11-261C10.1	-1.724787	SNORD116-20	-1.642067	TRBV4-2	-1.583042	AP000459.7	-1.527184
HMGA1P4	-1.72122	AC073094.4	-1.640226	IGKJ5	-1.578056	MTRNR2L4	-1.526437
MIRLET7A2	-1.718426	RNU6-497P	-1.637396	LOC101059948	-1.576825	ATHL1	-1.526266
RP11-719N22.1	-1.718273	SNORD88A	-1.634531	RNU6-722P	-1.57456	KRTAP5-9	-1.525133
RNU6-632P	-1.715534	SNORD88C	-1.633195	PRAMEF11	-1.573027	RNA5SP380	-1.524708
MIR514B	-1.714329	SNORD116-30	-1.629164	MND1	-1.569824	RNU12	-1.523706
CACNA1C-AS2	-1.712641	SNORD2	-1.62846	RNU6-415P	-1.568759	RP11-61A14.1	-1.52339
RN7SKP203	-1.707453	MIR519A1	-1.627665	RNU6-754P	-1.566849	SNORD116-23	-1.522815
SNORD26	-1.70678	RNU6-176P	-1.627187	SNORD115-27	-1.566111	HMGCS1	-1.521286
FGF5	-1.704957	RN7SKP230	-1.627104	SNORD116-14	-1.565756	SNHG19	-1.520681
RNU6-753P	-1.703753	RNU6-425P	-1.62341	RNA5SP298	-1.564891	RNA5SP459	-1.520107
RNA5SP19	-1.701584	RN7SKP168	-1.622885	SNORD59B	-1.563351	OR4N5	-1.518233
SNORA23	-1.700459	RNU6-1335P	-1.622372	CASC9	-1.562576	RNA5SP425	-1.515777
RNU6-321P	-1.69983	SNORA22	-1.621854	MIR519A2	-1.561094	SNORD53	-1.515103
FUNDC2P2	-1.699225	TPT1	-1.62056	RN7SKP74	-1.560575	AC092675.4	-1.513919
RNU6ATAC9P	-1.696918	RN7SKP66	-1.620093	KB-1615E4.3	-1.560134	MIR29B1	-1.513545
SNORD126	-1.692831	RNU6-1153P	-1.618289	SNORD97	-1.55619	LINC00395	-1.511028
LOC284632	-1.691533	RNU6-1214P	-1.613901	RNA5SP26	-1.556121	A2MP1	-1.509316
RNU6-936P	-1.691205	LOC101929721	-1.613342	RNU1-148P	-1.555953	RP1-202O8.2	-1.508923

Gene Symbol	Expression	Gene Symbol	Expression	Gene Symbol	Expression	Gene Symbol	Expression
RNU6-216P	-1.690771	SNORD116-27	-1.613098	SEC1P	-1.554985	SNORD27	-1.50708
LOC101929179	-1.68864	RNU6-1232P	-1.612848	SNORD50A	-1.554408	RNU1-36P	-1.506556
SNORA53	-1.6871	RNU6-340P	-1.612387	SCARNA14	-1.55319	AA06	-1.505592
RNU6-926P	-1.685638	RP11-400D2.3	-1.611611	LOC101928203	-1.552899	IGLJ4	-1.5049
LOC101929492	-1.684451	RNU6-135P	-1.610827	RNU1-100P	-1.550997	RNA5SP285	-1.502506
SNORD68	-1.68393	PRSS50	-1.610729	FAM90A12P	-1.550666	LOC100133286	-1.501725
RNU6-195P	-1.681934	SNORA71A	-1.60881	OR10H2	-1.549861	COL5A1-AS1	-1.4986
SNORD95	-1.67863	RNU6-477P	-1.607807	RNA5SP276	-1.547186	MIR3916	-1.495291
RNU6-1282P	-1.676166	RN7SKP245	-1.60578	C10orf71-AS1	-1.547131	EPPIN-WFDC6	-1.495039
RNU6-111P	-1.675299	RNVU1-19	-1.602899	RNU6-458P	-1.546883	RNU1-77P	-1.493345
RN7SKP80	-1.674602	RNU7-181P	-1.602739	RNU1-109P	-1.546822	RNU6-858P	-1.492999
ZNF733P	-1.672065	MSTO1	-1.602459	MIR3117	-1.546277	MIR548W	-1.490472
SPANXA1 // SPANXA2	-1.671696	DPRXP4	-1.601893	ARHGAP33	-1.545908	GNB2L1 // SNORD95	-1.487764
RP11-328J2.1	-1.669505	TRIM43 // TRIM43B	-1.600946	RNA5SP353	-1.545449	LOC101928253	-1.487428
HNRNPA3P5	-1.662484	SNORA68	-1.59891	SNORD15B	-1.54448	SNORD105	-1.486637
RNU6-1333P	-1.662442	SNORA76A	-1.597909	YME1L1	-1.544049	ENGASE	-1.48542
RNU6-1160P	-1.65924	SNORA49	-1.595771	IGHD3-9	-1.543253	RNU6-299P	-1.485356
RNU6-725P	-1.656535	RP11-998D10.7	-1.595044	MIR1197	-1.5432	MRGPRX4	-1.48435
RNU6-843P	-1.656393	OR51A4	-1.594664	SNORA84	-1.540273	RNU6-723P	-1.478688
TRAV8-3	-1.656263	SNORD66	-1.594602	SNORD1C	-1.53994	RNU6-712P	-1.47829
AC005077.5	-1.655751	IGHJ3	-1.592493	RNU6-1326P	-1.53889	MIR1914	-1.475534
RP11-401I19.1	-1.47521	RNU6-329P	-1.431078	RNA5-8SP4	-1.380494	RNU6-1324P	-1.334093
MIR4529	-1.474743	POM121L4P	-1.430959	AC093843.1	-1.380175	CTC-428G20.2	-1.334067
SNORD22	-1.474049	AKR7L	-1.429592	SNORD31	-1.379451	RBMY2FP	-1.333618
SNORD61	-1.471012	RNU6-826P	-1.429271	MIR4645	-1.378656	MIR133A1	-1.333184
RNU6-96P	-1.468525	SNORD63	-1.42806	ESRRAP2	-1.376453	RNU6-161P	-1.332612
RNU6-1186P	-1.467922	RNA5SP290	-1.427372	SNORD54	-1.375895	MIR3201	-1.332206
RNU6-485P	-1.46765	RNU6-68P	-1.42712	MIR4279	-1.375515	LOC100129055	-1.33146
RNU6-1272P	-1.467366	MIR4299	-1.424395	AC004878.8	-1.375161	RNU6-1126P	-1.330656
RNA5SP47	-1.465606	RNU1-103P	-1.421953	MT1F	-1.374429	RNA5SP379	-1.328957
RP11-703H8.9	-1.465239	RNU6-47P	-1.420429	RNA5SP426	-1.374323	TRAJ18	-1.327793
LOC93432	-1.465209	RP11-561I11.3	-1.417018	WI2-2373I1.2	-1.370813	LOC101929225	-1.327724
RNU6-455P	-1.464774	RP11-333A23.3	-1.416171	LINC00158	-1.368543	RNU1-33P	-1.326639
RNU6-1215P	-1.462559	LINC00888	-1.41608	SNORD34	-1.368048	RP11-326C3.7	-1.325996
MIR3200	-1.461004	RNU6-517P	-1.415486	LOC100507651	-1.365742	MAGEA1	-1.325816
LOC100506125	-1.460868	RP11-14I17.2	-1.414677	SNORD47	-1.362661	RN7SKP133	-1.323791
CSHL1	-1.458248	MIRLET7A1	-1.41413	C19orf83	-1.362362	RP11-439C8.2	-1.321852
RN7SKP220	-1.45798	LRRC7	-1.414008	RNU6-460P	-1.360477	RNU5A-1	-1.321769
MIR4717	-1.456827	VAMP8	-1.413533	PI4KA	-1.359996	TRAV6	-1.319776
KRTAP21-3	-1.456229	OR9A2	-1.413156	MIR329-1	-1.358774	KRTAP19-6	-1.318753

Gene Symbol	Expression	Gene Symbol	Expression	Gene Symbol	Expression	Gene Symbol	Expression
SNORA69	-1.454423	Z82214.3	-1.412988	SCARNA12	-1.357094	THBS3	-1.318707
RNU6-1340P	-1.45395	RNU6-136P	-1.411316	RNU6-736P	-1.356191	RP11-253D19.2	-1.318407
TRAJ14	-1.453895	TRDJ4	-1.410778	SCARNA27	-1.35494	ALS2CL	-1.318334
RNU6-614P	-1.45243	RP13-279N23.2	-1.410335	RNA5SP516	-1.354004	LOC100507445	-1.318316
CORO6	-1.451607	RNU6-643P	-1.408437	RNU1-130P	-1.353902	RNU6-437P	-1.317509
MIR128-2	-1.44911	RP11-367F23.1	-1.407998	LOC441455	-1.3532	SNORD69	-1.31708
RNU6-1143P	-1.448997	MIR4757	-1.40714	RNU6-661P	-1.352811	CBLC	-1.316854
RNU6-670P	-1.448645	SNORD110	-1.40713	CHEK2P2	-1.352797	RPL13A	-1.315551
RP11-356K23.2	-1.448326	RP11-619L12.3	-1.406746	SNORD55	-1.352323	RNA5SP55	-1.315505
RP11-69I8.2	-1.448006	RNU2-24P	-1.405985	AMY2A	-1.351214	RP11-619J20.1	-1.314092
SNORA64	-1.447738	RNU6-484P	-1.405973	C20orf203	-1.350766	RN7SKP293	-1.313893
RNA5SP200	-1.447314	SNORA44	-1.40295	RP4-735C1.6	-1.349779	AC093159.1	-1.312434
RP11-100G15.10	-1.446525	MIR4478	-1.402398	RNU6-1085P	-1.349151	RNA5SP359	-1.311811
LOC101929149	-1.445873	RRP7B	-1.401665	RP11-218D6.4	-1.349141	LOC344967	-1.311756
RP11-335O13.8	-1.445769	ZBTB40-IT1	-1.401596	RNU6-916P	-1.348675	RP11-466A19.8	-1.308936
RNU6-365P	-1.443276	RNU6-901P	-1.401508	TRAJ46	-1.348152	C1QL2	-1.308886
RNU6-1128P	-1.442919	SNORA8	-1.4001	OR1D5	-1.346529	RN7SKP231	-1.30791
RP11-444P10.1	-1.442754	CKM	-1.398651	AC114814.3	-1.346362	LA16c-4G1.3	-1.307112
SNORD30	-1.442403	PPBPP2	-1.398276	RP11-7I15.4	-1.345577	CTC-295J13.3	-1.306068
CASP1	-1.442132	RP11-12D16.2	-1.396312	LOC401134	-1.344997	SNORD42A	-1.305418
RNU6-571P	-1.440864	PIK3C2G	-1.395981	RTP1	-1.344744	RP11-62L18.3	-1.305166
RNU6-306P	-1.439333	NDUFA1	-1.395013	IGLL3P	-1.344316	SNORD44	-1.30501
CD274	-1.439302	RP11-501O2.3	-1.392181	MIR197	-1.343828	HMGN2P15	-1.304584
LOC100506272	-1.438994	STX1B	-1.391365	RNY3P8	-1.343128	RNU6-533P	-1.304116
RNU6-857P	-1.43899	CBLN4	-1.390128	SEPW1	-1.34295	RP11-716O23.2	-1.303917
RNU5B-3P	-1.437911	RNU6-1296P	-1.384184	GDPD3	-1.340943	SNORD50B	-1.302566
OSBPL7	-1.436151	SP7	-1.383531	RNU6-644P	-1.340828	RN7SKP98	-1.302232
RP11-465M18.1	-1.435179	SNORD65	-1.382744	SNORD51	-1.339474	SPANXN5	-1.301583
RNA5SP286	-1.43366	RNU6-240P	-1.382318	SNORA16A	-1.33886	SNHG10	-1.29838
RN7SKP255	-1.43365	LOC101927993	-1.380501	TERF2IP	-1.334384	RP11-561O23.7	-1.298298
AC106900.6	-1.297135	MIR4472-1	-1.271227	RNY3P4	-1.234365	LOC100505824	-1.210942
BMP3	-1.296117	MIR4676	-1.269133	RNU6-1180P	-1.233931	RP11-2C15.1	-1.210685
MIRLET7E	-1.295968	RP11-492A10.1	-1.267418	RNU4-24P	-1.23385	RPS6KA6	-1.210586
SNORD45A	-1.295218	ID3	-1.266948	RP11-110L15.2	-1.233579	SNORA80B	-1.209547
RNU6-598P	-1.295017	FAM163B	-1.265288	CHRM2	-1.233242	PER1	-1.208964
PPP2R2B	-1.293935	LOC401357	-1.264948	LOC102725382	-1.232345	RNU1-104P	-1.208062
HTR3E	-1.293915	PLCL2-AS1	-1.263744	AL157359.4	-1.230374	MIR499B	-1.207932

Gene Symbol	Expression	Gene Symbol	Expression	Gene Symbol	Expression	Gene Symbol	Expression
AC013448.2	-1.293654	SNORD116-26	-1.262974	LINC00682	-1.229954	RP11-1042B17.5	-1.207854
RNU6ATAC8P	-1.293571	MYL3	-1.262332	HFE2	-1.229625	LOC102724418	-1.207806
MIR1265	-1.291301	AOX2P	-1.261853	UBL4B	-1.229178	NBPF20	-1.206808
RNA5SP33	-1.290832	LINC00441	-1.260864	OR4M1	-1.229066	RNU6-1220P	-1.206066
TRBV3-1	-1.289278	RNU1-75P	-1.260809	AJ006995.3	-1.228893	RP11-202I11.2	-1.205612
RNU6-406P	-1.289262	RNU6-832P	-1.25974	LOC101928476	-1.228421	SNORA79	-1.20547
RNA5SP29	-1.286918	MSMO1	-1.258392	RP11-103H7.3	-1.228289	RNA5SP167	-1.205404
LOC101929448	-1.286815	RNA5SP375	-1.257556	LOC101930276	-1.228257	RNU6-382P	-1.204281
LOC101929486	-1.285612	RNU6-1140P	-1.256793	RP11-445P17.3	-1.228117	RNA5SP153	-1.203897
ZNF438	-1.285139	RNU6-235P	-1.256619	RNU1-96P	-1.227936	RBMY2EP	-1.20359
RP11-723G8.2	-1.283441	RNA5SP78	-1.256052	RPS2 // SNORA64	-1.226817	PGM5-AS1	-1.203579
CTC-558O19.1	-1.282695	LOC101928101	-1.255685	SUPT20HL2	-1.226521	RNU6-1234P	-1.203416
RNU6-435P	-1.282475	GUCY2C	-1.255471	MIR4480	-1.226263	RN7SKP188	-1.20338
RP11-798K23.4	-1.281704	RNU6-672P	-1.254991	SNORA55	-1.225207	RNU6-337P	-1.202742
RNU6-642P	-1.281183	LOC102725139	-1.252396	RNA5SP291	-1.223385	MIR4679-2	-1.202472
SNORD116-24	-1.28063	RN7SKP193	-1.251286	LOC100287846	-1.22318	RNU6-71P	-1.200311
RNA5SP323	-1.280051	RNA5SP214	-1.251056	AF178030.2	-1.22277	IGHA2	-1.200167
RP11-703I16.1	-1.279417	RNU6-61P	-1.248965	RN7SKP169	-1.22253	SELE	-1.199972
RP11-88H10.2	-1.278755	GDF2	-1.248716	PLAC9	-1.222171	HBB	-1.199624
MMP24-AS1	-1.278642	MTRNR2L10	-1.24649	RNU6-1222P	-1.22208	MIR4500	-1.19941
RNU1-69P	-1.278415	CENPH	-1.246371	RP11-706F1.2	-1.222076	WASH3P	-1.199046
ANP32C	-1.278181	RNU6-1022P	-1.2462	RP11-723D22.3	-1.222019	TUBA3C	-1.197992
RP11-391J2.3	-1.277996	TTTY11	-1.245406	MKRN7P	-1.221678	RNA5SP122	-1.196966
SYT14L	-1.277865	SNORD82	-1.245222	RN7SKP106	-1.221658	RP11-166N6.2	-1.195786
MIR885	-1.277051	KRTAP19-4	-1.244665	PRSS41	-1.221296	MIR548Z	-1.194331
RP6-102O10.1	-1.276989	RNU6-741P	-1.244382	RP11-363D14.1	-1.221007	RNA5SP448	-1.194189
RN7SKP178	-1.276982	RNU6-1088P	-1.244216	LHX5	-1.219926	MIR887	-1.193932
LOC101927533	-1.276946	RP11-638I2.4	-1.243709	RNU1-131P	-1.21846	RNU6-316P	-1.193751
RNU6ATAC21P	-1.276206	MIR526A1	-1.24369	MTRNR2L9	-1.218043	HIST1H3C	-1.192874
SNORD3D	-1.276009	RN7SKP213	-1.243467	MIR4518	-1.217331	SNORA70	-1.192744
KRTAP4-2	-1.275503	LINC00701	-1.243217	AC012314.20	-1.216367	RP11-85M11.2	-1.192159
MIR1266	-1.274446	CXXC4	-1.243035	GIMAP4	-1.216168	RP11-51B23.3	-1.19206
TRAJ48	-1.274408	LOC101928948	-1.241147	RNU6-1258P	-1.216159	RNU5F-8P	-1.191792
MIR4797	-1.274054	IGLV@	-1.241075	RNA5SP118	-1.215788	FEM1AP1	-1.191664
RNA5SP93	-1.273464	FDCSP	-1.239359	ESPN	-1.215297	MIR4530	-1.190321
LINC00243	-1.27321	MIR1283-2	-1.239161	RNU6-104P	-1.214788	LOC101927853	-1.189856
LOC101927693	-1.272781	LOC100506236	-1.237688	GFRA4	-1.214442	RP11-740P5.3	-1.189432
RNA5SP160	-1.27248	RNA5SP89	-1.236488	CDRT15L2	-1.2144	HIST1H2AK	-1.189285
LOC101927990	-1.272079	PIN4P1	-1.236102	RNU6-1016P	-1.214233	RNU6-1314P	-1.188835

Gene Symbol	Expression	Gene Symbol	Expression	Gene Symbol	Expression	Gene Symbol	Expression
LOC101928051	-1.271989	RNA5SP186	-1.23596	PIDD1	-1.213823	SCX	-1.188338
RP11-654G14.1	-1.271885	RNA5SP294	-1.23506	MIR4300	-1.211957	RNU6-332P	-1.18641
RNU6-141P	-1.271668	RNA5SP398	-1.234423	MIR3119-1	-1.211423	RNU6-948P	-1.186265
RP11-332M4.1	-1.186107	IGLV2-23	-1.167066	SNORD4B	-1.146938	OTOL1	-1.131127
RP11-1E4.1	-1.186068	RP11-310I24.1	-1.166903	SHD	-1.146882	H2BFXP	-1.130985
LOC101929014	-1.186052	LOC102723840	-1.166727	MIR1208	-1.146828	LOC100132831	-1.130522
RNU6-818P	-1.185757	HIST1H2BM	-1.166232	LOC102724732	-1.146812	RNU6-1087P	-1.130156
DMD-AS3	-1.185358	RP1-150O5.3	-1.166044	RNPEP	-1.146717	RNU6-1074P	-1.130064
PROSP	-1.184346	RNA5SP191	-1.1659	RNU6-429P	-1.146005	RNU6-689P	-1.129854
GCG	-1.183988	HCCAT5	-1.165658	HIST1H2BB	-1.145627	RP11-167N4.2	-1.129547
FLJ25694	-1.183915	SNORD76	-1.16552	MAGEC2	-1.145615	RNU5E-10P	-1.129135
RP1-155D22.1	-1.183828	SNORD12B	-1.165335	RP11-410L14.2	-1.144323	SNORD125	-1.129085
MIR4781	-1.183142	FCRL6	-1.164588	LRRC38	-1.143992	AKR7A2	-1.128941
RN7SKP247	-1.18302	OR52N2	-1.164295	AC004014.3	-1.143632	RP11-103H7.1	-1.128294
RNA5SP349	-1.182423	RNU6-635P	-1.164096	RP11-749H17.1	-1.143362	AC003985.1	-1.128216
RBM15	-1.181975	MIR3151	-1.163746	LOC284014	-1.142433	DDX12P	-1.128158
LOC101928769	-1.18157	TRGJP2	-1.163278	LOC102724657	-1.142224	SPANXN3	-1.127808
RN7SKP189	-1.180633	CCDC162P	-1.163086	RP11-733C7.1	-1.14215	RN7SKP111	-1.1278
RP11-103C3.1	-1.18022	CD1E	-1.162538	RNA5SP372	-1.142043	FAM72D	-1.127391
MKRN2OS	-1.18011	RP11-335E6.2	-1.162163	RP11-1006G14.2	-1.141971	RNA5SP267	-1.127352
MKRN3	-1.179627	CTD-2227I18.1	-1.161979	NDUFB7	-1.141343	FEV	-1.127208
RNU6-556P	-1.178933	RP11-831H9.3	-1.161749	OVOS2 // LOC100509445	-1.141047	RN7SKP112	-1.126749
LOC102723583	-1.178472	KRTAP1-5	-1.161666	CWH43	-1.139545	RN7SKP137	-1.126413
FAM72C	-1.177497	SGCZ	-1.160946	LOC101928912	-1.13921	TEX13A	-1.126357
RP11-495P10.1	-1.177215	SNHG7	-1.160826	RP11-475J5.6	-1.13914	MIR4658	-1.126135
LINC00703	-1.177033	AKT3-IT1	-1.160785	RP5-1050E16.2	-1.139097	RNA5SP161	-1.126073
CYP4F30P	-1.176756	NEFM	-1.160494	RP11-553K8.5	-1.13893	LINC00323	-1.126028
ACSM2A	-1.176318	MYH7	-1.160304	MIR920	-1.138649	RP11-541F9.2	-1.125956
LOC100293704	-1.176245	RNA5SP321	-1.159803	RNU2-57P	-1.138343	SMPD4P1	-1.125277
LOC100507468	-1.175755	RNU6-1229P	-1.158456	MIR3938	-1.138051	GRIP2	-1.124587
RNU6-1264P	-1.175563	LOC101928138	-1.158345	IFITM4P	-1.137995	RP1-65P5.5	-1.124552
ZNF99	-1.175443	RP11-382F24.2	-1.158178	ZKSCAN7	-1.137598	VAT1L	-1.124463
TRAJ28	-1.175228	RNU6-290P	-1.157609	RNU6-326P	-1.137366	TCEAL2	-1.123187
SNORA34	-1.17507	LOC101929355	-1.156903	MIR4266	-1.136507	SNORD116-15	-1.1224
RNU7-105P	-1.174662	RNU1-76P	-1.156519	RNU6-775P	-1.136332	FAS-AS1	-1.122333
HOXC12	-1.174532	RP1-27K12.4	-1.155096	SLC25A24P1	-1.135643	PRAMEF2	-1.121103
RNA5SP127	-1.173281	SNORD56	-1.155081	CEACAM6	-1.135529	LOC100653061	-1.120833
AL133249.1	-1.173252	DKKL1	-1.155011	HORMAD1	-1.134761	RNU6-949P	-1.120708
HMGN3	-1.173061	RNU6ATAC14P	-1.154721	RNU6-1172P	-1.134595	LOC101928733	-1.120607

Gene Symbol	Expression	Gene Symbol	Expression	Gene Symbol	Expression	Gene Symbol	Expression
LOC101929248	-1.172654	RNA5SP62	-1.154299	RNU4-52P	-1.134268	TPSD1	-1.120404
TRAJ9	-1.172292	FDFT1	-1.153848	RNU1-49P	-1.134013	SNORA19	-1.120378
MIR551B	-1.172278	NEU2	-1.152528	RP11-1149O23.2	-1.133761	RP11-417L19.2	-1.120099
RP4-781K5.6	-1.172173	MNS1	-1.151992	RNU6-1267P	-1.133724	ZIC4-AS1	-1.119747
SLC25A3P1	-1.171981	RP11-323I15.5	-1.151817	XAGE-4	-1.133136	MTRNR2L8	-1.118575
LINC00399	-1.171476	RP11-46F15.2	-1.151035	OR5F1	-1.133113	AC005324.6	-1.118474
RP11-756P10.4	-1.171047	RNVU1-14	-1.150844	UBQLN3	-1.133111	RP11-123O22.1	-1.118045
H1FNT	-1.170616	RNU6-454P	-1.150367	TMEM121	-1.133003	RP3-425P12.1	-1.117977
HSP90AA4P	-1.170335	OR1D2	-1.149612	SNORA13	-1.132908	RP11-348J24.1	-1.117412
RP11-875H7.1	-1.169394	MIR1260A	-1.14888	COL4A1	-1.132688	RMRPP5	-1.117245
RNU6-1191P	-1.167925	SNORD46	-1.14795	RP11-386G21.1	-1.132637	OR13C2	-1.116836
RNA5SP400	-1.167152	LINC00877	-1.147269	RNU6-1315P	-1.131829	AC079630.2	-1.116282
TUNAR	-1.16713	SNORD36B	-1.147068	RNU6-819P	-1.131727	RP11-269C4.2	-1.115279
LOC729815	-1.11494	RP11-493L12.5	-1.100847	MIR1537	-1.087574	MIR518D	-1.072417
RNU6-1063P	-1.114849	RNU6-633P	-1.100539	LINC01419	-1.087495	RNU6-968P	-1.072408
LOC101927687	-1.114673	RCN3	-1.100386	RNU6-717P	-1.087383	DNAJC22	-1.072158
RNA5SP42	-1.114594	NEUROD1	-1.100081	RP11-115J16.3	-1.087353	GYS2	-1.071988
HBCBP	-1.11459	LOC101928076	-1.099562	RNVU1-17	-1.087045	RNU6-1036P	-1.071714
RNU6-1303P	-1.112328	RP11-80H5.2	-1.099193	WHAMMP3	-1.086941	LOC100130548	-1.070743
AC011196.3	-1.112159	RNU6-557P	-1.099094	RNU6-208P	-1.086583	OR5AN1	-1.070714
AC010891.2	-1.112038	LOC100132529	-1.098933	LOC102724890	-1.086336	RP11-566H8.3	-1.070697
MIR612	-1.111929	CRABP2	-1.098378	LOC102724532	-1.086055	FBLL1	-1.070499
NPFFR1	-1.111516	OR5AC2	-1.098059	OR51B4	-1.085896	LINC01059	-1.070426
MT-TH	-1.111122	NDUFB8	-1.097977	C7orf62	-1.085825	LOC102724598	-1.070283
FREM3	-1.110613	PRM2	-1.09771	LINC00865	-1.085797	RNA5SP209	-1.070251
MST1	-1.110455	LA16c-2F2.8	-1.09747	LOC641515	-1.085591	UGT2B28	-1.070175
RNU6-1207P	-1.110223	RNA5SP394	-1.097264	AC004543.2	-1.085458	RP11-236P24.3	-1.069978
MC3R	-1.109816	HERC2P8	-1.096733	LINC01370	-1.085234	MIR4692	-1.069504
RNU6-920P	-1.10978	RP11-348J12.2	-1.096678	RNU6-1110P	-1.084857	CNTROB	-1.069484
SNORD1A	-1.109652	IGLV1-44	-1.096635	RNU6-1141P	-1.084415	RN7SKP149	-1.068874
LINC01255	-1.109412	RNU6-987P	-1.096034	HIST1H2AJ	-1.084288	RP11-231L11.1	-1.068848
LCE1F	-1.109255	TP53I3	-1.095708	RP4-806M20.5	-1.083402	RP11-897M7.1	-1.068569
LOC100129518	-1.109196	MIR708	-1.095684	RP11-108K3.3	-1.083074	RP11-674C21.9	-1.068039
RP11-434C1.2	-1.108615	LINC00028	-1.095645	RN7SKP55	-1.083016	RP4-800F24.1	-1.068016
KRTAP1-3	-1.108168	OR6T1	-1.095551	TRAV34	-1.082532	FDPS	-1.067929
MIR921	-1.107899	RP11-5N11.7	-1.09418	RNA5SP250	-1.082229	MYH6	-1.067564
RNU6-823P	-1.107697	RP11-486O13.2	-1.093819	RP11-100F15.2	-1.081315	PSG11	-1.067463
RN7SKP260	-1.10768	RNA5SP77	-1.093422	RNA5SP184	-1.081253	RNU6-554P	-1.067318
RIMS3	-1.107532	RP11-114N19.3	-1.092679	LOC102577424	-1.080775	RNU6ATAC26P	-1.067256

Gene Symbol	Expression	Gene Symbol	Expression	Gene Symbol	Expression	Gene Symbol	Expression
RNA5SP422	-1.107366	CXCL11	-1.09176	RNU6-339P	-1.080709	COL18A1	-1.067181
SULT1B1	-1.107189	SETP22	-1.091758	RNU6-994P	-1.079645	CTC-260E6.6	-1.067176
MIR181A1	-1.106694	ALG9-IT1	-1.09139	RNU6-401P	-1.079633	RP11-640N20.6	-1.067154
MIR130B	-1.106652	RNU6-303P	-1.091154	RNU6-815P	-1.079153	AC012501.2	-1.067139
LINC00524	-1.10642	LOC101927827	-1.091151	RNA5SP117	-1.078091	CEBPA-AS1	-1.066669
FGFR3	-1.106196	NFE4	-1.090716	RPL23 // SNORA21	-1.077639	KRTAP19-2	-1.066636
RNY4P18	-1.105338	NEAT1 // MIR612	-1.09056	MIR4305	-1.077519	MIR676	-1.066623
LINCR-0003	-1.105282	LOC100128563	-1.090076	RNA5SP94	-1.077391	OR11H12	-1.066211
LOC728763	-1.105109	RP11-793B23.1	-1.090054	CTC-359M8.1	-1.077101	AC093627.7	-1.066067
SNORD121A	-1.104963	COX17	-1.089722	LOC102724719	-1.076915	ARGFX	-1.065702
TUBGCP6	-1.104891	RP1-86D1.4	-1.08969	LOC100287072	-1.076915	RNA5SP249	-1.065422
GSDMB	-1.104826	RP11-646J21.2	-1.089506	RNU6-107P	-1.076887	LOC100996255	-1.065418
LOC729739	-1.104826	KRT8P41	-1.089176	MIR4421	-1.076336	TTC23	-1.065333
TRAV39	-1.104685	LOC101927856	-1.088972	LINC00385	-1.075356	RNU6-1320P	-1.065236
OR5H2	-1.104651	LINC01339	-1.088888	KRT18P11	-1.074856	RP11-223C24.2	-1.064995
CST2	-1.104429	RP11-297B17.3	-1.088808	RNU6-252P	-1.074378	MAGIX	-1.064843
RP11-97N5.2	-1.104111	RP4-765H13.1	-1.088528	RP11-4O3.2	-1.074305	MIR649	-1.064615
AC007680.2	-1.103215	RP11-962G15.1	-1.08834	MIR520D	-1.074113	OR5D18	-1.064362
LOC102723415	-1.102375	LOC102724571	-1.087918	RNU2-17P	-1.073937	RP11-356O9.2	-1.06431
UBXN7-AS1	-1.101759	OR10A2	-1.087752	FRMD5	-1.07371	KBTBD11-OT1	-1.06423
LOC100288152	-1.101574	REV3L-IT1	-1.087702	C10orf95	-1.072973	RP11-281A20.2	-1.063663
ADIRF	-1.101065	RNU6-577P	-1.087682	RNU6-887P	-1.072662	OR5AP2	-1.063521
CTAGE1	-1.10101	RABGGTB	-1.087615	RNA5SP178	-1.072483	RP11-46A10.2	-1.063303
LOC101929565	-1.063225	AC006373.1	-1.047684	RNA5SP98	-1.035288	RP11-27P7.1	-1.026798
OR3A3	-1.062448	UBE2Q2P1	-1.046871	CTD-2555I5.1	-1.035209	AC104076.3	-1.026249
SERPINA2	-1.061063	LOC101927621	-1.046821	PARP2	-1.035142	TPTE2	-1.025894
RP11-507B12.2	-1.060164	RP5-945I17.2	-1.04661	TOP3B	-1.03429	CTD-3105H18.7	-1.02575
XKR7	-1.059884	NSG1	-1.04656	LOC102723648	-1.034275	RNU6-414P	-1.025447
AL022344.5	-1.059842	RN7SKP244	-1.046539	RNA5SP435	-1.034025	SNORD42B	-1.02531
RNU6-777P	-1.059795	RP11-346J10.1	-1.045466	TRIM53AP	-1.033556	GS1-39E22.2	-1.025266
HES4	-1.059733	C11orf31	-1.045122	SPRR1B	-1.033425	ZDHHC8P1	-1.024843
TRDJ1	-1.059629	RNA5SP345	-1.044796	PTGIR	-1.033372	SNORD85	-1.024813
MIR517A	-1.059132	MEF2C	-1.044767	LOC339468	-1.032655	RNU1-140P	-1.02474
LINC01214	-1.059095	OR52M1	-1.044448	CPA2	-1.032221	RP11-38M15.11	-1.02462
LOC100507221	-1.058661	PRDM9	-1.043914	C3AR1	-1.032219	SNORD33	-1.02462
LINC01029	-1.058543	RNA5SP22	-1.04386	RN7SKP32	-1.032111	LOC401010	-1.024059
TMEM174	-1.058503	PIANP	-1.043601	SNHG6 // SNORD87	-1.0321	ACER1	-1.024032

Gene Symbol	Expression	Gene Symbol	Expression	Gene Symbol	Expression	Gene Symbol	Expression
EN1	-1.058173	RP11-1258F18.1	-1.043033	RP11-69C17.3	-1.031988	FAM230C	-1.023179
C10orf40	-1.058135	RNU6-561P	-1.042997	SLC4A1	-1.031795	LOC101928093	-1.022905
SNORD115-3	-1.057863	NDUFA13	-1.042985	RP11-488L18.8	-1.031354	EMCN-IT1	-1.022894
KIAA1751	-1.057646	RNA5SP444	-1.042955	RNA5SP174	-1.031338	RP11-4C20.3	-1.022686
RNU6-972P	-1.057544	RNU6-682P	-1.042631	RP11-519G16.5	-1.031301	NAMA	-1.022298
PMCHL1	-1.057096	PDC	-1.042504	AC018717.1	-1.031196	GS1-18A18.2	-1.021646
RNU6-456P	-1.057044	LOC101059949	-1.042024	RP11-665J16.1	-1.030928	LILRB4	-1.021543
RP11-91I20.3	-1.056398	RP11-655M14.12	-1.041709	PRSS35	-1.030894	LOC100131047	-1.021496
CYB5R2	-1.056351	RP11-603J24.14	-1.041558	RP11-966I7.3	-1.030056	LOC102724965	-1.021202
LOC101927347	-1.055578	RNU6ATAC42P	-1.041366	LOC101927577	-1.029664	RP11-360L9.7	-1.021118
UBTFL1	-1.05526	RN7SKP222	-1.040728	OVOS2	-1.029631	KIF19	-1.020944
RP11-388G22.1	-1.05523	ECRP	-1.04065	MPEG1	-1.029628	SPAG8	-1.020942
RP11-758I14.3	-1.054949	RNU6ATAC22P	-1.040526	C15orf56	-1.029125	GABBR1	-1.020809
RNA5SP225	-1.05482	AC019186.1	-1.040389	C9orf170	-1.029102	LOC101928306	-1.02051
ANKRD22	-1.054537	KRT17P2	-1.040019	IFI6	-1.029023	FAM180B	-1.020278
RNU6-929P	-1.054397	RNU6-767P	-1.039945	PNRC2	-1.028612	RNY4P19	-1.019487
OR10G8	-1.054378	ARF5	-1.039936	ARL9	-1.028444	RP11-386M24.3	-1.019358
RP11-278H7.4	-1.05433	RP11-203F8.1	-1.03977	RP11-296L22.8	-1.028401	RP11-536G4.1	-1.019301
CTD-2562J17.9	-1.053351	RP11-557C18.3	-1.039588	ANKRD20A3	-1.028398	RNU6-482P	-1.01884
AC018866.1	-1.052936	RP11-166N17.3	-1.039397	LINC00693	-1.028288	F11-AS1	-1.018728
AP000442.4	-1.052348	RP11-848D3.5	-1.039364	SPACA7	-1.028056	RNU4-41P	-1.018632
TRIM36-IT1	-1.052185	RP3-443C4.2	-1.038663	SNCB	-1.027949	AC104623.2	-1.018505
PI4KAP2	-1.052114	RNU6-283P	-1.038602	MIR3657	-1.02789	RP11-739N10.1	-1.018485
OR4N3P	-1.051549	RNA5SP496	-1.038537	SNAR-G1	-1.027792	GFI1	-1.018413
LOC645355	-1.050599	RP11-38H17.1	-1.038371	RN7SKP43	-1.027679	RNU7-185P	-1.018258
SRGAP2-AS1	-1.050465	IFNA13	-1.03828	SNORD114-28	-1.02749	CXCL3	-1.01806
RP13-1039J1.3	-1.050298	MYOM1	-1.037585	MVD	-1.027436	MAPK8IP3	-1.017427
RNU6-654P	-1.050237	FIGNL2	-1.037367	CTD-2353F22.1	-1.027405	LOC100505502	-1.017385
RNU6-696P	-1.049884	RP11-85O21.4	-1.037221	FGD5	-1.027388	LOC101928739	-1.017382
LOC102724306	-1.049805	KAT2A	-1.03711	AC096732.2	-1.027297	RP11-242P2.2	-1.017372
TRAJ5	-1.049762	RNU1-105P	-1.037106	LOC101929469	-1.027285	LOC101929167	-1.017026
RNU6-1057P	-1.049065	RNU6-237P	-1.036794	MIR3188	-1.027155	RNU6-520P	-1.016427
CD177P1	-1.0486	AC018685.2	-1.036385	RP3-471C18.2	-1.027138	ZPBP2	-1.016347
CECR9	-1.048271	ZFYVE28	-1.036233	RN7SKP128	-1.026918	AOX3P	-1.016281
RN7SKP180	-1.047968	RNU6-1271P	-1.036112	AC012442.6	-1.026802	RP11-395B7.2	-1.016147
RP11-424I19.1	-1.016123	HERC2P5	-1.005152	AC013402.5	-1.010149	CELF5	-1.001704

Gene Symbol	Expression	Gene Symbol	Expression	Gene Symbol	Expression	Gene Symbol	Expression
PAN2	-1.015336	LOC102724264	-1.004996	RP11-66A2.1	-1.009919	AL162151.4	-1.001533
CTD-2331D11.2	-1.015125	CYP2A6	-1.004496	RNU6-1078P	-1.00969	CYP2D8P	-1.001392
RPSAP9	-1.014841	RP11-616L12.1	-1.004378	MFI2-AS1	-1.009543	ABHD17AP3	-1.001229
MSH5	-1.014826	PROL1	-1.00431	RP11-124N3.3	-1.009244	RNU6-1161P	-1.001144
STAP1	-1.014797	RP11-26L20.3	-1.00425	RP11-626H12.1	-1.008894	ZNF295-AS1	-1.000719
AC006026.13	-1.014654	KRTAP19-3	-1.004213	LOC102724601	-1.007756	RN7SKP39	-1.000528
HMX3	-1.014539	IVL	-1.004172	RNU4ATAC5P	-1.00758	MIR302E	-1.000511
OR1L4	-1.014504	RNU1-61P	-1.00411	ZNF366	-1.007047	SCN3A	-1.000505
OR3A1	-1.014279	RP11-624D11.2	-1.00398	RNU6-1279P	-1.006964	RP11-586K2.1	-1.000445
RP11-654A16.3	-1.014133	LOC101928150	-1.003845	EEF1DP3	-1.006285	RNU6-171P	-1.000433
MIR4788	-1.013985	RNU6-491P	-1.003433	CD99	-1.006233	MIR4718	-1.011135
GSTA3	-1.013298	RP11-27G13.1	-1.002895	RP11-627D16.1	-1.005839	RNU2-45P	-1.01109
AC004009.3	-1.013221	FAM182B	-1.002735	TRAJ43	-1.005798	RP11-807H7.2	-1.010672
GTF2IRD1P1	-1.013049	RNU6-856P	-1.002672	RNU2-25P	-1.005775	C1orf68	-1.010568
LINC00624	-1.012981	MIR659	-1.0026	LOC100129722	-1.005705	CTD-2113L7.1	-1.010558
LOC100506929	-1.012945	RNU6-931P	-1.002547	MIR129-2	-1.005626	RP11-758M4.4	-1.010327
RP11-10B2.1	-1.012914	RNU6-177P	-1.002358	MIR4760	-1.005454	RLN2	-1.010259
MIR4764	-1.012856	RPL7A	-1.002318	OR2T4	-1.012336	RNA5SP27	-1.011801
NOSTRIN	-1.012415	RNU1-20P	-1.001843	RN7SKP64	-1.011893	RP11-353P15.1	-1.01156

Table 7.9: List of genes that 1 fold up regulated in K1E7 cells following Metformin treatments (0.3 mM) for 6 days.

Gene Symbol	Expression	Gene Symbol	Expression	Gene Symbol	Expression	Gene Symbol	Expression
PPP1R10	18.396358	RP11-745L13.2	3.583871	EFNB2	2.700318	DENND5B	2.306622
IPW	18.180253	ZBTB20	3.553499	MMP1	2.699085	MIR616	2.29945
HCG8	13.96817	LOC100287934	3.497951	IL33	2.677546	AGFG2	2.298074
IER3	10.379987	LOC100287497	3.454405	RHOQ	2.643028	TNFRSF10D	2.297076
FLJ22447	8.675055	NT5E	3.449514	DNAJC6	2.634513	RP11-314N13.3	2.288203
C6orf47	8.49042	CLDN16	3.432416	VEZF1	2.621706	RNU6ATAC18P	2.280939
PPT2-EGFL8	8.417027	TSC22D2	3.419841	MIR31HG	2.611304	SLC35B3	2.280711
MTRF1L	7.367797	F8A1	3.344814	ZFP36L2	2.603079	bP-21201H5.1	2.28063
LOC100132167	7.181866	TRIM25	3.327166	LOC100288637	2.585811	UBL3	2.278935
LINC01000	6.776727	PLCG2	3.292972	TIGD2	2.5711	RNU2-34P	2.271111
MIR1236	6.620298	CDYL2	3.284184	RP4-791M13.3	2.561201	ITGB3	2.267268
TRIM27	6.498174	PCF11	3.221567	RP3-368A4.5	2.550582	MIR590	2.267204
LOC101927880	6.082773	HCG18	3.214265	EDNRA	2.545605	ST8SIA6	2.265311
MIR3671	5.918655	LOC728339	3.195197	SERPINE1	2.54529	ERRFI1	2.255162
PRKXP1	5.87266	MIR573	3.195186	RPL23AP53	2.536122	TOB1	2.250046
RP11-760D2.12	5.510526	TNKS	3.169761	CASC7	2.533043	TRAK2	2.245783
LINC00963	5.447429	DKK1	3.154172	CHAC1	2.532166	BMP2K	2.243308
RNF185	5.364801	PDCD6IP	3.11658	THBD	2.524459	SLC16A6P1	2.240645
LOC101929475	5.292922	EIF3J	3.106675	SLC7A5	2.517353	SKA3	2.238547
PARP4	5.132557	DLGAP1-AS2	3.097128	CLDN1	2.491395	LRRC37BP1	2.237285
LOC100506870	5.036196	VLDLR-AS1	3.078112	OSMR	2.478584	SIRPB1	2.23626
IL1B	5.019607	RNU7-14P	3.025246	MYPN	2.471146	FOSL1	2.230029
INTS6	5.013701	HNRNPA1L2	3.018409	FZD1	2.454462	IL11	2.227204
BRD2	4.959461	LOC100294341	3.009071	EIF5	2.448106	EGFR	2.220315
PSAT1	4.603824	ULBP1	3.007854	LINC00622	2.438816	CABLES1	2.219924
DUXAP10	4.565214	CSF3	2.973273	CLGN	2.436664	DOCK11	2.214385
MIR1184-1	4.477308	CYP24A1	2.962964	PSPC1	2.425345	ZNF836	2.213354
CD177P1	4.403834	MOB3A	2.923767	SLC1A5	2.419625	MIR4277	2.208876
PIK3CA	4.385445	TAS2R14	2.922926	TMSB4X	2.406367	ASS1	2.198921
PTPRJ	4.256055	CTH	2.905041	RP11-360F5.3	2.39891	SRGAP2C	2.198449
MAT2A	4.234648	LGR5	2.87056	PRKAA2	2.393396	MIR421	2.197534
AC003092.1	4.226591	LOC90784	2.859262	MIR4521	2.388046	SOCS6	2.192387
LINC01111	4.225352	KIR2DL5B	2.848919	NPAS2	2.376644	LOC283070	2.192075
MIR21	4.22201	AMIGO2	2.845933	SLC38A1	2.376627	SLC48A1	2.190653
HIF1A-AS2	3.994359	LINC01296	2.841038	GEN1	2.373196	DLGAP1-AS1	2.186441
VLDLR-AS1	3.921012	CDKN2AIPNL	2.812056	USP27X	2.364508	RP11-841O20.2	2.179833
C10orf12	3.896996	SLC6A9	2.812053	NLRP10	2.363244	ADAMTS5	2.177336
USP32	3.886046	PAQR5	2.805897	ZNF807	2.3632	LINC00973	2.176555
CD22	3.859482	AC104135.3	2.790624	RP11-274H2.3	2.362245	ZNF45	2.172775
ASNSP1	3.846234	PTGS2	2.789166	CDK13	2.351837	ZNF480	2.169903
KRCC1	3.82766	LOC400743	2.77726	ZNF554	2.351616	RP11-70J12.1	2.169523
NABP1	3.803141	SMAD2	2.766045	STC2	2.346575	PTPN13	2.163285

Gene Symbol	Expression	Gene Symbol	Expression	Gene Symbol	Expression	Gene Symbol	Expression
RP11-3L8.3	3.757711	LINC00641	2.744724	LOC101930106	2.333776	FKTN	2.161884
SLC7A11	3.726679	IL7R	2.742733	SHISA2	2.333452	DRAM1	2.161508
LINC01293	3.702518	SLC16A13	2.72888	FOS	2.330317	ZFX	2.160125
SERTAD4	3.696954	LOC100506178	2.724689	LOC101927841	2.322424	LINC-PINT	2.15821
LOC101930489	3.677426	LOC729987	2.717962	SLC30A1	2.321284	ZNF770	2.156218
SLC16A6	3.650859	GABRG1	2.715668	MOCS3	2.316791	ANKRD1	2.151857
NCOA5	3.631526	ECH1	2.714425	ZBTB38	2.314818	CTB-32H22.1	2.150359
RFX3	2.143829	IL1R1	2.042979	BCAT1	1.918492	TSPAN2	1.848103
NCOA7	2.141958	YAE1D1	2.041803	RNF185-AS1	1.916905	MYC	1.845482
SLC25A32	2.140819	SNX9	2.039378	DEPTOR	1.916657	AKIRIN2	1.845385
AJUBA	2.14075	LOC100996579	2.03929	FLJ42627	1.91595	LINC00328	1.83894
NR2F2	2.138533	LINC00969	2.036891	TET1	1.91316	DPY19L3	1.83668
RP11-265D17.2	2.133485	RP9P	2.035751	PDE1C	1.912923	GPR56	1.836429
NEO1	2.131532	DDX19B	2.034526	SMOC1	1.910278	ZCCHC8	1.836125
DGCR8	2.130928	VCAM1	2.032793	ZBED8	1.906282	SLFN5	1.834535
FZD2	2.130085	KRT80	2.02258	E2F8	1.904929	LMBRD2	1.833772
TNFAIP6	2.127778	POLI	2.017741	TFAP2C	1.903646	NID2	1.83201
ZNF566	2.127256	EIF5A2	2.017046	LRIF1	1.903429	RRN3	1.831454
DUSP1	2.124598	KDM7A	2.013799	GUF1	1.903137	VLDLR	1.831256
ZC3H12C	2.123501	GTF2A1	2.012097	DDX3X	1.902463	MAN1A2	1.831226
EMP1	2.123099	DAPK1	2.009512	SNHG1	1.901983	SBNO1	1.829316
FPR1	2.120273	SLC12A2	2.008491	GARS	1.901695	ASNS	1.828851
GREM1	2.119657	PANX1	2.004658	PROSER1	1.900411	PLAU	1.828087
SACS	2.118555	SLC6A15	1.999921	PTCH1	1.90025	RNU6-342P	1.824741
CHAC2	2.116019	ARHGAP35	1.997141	F3	1.897553	LATS1	1.824263
SNTB1	2.110157	KCNH1	1.996022	WARS	1.897509	PTGES	1.824161
CYP4V2	2.109592	VTRNA1-3	1.986014	ELTD1	1.894138	MIR3189	1.819376
UBASH3B	2.108435	UBE2J1	1.985595	ZYX	1.893617	PRICKLE1	1.81923
RAB27B	2.104826	TLE1	1.975845	UPF2	1.893116	HTRA1	1.81714
FAM168B	2.098751	SLC46A3	1.974903	DKFZP586I1420	1.891918	ZNF616	1.814841
AMD1	2.097939	LOC101928161	1.971175	PTGIS	1.889755	FOXN3-AS1	1.81464
SGPP2	2.096126	RNU6-737P	1.967519	SLC35B4	1.888547	PM20D2	1.813977
SEMA7A	2.095867	MURC	1.961502	AC002117.1	1.88551	PMS2CL	1.813099
MAP3K2	2.09431	HERC2P9	1.960307	BRCC3	1.883176	IL6	1.812095
RN7SKP103	2.092165	NEDD4	1.959699	ZNF451	1.882136	ANTXR2	1.81045
INA	2.091255	SOS2	1.954544	DNAJC16	1.879633	ZNF749	1.809319
LOC100129033	2.090994	TRIB1	1.953029	RNY1P5	1.878979	FAM169A	1.808473
ARL14EPL	2.089754	RWDD2A	1.947853	CSGALNACT2	1.878331	KLHL5	1.807048
DUSP4	2.08767	EPC2	1.943185	RP11-51L5.3	1.877737	CHST15	1.806131
IL6ST	2.085031	GLYR1	1.942764	LOC100288842	1.875847	MIR1305	1.805875
ALDH1L2	2.082424	SNURF	1.939961	USP34	1.87583	LINC00941	1.80328
DCLRE1A	2.074959	RNA5SP514	1.939677	TTC39C	1.873594	ZC3HAV1	1.801853
TPTEP1	2.073601	AF127936.7	1.939403	CREG1	1.872638	CUL3	1.801803
CD200	2.071668	SLC37A2	1.935587	TINAGL1	1.872494	SRSF8	1.801532

Gene Symbol	Expression	Gene Symbol	Expression	Gene Symbol	Expression	Gene Symbol	Expression
SCN9A	2.069506	SLC38A2	1.93174	PTPN21	1.867221	PTPLAD1	1.800976
SNAI2	2.067916	MXRA7	1.931705	CDR1	1.867099	TXNL4B	1.800952
SLC7A1	2.060234	ELK3	1.930185	SLC36A4	1.863081	ATE1	1.800444
RP11-760H22.2	2.059532	ZNF510	1.928199	RP11-350F4.2	1.860596	SEMA3C	1.800292
MOSPD1	2.057721	DHRS3	1.92713	MTM1	1.858839	IGIP	1.7982
EPHB2	2.05737	EFR3A	1.926876	BCL2	1.858283	TUBE1	1.798166
TTPAL	2.056755	PTER	1.925035	BRWD3	1.854428	FBXO28	1.797531
ZCCHC14	2.055231	PDE4DIP	1.922442	SH2D4A	1.853101	SIN3A	1.794683
CEACAMP7	2.05205	PHLPP2	1.921791	CDCP1	1.852996	GCSHP3	1.793769
KCNK3	2.047872	MIR622	1.920585	TIGIT	1.852878	CEP170P1	1.792686
RNU7-12P	2.046575	FOXE1	1.919704	ITGB8	1.849672	PSPH	1.792622
RAB23	2.043914	POLR3C	1.918577	ZNF114	1.84827	RP11-152P17.2	1.791818
CLOCK	1.78992	RCOR3	1.74372	LRRC58	1.701534	SFTA1P	1.6662
RNU6-552P	1.788636	HIPK2	1.739355	KCNQ1OT1	1.700439	GPR137B	1.666123
ASB7	1.788473	MIS12	1.739009	ABCC4	1.699939	EP300	1.66553
GAB1	1.786602	VEGFA	1.737879	AHR	1.699907	LOC644135	1.664838
RNU7-22P	1.786594	ESCO2	1.736728	SDCBP2-AS1	1.699864	PIGM	1.66414
MIR548H3	1.784082	TJP1	1.735386	PUS7	1.698751	SLC39A14	1.66384
MIR645	1.7837	NCOA1	1.735349	NCOA6	1.698281	KIAA1614-AS1	1.661423
RP11-531A24.5	1.782452	MIR550A2	1.734352	RAD51D	1.698	ZNFX1	1.660288
ZBTB2	1.78243	SLC35F6	1.734014	HNRNPA1P33	1.69766	TSEN2	1.659682
IL1A	1.782171	OSBPL6	1.732734	PA2G4P4	1.697442	CHAMP1	1.658388
ODC1	1.781665	TRIB3	1.732405	SLC25A33	1.696959	RP11-221N13.3	1.658131
CDC6	1.780991	LOC389906	1.731913	APPBP2	1.695547	FAM135A	1.657188
CEP19	1.779285	PCNXL4	1.73142	SOAT1	1.695361	DSC3	1.656548
NRP1	1.77921	SLC9A7P1	1.731332	LGR4	1.694303	POGLUT1	1.656156
LURAP1L	1.778317	PPT2	1.730819	PTX3	1.693039	TRIM61	1.655637
VPS4B	1.777982	INTS5	1.73061	SLC30A7	1.692324	SOS1	1.655123
IFNAR1	1.776111	UTP20	1.730265	MOCOS	1.691342	CLMP	1.654763
ZSCAN29	1.775774	KLHDC1	1.72936	LOC100507516	1.690573	DOCK9	1.654632
CREBBP	1.772983	ARHGAP29	1.728854	DOCK7	1.689326	ZCCHC2	1.654386
EGR1	1.770654	KIAA1549	1.727039	ITGA2	1.688345	ST6GALNAC3	1.653842
RNF2	1.770441	SNX18	1.726307	VDR	1.686183	UBLCP1	1.653543
ZNF382	1.770258	NDST1	1.726079	SLC7A2	1.684968	SGPP1	1.653503
RNF157	1.76798	OXTR	1.726	RMND1	1.684094	SLC1A1	1.653435
XPOT	1.767514	ARID2	1.725809	TNFRSF12A	1.683306	SPIN3	1.652619
BRCA2	1.767387	SDAD1	1.725691	H1F0	1.683254	ERCC6L2	1.650905
PARP8	1.765333	SLC35A4	1.724311	ZNF280C	1.682776	REPS1	1.650871
ZNF543	1.761874	AJAP1	1.724183	RNU6-795P	1.682551	NUAK1	1.650607
MGC27345	1.760415	RP11-290L1.3	1.723926	PLEKHA3	1.68216	DAZL	1.650314
CYP20A1	1.760145	ADAM12	1.719408	RNA5SP462	1.682087	KAT6B	1.648313
ZDHHC5	1.757528	DIS3L	1.718074	RC3H2	1.681834	RB1CC1	1.64733
TRIM24	1.757328	MMGT1	1.717454	MT-TL2	1.678737	HGSNAT	1.647241
JUN	1.75647	SLCO4A1	1.715966	OTUD4	1.678462	KCNMA1	1.646335

Gene Symbol	Expression	Gene Symbol	Expression	Gene Symbol	Expression	Gene Symbol	Expression
RPL23AP32	1.756319	TAF2	1.715794	FOXN2	1.678402	PLLP	1.645048
MIR1299	1.7563	ETV4	1.714928	ARHGEF28	1.677537	LOC645553	1.643692
RNU7-193P	1.756214	RRAGC	1.714511	RNU6-917P	1.677435	RP11-449J1.1	1.643619
COQ10A	1.75581	PDE12	1.713194	RP5-1087E8.3	1.677424	LA16c-60G3.8	1.643028
C18orf8	1.754843	PAPPA2	1.712624	USP7	1.676185	PMEPA1	1.642315
SGPL1	1.754667	RASGRF1	1.710491	METTL4	1.675794	ZDBF2	1.64205
B3GALTL	1.75428	ME1	1.709676	PTPRK	1.674733	USP6NL	1.642002
NBEAP1	1.752546	RMND5A	1.708225	DNAJC13	1.674005	DHRS13	1.64177
AGL	1.751588	C3	1.708101	SLC38A4	1.673228	ZWILCH	1.640371
SLC1A4	1.751068	RP11-389O22.1	1.707705	EOGT	1.672845	NCK2	1.640021
MEIS3P1	1.749582	APOLD1	1.707253	KLF5	1.669997	NEDD4L	1.639741
RALGPS2	1.748452	ZKSCAN2	1.704567	TMEM171	1.669907	WASF1	1.639088
ZNF280B	1.748173	CCDC68	1.70398	LINC00294	1.66893	SESN2	1.638715
ZBTB44	1.747966	MIR548V	1.7036	AP000695.6	1.66886	FBXL3	1.638045
N4BP2	1.747314	INTS7	1.702671	LOC101060691	1.667846	USP53	1.638026
CLSTN2	1.74692	ADM2	1.702531	LINS	1.667118	ARHGAP12	1.636429
LOC284926	1.74582	C1orf109	1.702395	TCP11L2	1.666627	MIR614	1.636091
SPEN	1.636081	FBXO32	1.601066	RNU7-50P	1.570298	ASAP2	1.544552
CPPED1	1.635599	KIF5B	1.600403	CYP4F26P	1.569256	FNTA	1.543467
RABEP1	1.634311	LAMB3	1.600055	JMY	1.568123	STAM	1.543034
SLC7A6	1.633565	RPP40	1.599206	SLC7A5P1	1.56807	TIAM1	1.542935
VAMP4	1.632099	C7orf31	1.598038	GOPC	1.567827	LMBR1	1.542913
AFF1	1.63109	SRGAP1	1.597572	SSH1	1.567811	DUSP6	1.542131
VGLL3	1.630561	TMX1	1.597531	OTUD1	1.567602	SLC16A3	1.541486
IFNE	1.629674	SLC30A6	1.596849	LOC101926917	1.564761	IRF2BP2	1.541025
ZNF37BP	1.629388	CDH4	1.596599	ORC5	1.564005	SIRPD	1.540921
RP11-11N9.4	1.628769	NFAT5	1.596037	DSC2	1.563897	RP11-473I1.9	1.540698
RP11-63P12.7	1.626747	SHC3	1.595951	EML4	1.563746	KIAA1644	1.539797
ANGPTL2	1.625912	RAPGEF3	1.595901	AP4E1	1.563739	BICC1	1.539705
LOC100506255	1.625411	AP5M1	1.595544	ASH1L	1.563651	RP11-692D12.1	1.539357
USP38	1.62488	ZNF786	1.595516	RIN2	1.562456	MIR3142	1.539357
STXBP5	1.623868	SIK2	1.594961	MMP24-AS1	1.561526	LINC00476	1.538922
USP24	1.623373	ZNF571	1.594173	SLC30A9	1.560926	NGF	1.538579
SPPL2A	1.622904	CAPN7	1.593797	DPP4	1.560828	SLC38A7	1.538341
RNU6-1065P	1.62259	LARP4	1.593684	RCHY1	1.560376	LOC101930415	1.537579
STAM2	1.621963	NOP2	1.593	C17orf80	1.559804	ZC3H11A	1.537399
ADAM1A	1.621258	DHRS7B	1.589735	FMNL2	1.558952	SIM2	1.537254
HELQ	1.62117	IRS2	1.589264	PAIP2	1.558525	TNRC6C	1.536722
RAI14	1.620979	HEATR1	1.58843	SFMBT1	1.558096	ANKRD28	1.536264
SMIM2-AS1	1.620877	NRIP1	1.587883	MIR1224	1.558043	ROCK2	1.535472
AC003092.2	1.619539	RPS6KA5	1.587711	ROR1	1.557849	SLITRK4	1.53484
BAZ1B	1.61838	RIOK1	1.5874	TOE1	1.557604	ACTR3BP2	1.534471
ZNF768	1.618169	GPATCH8	1.585807	PRR14L	1.556856	KIAA1033	1.533985

Gene Symbol	Expression	Gene Symbol	Expression	Gene Symbol	Expression	Gene Symbol	Expression
ABHD5	1.616489	LRRC15	1.584497	ERCC4	1.556852	ZNF557	1.533238
LOC101927287	1.616235	ZNF148	1.583097	RMI1	1.556851	CRTC3	1.532527
LINC01355	1.615884	RRP1B	1.581985	LITAF	1.556808	TMEM170B	1.531543
CLCN3	1.615855	ZDHHC21	1.581645	ZNF613	1.556659	ACSL1	1.53126
ANAPC1	1.615255	RN7SKP233	1.581046	ARHGAP21	1.555701	ZZZ3	1.53123
LIMS3-LOC440895	1.613074	GPR84	1.580709	CDK8	1.554758	ETHE1	1.531097
PBDC1	1.612459	WRN	1.580576	HIPK3	1.554418	PAK2	1.530761
IL24	1.612094	ZNF620	1.579919	BACH1-IT2	1.552076	SEPT7P2	1.530563
DCLK1	1.611458	CCNYL1	1.579247	DOLK	1.551975	ZNF284	1.529801
AGPAT9	1.610974	RBM26-AS1	1.57797	LEPREL1	1.551631	GFPT2	1.529722
LOC100130428	1.610967	ZFYVE9	1.577871	DDAH1	1.551444	TTPA	1.52919
PKN2	1.610821	LACC1	1.577764	DHX32	1.551334	GTF2IRD2B	1.528708
PWARSN	1.610572	CLEC2D	1.577601	DOCK5	1.551318	ZNF594	1.528352
SYDE2	1.610369	FAM89B	1.576516	NCOA3	1.551199	IFIT5	1.528192
FOXD1	1.610332	PXK	1.576018	RP11-21L19.1	1.551136	FTSJ1	1.527039
PKD2	1.609927	RP11-864G5.3	1.575954	RP5-864K19.4	1.551076	TPTE2P5	1.526762
C5orf22	1.609657	FTX	1.575772	SLC35A5	1.549874	TBCEL	1.526207
CHTF8	1.607349	PLAT	1.573257	FLJ31306	1.549423	SNX2	1.524556
GTF2H1	1.606428	MT1E	1.572997	LOC100128281	1.548419	ALKBH1	1.523901
ATF1	1.606089	RAB4A	1.572824	N4BP1	1.547936	LIFR	1.522688
CPT2	1.605741	BTBD7	1.572024	AKAP11	1.54672	RNY4P16	1.522136
FAM49A	1.605301	CCNJ	1.571715	C2orf42	1.546037	CHST11	1.520704
MBTPS2	1.601968	RP11-115J23.1	1.571193	PLAGL2	1.545879	GPATCH2L	1.517324
FAM208B	1.517152	JAM2	1.493546	C21orf91	1.467402	TAB3	1.439521
SRSF6	1.51683	FLJ38717	1.493111	TNFAIP2	1.463938	PPIP5K1	1.439348
LONRF3	1.516118	ENTPD7	1.492494	JAGN1	1.463534	EVI5	1.439308
ZBTB24	1.515437	SERPINB2	1.492354	STOX1	1.462698	ARL6	1.438975
RNU6-729P	1.51534	CTSO	1.491522	AC002480.4	1.462223	RBBP6	1.438948
MBLAC2	1.514796	SGOL1	1.491217	ZXDB	1.4618	SHMT2	1.437801
TRAPPC10	1.513891	RPF2	1.490045	ZNF614	1.461071	SLC31A1	1.436611
AGPAT5	1.513805	DCAF10	1.489306	OSBPL8	1.460799	LOC101929787	1.436437
TAS2R20	1.51367	ZNF189	1.489108	DSCC1	1.460642	KIAA0430	1.43625
AP000695.4	1.513253	SUCO	1.488958	CNIH3	1.460501	BRWD1	1.436022
MAFIP	1.51291	LBR	1.487698	ERN1	1.460311	C5orf30	1.436002
TMEM184C	1.512569	INHBB	1.487305	RP11-394J1.2	1.460249	RALGAPA2	1.435998
SCN8A	1.512562	TMEM104	1.487042	IL31RA	1.459969	MCTP1	1.435791
WAPAL	1.512239	CAMSAP2	1.486762	UBIAD1	1.458976	ZNF70	1.435748
RP11-337C18.8	1.5121	ATMIN	1.486534	UBE3A	1.458512	LOC101929705	1.435428
LOC645513	1.511724	ABHD3	1.486331	TP53BP2	1.457955	ZNF319	1.434824
NIPA1	1.51135	SNAP29	1.48632	UCN2	1.457804	SENP6	1.43459
MTMR9	1.511248	TGFBR2	1.486215	ANKH	1.457617	RP11-428P16.2	1.434176
PRKCI	1.510416	APBB1IP	1.486064	WIPF1	1.456883	SLC9A8	1.433236
UBXN2B	1.509993	LOC100129034	1.484602	ADCY9	1.456601	GPT2	1.432408
IL18	1.509688	LOC100131691	1.484523	INO80D	1.456383	EIF4G2	1.432407

Gene Symbol	Expression	Gene Symbol	Expression	Gene Symbol	Expression	Gene Symbol	Expression
TSTD2	1.509433	MRPL42	1.4832	TRAM1	1.455212	POLR1B	1.431811
CPEB4	1.509287	CIRH1A	1.483088	PPP2R3C	1.45486	TMEM216	1.431442
CDC14A	1.50894	TMEM127	1.483064	NEDD1	1.454665	ABLIM3	1.430771
RNU6-945P	1.508327	SRXN1	1.482562	EEFSEC	1.454555	BACE1-AS	1.429879
STAMBPL1	1.507999	SQSTM1	1.48098	FLG-AS1	1.454022	TMX3	1.429562
RN7SKP97	1.507858	ADAMTS12	1.480737	CTNS	1.453683	SCAF4	1.427791
C9orf41	1.507848	DGKE	1.479801	SLC27A4	1.453395	SMOX	1.427552
SMEK2	1.507516	FAM217B	1.477998	KIAA0513	1.452723	ENOX2	1.427221
RAB22A	1.507414	ACVR2A	1.477882	DNER	1.452283	RP11-283G6.3	1.426543
SLC38A9	1.50712	RAD50	1.477428	DCLRE1C	1.451439	CLCN5	1.426277
NPC1	1.506433	AKAP12	1.476506	ZNF658	1.450561	ZSWIM7	1.42614
E2F5	1.506412	LOC731157	1.476149	ERCC6	1.449839	RP11-432J22.2	1.426051
IFNA5	1.505934	USP1	1.475617	TMEM170A	1.447485	MYO9A	1.42569
ESCO1	1.505563	SF3B4	1.474387	MKKS	1.447453	AC073046.25	1.425458
ATP13A3	1.504597	HSCB	1.473746	UBAP1	1.446822	BCOR	1.42543
LINC00997	1.504594	LOC100132705	1.473384	ASUN	1.446407	HAUS6	1.425339
MIR4706	1.503593	AGGF1	1.473243	LOC100506083	1.446051	KCNIP3	1.425308
LRRC8D	1.502046	AGO3	1.473011	ZNF268	1.445874	ZBTB40	1.424618
FTSJ2	1.498982	ELOVL4	1.47185	ZFHX3	1.445201	CTR9	1.424035
TIFA	1.498214	ALDH1B1	1.471296	GLIPR2	1.445102	ZMYM4	1.423858
HIST1H2AB	1.498048	DPP8	1.470887	ELF1	1.444913	NDUFC2-KCTD14	1.423383
USP10	1.49792	RP11-7F17.7	1.470376	DCBLD2	1.444389	CEP120	1.422738
C1QTNF1	1.497697	FBXL4	1.470242	RP11-154D6.1	1.443486	RNU6-623P	1.421597
SRSF1	1.496238	C3orf35	1.469421	ITPR2	1.442371	KIAA1804	1.421583
G0S2	1.495243	CD3EAP	1.46873	WDR66	1.441458	SMG1	1.420775
GPR65	1.495142	ANKS6	1.46872	TIMM22	1.441366	TCAIM	1.420272
BDKRB2	1.4942	TMEM192	1.468279	RIPK1	1.440426	SLIT2	1.419477
PKI55	1.493913	RP11-253E3.3	1.467753	SLC16A1-AS1	1.4398	CDA	1.419115
Z83851.4	1.418785	TSPAN14	1.397822	TANC2	1.377635	CPTP	1.35766
EFTUD1	1.418691	PAX8	1.39734	MDC1-AS1	1.377512	TNPO1	1.35742
CUL5	1.417213	DCP1A	1.397011	EPHB1	1.376693	CCDC138	1.357252
CAB39	1.417188	TULP4	1.396604	SESN3	1.376296	HOMER1	1.356849
EVA1A	1.417142	IARS	1.395456	RNU4-9P	1.376138	FAM86DP	1.356761
KCNIP1	1.416818	MTMR10	1.39508	SCARA3	1.37603	PSMD5	1.356013
SLC15A4	1.416405	STC1	1.394048	CBL	1.375654	RFX8	1.355878
MKL2	1.415597	LCMT2	1.393982	FNIP1	1.375525	SPAST	1.355427
KIRREL	1.415589	CNOT1	1.393839	EPS15L1	1.375502	PREX1	1.355376
TUBD1	1.415307	MED1	1.393589	GAS6-AS2	1.375053	EML5	1.355225
ANPEP	1.414548	MTF1	1.393486	RNU7-96P	1.374904	RNY4P17	1.354979
USP32P2	1.412629	RNU6-302P	1.39337	GULP1	1.373886	SH3BP4	1.354902
SLC9A6	1.412229	USP12	1.393049	OPN3	1.373862	CLN8	1.35482
ZNF652	1.411916	LOC100289650	1.392468	HELZ	1.373503	DNAJC10	1.354256
RSPRY1	1.411847	ENTPD5	1.390745	ZNF644	1.373026	CDC42BPA	1.354214

Gene Symbol	Expression	Gene Symbol	Expression	Gene Symbol	Expression	Gene Symbol	Expression
ABTB2	1.411704	ABHD6	1.390414	PEA15	1.372827	DMXL1	1.354016
TRAM2	1.411283	OCLN	1.390171	NARS2	1.372602	AARS	1.35386
RAB6A	1.410723	ADAL	1.389439	CTD-2555O16.2	1.372595	AMTN	1.353526
IFIT1	1.41058	ERGIC1	1.389249	NEXN	1.372481	RP11-344N10.5	1.353261
ASXL2	1.410483	SLC2A1	1.389242	IFT88	1.37248	QRSL1	1.35304
KIAA0196	1.410328	TARS	1.388617	SUPT20H	1.371767	RSC1A1	1.352768
RNF144B	1.410226	RP4-816N1.7	1.387688	NQO1	1.37156	CNST	1.352705
COG2	1.410165	PRKG2	1.386621	LOC100507530	1.37091	CDK19	1.352417
MORC3	1.410057	HERPUD2	1.385828	SRR	1.370899	LINC00337	1.352363
MAFG-AS1	1.409312	PHF3	1.385753	SMIM13	1.370502	NHEJ1	1.352306
FAM208A	1.408428	MCIDAS	1.385696	RP6-206I17.1	1.369637	ANKRD40	1.35228
TROVE2	1.40791	KLF10	1.385686	CINP	1.369414	RPS6KB1	1.351969
LYSMD3	1.407643	MRPL45	1.385385	MOB1B	1.368512	MYCBP2	1.351784
CITED2	1.407412	ZBED4	1.384752	TEX2	1.368378	LOC102723919	1.351293
IGKV1-17	1.407109	COMMD2	1.384052	PEX12	1.367892	OGFRL1	1.350403
LOC389831	1.406581	ALG2	1.383817	KDSR	1.367024	TTC30A	1.350185
TBX20	1.406547	LAMC2	1.383816	TXLNG	1.366143	TRNT1	1.349976
ZMYND11	1.406281	PALB2	1.3832	SLC35E1	1.366058	ATP2B1	1.349907
MCM8	1.405027	TOR1B	1.382883	GDA	1.366039	UBE4B	1.349833
ZFR	1.40438	TMEM43	1.382754	GPAM	1.365405	MTDH	1.349667
TBL1XR1	1.404047	RALGAPA1	1.382259	PIGW	1.365229	NANS	1.349066
HKDC1	1.403702	RFXAP	1.381933	RN7SKP88	1.364836	UTP15	1.348905
APBB2	1.403631	MYO5A	1.381926	ELK4	1.364247	TMEM185B	1.348299
OR2A1-AS1	1.402576	CPN2	1.381566	RPRD2	1.364145	RAD17	1.348068
SLK	1.401072	RAB3B	1.381192	MAP3K15	1.363872	EDA2R	1.34788
FASTKD3	1.401027	LOC101927326	1.380802	MIR4731	1.363169	KDM4D	1.347677
AFTPH	1.400808	ATP2C1	1.380672	ATG2B	1.362966	PPP2R3A	1.346784
LOC100134040	1.400583	MALT1	1.380635	HECTD2	1.362786	HEG1	1.346006
MGC70870	1.400437	FGF2	1.380116	ATP11C	1.361578	WAC-AS1	1.345376
C9orf64	1.400043	FITM2	1.379964	GSK3B	1.360975	MRFAP1L1	1.345103
HECTD1	1.399922	PHF23	1.379045	CPM	1.36067	MYO1B	1.343488
PAG1	1.39979	USP25	1.378394	CCNI	1.359333	CD44	1.342396
ZNF689	1.399228	TMEM194A	1.378307	SLCO3A1	1.358797	FAM126A	1.342287
CGRRF1	1.397822	AAED1	1.377967	GPS2	1.358376	MEX3C	1.341886
RP11-685N10.1	1.34174	RP11-513D5.2	1.323929	DNAJC1	1.304436	RP11-632F7.3	1.282305
CCDC6	1.341476	PLEKHG7	1.32384	S1PR1	1.304211	TENM3	1.282008
WASL	1.341432	KCTD9	1.323602	PRKAA1	1.304198	LOC729218	1.281832
ZSCAN30	1.341231	CHUK	1.323417	DNASE2	1.304134	MIR4798	1.281799
LINC01234	1.340526	RPL7AP28	1.323188	GOSR1	1.302506	USP8	1.281727
DEGS1	1.340292	RP13-143G15.4	1.321899	FOXF2	1.302422	LDOC1L	1.281366
RP11-513I15.6	1.33992	FAM89A	1.321229	NF1	1.302028	MIR4252	1.281248
ANKRD42	1.339382	CEP104	1.321101	MLXIP	1.299884	NEK7	1.28095

Gene Symbol	Expression	Gene Symbol	Expression	Gene Symbol	Expression	Gene Symbol	Expression
FOXC1	1.338869	CTD-2116N20.1	1.319868	NEGR1	1.299653	GPRC5C	1.280754
SPDL1	1.338263	CDC42EP2	1.319571	CNOT10	1.29961	GRB10	1.279955
YIPF4	1.33817	RNF6	1.319421	MAP1B	1.298814	LMLN	1.278812
GNPNAT1	1.3379	PTDSS1	1.318813	BMP2	1.29877	NT5C2	1.278628
TAPT1-AS1	1.337838	TST	1.318697	CA5B	1.298759	CCNT1	1.278534
FAM13B	1.337773	AASDHPPT	1.318649	POLR3B	1.297936	DFFA	1.27826
ACTBL2	1.337643	THRB	1.317908	MARS2	1.297518	SLC30A4	1.277958
NSAP11	1.337141	LIAS	1.317793	SLC35G2	1.297178	PTPN12	1.277798
RNU6-960P	1.336786	BRPF3	1.317766	FHOD3	1.295922	C6orf15	1.277282
SH3RF1	1.336614	HIPK1	1.31711	CCDC50	1.295272	AXL	1.27711
SETD7	1.336279	MED13	1.316936	SIRPA	1.29397	SLC35A3	1.276942
ABCE1	1.336252	ZNF592	1.31685	AP5B1	1.293766	RARG	1.276789
ARL13B	1.335781	PLCE1-AS1	1.316719	HNRNPA0	1.293626	SLC1A3	1.276714
GS1-259H13.2	1.334701	PCGF5	1.316559	CASD1	1.293487	DFNA5	1.276496
PIK3C2A	1.334699	USP42	1.31652	C5	1.293263	CLIP4	1.276099
GTF3C4	1.334464	MBNL2	1.31573	KAT2B	1.292993	LOC102724851	1.275713
PPARA	1.334194	TTC13	1.315128	LOC100507577	1.292849	EHBP1	1.275111
PHGDH	1.332714	C12orf49	1.314833	LOC100287072	1.29271	PAPD4	1.274444
NNT	1.332005	TBRG1	1.314255	SPATA2	1.292363	RNA5SP140	1.273958
MIR548H2	1.331638	ZNF41	1.313755	XPR1	1.291301	PRKD3	1.273607
LPXN	1.331593	ZNF2	1.312331	FAM118B	1.291298	LOC647859	1.273436
CCND1	1.331442	OSBPL11	1.312193	FAF2	1.291179	ARMCX2	1.272956
ATL3	1.331154	HRK	1.311553	PIKFYVE	1.291116	MIR181B2	1.272752
CTBP1-AS2	1.330835	RAD23A	1.311351	C4BPB	1.29109	VKORC1L1	1.272721
RPAP2	1.330816	CTD-2647L4.4	1.310436	ARRB2	1.288526	LOC399815	1.27123
RAB42	1.330498	TMEM179B	1.3104	C5orf51	1.287892	ARHGEF6	1.270944
CENPBD1	1.33032	ZRANB1	1.310215	CPSF2	1.287741	CSNK2A3	1.270937
C9orf85	1.330045	LINC01433	1.309855	NOP58	1.286867	AP000704.5	1.270723
IREB2	1.328996	GDAP2	1.30978	FASTKD2	1.286672	LINC01128	1.270707
AGTPBP1	1.328773	LOC100506498	1.309323	MTSS1L	1.286026	FAM86MP	1.27036
ZBTB25	1.328566	NIFK	1.309274	SH3PXD2B	1.285991	NUPL1	1.27013
ASF1A	1.328137	FBXO10	1.309248	C9orf91	1.285711	POLR1A	1.270009
TMEM57	1.328053	NSMAF	1.307543	PRICKLE2	1.284794	CDY2A	1.269933
PNPLA8	1.328029	ZNF287	1.30638	DOCK4	1.28444	R3HCC1L	1.269795
TMEM131	1.327636	LOC389602	1.306207	SLC25A13	1.283959	DBT	1.269508
CSRP2BP	1.32684	PORCN	1.305967	RNU6-1029P	1.283948	POP1	1.269235
RNU6-811P	1.324877	LDLRAD3	1.305433	TMEM38B	1.283293	BVES	1.269155
MYO6	1.324826	FAM122A	1.305241	NCR3LG1	1.282793	PNO1	1.269093
PLOD2	1.324691	HSDL1	1.304901	SHISA9	1.28279	SMCHD1	1.268471
MEPCE	1.324318	DUSP14	1.304681	UTP14A	1.282785	ZNHIT6	1.267512
PMAIP1	1.324242	FAM20C	1.304663	SPRTN	1.282696	PID1	1.267384
PDCD4	1.267007	MTFMT	1.252153	HEATR5A	1.237303	MTRR	1.222764
ITGA1	1.266801	ZHX2	1.251953	BCL2L13	1.236654	DDX21	1.222337

Gene Symbol	Expression	Gene Symbol	Expression	Gene Symbol	Expression	Gene Symbol	Expression
RAP1GDS1	1.266561	SLC39A6	1.251279	BCL10	1.236285	DCP1B	1.222283
LOC441461	1.266259	ST3GAL1	1.250956	MTHFD2	1.236262	FAM60A	1.221706
AGO4	1.266108	AC083899.3	1.250718	ASNSD1	1.236098	SLC26A2	1.221702
USP46	1.26549	NIPAL2	1.249977	PARD3	1.235664	ZNF507	1.221636
UBE2Q2	1.264791	RNU6-529P	1.249405	TSHZ3	1.235443	CSNK1G3	1.221174
DIP2A-IT1	1.264347	NSRP1	1.249174	UBE2Q1	1.235297	PITPNA	1.221104
TPT1-AS1	1.264112	WDR3	1.2491	MIR29C	1.234988	NOC3L	1.220807
EXOSC5	1.263763	PRUNE2	1.248993	MIR25	1.234177	FAM175B	1.220637
LINC00665	1.263449	ABHD17C	1.248225	RPL13P5	1.233943	ZNF250	1.22022
RN7SKP268	1.262646	RP13-631K18.5	1.247942	B4GALT1	1.233482	RAP2CP1	1.22014
CAND1	1.261895	FAM86C2P	1.247877	PRKACB	1.232335	MTSS1	1.219847
EBLN3	1.261489	LOC101927116	1.247255	NBEAP3	1.232326	DBNDD2	1.219742
KIAA2026	1.261036	ZBTB14	1.246778	LARP4B	1.232262	C19orf12	1.219582
WDR52	1.260824	AP1G1	1.246598	SLC3A2	1.232218	PAPOLA	1.219228
TXNRD1	1.260633	ARMC9	1.246482	XPO4	1.231575	IGLV1-40	1.218093
RNF180	1.260188	KANK2	1.246212	LOC101926941	1.231571	SPG20OS	1.217874
SH2B3	1.259427	FAM172A	1.246062	MSRB3	1.229298	TAS2R30	1.217598
C1orf43	1.258509	RAB29	1.246003	NBPF25P	1.229284	MIR619	1.217316
C10orf25	1.258493	S100PBP	1.245932	NRROS	1.229123	TMCC3	1.217264
FUS	1.258299	GPRC5A	1.245853	CDC42EP1	1.228986	SLC35F5	1.217257
TMEM156	1.258235	ZXDC	1.245675	PDGFA	1.228909	TRAPPC6B	1.216899
EYA4	1.258229	RNU6-918P	1.245514	ZMIZ1	1.228337	SNRNP27	1.216372
IDH3A	1.257843	ANAPC16	1.245506	RGL1	1.228333	TMEM251	1.216016
CYP2E1	1.257577	CHIC2	1.245393	AC005037.3	1.228261	USP28	1.215901
CCDC183-AS1	1.257362	MIR654	1.245265	ROCK1	1.227693	ABLIM1	1.215288
ARSG	1.257157	SEL1L3	1.244993	HIST1H3E	1.227191	RCN1 // DKFZp686K1684	1.215097
FCHO2	1.257116	MIR28	1.244726	KLF11	1.227113	JOSD1	1.214777
CASK	1.257036	SH3BP5	1.244549	ELOVL6	1.226487	ARID5B	1.214632
CLHC1	1.256684	SVILP1	1.243699	LOC100130876	1.226435	USP13	1.214518
DERL2	1.256662	C1orf233	1.243295	HSD17B1	1.226434	TBC1D9	1.214425
TOX2	1.256455	USO1	1.242737	QPRT	1.226337	DHRSX	1.214255
PNMA1	1.256104	CTC-378H22.2	1.242624	LOC101929099	1.225724	ZNF75A	1.214061
RP1-101K10.6	1.255986	RP11-3D4.2	1.242155	DNAJC15	1.225457	TNFRSF9	1.21388
DDX58	1.255924	MAGI2-AS3	1.242126	CRISPLD2	1.225358	INHBA	1.213716
GPR125	1.255797	FBN2	1.241543	SIGMAR1	1.224755	DAGLB	1.213689
GALK2	1.255154	DUSP5	1.240768	PSKH1	1.224735	RAPGEF1	1.213506
KLC1	1.255046	FADS1	1.239585	RPAP3	1.224445	ACVR1	1.213268
RP11-351I24.1	1.254619	PTPN14	1.239482	RHOF	1.224033	SLC41A2	1.212879
USP37	1.254497	NUFIP1	1.239115	ZBTB8A	1.223982	BTBD9	1.212075
MFSD12	1.254488	ATP11B	1.239058	AVL9	1.223962	LINC00869	1.211897
LRRC16A	1.254376	HTR1D	1.238856	UBTD2	1.223876	MIR513A1	1.211702
TMTC3	1.254323	THEM4	1.238752	HS2ST1	1.223783	NEK4	1.210802

Gene Symbol	Expression	Gene Symbol	Expression	Gene Symbol	Expression	Gene Symbol	Expression
PHF20L1	1.253891	40787	1.238633	GFRA1	1.223758	VANGL1	1.210203
SACM1L	1.25388	CYBRD1	1.238534	MIR3665	1.223498	ANKRD13C	1.210118
GNA11	1.253196	NCKAP1	1.237966	AC046143.3	1.223093	SUZ12	1.20985
LPHN1	1.252801	SUV420H1	1.237663	QTRTD1	1.223072	KIAA0895	1.209691
MID2	1.252505	RP11-196H14.3	1.237447	CASC10	1.222906	TMEM181	1.209391
RNU7-110P	1.209082	C9orf69	1.191625	LOC441155	1.177516	PPAPDC2	1.162867
UBE3B	1.208612	TMEM158	1.191173	ADRB2	1.177481	KYNU	1.162838
SMARCAD1	1.208563	PTPLB	1.191061	OXSR1	1.176901	RNU6-575P	1.162829
ABCC3	1.208132	C10orf88	1.19039	DOCK1	1.176159	COX11	1.162503
SLC25A46	1.207225	RRM2B	1.190326	SDE2	1.175604	ARHGAP5	1.162473
MBNL1	1.206768	TMEM65	1.189977	ABCF2	1.175166	ZNF252P	1.161729
WDR44	1.206263	NAIP	1.189938	COA5	1.175128	MET	1.160669
IGF2BP3	1.206069	CUL1	1.189618	CBX4	1.174959	CDC42EP3	1.159961
ANO6	1.20494	ZNF106	1.189083	PCNX	1.174474	MIR4267	1.159837
TCP11L1	1.204884	FZD7	1.188988	PCMTD2	1.174383	TRMT6	1.15969
GGCX	1.204642	LOC286437	1.188696	RPS6KA3	1.174154	ZNF691	1.159623
RBBP8	1.204619	AC068286.1	1.18866	MKX	1.173955	DNAJB6	1.159166
SLC25A24	1.204276	PPIF	1.188158	KDM6A	1.173641	NET1	1.158782
ZNF33B	1.204197	PLEKHM2	1.188137	CLPTM1	1.17348	DTX2	1.158476
IFNGR2	1.204166	LOC100130691	1.188121	RNASEH2B	1.173388	TSSK3	1.158318
PMS2	1.203154	ERBB2IP	1.188052	CRK	1.173317	MKNK2	1.157744
ZNF639	1.202794	ZFP91	1.187847	PPP6C	1.172981	ANGPTL4	1.157629
CARS	1.202684	SYT14	1.187793	RNU6-14P	1.172817	RP11-380G5.2	1.157627
WDR35	1.201383	MTHFD1	1.18765	UEVLD	1.17274	SNX16	1.157533
LOC283588	1.201145	IFT80	1.187563	DYM	1.172058	LIMA1	1.157411
PSMD11	1.200916	TRIM33	1.187343	FBXW11	1.171923	CENPN	1.157365
MID1IP1-AS1	1.200117	RNF13	1.187103	LRRC37A2	1.171518	GOLPH3	1.157338
SEPSECS	1.199973	GSPT1	1.186137	IFT22	1.17139	EMC3-AS1	1.157287
HN1	1.199955	EID2	1.186032	PDE7A	1.170772	BMPER	1.156802
PSME3	1.199867	AP000525.9	1.185137	SPG20	1.170411	40422	1.156366
PHF10	1.199867	GNG5	1.184033	HLTF	1.170099	LOC100506731	1.156114
ZBTB1	1.199388	ANKIB1	1.183669	TMEM51	1.169978	GAS5-AS1	1.155622
BNC1	1.19934	RNU6-433P	1.183633	AC099850.1	1.168921	WDR36	1.155442
DMWD	1.199128	NF2	1.182665	BMPR2	1.168816	ACOT9	1.155421
ABCA1	1.198888	HIST1H3G	1.181867	CTCF	1.168534	BACH2	1.154412
HARBI1	1.198329	UGGT2	1.181745	RICTOR	1.168482	TPCN1	1.15436
CGGBP1	1.198012	IMPAD1	1.181364	IQCK	1.167128	SLC43A3	1.153918
LL0XNC01-250H12.3	1.197312	AGFG1	1.180855	RNA5SP273	1.166593	URB2	1.153669
RNA5SP385	1.197249	SVIL	1.180845	TIA1	1.166474	DNAJA1	1.153498
GDF15	1.196983	RP11-111F5.3	1.180587	PPIAL4B	1.165843	BTF3L4	1.153433
ZBTB6	1.196409	FBXO30	1.180522	MIR570	1.165805	ANKRD29	1.153361
CYP2U1	1.196261	MEF2A	1.180388	RNA5SP518	1.165734	PTP4A1	1.153284

Gene Symbol	Expression	Gene Symbol	Expression	Gene Symbol	Expression	Gene Symbol	Expression
EIF1	1.196059	TRMT10B	1.180234	SPOPL	1.165389	RP11-534L6.5	1.153017
ZFAND4	1.195863	AMMECR1	1.180056	FAM129A	1.165364	CSTF1	1.152742
SKIL	1.194692	AKR1B1	1.17997	YTHDF3	1.165095	EIF4EBP1	1.152489
ZC3H8	1.194567	UPF3B	1.179664	UBXN2A	1.164813	KIF13A	1.152246
FER1L6	1.194371	MAP4K4	1.17963	ZNF146	1.164143	FBXO27	1.152027
PPAPDC1A	1.193984	MICALL1	1.179585	GNPDA1	1.164097	MPND	1.151698
SLC16A2	1.193177	TRIM8	1.179527	MED17	1.16408	STARD7-AS1	1.151366
ADARB1	1.193156	KRAS	1.179191	AC011431.1	1.164036	PGPEP1	1.15128
BNIP3L	1.193043	MIR181A2HG	1.17842	MAD2L1BP	1.163841	PTRH2	1.150957
ATP6V1C1	1.191967	BCAS2	1.178262	EPB41L5	1.163647	RNU6-773P	1.150469
ELP3	1.191934	RUNX2	1.177764	LINC00862	1.163275	ULBP3	1.150421
LIG4	1.191653	SWAP70	1.177602	SRP68	1.163083	SAAL1	1.150105
SPATS2L	1.150043	NME6	1.139001	EPS15	1.127541	RP11-167J8.3	1.115795
SIMC1	1.15001	EIF3A	1.138884	CRTAP	1.127383	UBR3	1.115533
UBN2	1.149361	GPR135	1.137787	KRT81	1.12729	CXCL8	1.115484
CLDN12	1.149292	NFKB1	1.137588	MKLN1-AS	1.127214	AC074183.4	1.115421
VWA8	1.14928	RPS15A	1.13749	GUCY1A2	1.127138	MIR635	1.115166
RNF111	1.148862	HS3ST3A1	1.137358	FAR1	1.126691	EXOC6B	1.115004
STK17A	1.148815	RP11-164P12.4	1.137196	MLLT10	1.126639	RSPH3	1.114905
RBMS2	1.148534	ZNF462	1.137151	EDEM3	1.126477	ST6GALNAC6	1.114749
CBS	1.148142	LINC00571	1.136974	HDAC3	1.126308	CTTNBP2NL	1.114207
ATP6V0A2	1.148034	ANXA3	1.136294	B4GALT5	1.125836	CYB5D2	1.113995
LOC646021	1.147895	RP11-274J7.2	1.136063	CD109	1.125768	VAPB	1.113919
PROSER2	1.147765	NAA50	1.135538	RP11-597A11.6	1.125601	CA2	1.113616
SCGB2B2	1.147726	CCDC97	1.135475	MAPKAP1	1.125463	PPM1D	1.113607
ATM	1.147129	FBXL20	1.135372	API5	1.125218	NCOA2	1.112979
AAK1	1.146837	HS3ST3B1	1.135113	NLK	1.124262	BAMBI	1.11279
GREB1L	1.146646	SECISBP2L	1.134974	SEMA3A	1.12405	YIF1B	1.112776
C6orf47-AS1	1.145754	GPR19	1.134513	PDZD8	1.123656	LOC101929709	1.112739
CASP2	1.145662	PRMT3	1.134328	MGAT2	1.123486	ALKBH8	1.112432
LIN54	1.145547	CLIC4	1.13422	RAB3GAP2	1.12347	SERPINE2	1.11233
DTX2P1-UPK3BP1-PMS2P11	1.145451	ARAP3	1.133921	PRPF38A	1.12331	PHTF2	1.112097
LINC01138	1.14535	C11orf54	1.133727	FAM111B	1.123259	MUL1	1.111976
ARHGEF2	1.144842	PSPN	1.133387	KLRAP1	1.123175	LOC101928829	1.111831
KLF6	1.144343	DLAT	1.133384	LOC648987	1.122836	CCDC92	1.111703
BCL7B	1.144297	UBQLN2	1.133272	RP1-239B22.5	1.122569	AATF	1.111575
KLHL42	1.144188	NFIB	1.133065	RNF138	1.12246	UCHL3	1.111541
WBP4	1.143998	RAB32	1.132704	MIR32	1.122211	PARD6B	1.111228
CROCCP3	1.14353	NAA35	1.132389	BTBD11	1.121493	TMEM133	1.111102
DDX60	1.143424	CCDC25	1.13234	PXDC1	1.121307	FANCF	1.111033
TAB2	1.142764	ABCA3	1.132339	SCRN3	1.120481	SPECC1L	1.110972
EPM2A	1.142717	NUDT4P1	1.13203	NFATC3	1.120435	TMEM209	1.110964

Gene Symbol	Expression	Gene Symbol	Expression	Gene Symbol	Expression	Gene Symbol	Expression
XYLT1	1.142325	LBX2-AS1	1.131711	PARP16	1.12043	LINC01123	1.110957
FJX1	1.142096	RN7SKP78	1.131569	DENND4A	1.120086	GNAO1	1.110914
APPL2	1.141867	GALNT3	1.130654	FZD6	1.119793	RP11-486O13.4	1.110518
DGCR14	1.141474	CDK6	1.130502	TTC7B	1.119772	RGMB	1.110488
TCF20	1.141228	TET3	1.130275	BAG2	1.119551	ZNF774	1.109881
AC092835.2	1.141221	HPS5	1.129808	SIK3	1.119452	CCSER2	1.109473
TNPO3	1.141127	RN7SKP16	1.12965	ARL4C	1.119257	C17orf51	1.109151
DHX36	1.141038	TTC3	1.129451	MOSPD2	1.119215	LOC284581	1.109146
NRBP1	1.140706	KRIT1	1.12929	NPAT	1.119093	S100A10	1.108997
PLAC8	1.140652	GLRX2	1.129184	DCAF5	1.118853	KLF12	1.108645
APLF	1.140586	HIVEP2	1.128968	FCHSD2	1.118744	ASAP1	1.108091
PHC1	1.140343	GSE1	1.128762	TMEM220	1.118481	NTNG1	1.107978
CARF	1.1403	CTBP2P4	1.128686	MTMR6	1.118059	USP47	1.107689
TRIM32	1.140169	RDH10	1.128678	ETS1	1.117641	CLCF1	1.107433
SYNCRIP	1.140052	CNOT4	1.128653	WDR45	1.117377	ERI2	1.107385
MTMR12	1.139652	SMAD4	1.128574	FGF5	1.117219	SAMD12-AS1	1.107364
PLEKHA1	1.139347	MICAL2	1.128242	AMPD3	1.116797	TESK1	1.107248
ZMPSTE24	1.139193	RP1-102E24.8	1.127832	LOC101929530	1.116647	SAV1	1.10693
RP11-655C2.3	1.139036	TAS2R10	1.127757	RAB11FIP2	1.115894	HBEGF	1.106894
CNKSR3	1.106533	PROSC	1.097967	C10orf76	1.08664	FRMD4A	1.077572
LINC00649	1.106533	DDX39B	1.097922	GATSL2	1.086633	VAC14	1.077465
FAF1	1.106465	DIRAS1	1.097335	MIR194-2	1.085933	SKA1	1.077417
PROS1	1.106442	CHST12	1.097299	LRPPRC	1.085694	ZNF227	1.077297
KIAA0232	1.106028	LTV1	1.097053	RSU1	1.085645	PCM1	1.077112
ID1	1.105908	SCYL2	1.096558	RP4-633O19__A.1	1.085593	SNX13	1.07689
AGPS	1.105707	HSPH1	1.09645	RNU6-1082P	1.084957	LINC00152	1.076841
FAM160B1	1.105698	STK38	1.096049	STAG2	1.084898	CHD7	1.076735
RNU1-59P	1.105653	SGTB	1.09587	SGMS1	1.084851	SIK3-IT1	1.076573
HEXB	1.105566	SCAF8	1.095584	IER5L	1.08452	GATM	1.076364
BCL9L	1.105416	LOC100131802	1.094507	WSB1	1.084314	ZNF611	1.076339
NCKAP5	1.105376	BPGM	1.094147	DHX33	1.084245	IDS	1.075225
MEGF9	1.105347	SATB2	1.093986	TMEM38A	1.084038	CHRAC1	1.075221
SHFM1	1.10534	STAG1	1.093921	PLEKHA5	1.084024	TRIOBP	1.07493
QPCT	1.10497	MIR3661	1.093792	SUCLG2-AS1	1.083719	SCAMP4	1.074507
NUDT5	1.104941	RIPK2	1.093525	KIAA1109	1.083635	SENP5	1.07438
CACHD1	1.104747	LYPD1	1.093163	JPX	1.083561	RP11-156E6.1	1.074365
KIAA1551	1.104735	TFB2M	1.09303	CA5BP1	1.083429	MAN1A1	1.074194
POLR3H	1.104442	MIR505	1.093008	FRMD6	1.083305	CDC42SE2	1.074153
CNPPD1	1.104413	QSER1	1.092504	C6orf120	1.083059	PARG	1.073691
MFHAS1	1.104322	ARMCX6	1.092022	TP53TG3B	1.08254	KGFLP1	1.073446
ZBTB41	1.10419	SOCS4	1.091869	RNF19B	1.082477	ITGA3	1.07325
BBS7	1.103919	CDK9	1.091706	ARFGEF1	1.082429	MIR3065	1.073166
EIF4G3	1.103182	TOR1A	1.091165	FOXN3	1.082022	MON1B	1.07308

Gene Symbol	Expression	Gene Symbol	Expression	Gene Symbol	Expression	Gene Symbol	Expression
ZNF518A	1.103043	ADSL	1.09114	THOC5	1.08174	GIT2	1.072817
C7orf69	1.102933	MRS2	1.09101	RP11-314A15.2	1.081535	ENAH	1.072564
AMMECR1L	1.102521	TMEM69	1.090937	NR1D2	1.081347	CBLL1	1.072515
SRGAP2	1.102267	FLRT2	1.090806	AC159540.1	1.081275	UTP11L	1.072504
GADD45A	1.101968	GGTLC2	1.090462	SH3GLB1	1.08106	PPP3CB-AS1	1.072291
SLC45A4	1.101847	C7orf49	1.090288	GRPEL2	1.080912	MGA	1.072105
RP11-561O4.1	1.101638	CERS2	1.09027	F11R	1.080658	RPS6KC1	1.07207
EGLN1	1.101375	RASSF3	1.090134	S100A16	1.079887	TRIM37	1.071881
TIMMDC1	1.10124	LOC103344932	1.09008	TTYH3	1.079591	VWA9	1.07142
LRRC47	1.101196	ZNF117	1.08998	KRTAP5-4	1.079505	EHD2	1.071387
AC104651.1	1.101104	SLC25A44	1.08994	NHLRC1	1.079456	RAB7A	1.07065
RPP38	1.100986	RP11-110I1.12	1.089628	LIN7C	1.079289	PIK3R1	1.070531
TOP3A	1.10088	SIKE1	1.08954	PPAP2A	1.079263	SEC24A	1.070514
RP11-41O4.1	1.100866	DSP	1.08946	PTPN11	1.0789	TTL	1.070284
RP11-589M4.1	1.099925	LOC100506548	1.089175	PDS5A	1.07869	NETO2	1.070188
DIRC2	1.09985	TPRA1	1.089074	LOC286370	1.07851	KIAA1279	1.070149
ITGAV	1.099826	CCDC30	1.088955	RLF	1.078509	RBM41	1.069826
AP001347.6	1.099576	NUDT3	1.0881	WDFY3	1.078479	TRIM44	1.069695
TAS2R3	1.099387	PLGLA	1.08728	RP4-798A10.2	1.078364	PHLDA1	1.069352
PYGO1	1.099299	XX-C2158C6.3	1.087263	LINC00173	1.078208	SP4	1.068681
SERTAD2	1.098957	MIR3908	1.087244	LOC100129550	1.078155	LOC374443	1.068677
NOL10	1.098828	C16orf70	1.087029	PRUNE	1.078087	FAM173B	1.068613
FAM27E2	1.098296	PPP4R1	1.086909	HPS3	1.078004	CACNG4	1.067932
DDX1	1.098202	MTOR	1.086826	TLN2	1.077952	XKR6	1.067017
LYPD8	1.098115	RAB21	1.086698	TAF4B	1.077572	C11orf63	1.0669
RNA5SP408	1.066541	CCDC144A	1.056366	NNMT	1.045293	SMURF2	1.03542
LOC642361	1.066369	NRBF2	1.056223	CLTCL1	1.044601	NUB1	1.035416
SFR1	1.066148	ARNTL2	1.055978	SRGAP2-AS1	1.044546	XRCC1	1.035318
TTC9	1.065865	ACTR8	1.05587	NIPAL1	1.044533	SPOP	1.035287
NALCN	1.065732	LOC541472	1.055738	SNX6	1.044426	PTK2B	1.034762
LINC00667	1.065671	AFAP1L2	1.055313	COA7	1.044337	PPP2R5E	1.034715
RP11-79P5.2	1.065252	UTP3	1.05515	RPP14	1.044134	TP53RK	1.034383
SNHG16	1.064456	RP11-1103G16.1	1.05401	SIPA1L3	1.043917	OSER1-AS1	1.034178
SIRT1	1.064307	POC1B	1.053337	ABL2	1.043878	ZMAT3	1.034008
EAF1-AS1	1.064305	SERPINB8	1.053288	NIP7	1.043539	RASGRP3	1.033909
ARMCX4	1.064123	TM4SF19	1.053222	DHCR24	1.0434	PKP2	1.033761
ECM2	1.064117	TCTN3	1.053118	MAP4K3	1.042916	EIF1AX	1.033625
SDHAP2	1.064067	ZSCAN16	1.052486	THAP11	1.042817	KIN	1.033324
ALMS1	1.06395	TOB2P1	1.052085	RP11-521B24.5	1.042659	TMEM128	1.033246
CD55	1.063918	TPP2	1.05203	CCAR2	1.042598	DUSP28	1.033079
MIR4755	1.063711	SPIN1	1.051855	DUSP7	1.042415	CCDC71	1.033
RP11-255A11.2	1.062897	PARP6	1.051795	UGDH	1.042393	IRAK2	1.032947
LARS	1.062746	GNPDA2	1.051375	BMPR1A	1.042355	CHIC1	1.032846

Gene Symbol	Expression	Gene Symbol	Expression	Gene Symbol	Expression	Gene Symbol	Expression
PUM2	1.062678	PXMP2	1.051185	39873	1.041852	SLAIN2	1.032783
SLTM	1.06208	MIR4720	1.051125	C15orf41	1.041712	ARID4A	1.032755
MPHOSPH8	1.062064	MIRLET7I	1.051011	PLD1	1.041494	RNU6-126P	1.032519
NTAN1	1.061977	LRCH2	1.050923	IL4I1	1.041444	TNKS2	1.032335
E2F3	1.061963	NFE2L1	1.050798	RP11-244F12.2	1.041238	LPGAT1	1.031459
LOC100652999	1.061818	EZR	1.050743	NSD1	1.041226	ZEB1	1.030765
IFT52	1.061693	SLC20A1	1.05015	MIR3135B	1.041174	CHD1	1.03045
TTLL12	1.061507	SLC23A2	1.050085	PTPRE	1.041017	CNBP	1.030424
ZBED5-AS1	1.061448	DLEU2	1.049873	MPI	1.040881	PPAT	1.029803
FEM1B	1.061358	EVC	1.049856	ATP2B4	1.040766	MID1	1.029698
DNAJB12	1.061255	LOC391322	1.049714	DCTN4	1.040687	KPNA4	1.029624
TRPS1	1.060366	CLASP2	1.049199	OGT	1.039964	ABHD17B	1.02934
ANAPC13	1.060292	LOC644450	1.048931	TFDP2	1.039193	MIR548T	1.029328
ARMC10	1.060223	CRYBG3	1.048734	ZSWIM4	1.03902	HSBP1L1	1.029298
WBP1L	1.060112	ZNF599	1.048114	RNU6-522P	1.038477	LINC00638	1.029131
LRCH3	1.059565	ENG	1.047819	AHCTF1	1.038189	AC009505.2	1.029033
TRA2B	1.059162	WNK1	1.047629	AC005014.5	1.03809	PHIP	1.028906
UHRF1BP1	1.058987	ZNF248	1.047531	MED13L	1.038004	RTN4	1.02878
GOLGB1	1.058811	PIGA	1.047422	MAP1LC3B2	1.03791	MIR31	1.028379
AIMP2	1.058612	B3GALT6	1.047388	AC067956.1	1.037718	STIM2	1.028184
AGO2	1.0586	CTSD	1.047276	PDPK1	1.037567	RECK	1.028112
SMARCD1	1.058481	LOC101929112	1.04673	WDR82	1.037462	BAZ1A	1.028106
OTUD6B-AS1	1.058277	NDUFAF1	1.046661	SLC16A7	1.037451	RNU4-36P	1.028102
SOCS3	1.058039	TMEM67	1.046566	N4BP2L2-IT2	1.037267	FAM171A1	1.027955
RAB9A	1.057956	TSEN15	1.04639	KIR2DL2	1.036977	C8orf88	1.027698
R3HDM1	1.057924	MIR761	1.046271	CDKL5	1.036975	NIPBL	1.027488
GAREM	1.057474	WSB2	1.046048	TLE4	1.036664	GALNT1	1.027039
ANKRD12	1.056866	EXT1	1.045976	ZCCHC17	1.036627	ITPK1	1.026614
RAB31	1.056763	SPRY3	1.0459	SAP130	1.036604	ARHGEF12	1.026461
USP33	1.056645	LINC01184	1.045528	MIR604	1.036479	CHMP2B	1.026359
SERINC2	1.056583	MIR4632	1.045308	RYK	1.036088	C1orf220	1.026326
NCOA4	1.026214	MGARP	1.017706	LINC01125	1.007988	TAF15	1.002056
SMAGP	1.025848	SLC25A43	1.017655	PTPRG	1.007899	GSKIP	1.002001
CD1B	1.025806	SRP72	1.017619	ALKBH3	1.007641	SLMAP	1.001506
RWDD2B	1.025698	MIR626	1.017574	SIGLEC15	1.007555	PLK4	1.001422
GCLM	1.025646	FBXL17	1.016882	SPRY2	1.007523	SHOC2	1.001253
MME	1.025531	MID1IP1	1.016519	APCDD1L	1.007426	ZNF607	1.001149
LOC101928020	1.025494	CTBS	1.016315	CCDC47	1.007329	NHS	1.000746
ENTPD4	1.025298	DICER1	1.015704	SRPR	1.007313	NEK3	1.000699
C22orf46	1.02507	FAM213B	1.015541	SYNC	1.006925	MAP3K8	1.000412
IPO5P1	1.024981	NAA30	1.015472	FAM171B	1.006854	VPS54	1.000173
IGLJ5	1.024974	RP11-25E2.1	1.015232	IL1RL1	1.006651	RP11-503E24.2	1.009823
ZCCHC5	1.024504	LOC101929302	1.015026	ARHGEF18	1.006321	ZBTB9	1.009682
SORT1	1.02447	ADRBK2	1.014746	CHKA	1.005964	GPD2	1.009566

Gene Symbol	Expression	Gene Symbol	Expression	Gene Symbol	Expression	Gene Symbol	Expression
SLC12A6	1.024335	ANKRD30B	1.014434	RMND5B	1.005693	LHX4-AS1	1.009557
AP4M1	1.024191	SUPT6H	1.014269	SLC25A40	1.005613	MRPL1	1.009268
FAM86EP	1.023982	RNA5SP500	1.01416	AVPI1	1.005159	BLM	1.009266
NIN	1.023958	PLA2G15	1.0139	MIR769	1.005002	NOMO1	1.00926
GIN1	1.023543	ANKRD16	1.013152	PRLR	1.004958	JAK2	1.009138
FAM102B	1.023446	NAF1	1.01315	PARP4P2	1.004874	RTP3	1.009128
IKBIP	1.023278	HOOK3	1.01311	LOC493754	1.004564	IGKV1-39	1.009037
GCOM1	1.023206	ASCC2	1.013052	SEC11C	1.004172	RAB30	1.008787
HECW2	1.02298	NT5DC2	1.012766	SP2	1.004115	RNU6-612P	1.008535
IFIT2	1.02269	MLLT4	1.012762	FZD8	1.004045	CCDC101	1.008173
LRRC8E	1.022572	RNA5SP70	1.012389	RAP2A	1.003902	ZSCAN5B	1.021091
TAX1BP1	1.022356	ANTXR1	1.011957	ASPHD2	1.003633	ITCH	1.021067
FUT11	1.022091	ORMDL1	1.011937	KLF3	1.003607	RBM24	1.020578
SPTLC2	1.021971	TES	1.0117	PPAP2B	1.003552	STEAP3	1.020562
LOXL2	1.021858	IDNK	1.011652	LYST	1.003532	CCDC103	1.020159
VPS72	1.021793	RNA5SP355	1.011604	LSG1	1.003384	FAM200A	1.019979
NUPR1L	1.021672	SLC22A4	1.01136	WNT5A	1.003003	TBC1D31	1.01983
PPP3CA	1.021672	BLZF1	1.010509	RNU4ATAC16P	1.002975	GABRE	1.018605
PAQR7	1.021549	USP31	1.010308	C7orf25	1.002944	SENP1	1.018475
ARHGAP39	1.021346	MERTK	1.010129	PATZ1	1.002931	ZER1	1.018308
RGPD1	1.021325	C2CD2	1.01012	PIAS2	1.002699	PYROXD1	1.018254
RNU2-5P	1.021254	NXPE3	1.010083	ZNF271	1.002689	GNPTAB	1.018109
ZNF384	1.021249	SRCAP	1.00987	ARHGAP11A	1.002432	RP11-642D21.2	1.018025